EXTREME VALUE ANALYSIS OF DEFECTS ON AM PARTS

S. Beretta, S. Romano – Politecnico di Milano, Dept. Mechanical Eng., IT

A. Brandao, J. Gumpinger – European Space Agency, Noordwijck, NL

A research with the support of RUAG Space, Product Unit Structures

Summary of the presentation

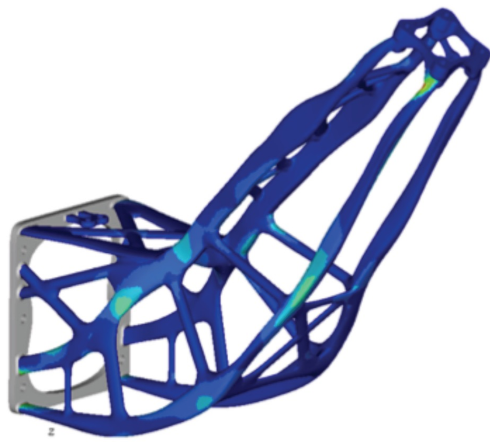

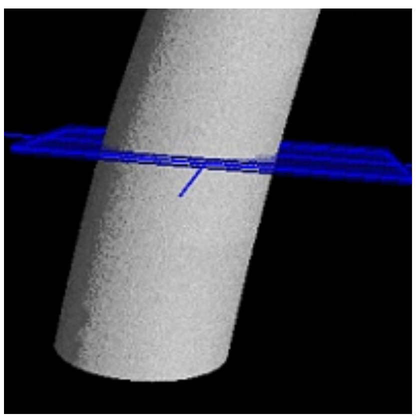

- **Introduction & motivation**
- **Extreme value analysis for CT scans**
  1. Sampling strategies;
  2. Analysis in terms of volumes;
  3. Geometric features of extreme defects;
- **How to reduce CT scan effort**
  5. Choice of the threshold;
  6. Minimum material volume to be scanned;
- **Application to component**
  7. prospective application onto a component;
  8. Fatigue assessment.
- **Conclusions**

Literature review

Defects have a large influence on the fatigue limit. They can be treated as short cracks according to Murakami's projected root area and described by the **Kitagawa diagram**.

AlSi10Mg, R = -1

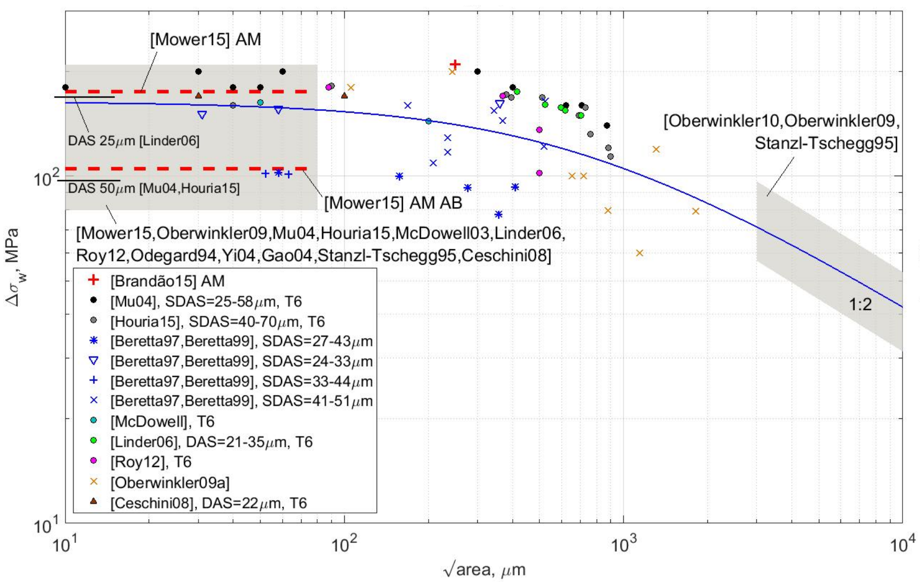

Ti6Al4V, R = 0

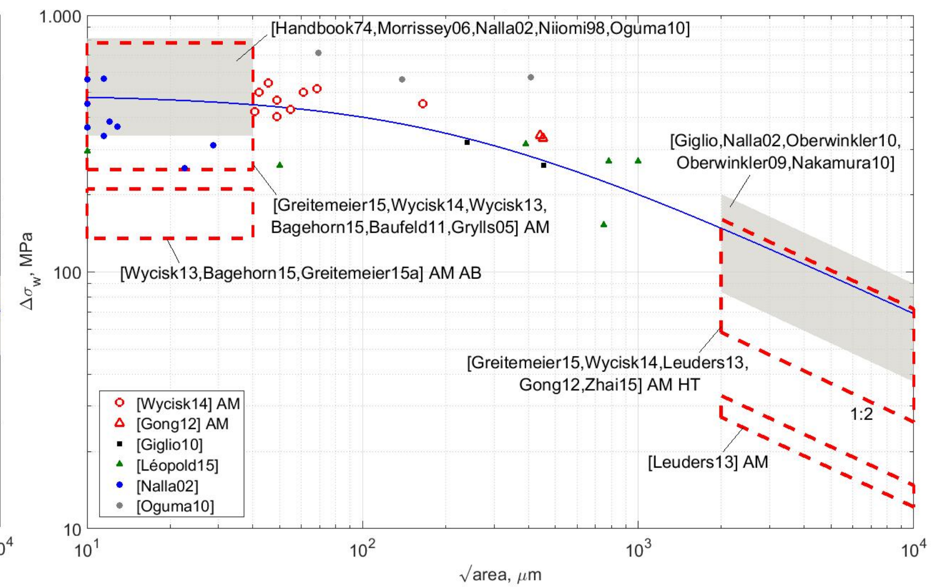

- Fatigue properties of AM are very similar to those of standard processes;
- Large reduction of fatigue resistance for as-built samples (they can be modeled as equivalent surface defects);
- Intrinsic variability of the fatigue limit due to several factors (process/microstructure).

Extreme value statistics for defects

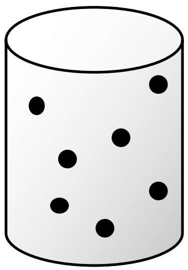

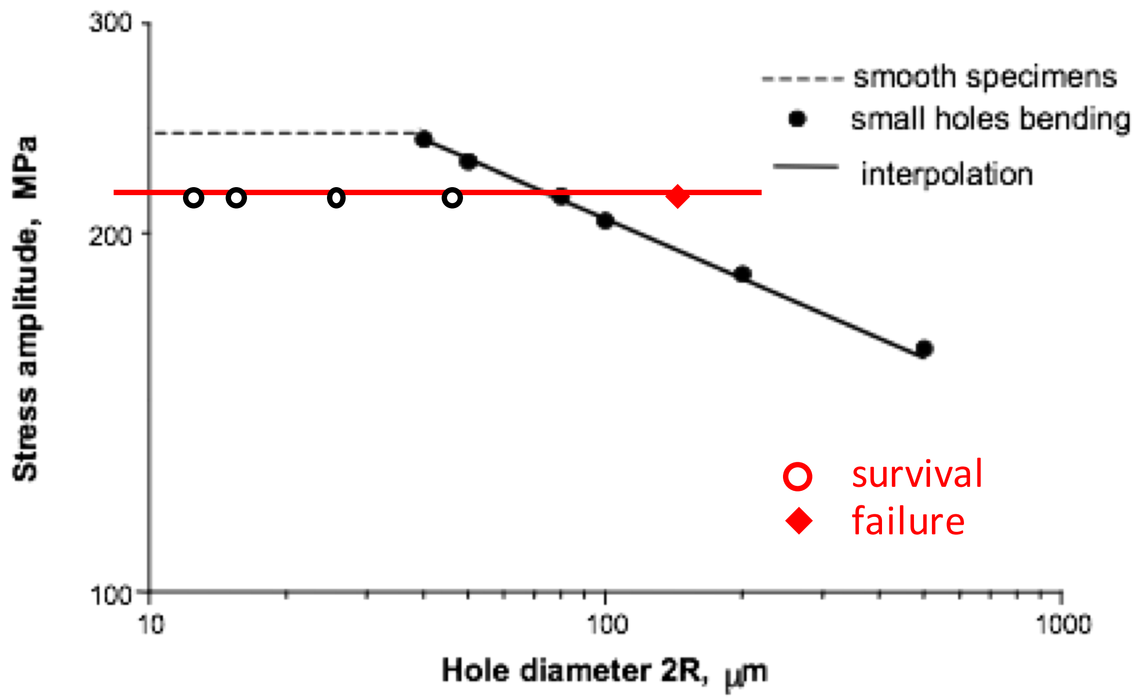

the fatigue is controlled by the **extreme values** of the population of defects **not** by the average dimension

analysis of extremes based on **extreme value sampling** at the end of the 90's

ESIS P11-02
ASTM E2283-03

Statistics of extremes strategies

Peaks-over-threshold

In a given volume, all the defects over a certain threshold are considered.

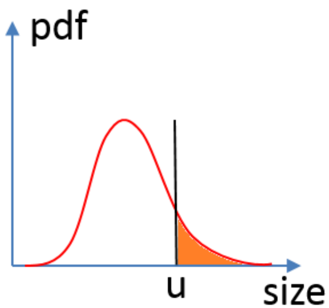

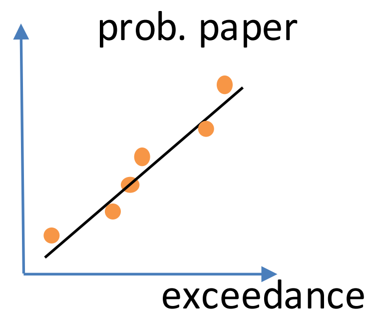

- no standard (but good books);
- all the measurements above *u* are treated;
- **Exponential distribution** (d →∞);
- Extrapolated distribution for the maximum defect in a given volume is the **Gumbel distribution**

Block maxima

In a given volume, only the largest defect is considered.

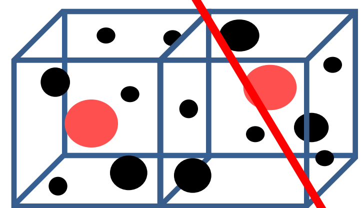

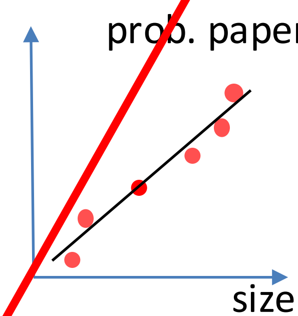

- considered in ASTM E2283-03;
- it is applied very naturally with polished sections;
- a bit 'innatural' to pick up the maximum defect in a given sub-volume.
- **Gumbel distribution** (d →∞)

Activity

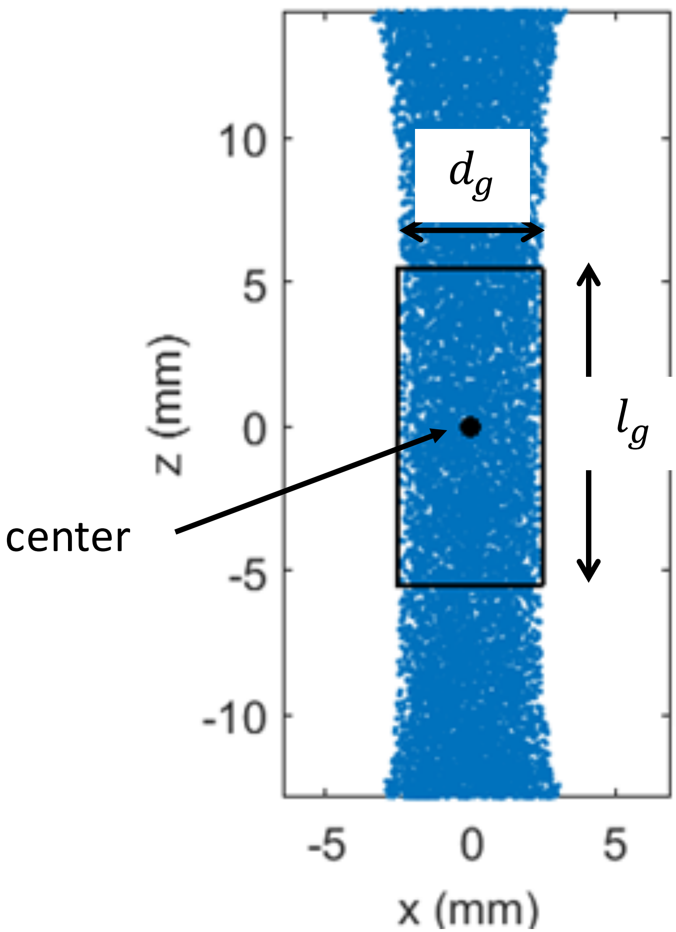

At the beginning only the data in the gage length were considered

- CT scans for a series of specimens that were provided by RUAG Space, Product Unit Structures,
- together with a component were analyzed with CT scans at ESA;
- Analysis with the statistics of extremes with POT method.

Name	Print direction	N	V_{max}
F2H	horizontal	12740	0.0119
F3H	horizontal	15851	0.0142
H25	horizontal	22345	0.0121
O26	vertical	6600	0.0107
U25	vertical	10880	0.0222
V26	vertical	20871	0.0038

Volume distribution

A comparison on defect size V and $\sqrt[3]{V}$ is done considering only the gage volume. Some difference among the specimens.

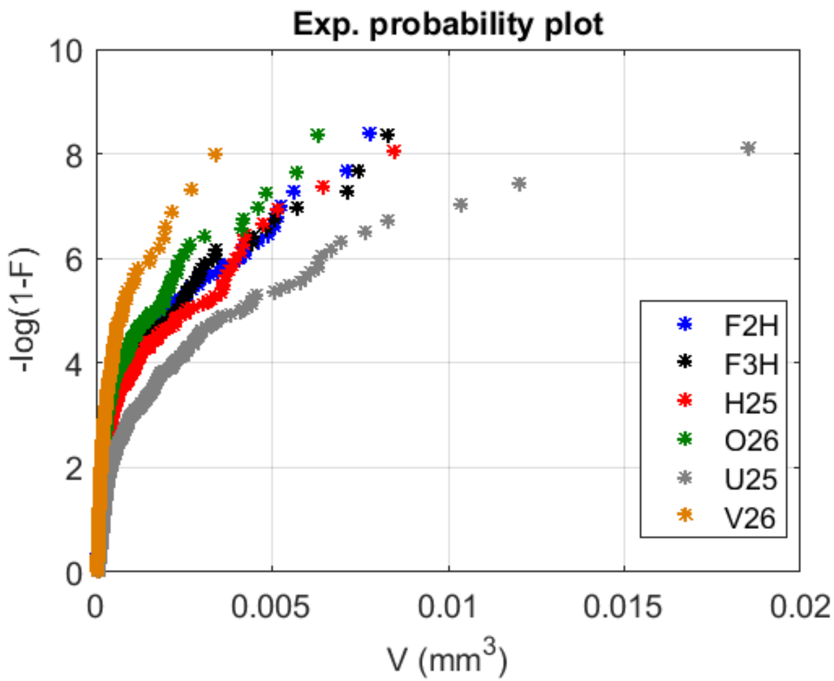

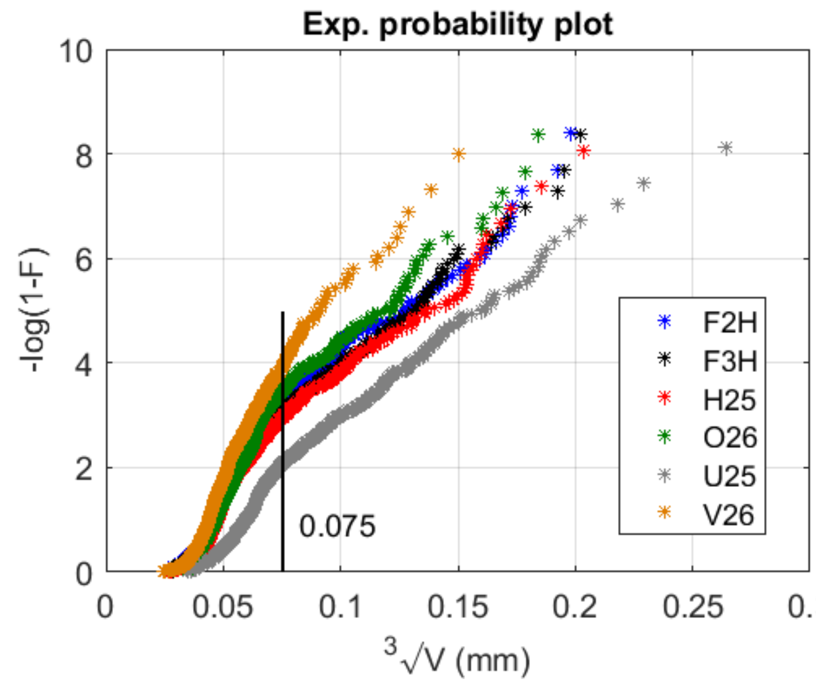

- Above a threshold of 0.075 mm, the flaw distribution of the exceedances is an exponential;
- this corresponds to the well established results for inclusions in steels (√area is a Gumbel)

Example of analysis

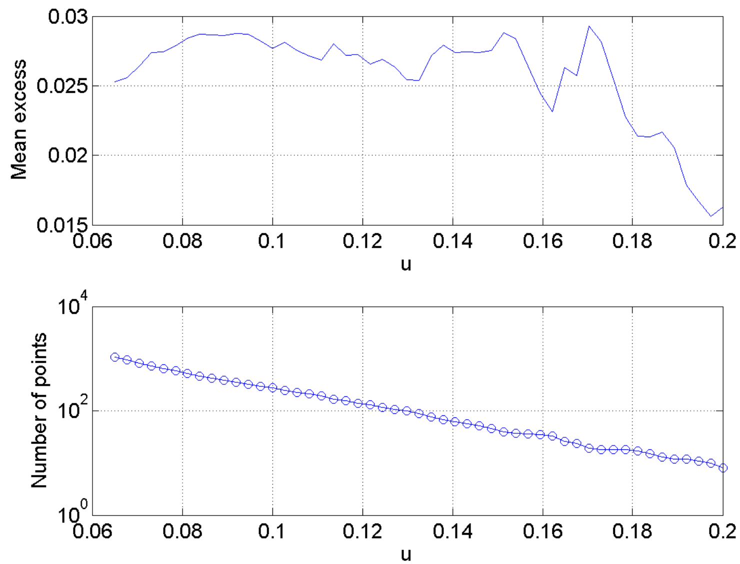

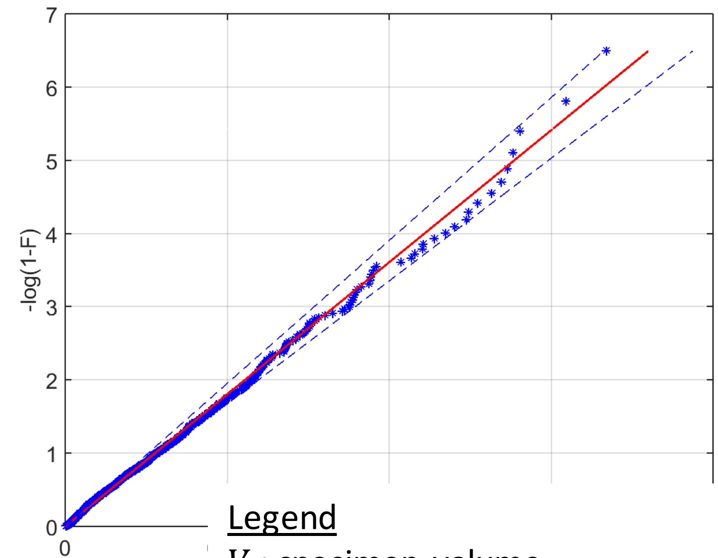

<u>Legend</u>
V_c: specimen volume
V_s: scanned volume
n: number of defects exceeding *u*
T: return period of the max. defect

1. Fix a threshold for the volume: $u = 0.075$
2. Calculate the mean excess: $\mu = mean(\sqrt[3]{V} - u)$
3. Return period of the defect exceeding *u* in a bigger volume: $T = \frac{V_c}{V_s} \cdot n_u$
4. Define the maximum defect with return period T in terms of diameter and volume:

$$d_{max,T} = \mu \cdot \log T + u \qquad d_{max} \in LEVD \begin{Bmatrix} \lambda = d_{max} \\ \delta = \mu \end{Bmatrix}$$

Estimation of extreme defects

Predictions of maximum defects have been compared with maximum defect detected on the entire specimen (not only the gage lenght).

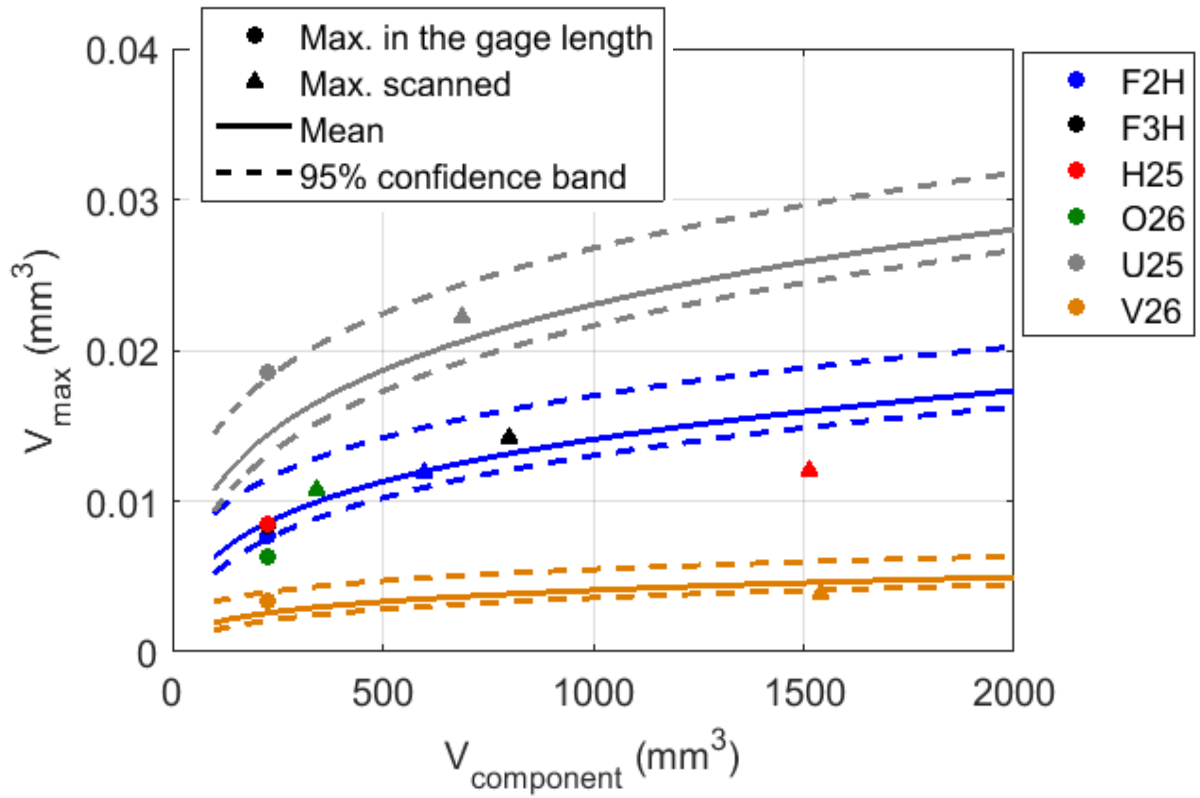

Considering the low number of defects used in the estimation of maxima (only those in V_g), the prevision is quite good.

Defects → fatigue

From Murakami we know that:

$$\Delta K = 0.65 \cdot \Delta S \cdot \sqrt{\pi \sqrt{area}}$$

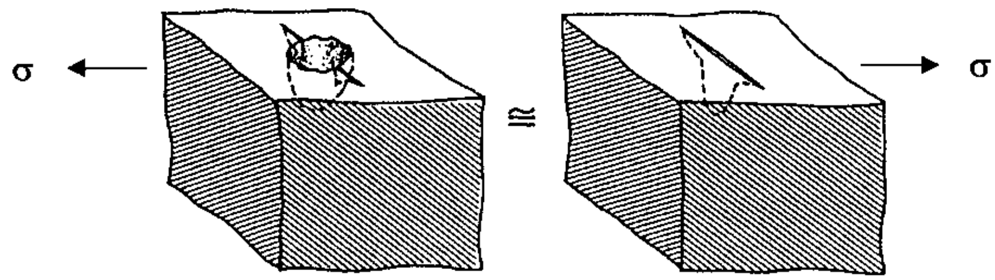

The projection along the stress direction (PZ) can then be used to define the $\sqrt{Area}$ parameter, essential for the Kitagawa diagram.

In order to perform good estimations of the fatigue life, the extreme value analyses have to be carried out on the $\sqrt{Area}$ parameter.

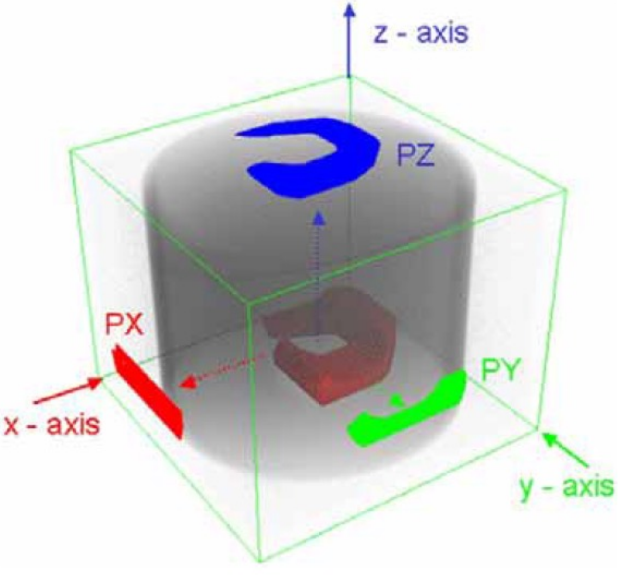

POT on $\sqrt{A}$

Even considering $\sqrt{A}$, distributions are very similar, except for U25 and V26.
Once again, only the defects in the gage volume are taken into account.

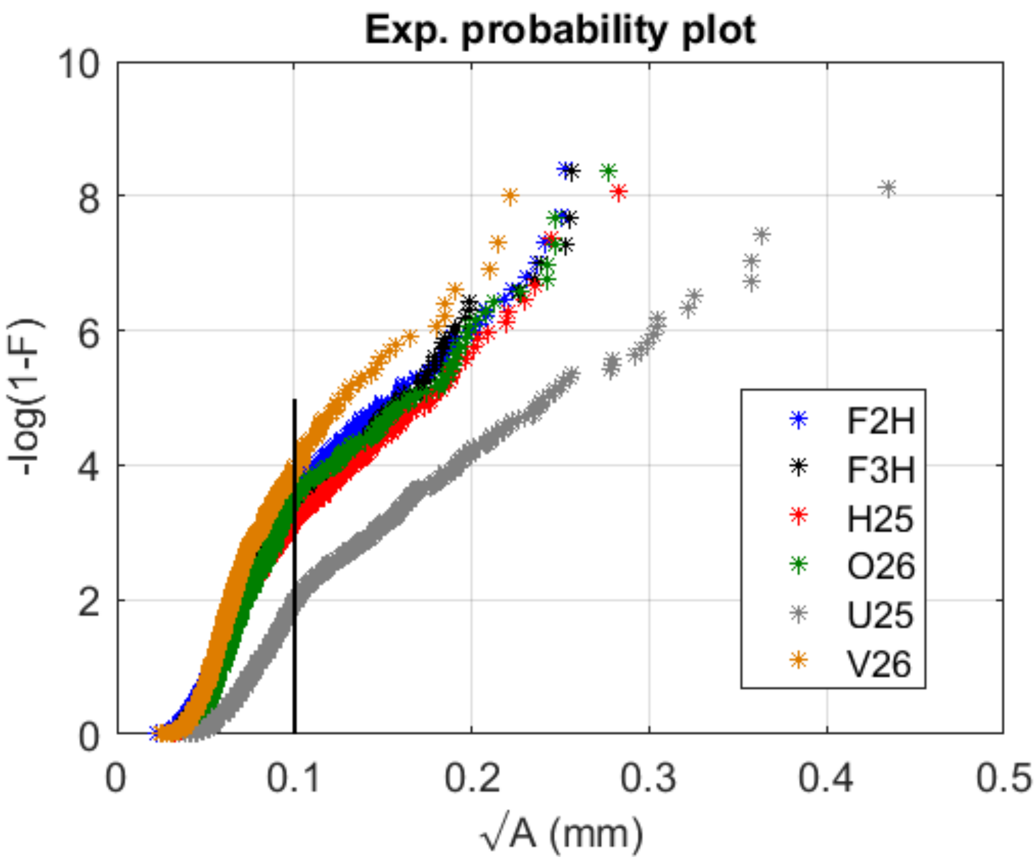

POT threshold:
$\sqrt{A_{th}}$ = $100\mu m$

The analysis of √area confirms that the exponential fit can be adequate

Summary of the application

- Comparison of the specimens considering the √area of defects perpendicular to specimen axis;
- Important defects have $\sqrt{A} > 100\mu m$ (final flat part of Kitagawa diagram);

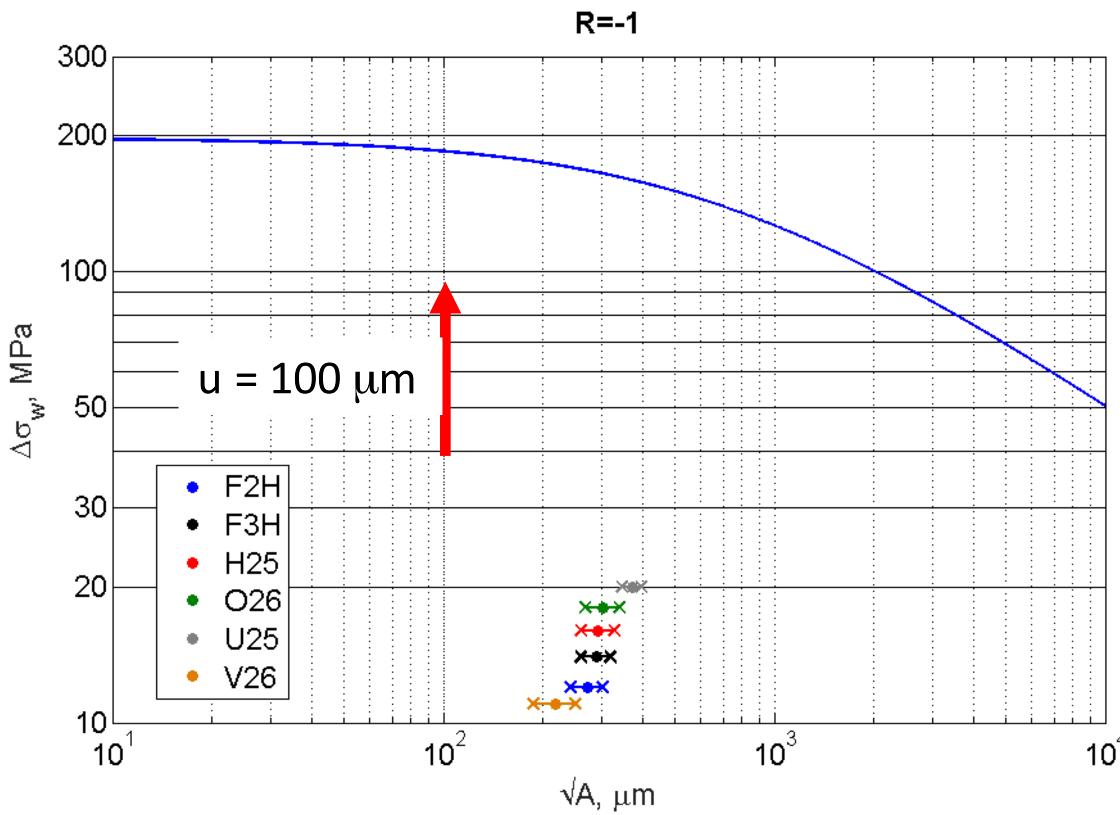

threshold *u* has a meaning also from the point of view of Kitagawa diagram (only defects exceeding 100 μm are detrimental)

1) Our estimates of maximum defects from a small material volume are really precise ?

2) How much effort do we have to spend (scanning time, material volume) for obtaining good estimates if we had to estimate the maximum defect on a big component ?

Block Maxima on defect area

The reference distribution obtained by 'Block maxima' sampling a much larger material volume has been estimated through the POT by taking different values of u.

The threshold varies from u=100 µm to u=150 µm and 200 µm.

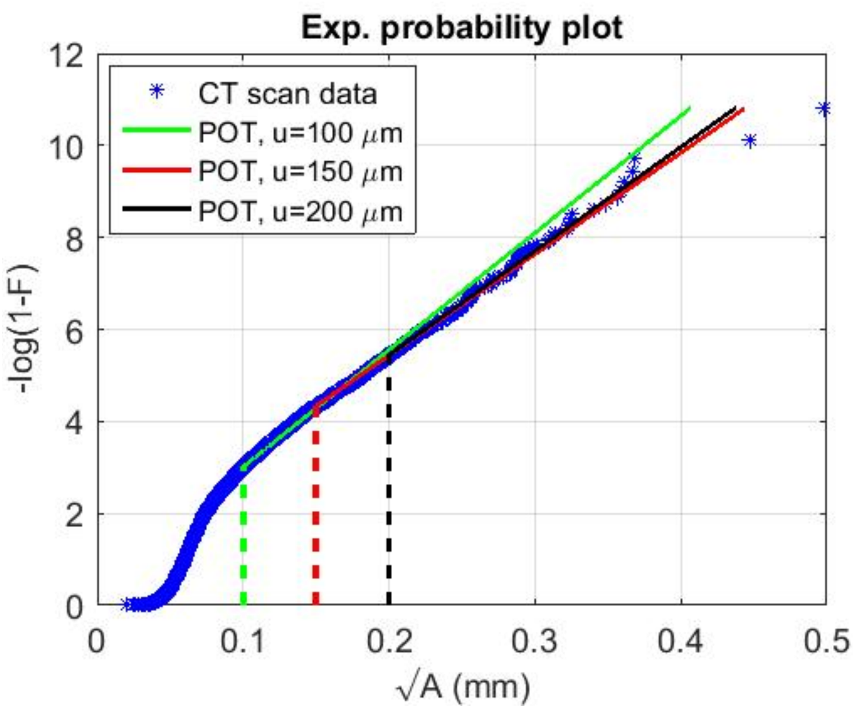

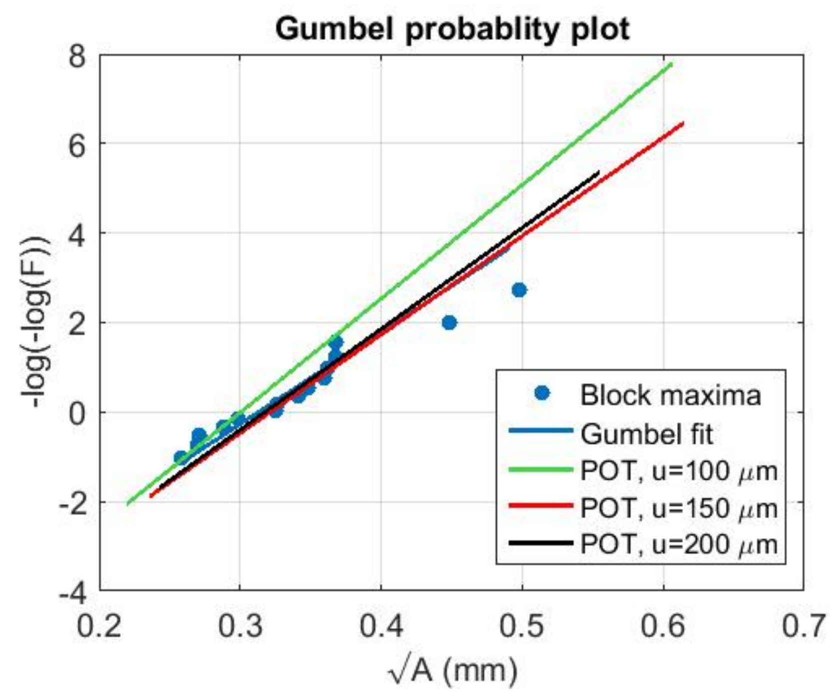

The estimations based on the two POTs described are in line with the maxima found, and in particular the estimation is very accurate fixing u=150 µm, while using u=100 µm we underestimate the real maxima. No further improvement for 200 µm.

Low resolution scan

We are analyzing defects above 100-150 mm
→ it would be worth reducing resolution ?

Specimen F3H was tested considering two CT resolutions:

- High resolution: pixel size 15 µm;
- Low resolution: pixel size 30 µm.

The goal is to verify if decreasing the resolution some time needed for CT could be saved, without loosing in accuracy when describing the extreme defect distribution.

- Distribution of POT is almost the same!
- Significant time saving from 7.5 h to 2.3h !

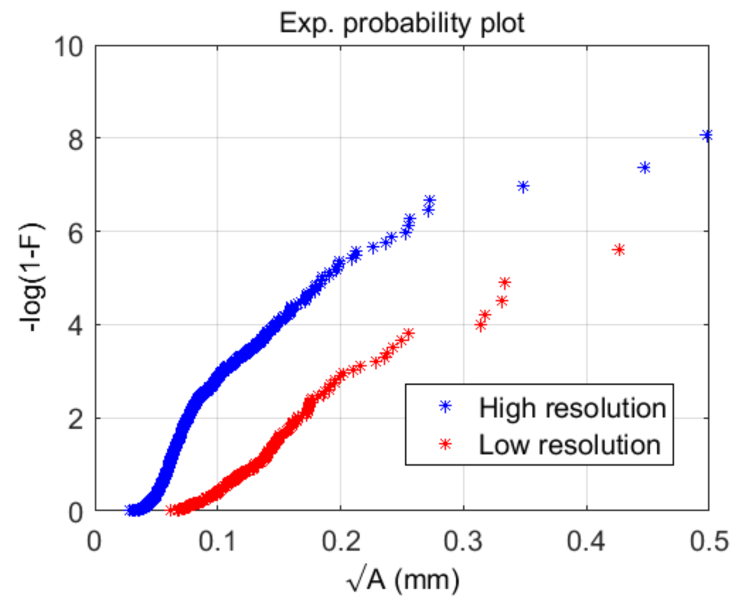

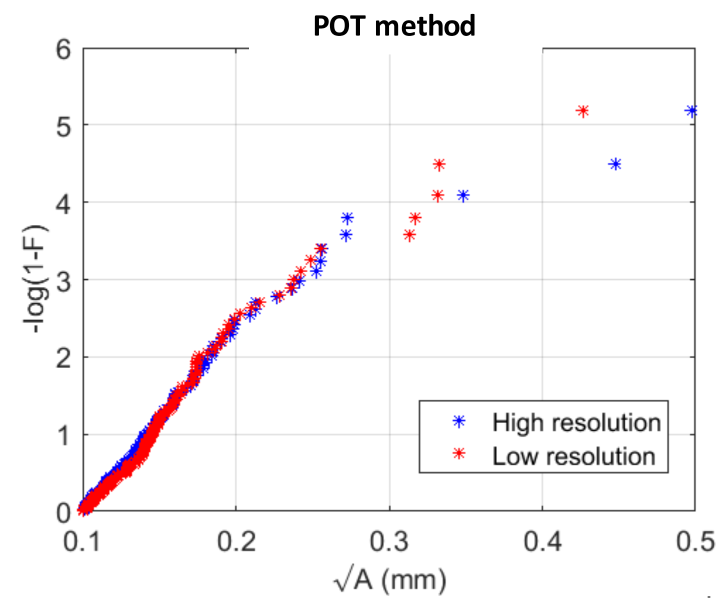

Minimum material volume

Monte Carlo simulations have been performed in order to understand the influence of this variability, sampling 3, 5 or 10 subvolumes of the 15 ones and fitting the exponential distribution on the exceedances over the threshold *u*.

3 subvolumes | 5 subvolumes | 10 subvolumes

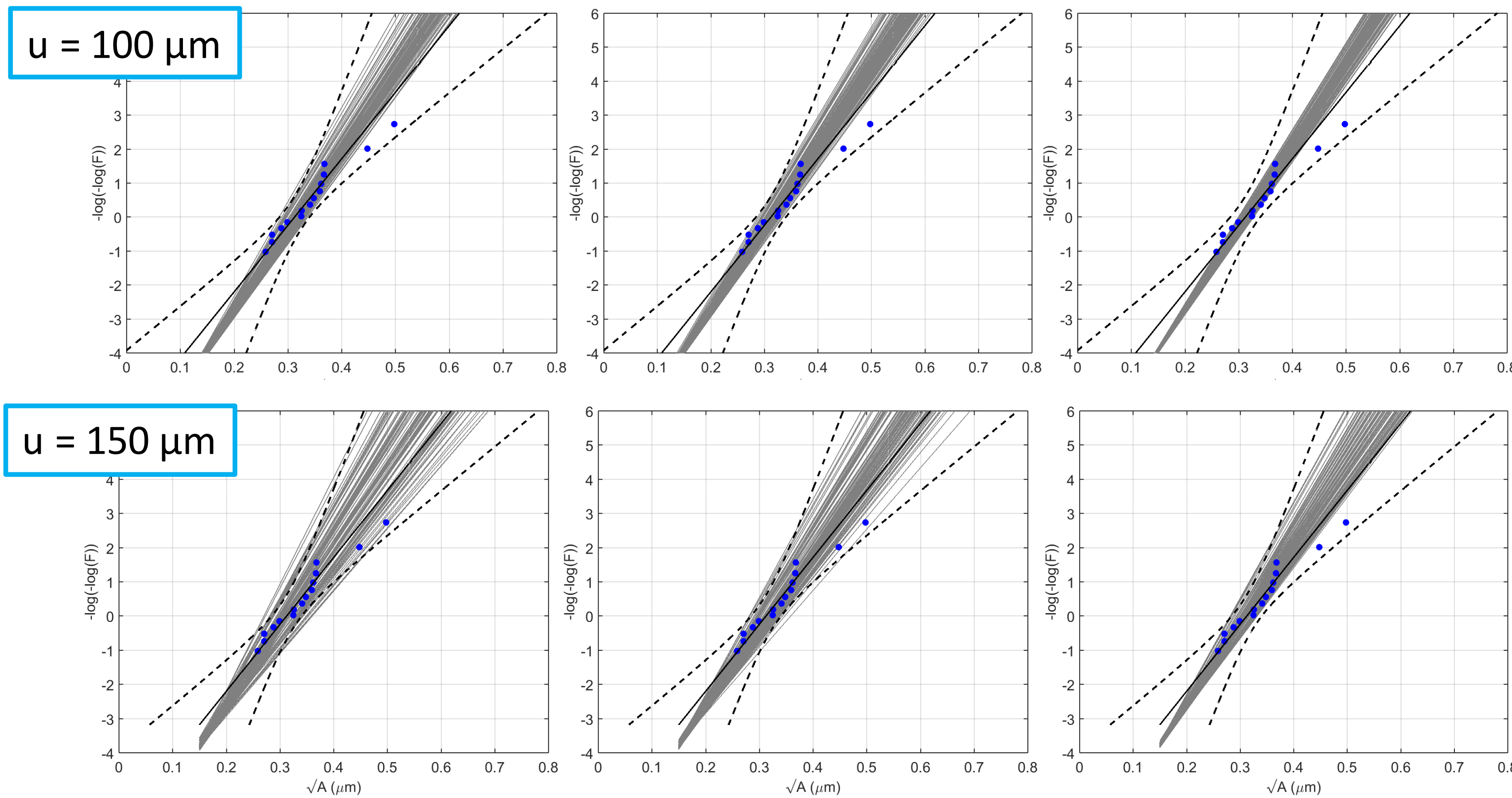

The distribution matters !

Even if the two maxima are not perfectly in line with the estimation, both the LEVD and the composed distribution found by statistic of extremes on a volume equal to 7,5 V_{gage} (the whole volume divided by 2, the return period of these points) yields a good prevision.

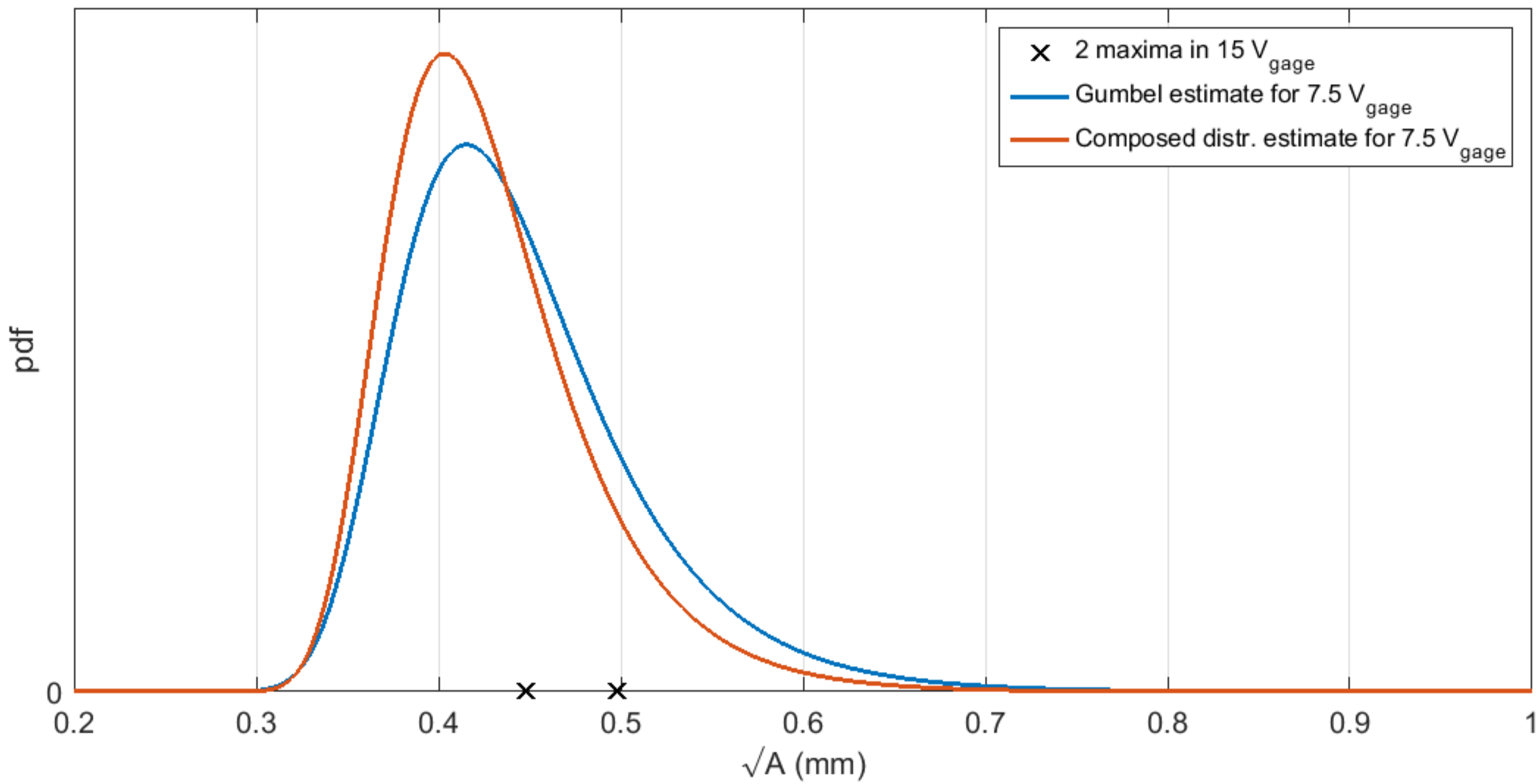

Bracket parts

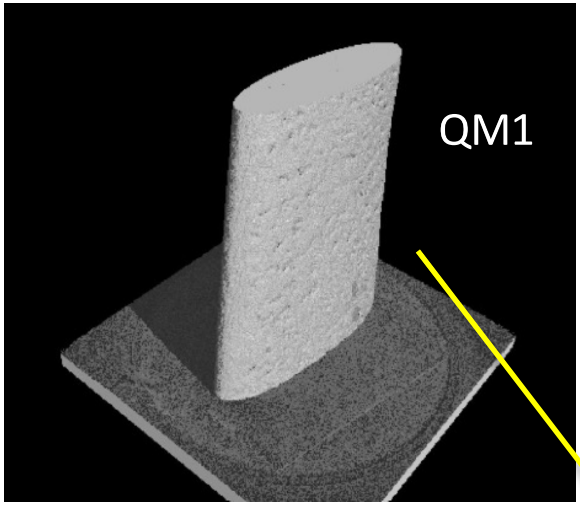

Two small parts of the component were analyzed by CT: QM1 and QM2.

Their volumes are:

- V_{QM1} = 15500 mm^3
- V_{QM2} = 3870 mm^3

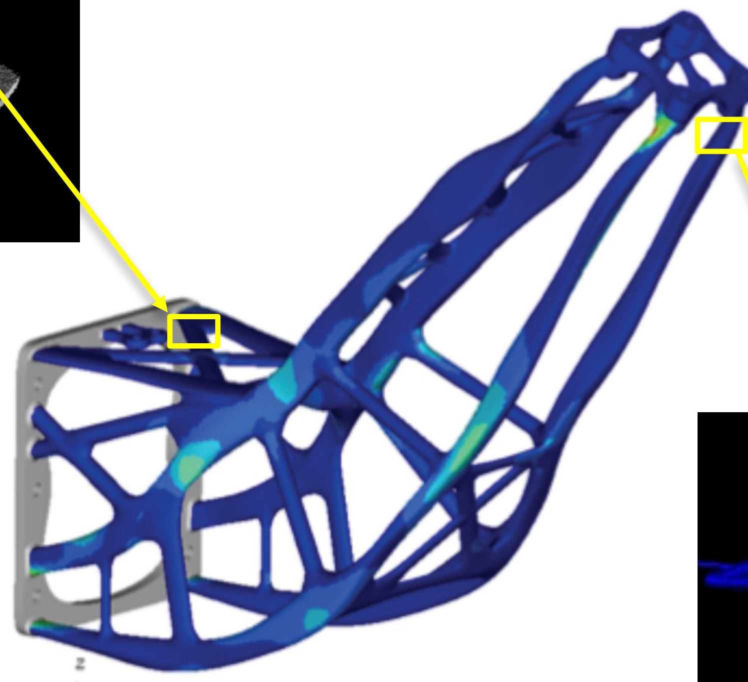

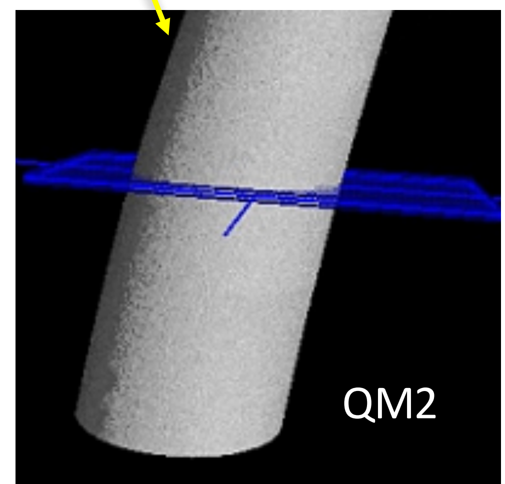

Application of the previous ‘rules’ was successfull

Prospective fatigue strength - 1

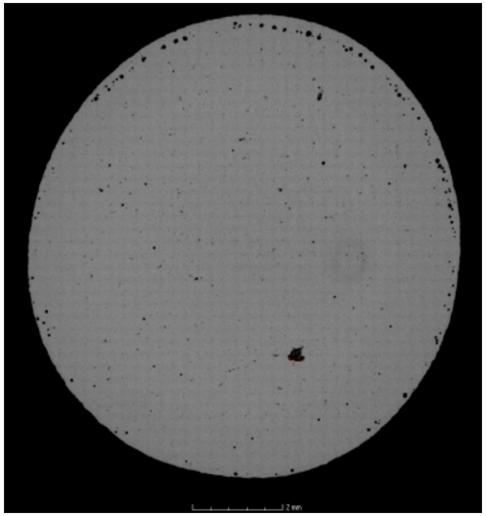

CT scans of the component reveal that, apart internal volumetric defects, there are regions of sub-surface pores

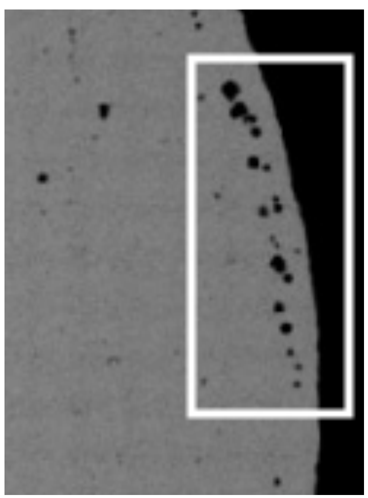

If we treat them as a 2-D crack:

$$\sqrt{area}_{sup} = 650 - 790 \ [\mu m]$$

Prospective fatigue strength - 2

Prospectively, this is the scenario for fatigue assessment considering average strength of AlSi10Mg

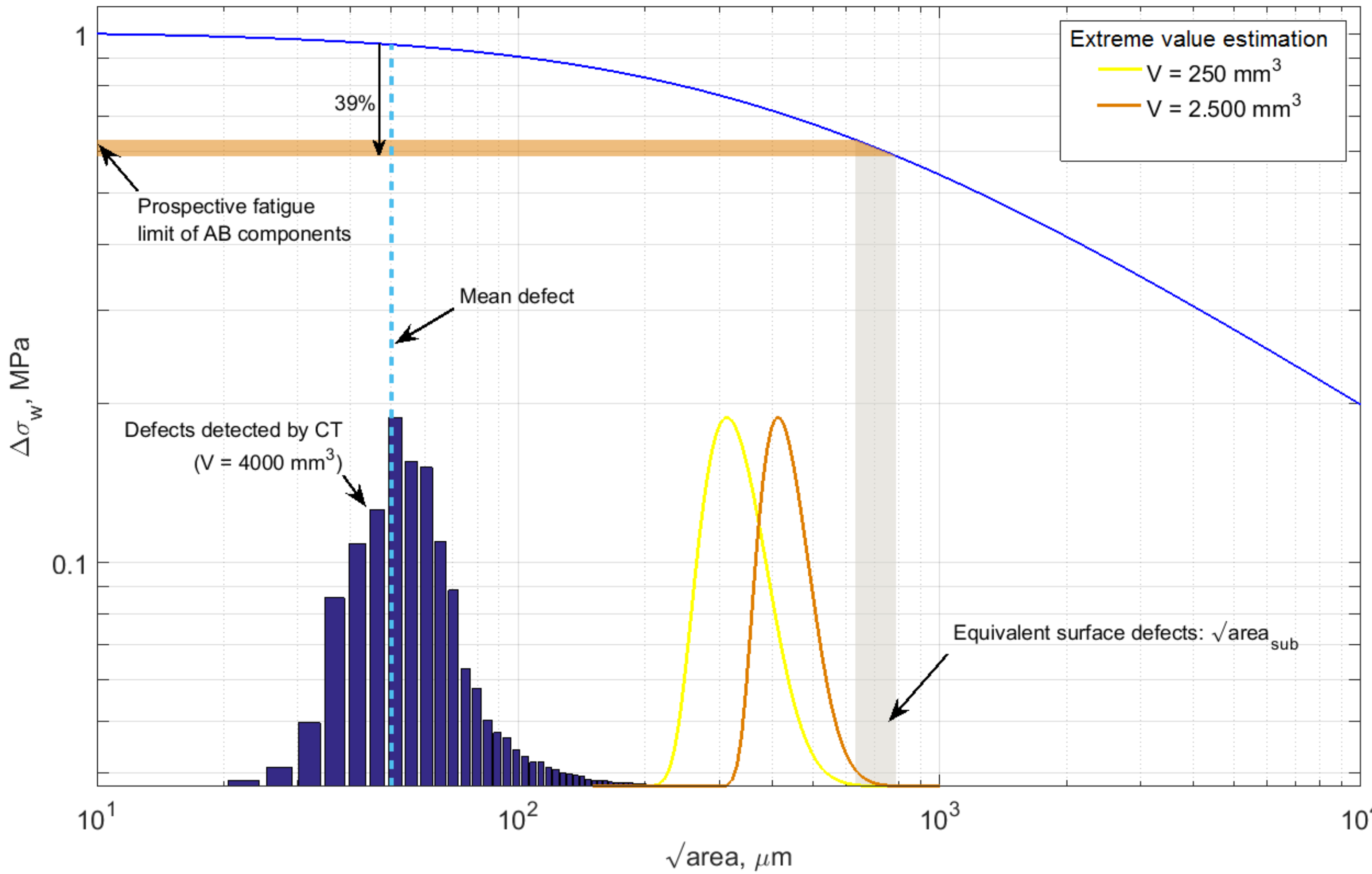

The sub-surface defects appear to be more detrimental than the internal ones

Conclusions

In this presentation I have discussed some applications of the statistics of extremes to AM parts:

- it has to be used because fatigue strength is controlled by the maximum defect in a given volume;
- features and methods developed in the '90's for inclusions are still valid and it is worth adopting that wide background (e.g. ASTM E2283-03);
- It looks that the 'Peak Over Threshold approach' is the most simple to apply for CT scan measurements;
- It is possible to determine the minimum requirements for the scan of a component (threshold, minimum volume) that also allow to reduce the effort of defect sampling;
- prospective application to fatigue is very simple through the Kitagawa diagram.

Essential references

[1] Y. Murakami. Metal Fatigue: Effects of Small Defects and Nonmetallic Inclusions. Else- vier, Oxford, 2002.
[2] Y. Murakami and M. Endo. Effect od defects, inclusions and inhomogeneities on fatigue strength. Int. J. Fatigue, 16:163–182, 1994.
[3] Y. Murakami. Inclusion rating by statistics of extreme values and its application to fatigue strength prediction and quality control of materials. J. Res. Natl. Inst. Stand. Tehcnol., 99:345–351, 1994.
[4] S. Coles. An Introduction to Statistical Modeling of Extreme Values. Springer, London, 2001.
[5] R.D. Reiss and M. Thomas. Statistical Analysis of Extreme Values. Birkhauser Verlag, Basel, 1997.
[6] Y. Murakami and S. Beretta. Small Defects and Inhomogeneities in Fatigue Strength: Experiments, Models and Statistical Implications. Extremes, 2(2):123–147, 1999.
[7] ASTM E2283-03. Standard practice for Extreme Value Analysis of Nonmetallic Inclusions in Steels and Other Microstructural Features. American Society for Testing And Materials, 2003.
[8] Beretta, Stefano, Clive Anderson, and Yukitaka Murakami. "Extreme value models for the assessment of steels containing multiple types of inclusion." *Acta materialia* 54.8 (2006): 2277-2289.
[9] S. Beretta, S. Romano, A comparison of fatigue strength sensitivity to defects for materials manufactured by AM or traditional processes, International Journal of Fatigue, Available online 22 June 2016, ISSN 0142-1123, http://dx.doi.org/10.1016/j.ijfatigue.2016.06.020.

The authors would like to acknowledge the support of RUAG Space, Product Unit Structures, Zurich (CH)

National Aeronautics and Space Administration
Marshall Space Flight Center

Overview of Fatigue and Damage Tolerance Performance of Powder Bed Fusion Alloy N07718

William Campbell
NASA MSFC
Huntsville AL

William Tilson
Jacobs ESSSA Group
Huntsville AL

ASTM/NIST Workshop on Mechanical Behavior in Additive Manufactured parts

May 4, 2016

MSFC PBF Capability

- Selective Laser Melting (SLM)
  - Heat source is a 200 W laser
- Concept Laser M1 Cusing SLM machine
  - 250 x 250 x 250 mm^3 build volume

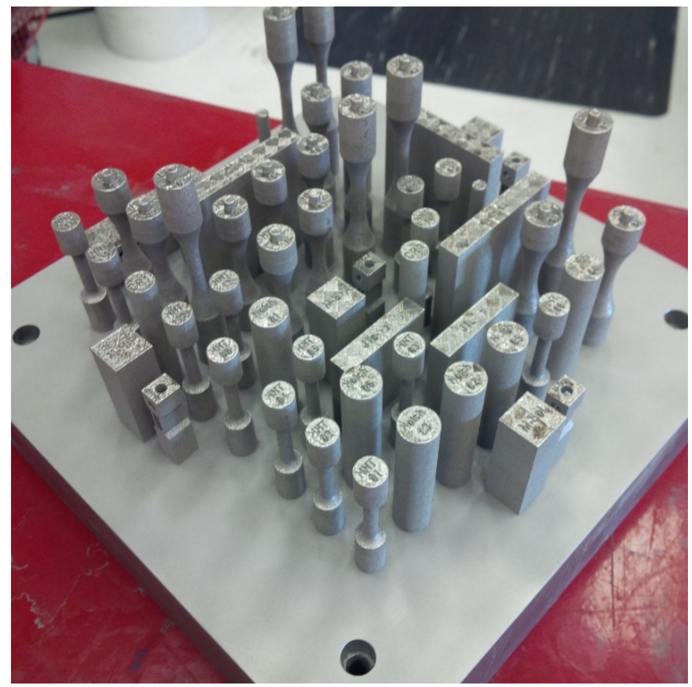

SLM 718 Post-Processing

- Stress Relief: 1065°C for 1.5 hours; furnace cool.
- HIP: 1165°C, 100 MPa, 3-4 hours
- Solution (AMS 5664): 1066°C for 1 hour; air cool.
- Age (AMS 5664): 760°C for 10 hours; furnace cool to 650°C; treat for total of 20 hours.

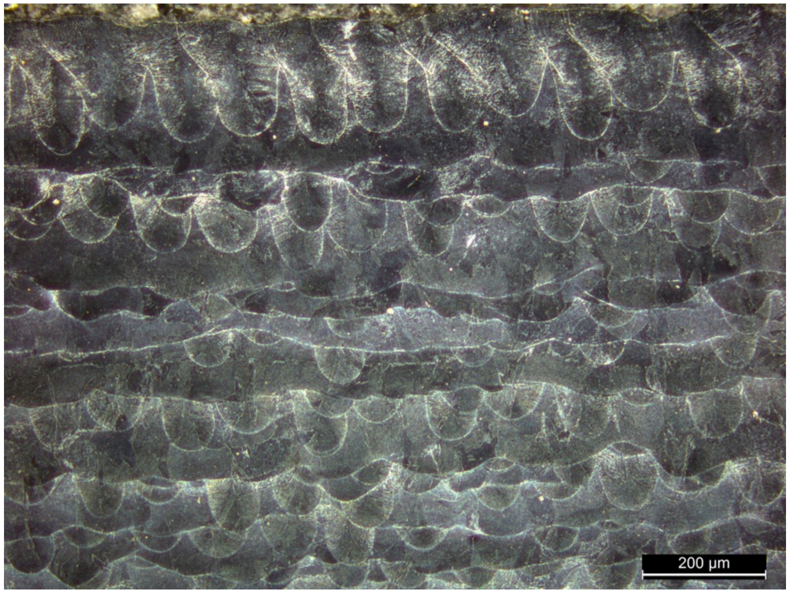

As-built microstructure

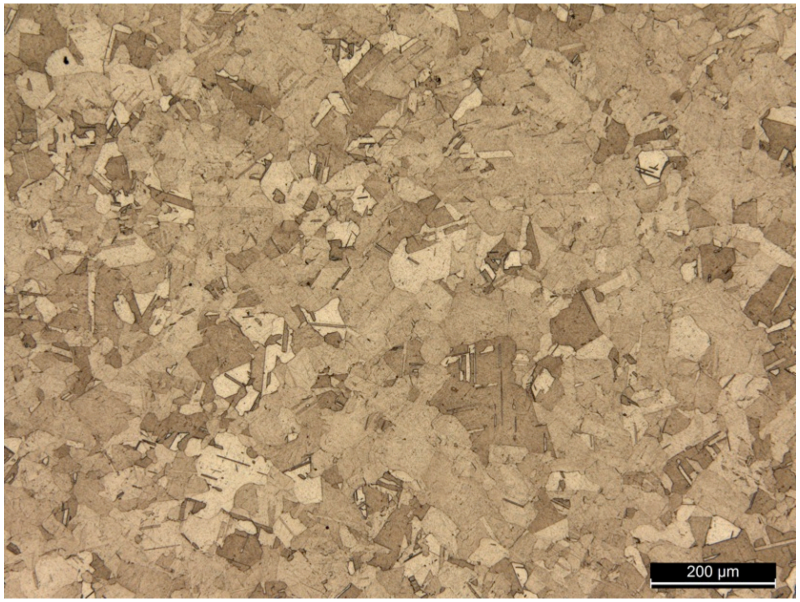

Heat treated microstructure

Typical Build Properties

- Typical tensile witness test curve for SLM 718.
  - Ultimate Tensile Strength: ~ 1380 MPa
  - Yield Strength: ~ 1170 MPa
  - Fracture Elongation: > 20%

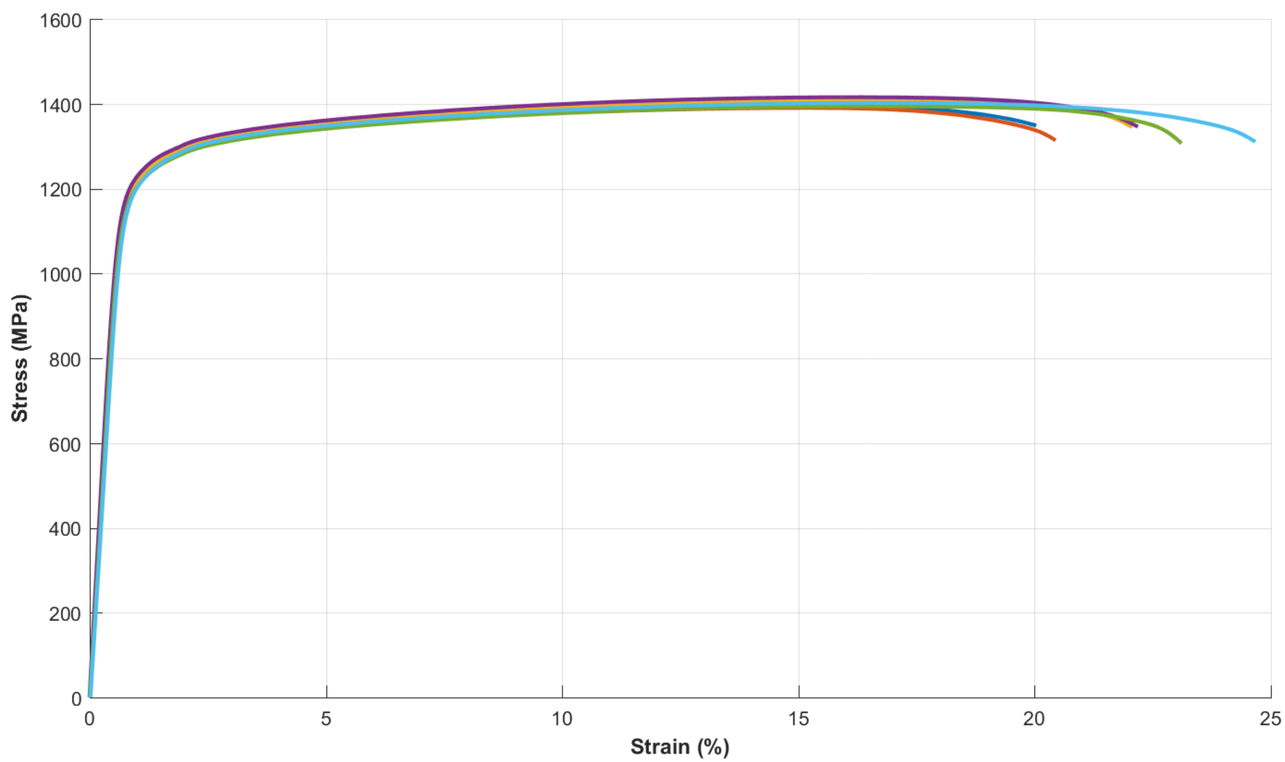

Defective Build

- A build of test specimens was produced; all indications were that the build was successful.
- Witness tensile testing revealed lower than expected material properties.

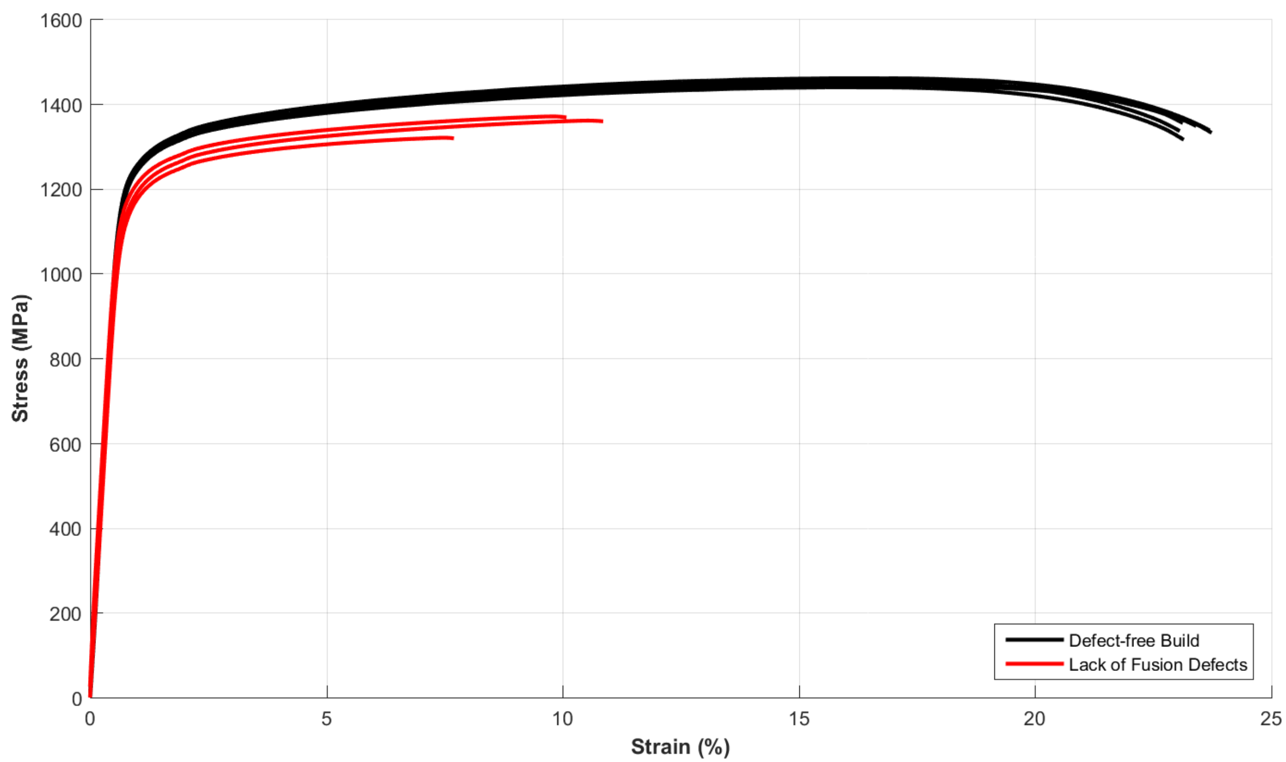

Defective Build

- Metallographic examination revealed lack of fusion defects in the material.
- Source was eventually determined to be a clogged ventilation duct that was allowing combustion by-products to settle on the powder bed.

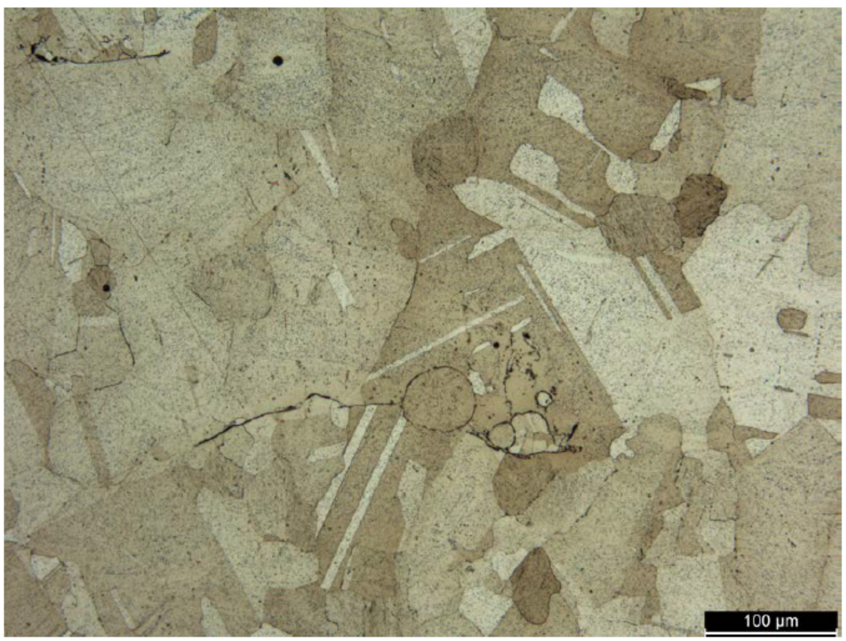

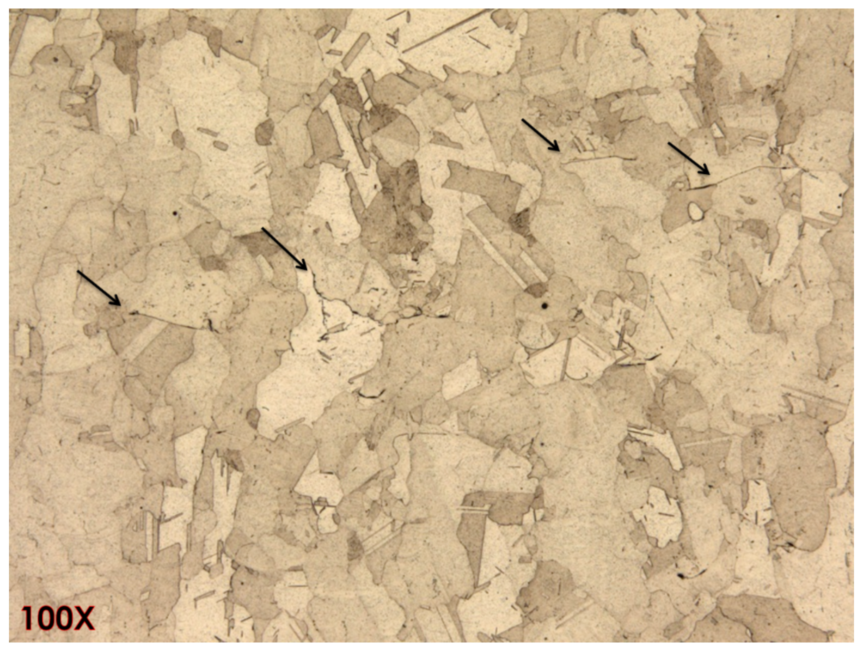

Low Cycle Fatigue of SLM 718

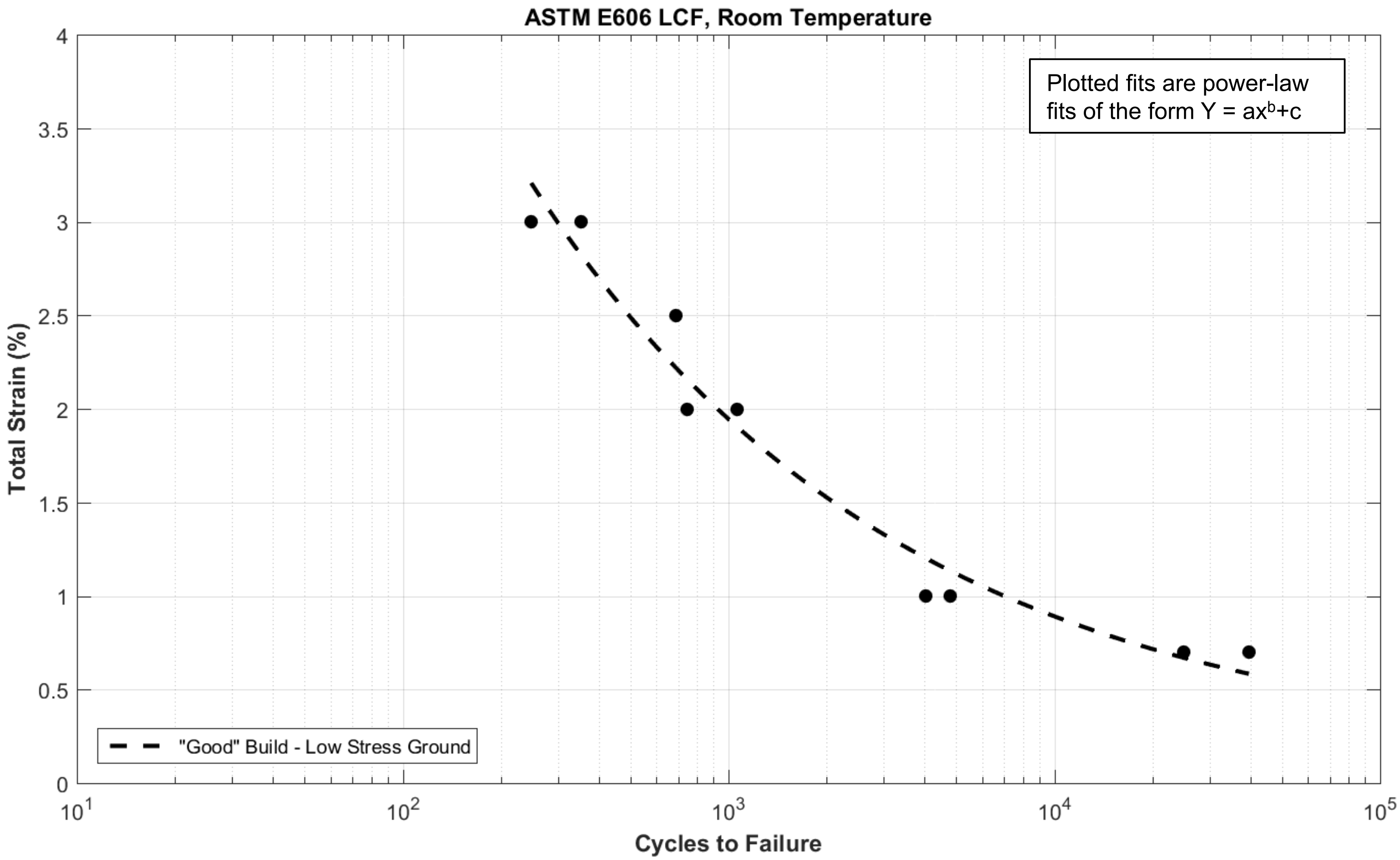

- “Reference” data – Low Stress Ground, R = -1, Defect-free build

Low Cycle Fatigue of SLM 718

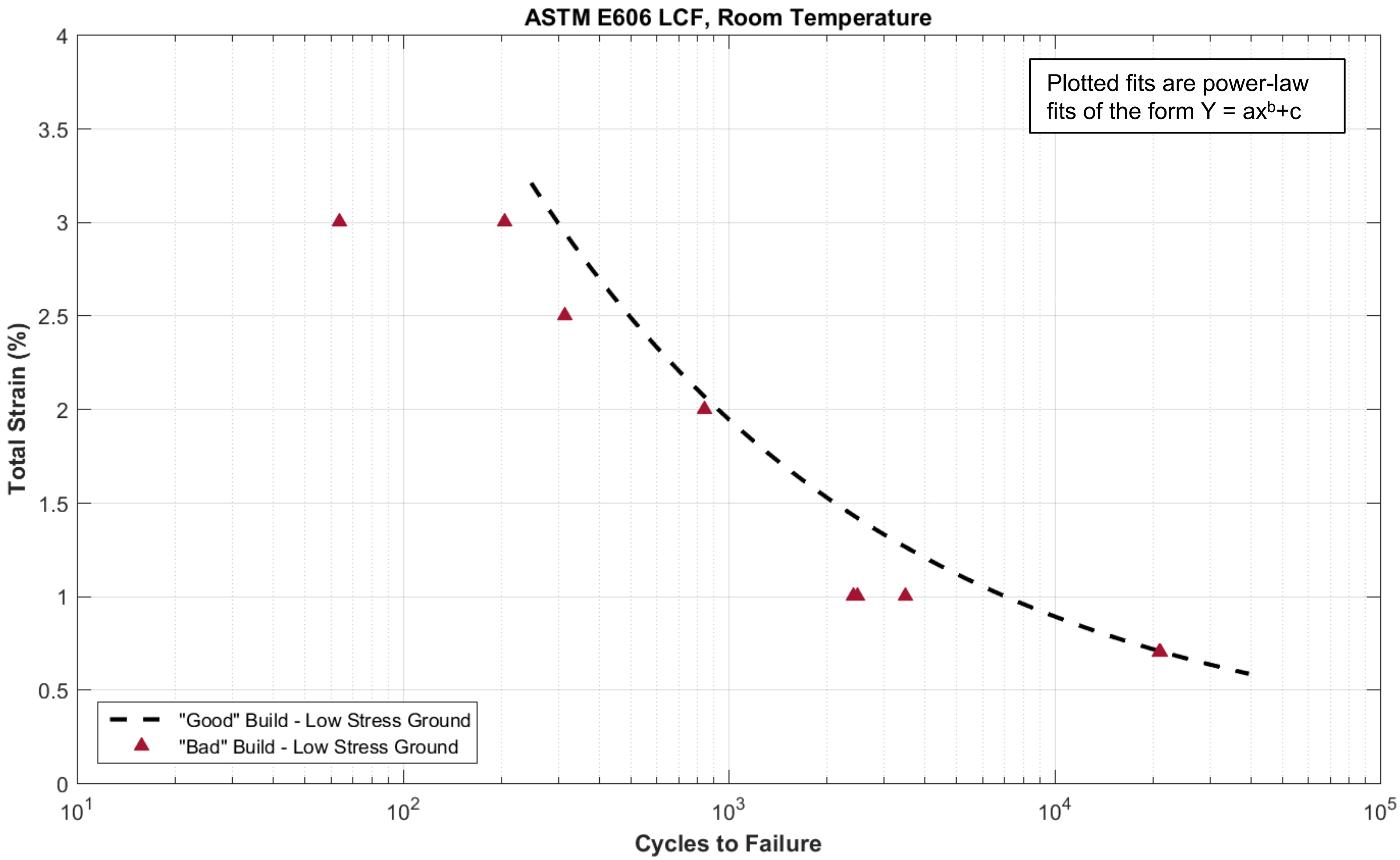

- Compare to build with defects – slightly lower fatigue life

Low Cycle Fatigue of SLM 718

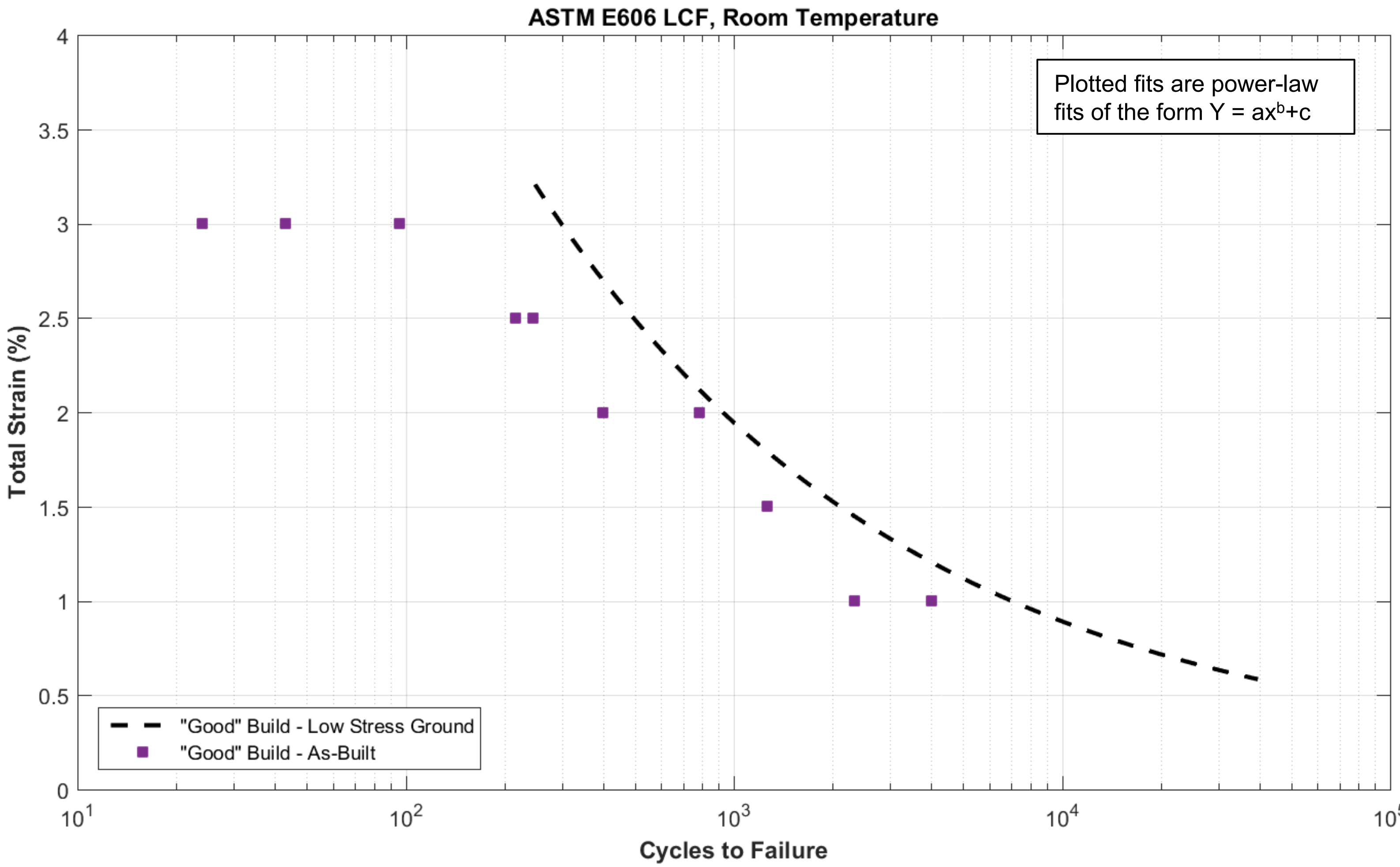

- Defect-free build with as-built surface finish; fatigue life even lower

Low Cycle Fatigue of SLM 718

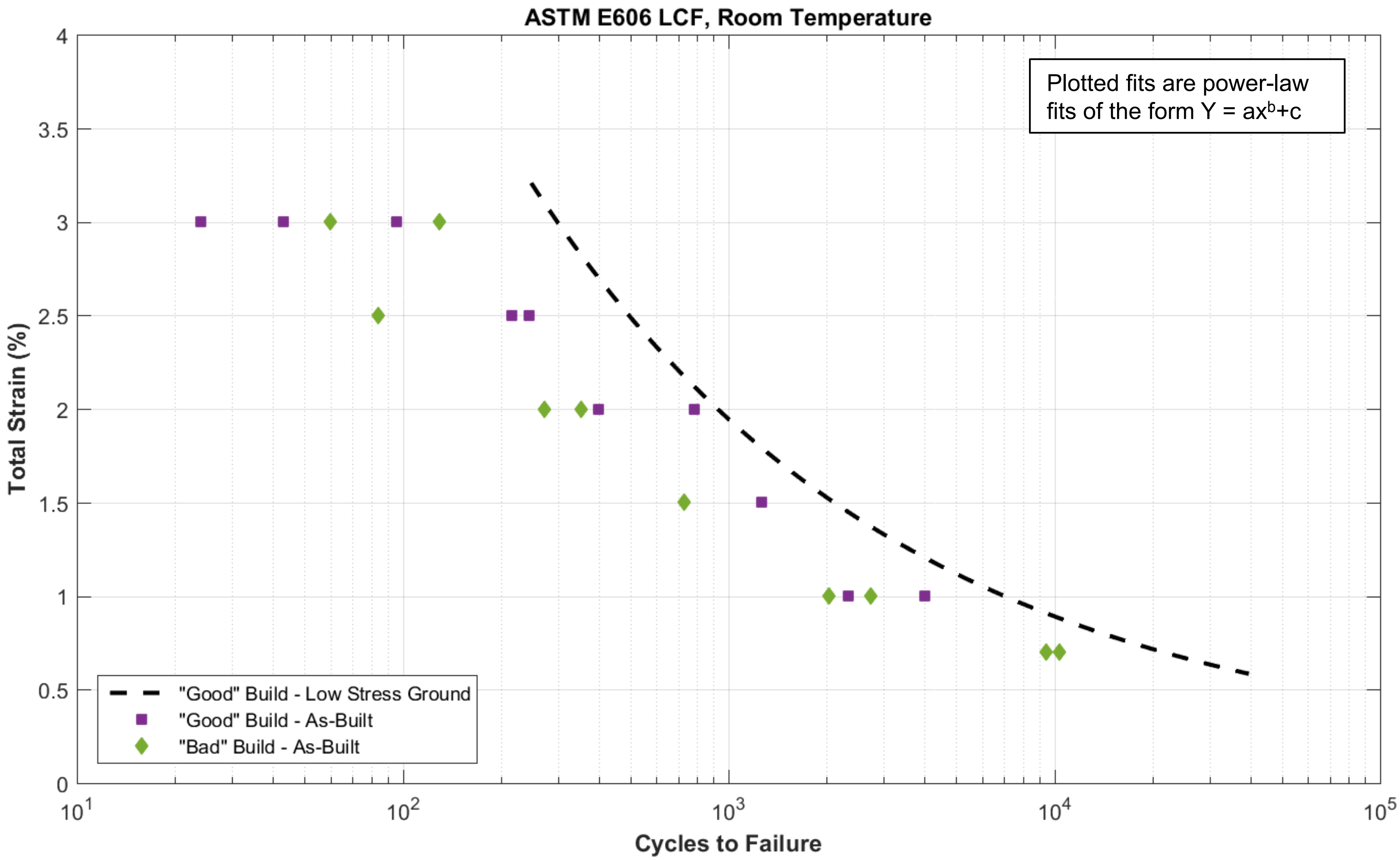

- As-built surface finish, with defects; surface finish has more effect than internal defects.

High Cycle Fatigue of SLM 718

- Key Variables
  - Orientation
    - Z – loading axis perpendicular to powder bed plane.
    - XY – loading axis parallel to powder bed plane.
    - 45° – loading axis 45° from powder bed plane.
  - Surface Finish
    - Low Stress Ground – ASTM E466 finishing procedure
    - As-Built – Surface finish from the SLM machine
  - Temperature
    - Room Temperature (RT) – nominal lab conditions, 70-75°F
    - Liquid Nitrogen (-320°F)

High Cycle Fatigue of SLM 718

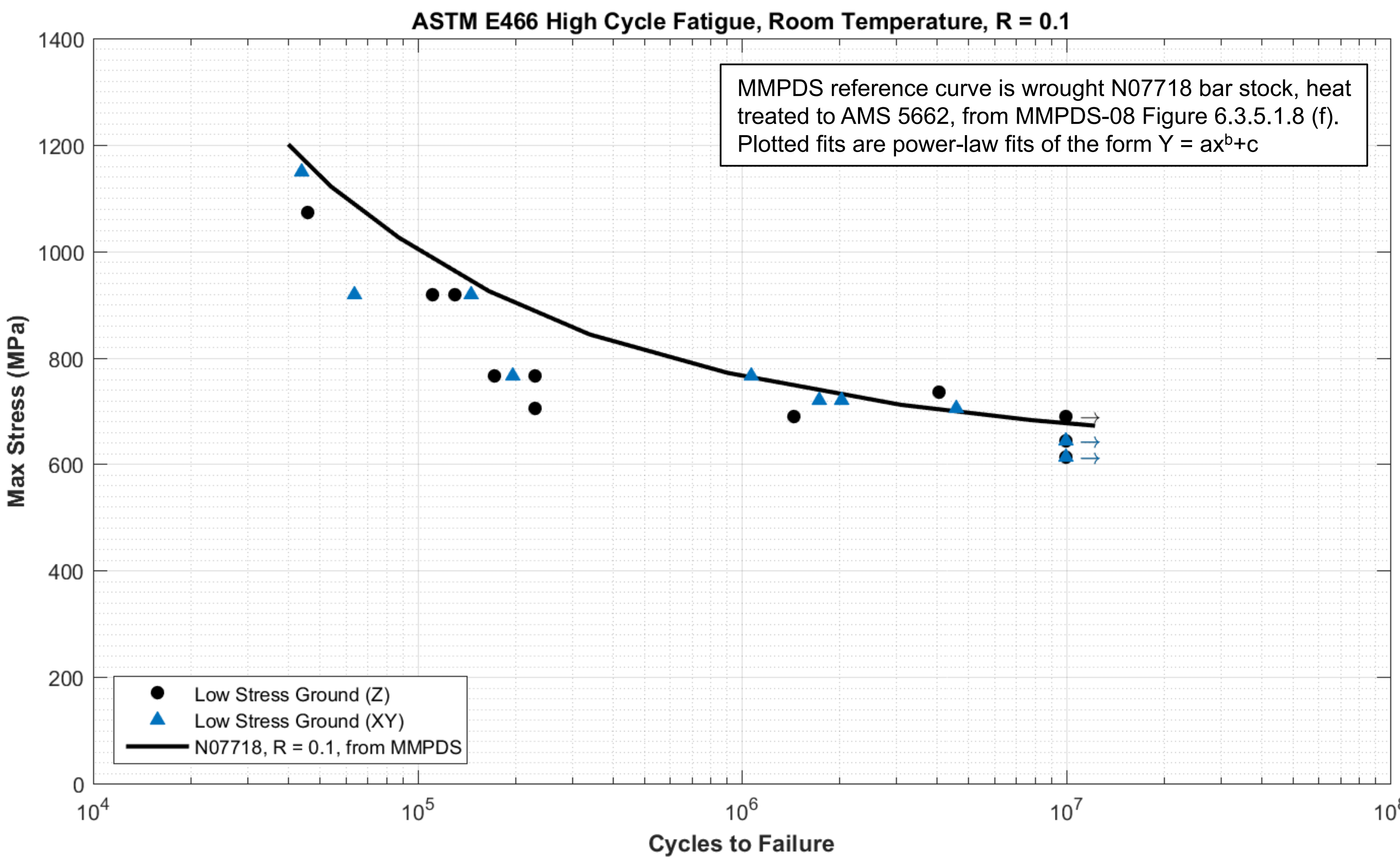

- Low stress ground; minimal effect from orientation

High Cycle Fatigue of SLM 718

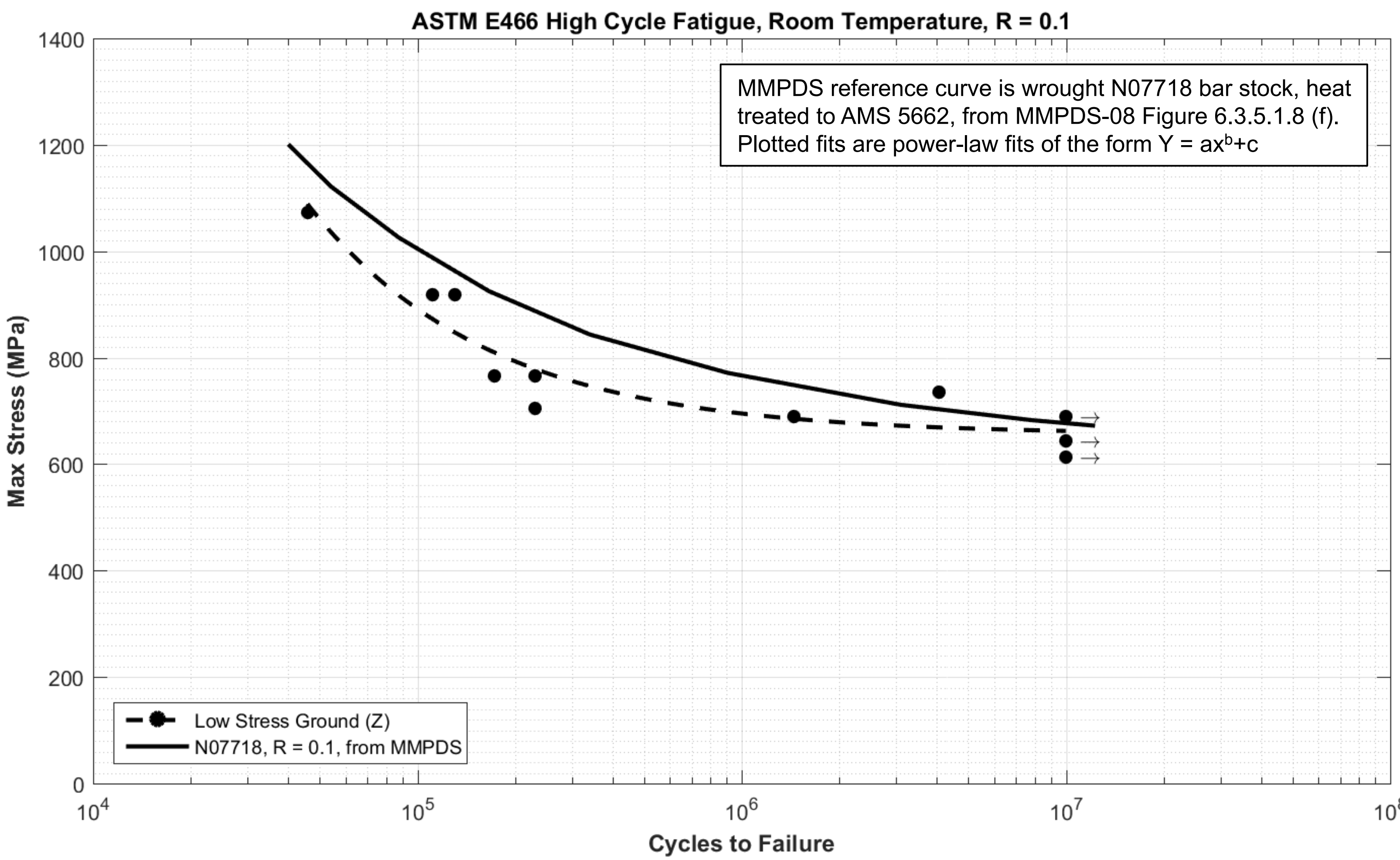

- “Reference” data – Low Stress Ground, Room Temperature, R = 0.1

High Cycle Fatigue of SLM 718

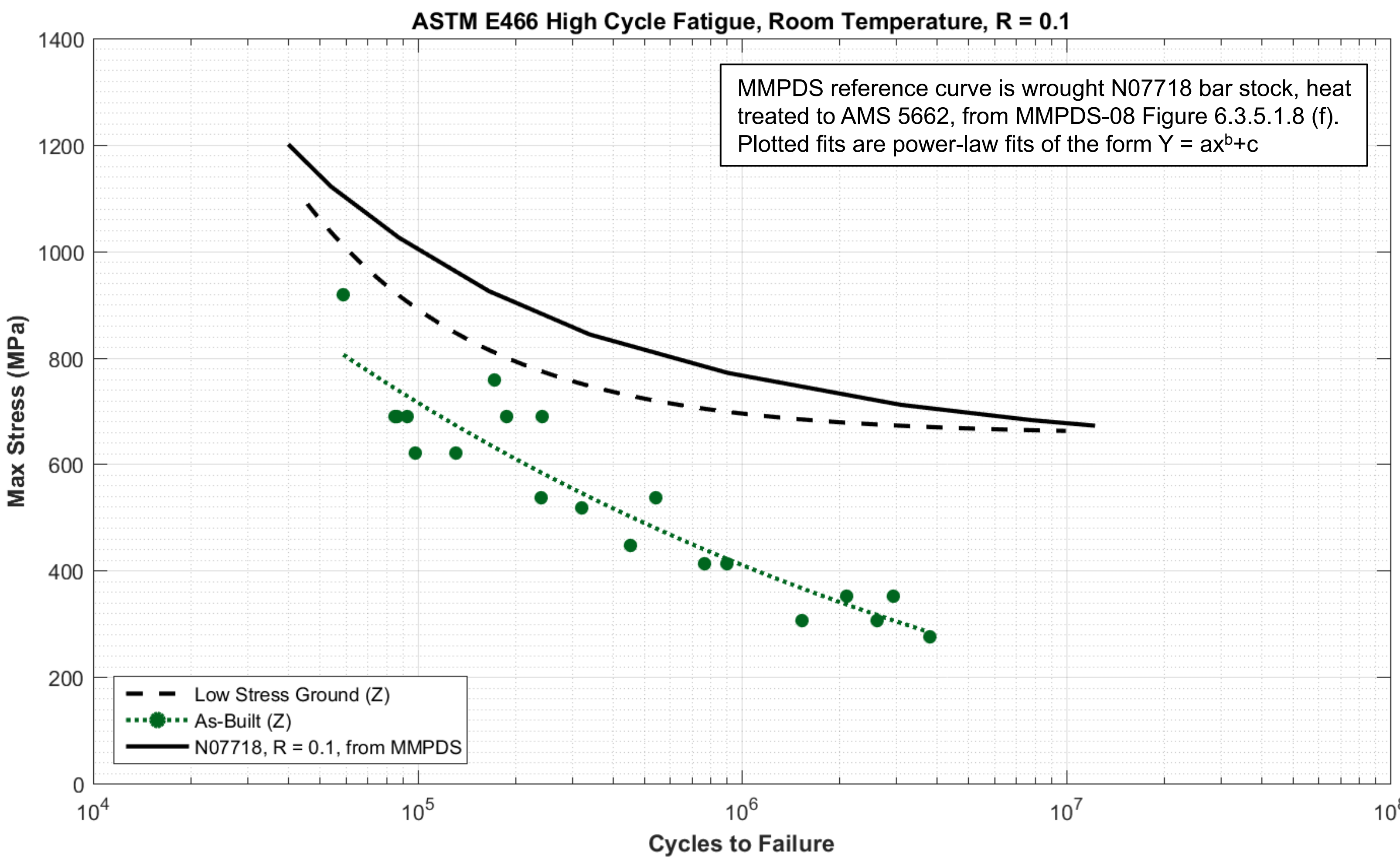

- Z-oriented, As-built surface finish; decreased fatigue life

High Cycle Fatigue of SLM 718

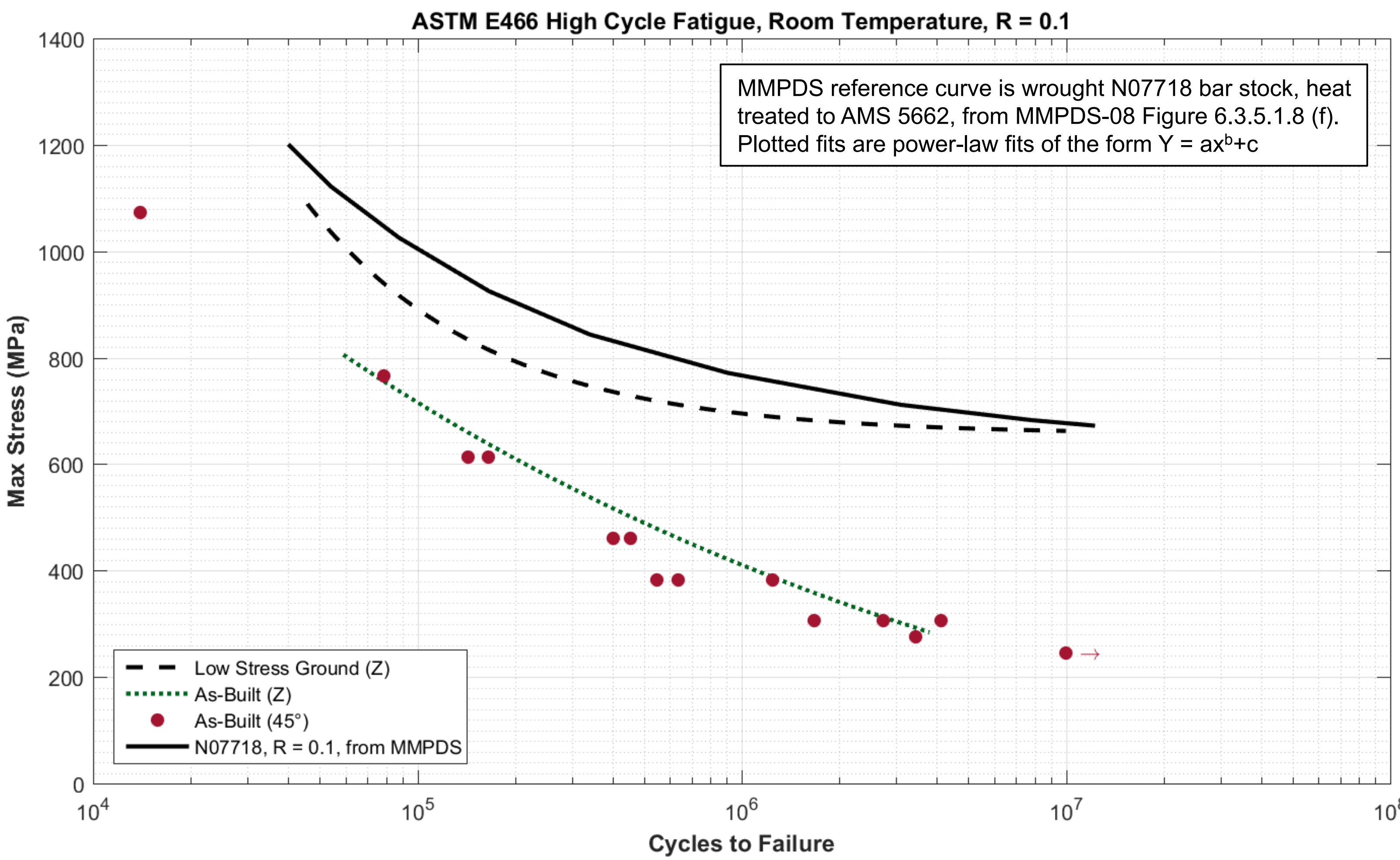

- 45°-oriented, As-built surface finish; similar fatigue life, 45° tend to be rougher than Z

High Cycle Fatigue of SLM 718

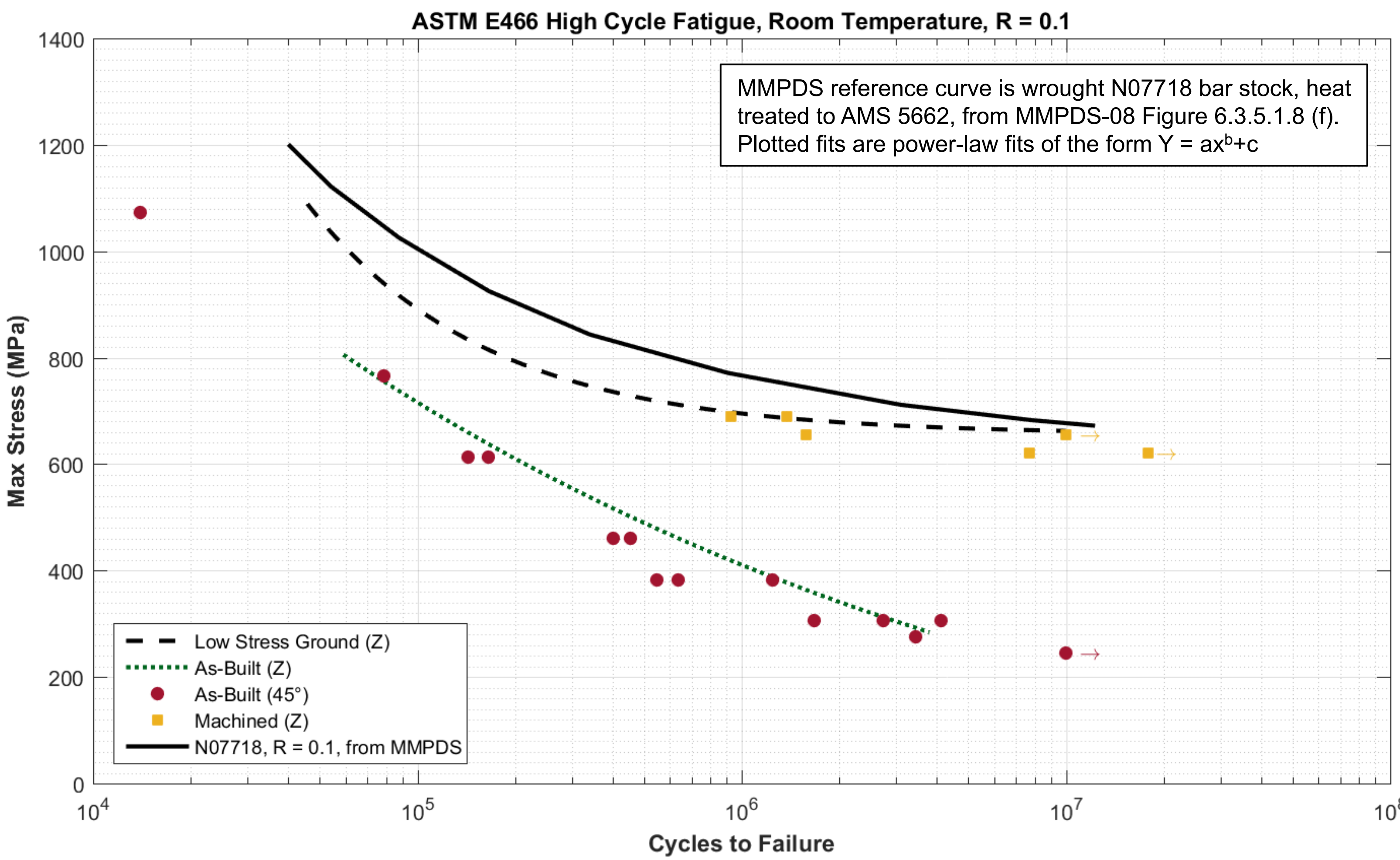

- Z-oriented, lathe-turned surface finish; quicker machining turnaround, slight decrease in life from low stress ground.

High Cycle Fatigue of SLM 718

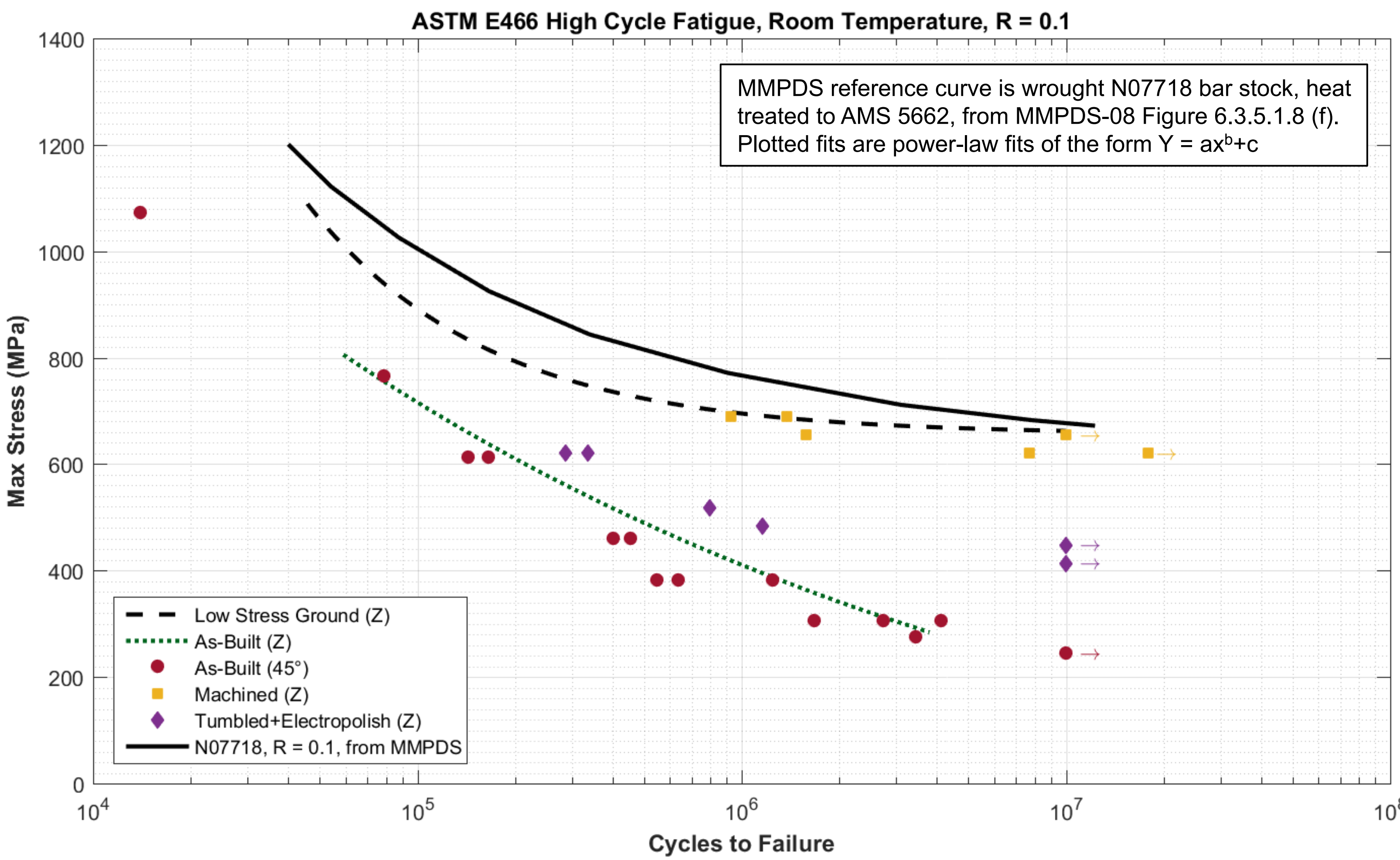

- Z-oriented, Tumbled then Electropolished; investigated for part finishing.

High Cycle Fatigue of SLM 718

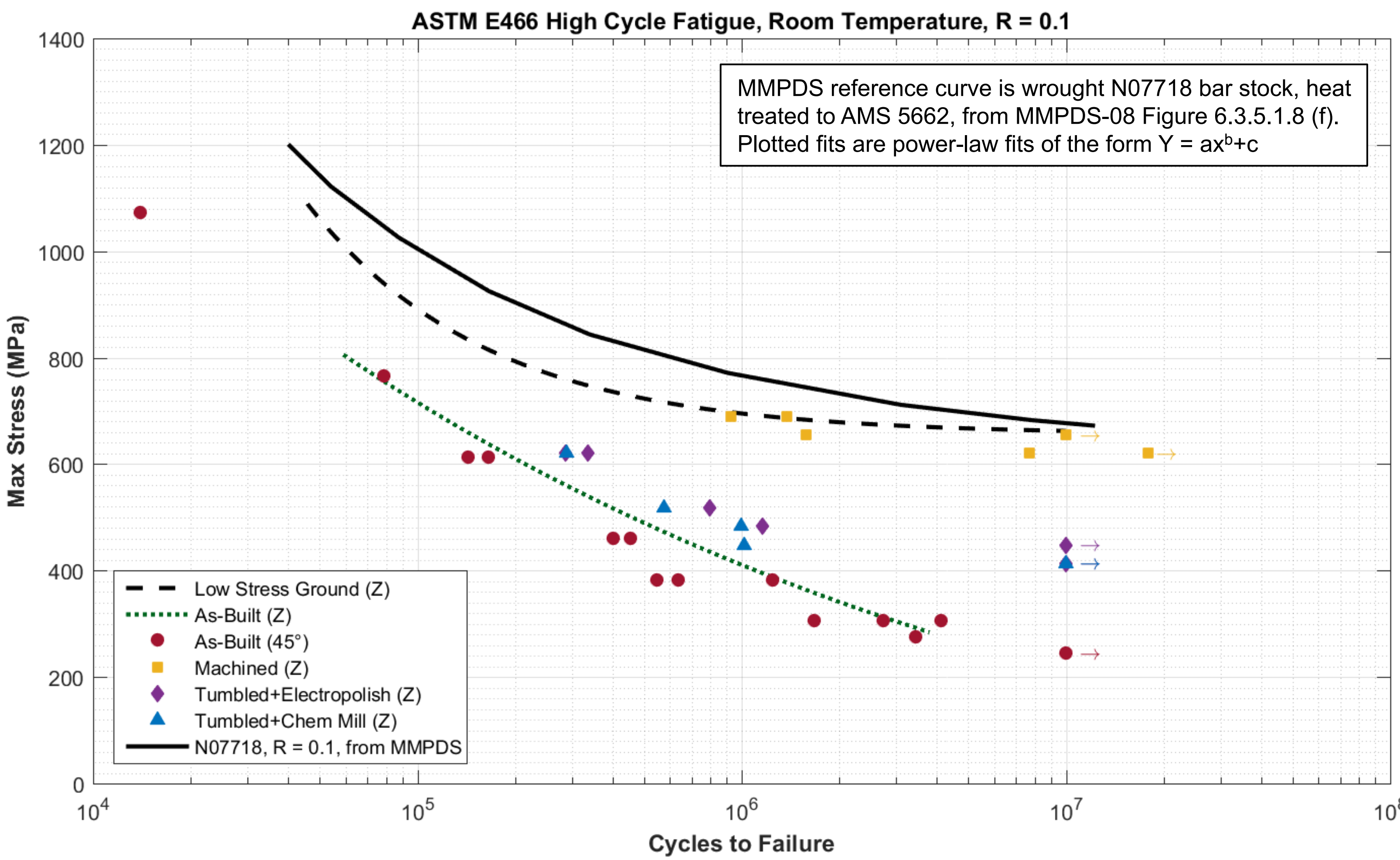

- Z Oriented, Tumbled then Chem Milled; investigated for part finishing.

High Cycle Fatigue of SLM 718

- Fatigue life decreases with increasing surface roughness.

Low stress ground

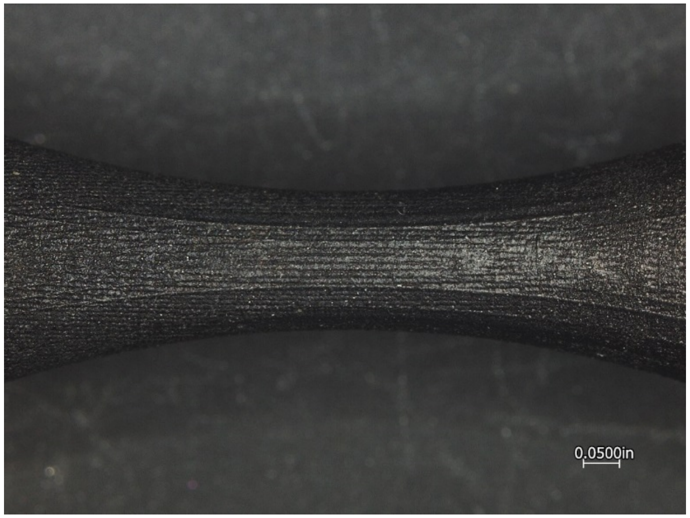

As-built

Tumbled & Electropolish

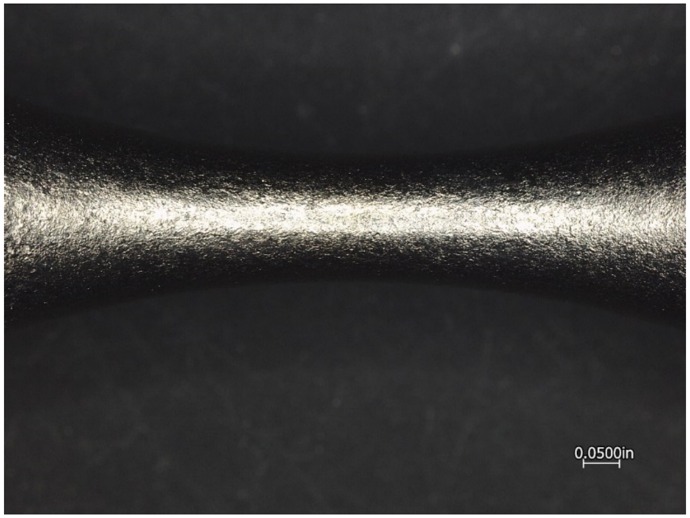

Tumbled & Chem Mill

High Cycle Fatigue of SLM 718

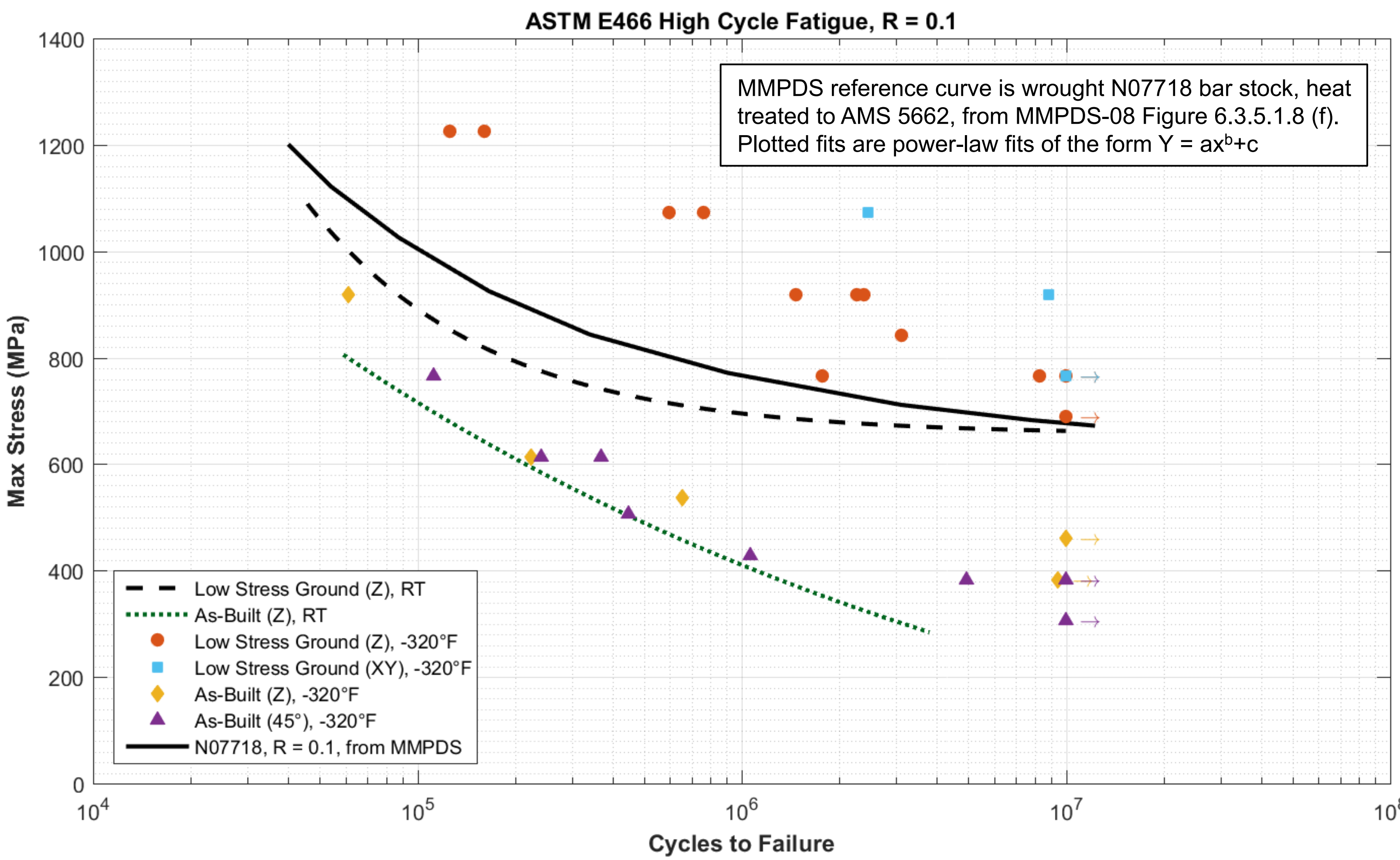

- Tests in LN_2 (-320°). Some increase in life for as-built surfaces; more increase for low stress ground.

Vendor Round Robin

- Identical builds were procured from three third-party SLM vendors; one build was provided by MSFC.
- The specimens were heat treated per MSFC guidance, although allowances were made for vendors with existing mature processes.
- A series of comparison testing was of the material.

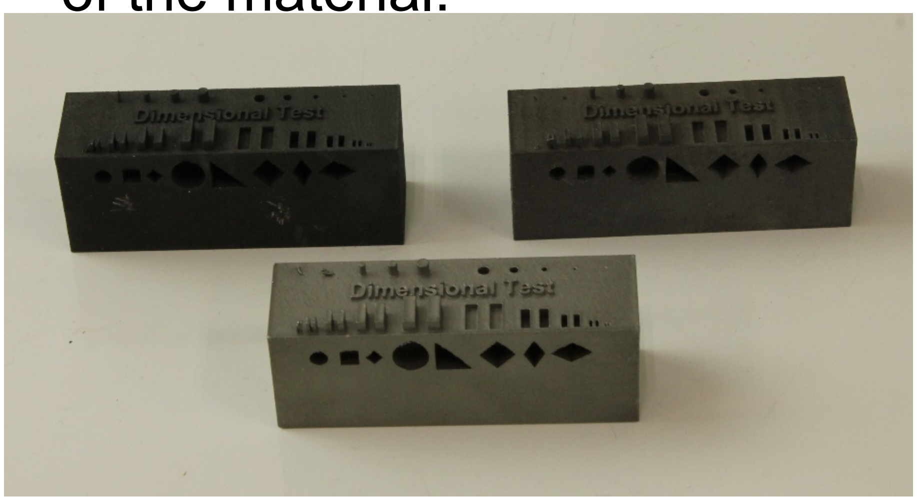

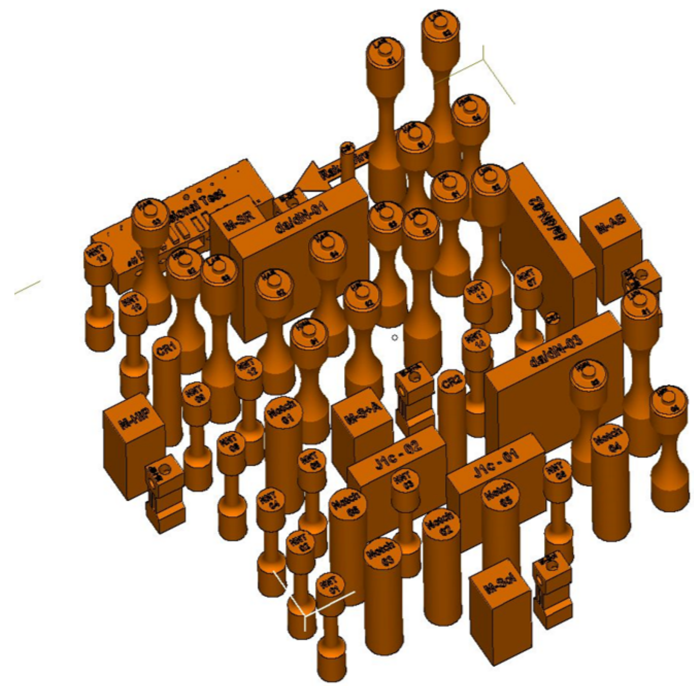

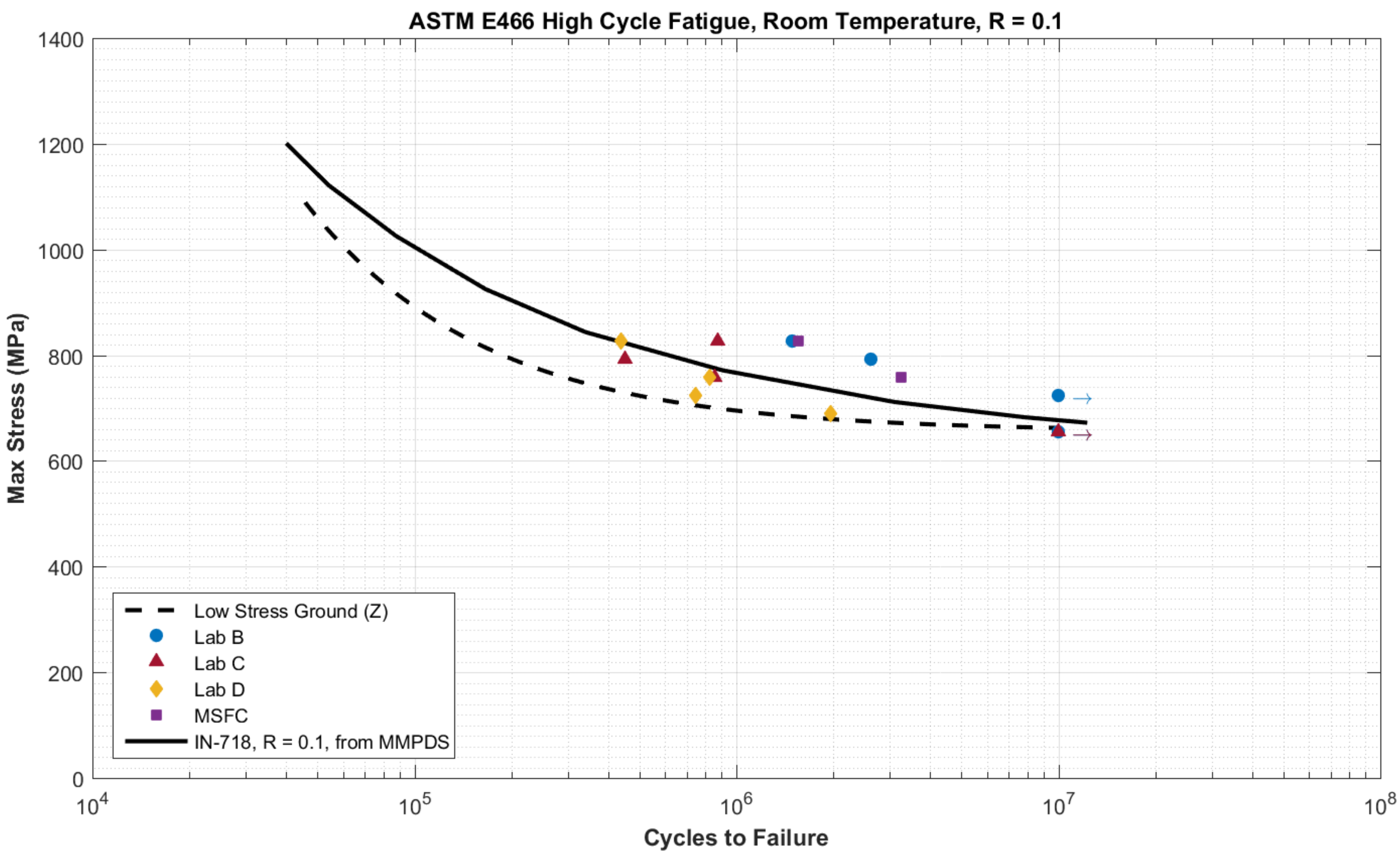

- Z-oriented, low stress ground surface finish; compared to M1 and wrought reference curves

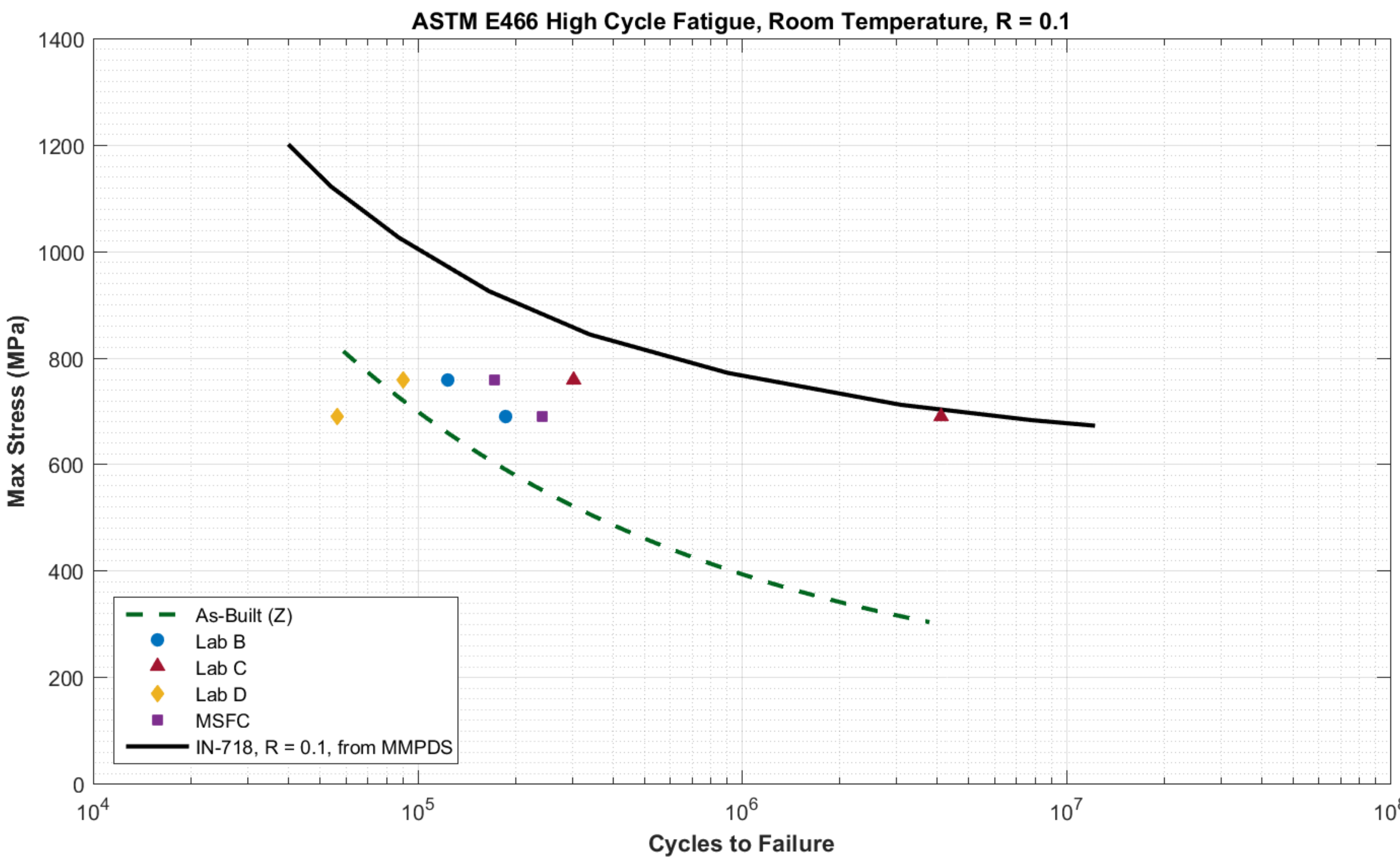

- Z-oriented, "as-provided" surface finish; compared to M1 and wrought reference curves

Fatigue Crack Growth Results

- Round Robin Results
  - 3 specimens from each build
  - Z-XY test orientation
  - Post-processing same as fatigue specimens
- Testing Methodology
  - Tested according to ASTM E647
    - “Standard Test Method for Measurement of Fatigue Crack Growth Rates”
  - R = 0.1 and R = 0.7 data shown
  - Compression pre-cracking procedure (CPC)

Compression Pre-Cracking

- Compression-compression loading used to generate a crack at the notch root of a c(T) specimen.
- May produce more conservative threshold and near-threshold crack growth rates.
- Following CPC procedure detailed by Newman and Yamada.

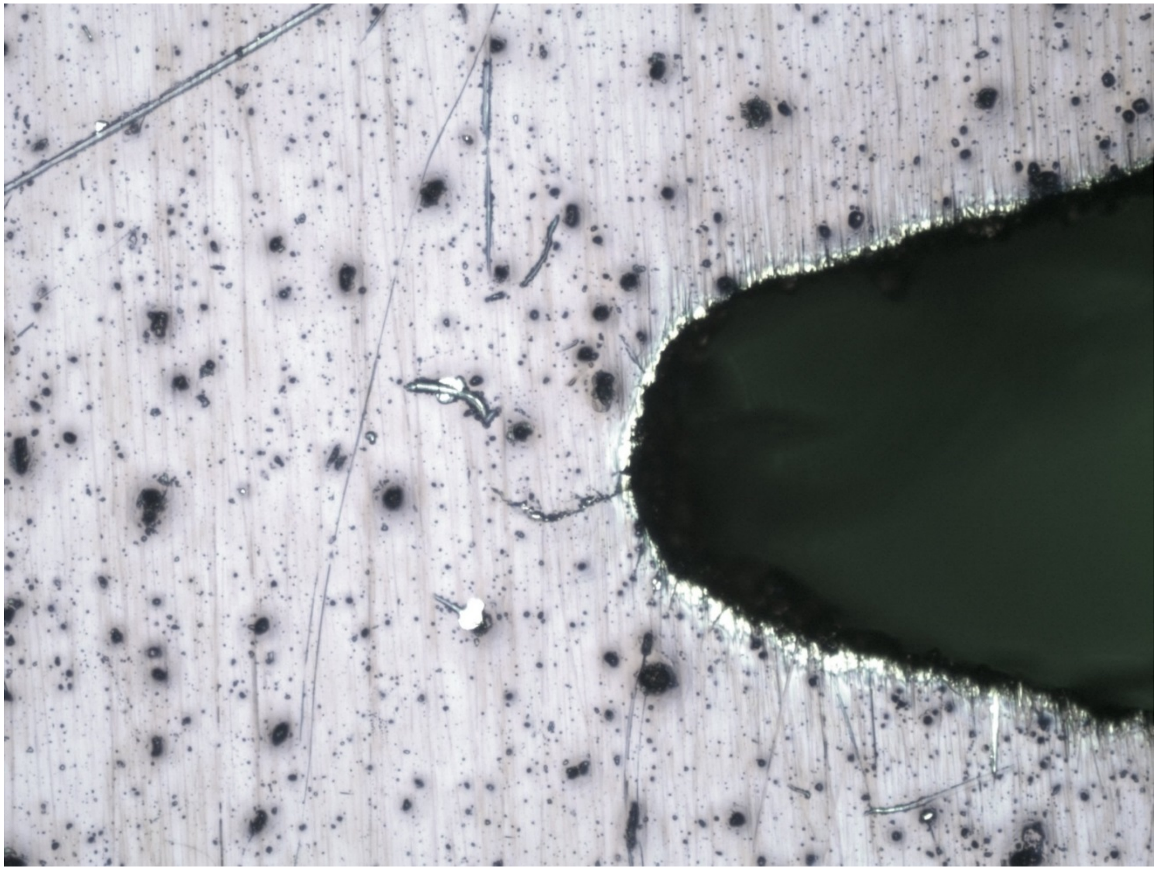

Fatigue Crack Growth

- Wrought Inconel-718 alloy obtained from Boeing-Rockwell. Tested using the ASTM LR test method and CA loading.

- Garr KR, Boeing-Rocketdyne Propulsion and Power Company, private communication; 2004.

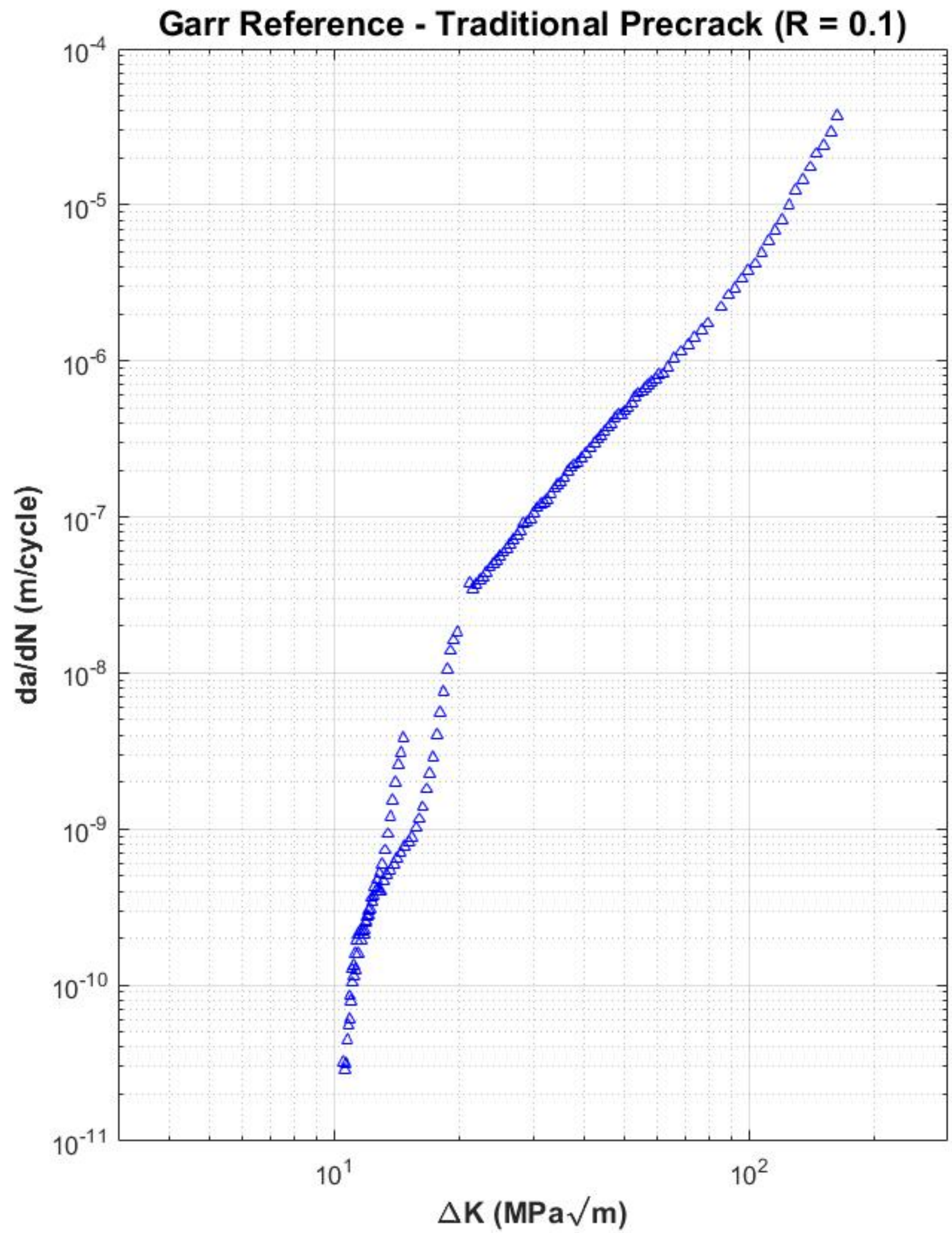

Fatigue Crack Growth

- Wrought Inconel-718 alloy obtained from Boeing-Rockwell. Tested using the CPLR test method and CA loading.

- Newman, J.C., Jr. and Yamada, Y., "Compression Precracking Methods to Generate Near-Threshold Fatigue-Crack-Growth-Rate Data", International Journal of Fatigue, Vol. 32, 2010, p.879-885.

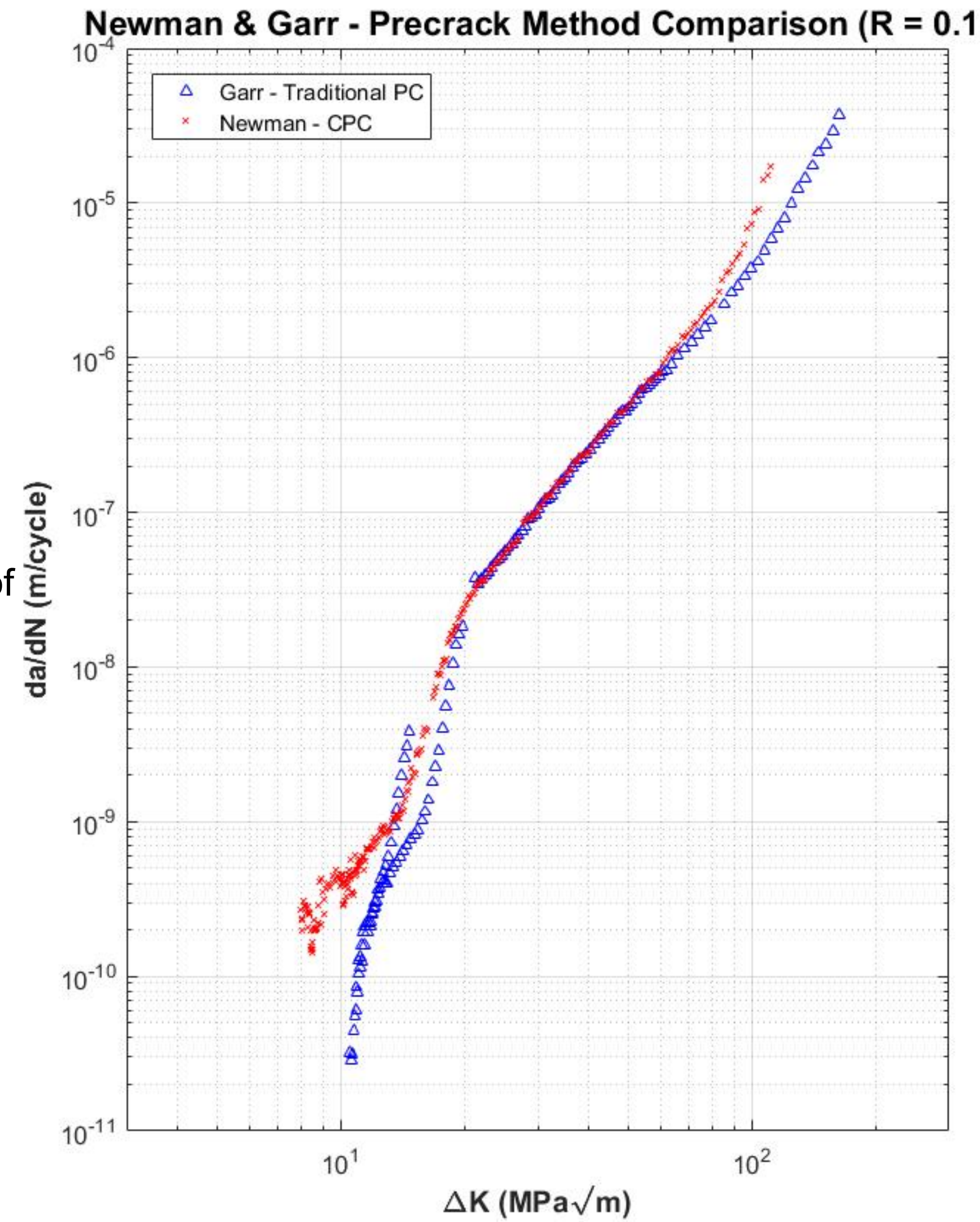

Fatigue Crack Growth

- SLM 718 M1 Machine included as a reference. This data is not part of the Round-Robin.
- Produced using ASTM LR and CA loading.

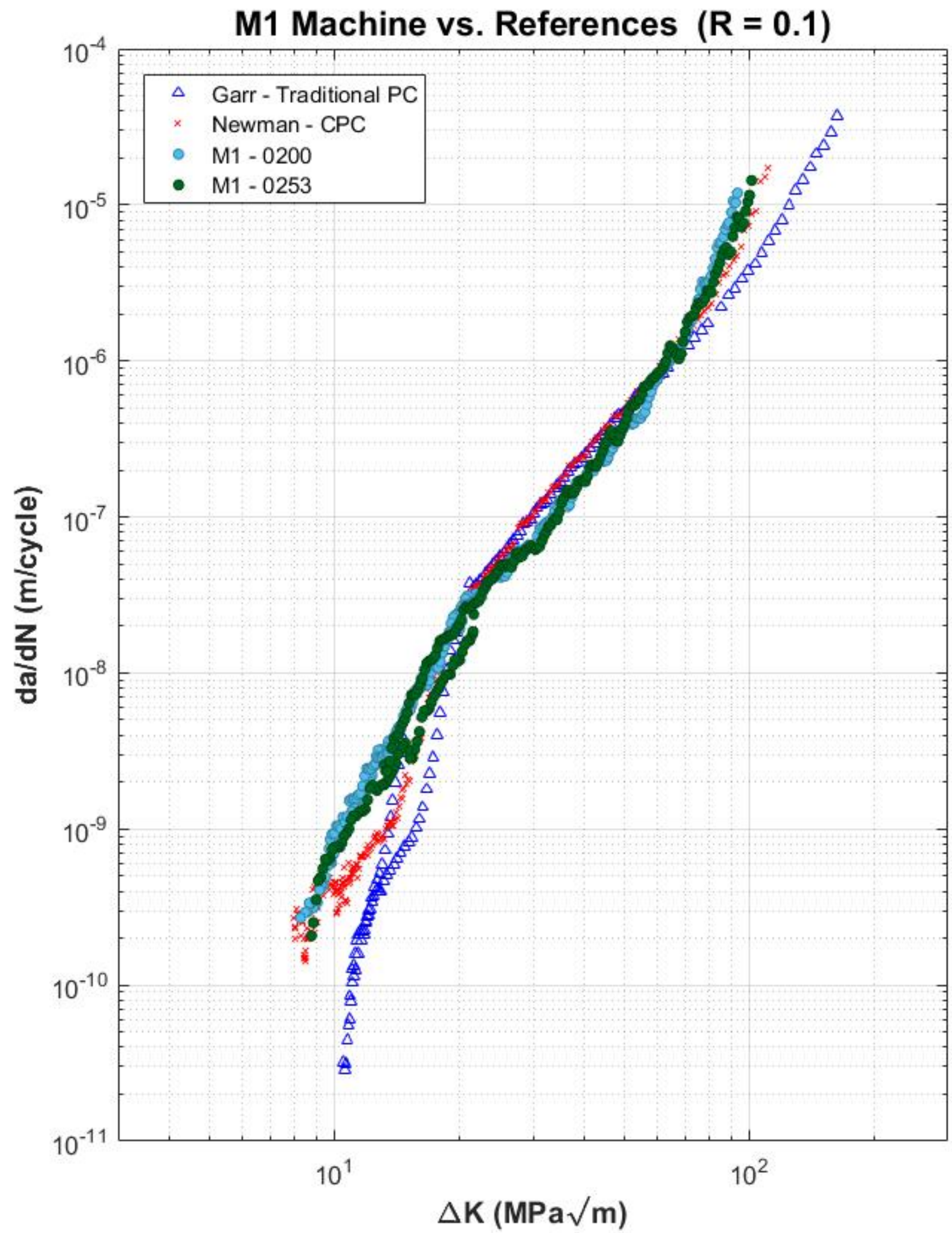

Fatigue Crack Growth

- MSFC Round-Robin data. Consistent with M1 data.

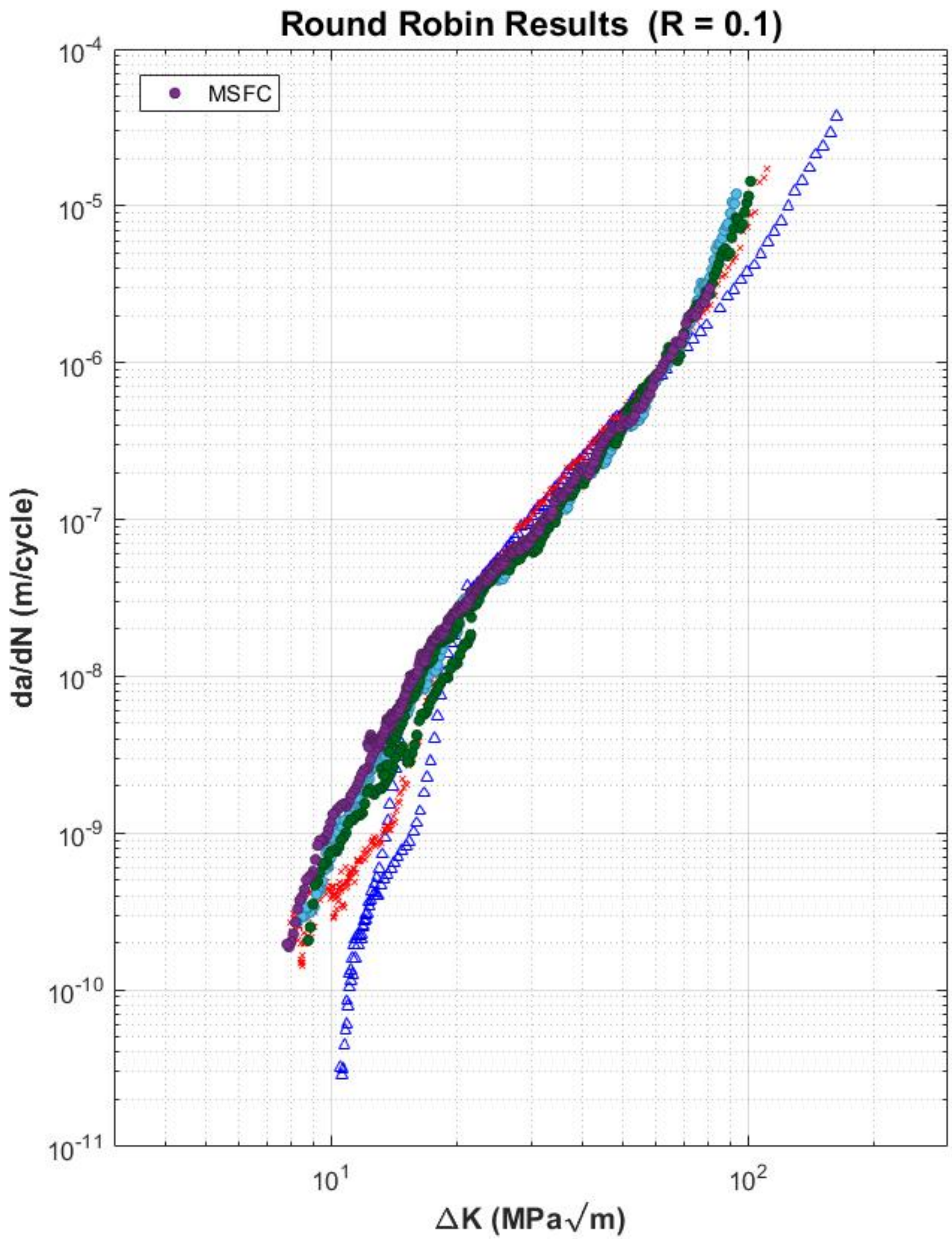

Fatigue Crack Growth

- Lab B - Higher observed growth rates than M1 data.

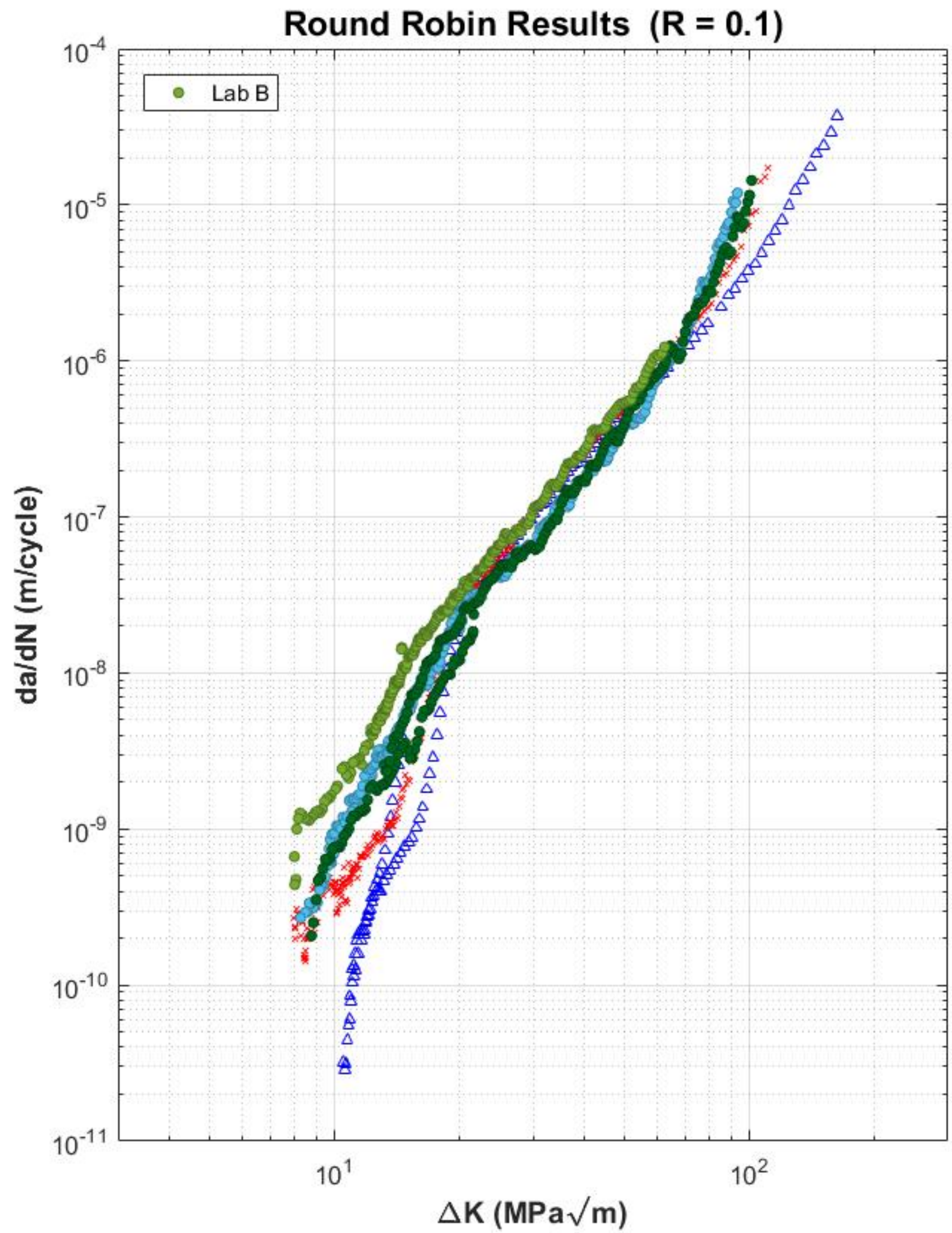

Fatigue Crack Growth

- Lab C - Consistent with M1 data.

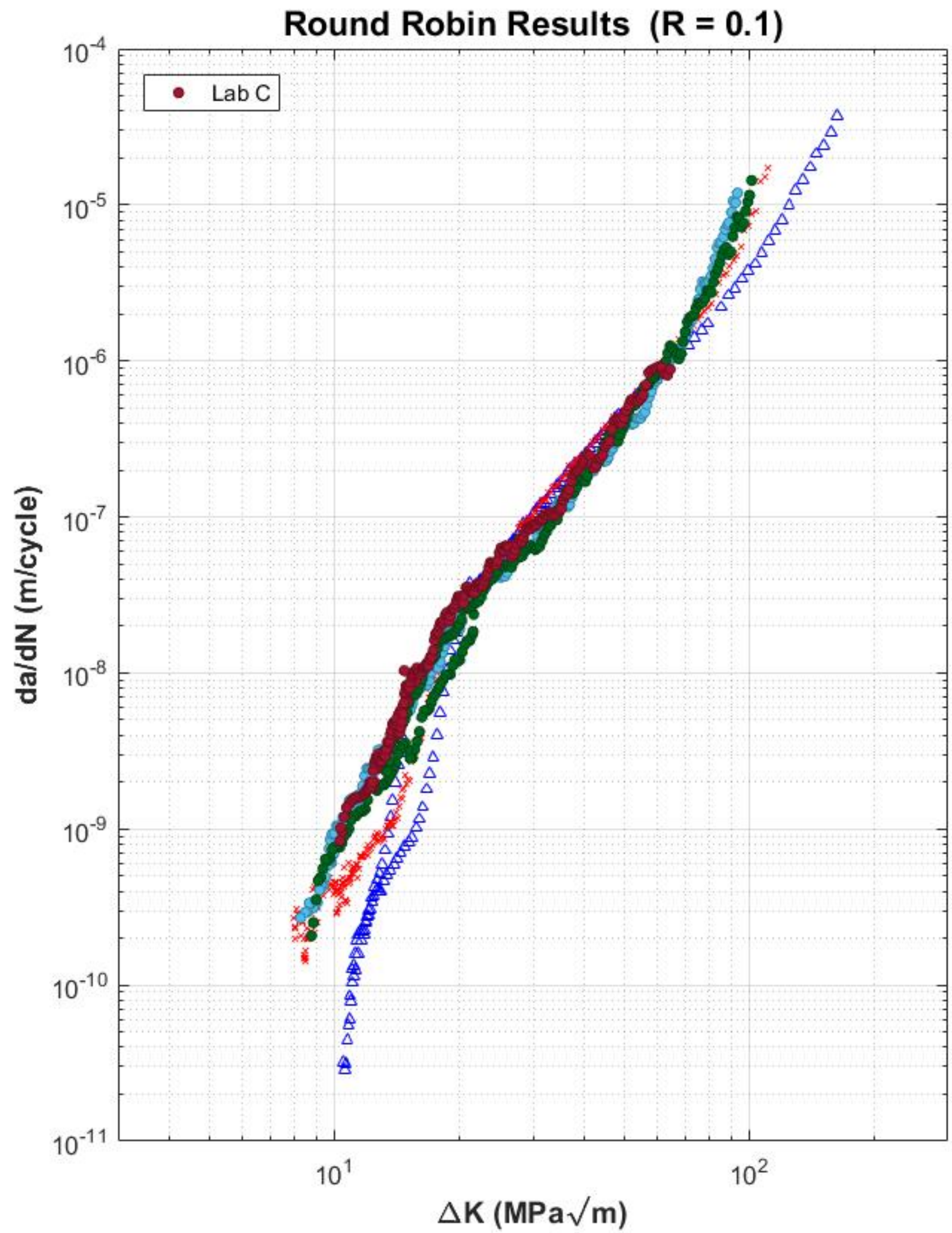

Fatigue Crack Growth

- Lab D - Consistent with M1 data. CPLR only.

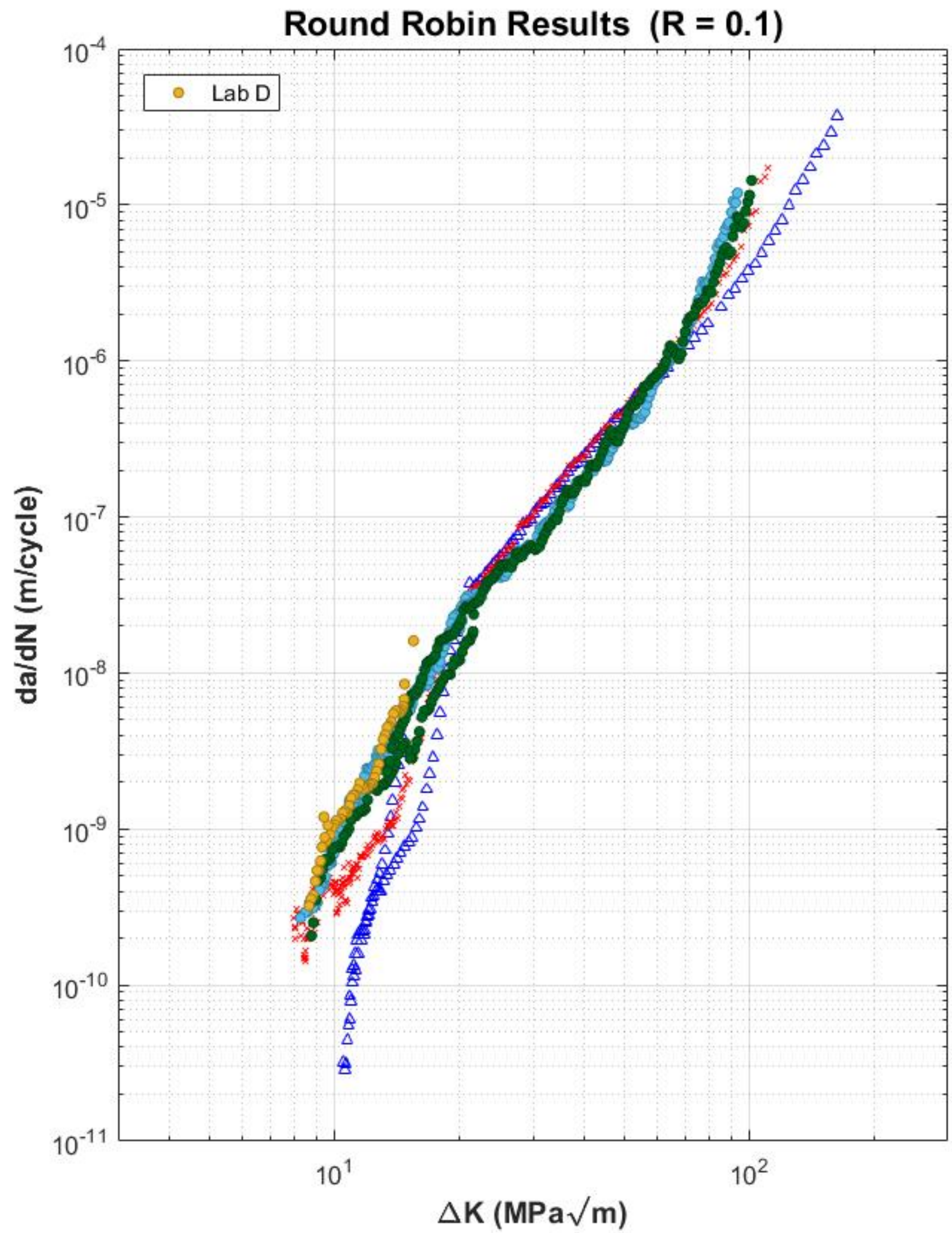

Fatigue Crack Growth

- Only Lab B had any distinction from the M1 data.

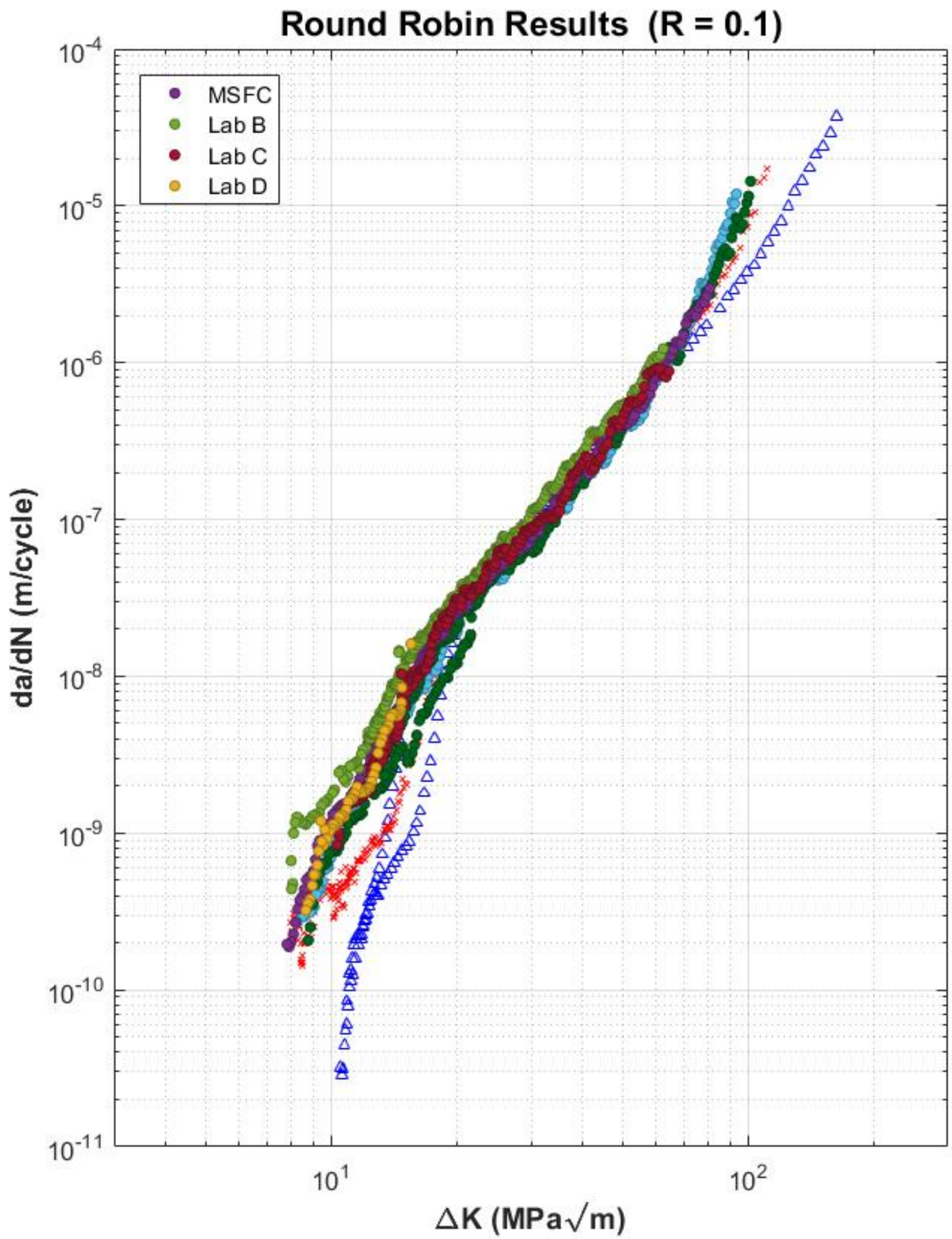

Fatigue Crack Growth

- Wrought Inconel-718 alloy obtained from Boeing-Rockwell. Tested using the ASTM LR test method and CA loading.

- Garr KR, Boeing-Rocketdyne Propulsion and Power Company, private communication; 2004.

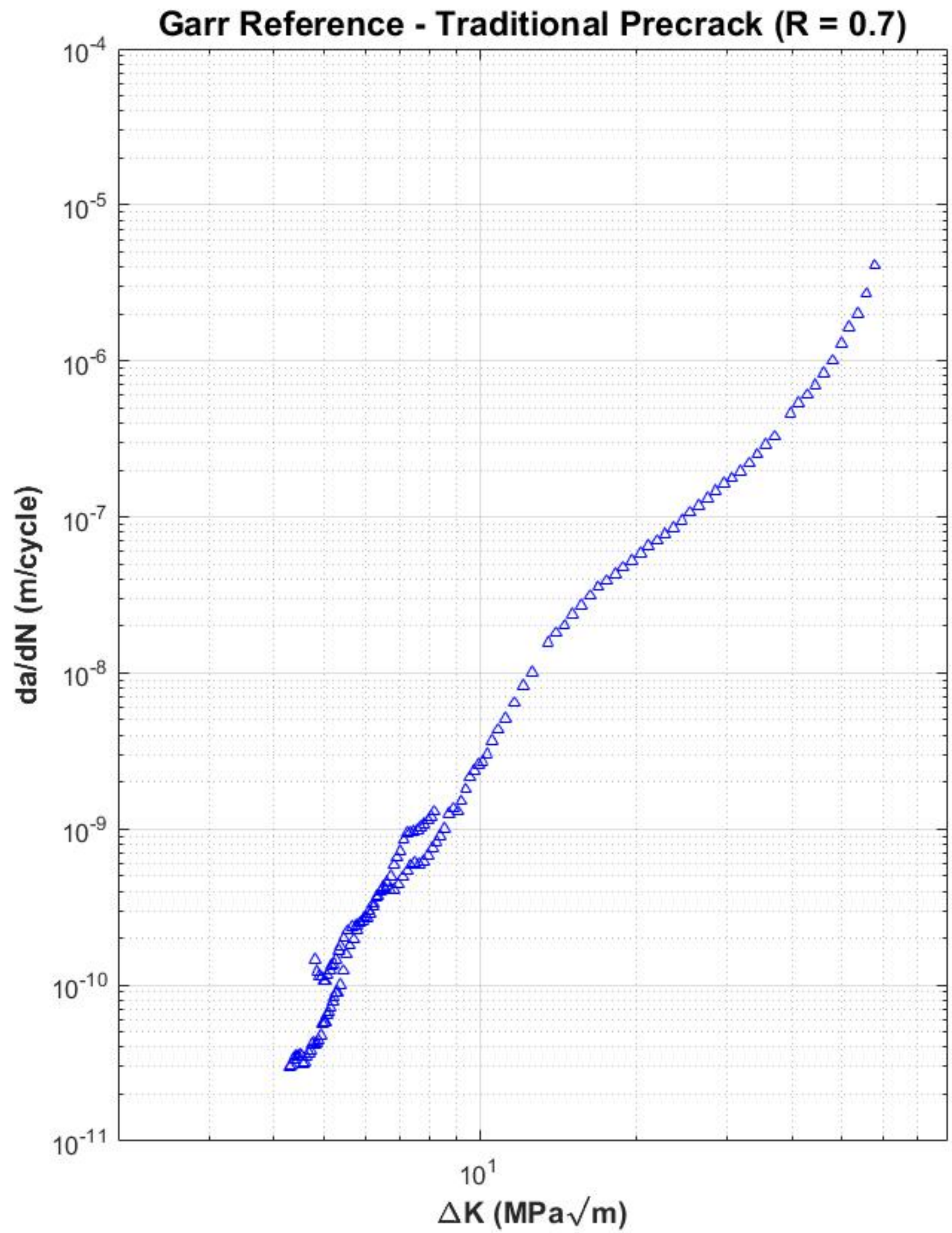

Fatigue Crack Growth

- Wrought Inconel-718 alloy obtained from Boeing-Rockwell. Tested using the CPLR test method and CA loading.

- Newman, J.C., Jr. and Yamada, Y., “Compression Precracking Methods to Generate Near-Threshold Fatigue-Crack-Growth-Rate Data”, International Journal of Fatigue, Vol. 32, 2010, p.879-885.

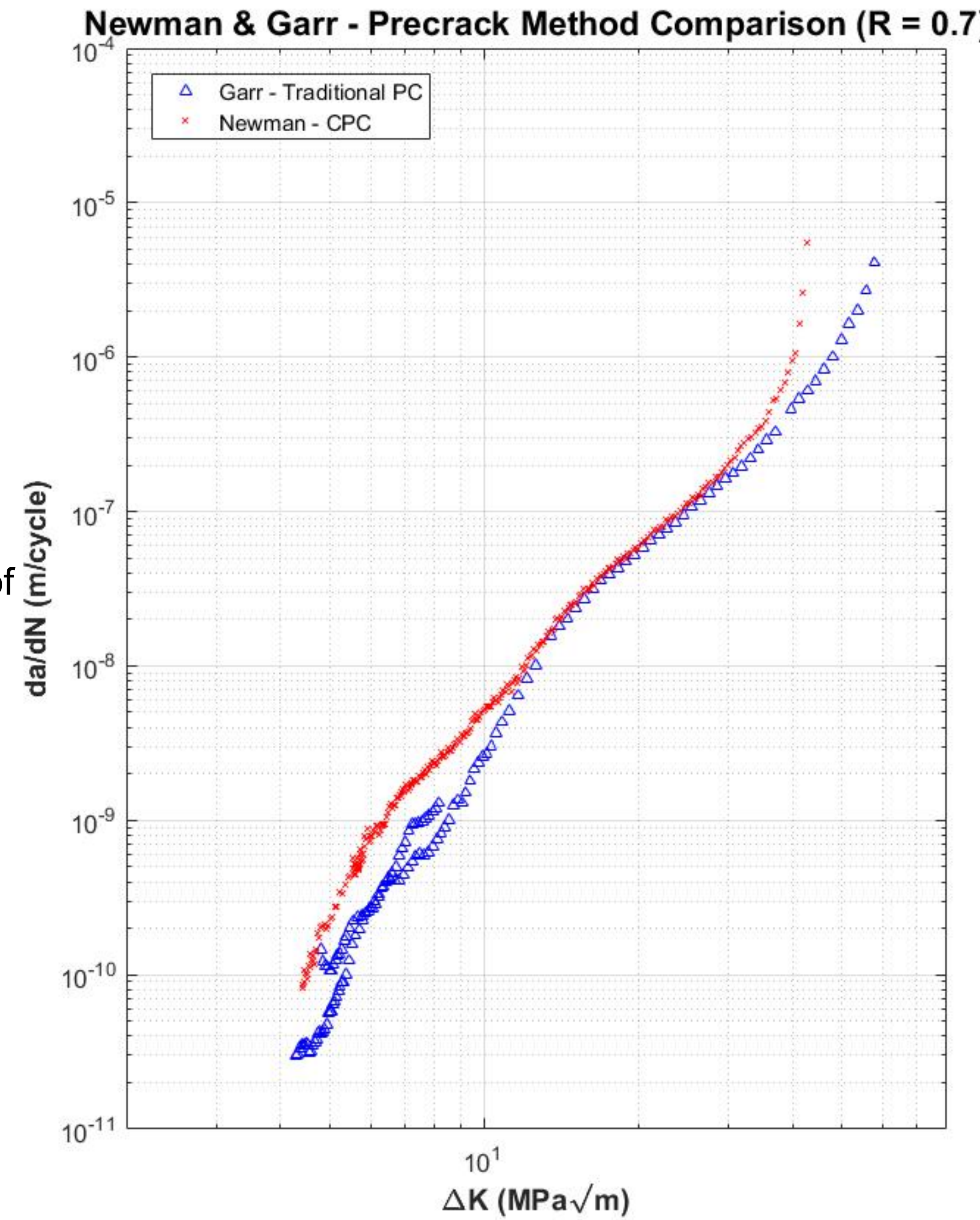

Fatigue Crack Growth

- Higher observed growth rates compared to wrought 718 near-threshold.

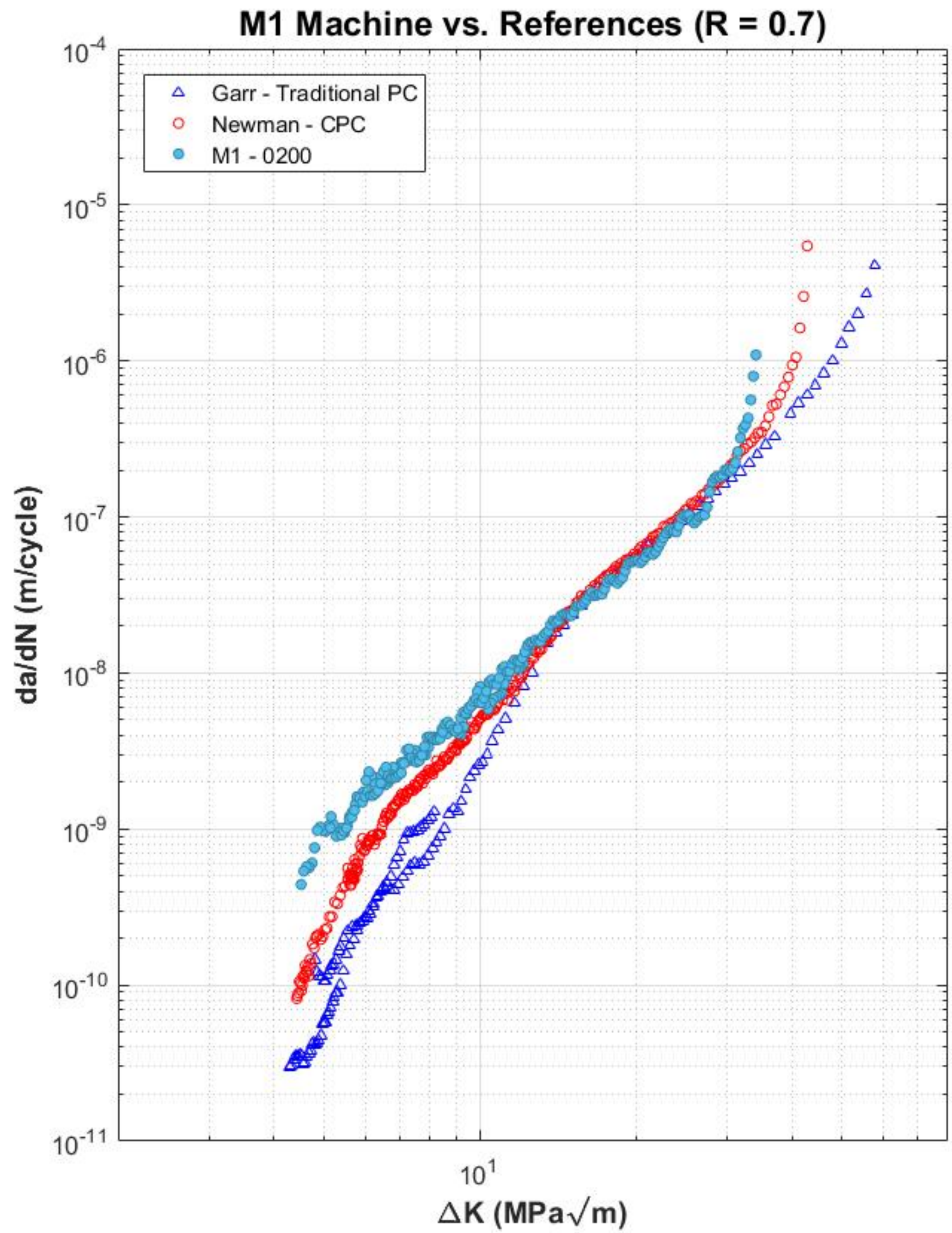

Fatigue Crack Growth

- MSFC - Consistent with M1 data.

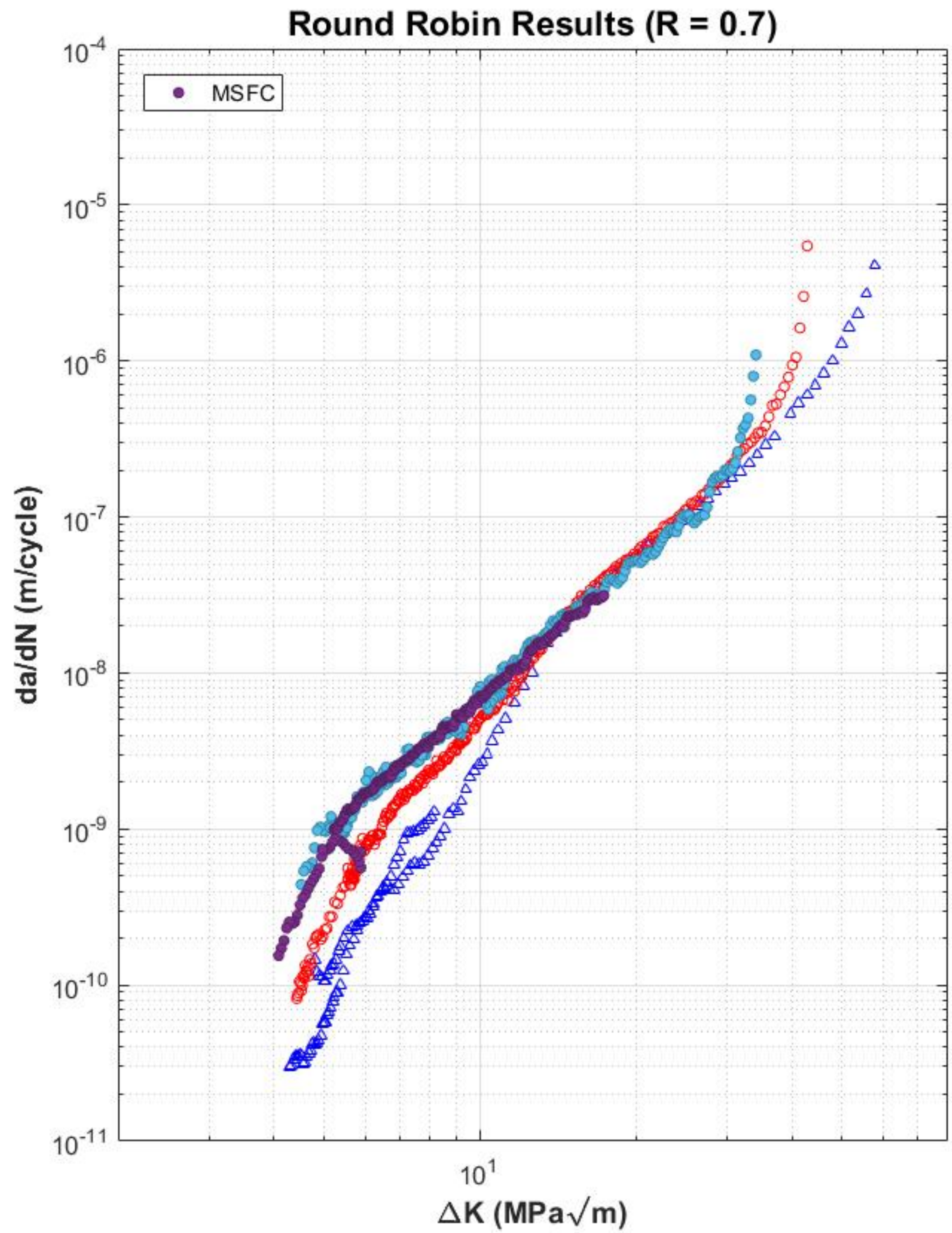

Fatigue Crack Growth

- Lab B - Consistent with M1 data.

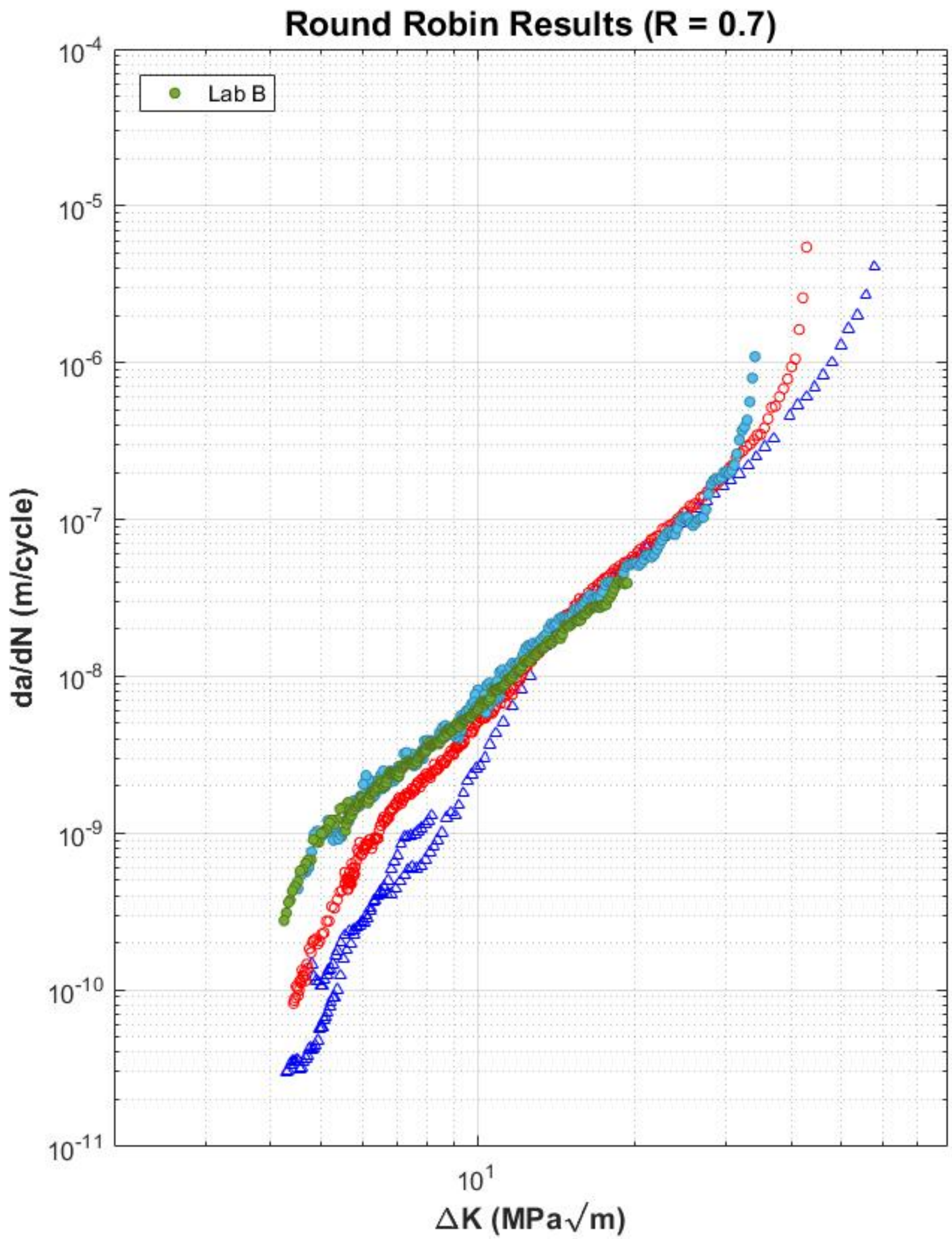

Fatigue Crack Growth

- Lab C - Lower crack growth rates near-threshold compared to M1 data. More closely follows Newman data.

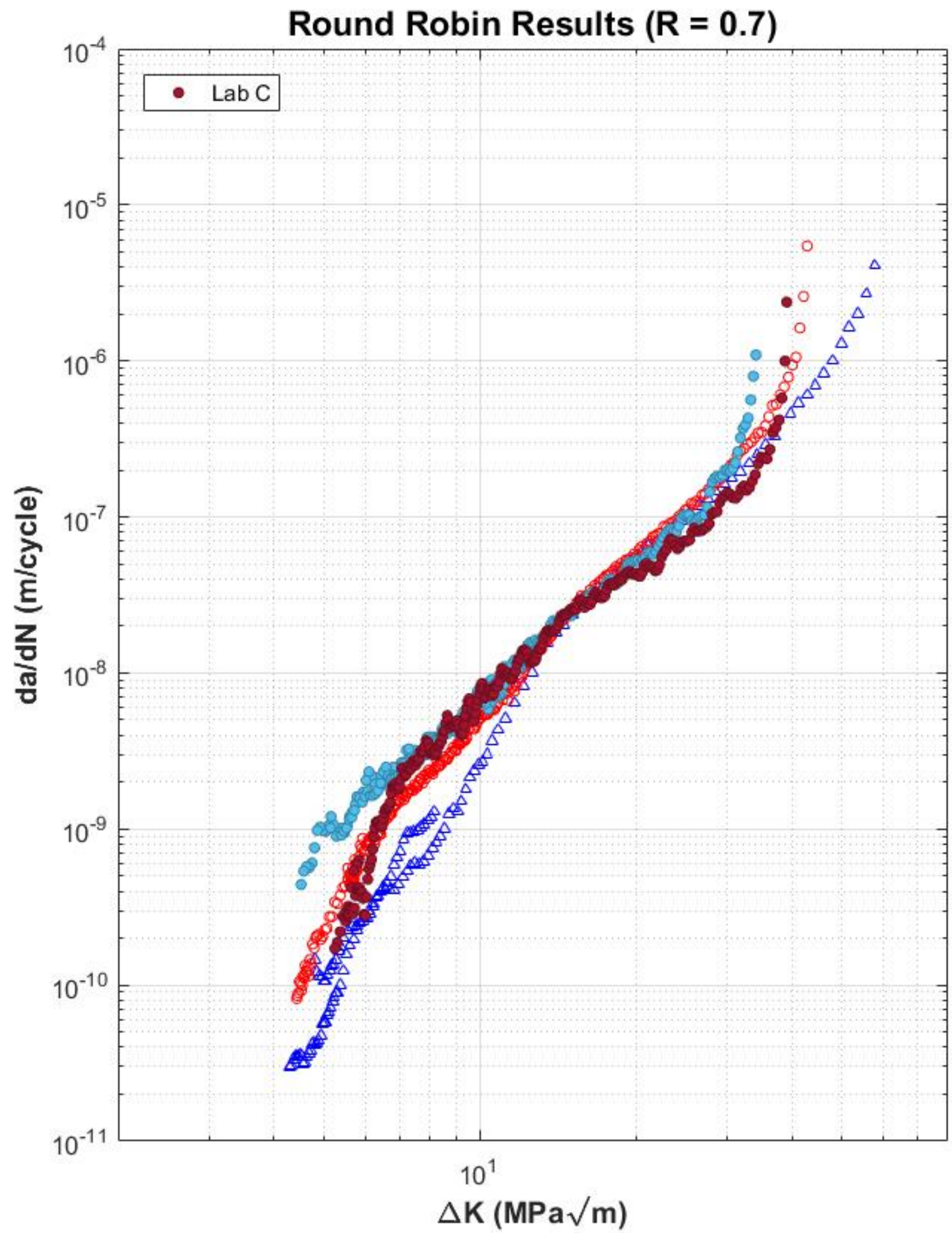

Fatigue Crack Growth

- Lab D - Lower crack growth rates near-threshold compared to M1 data. More closely follows Newman data.

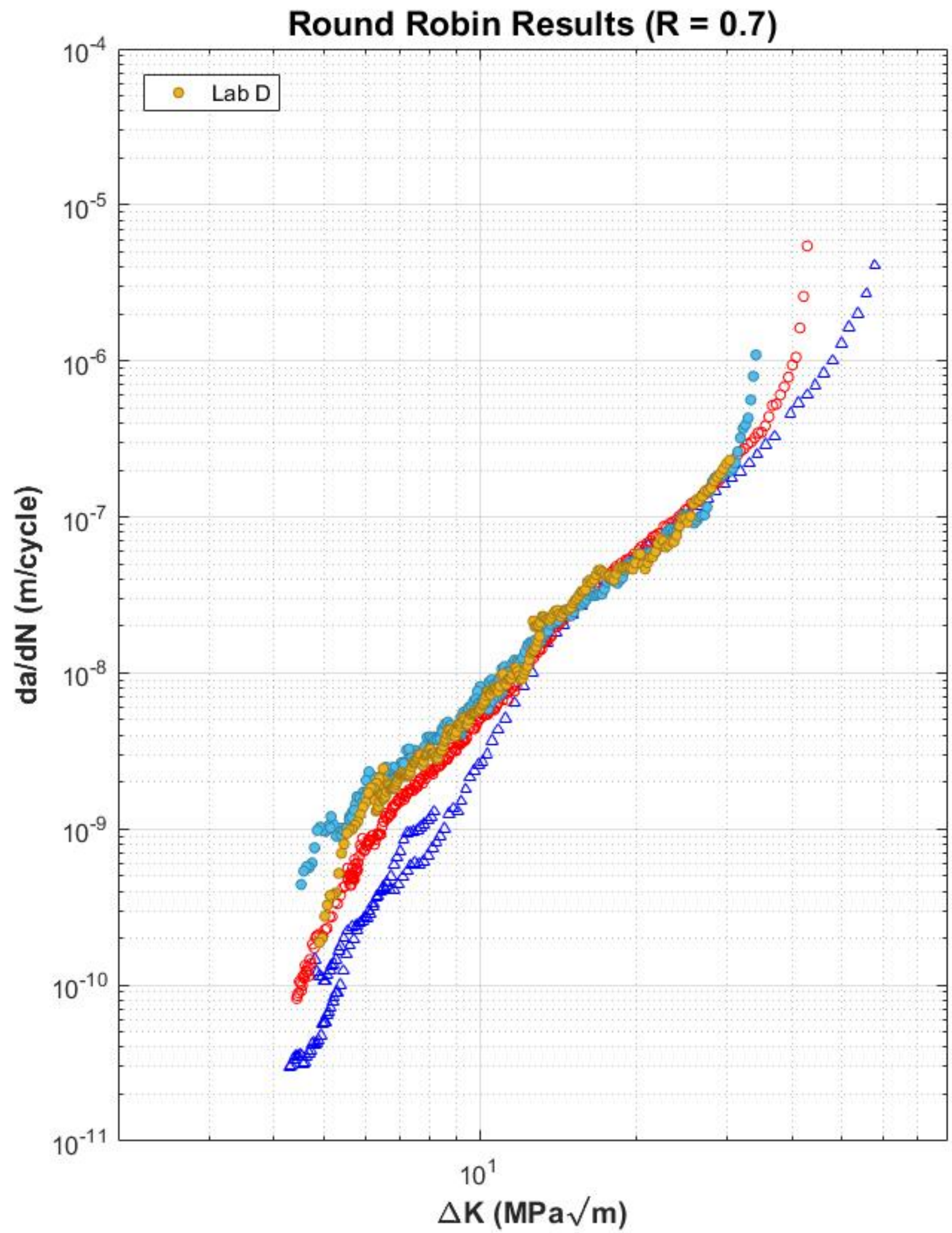

Fatigue Crack Growth

- MSFC & Lab B: Consistent with M1 data

- Lab C & Lab D: Consistent with Newman data

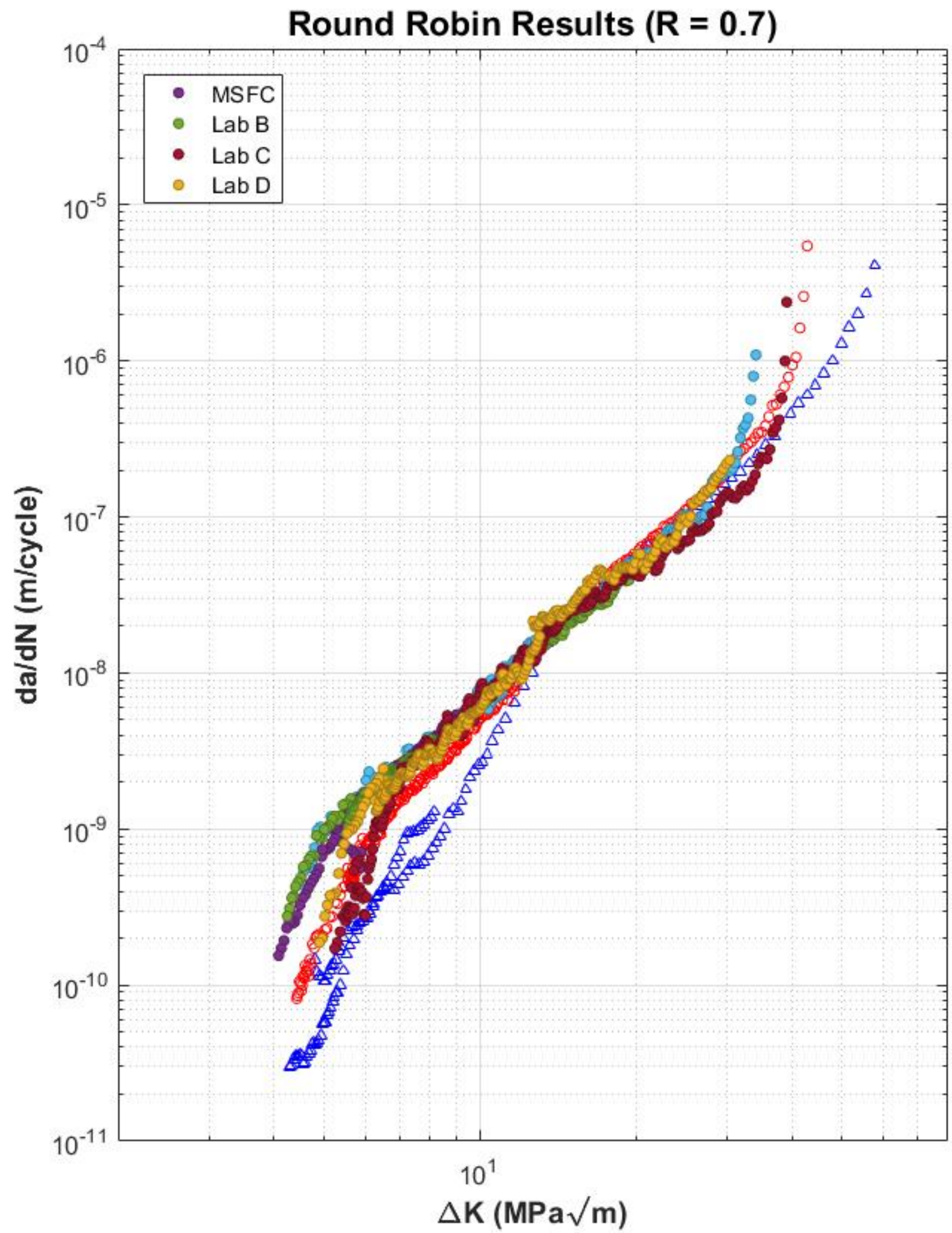

Fracture Toughness Results

- Round Robin
- SLM 718
  - Stress relief, HIP, ASM 5664 Heat Treatment
- ASTM E1820
  - J-R vs Δa
  - Legend lists J_{IC} value obtained from ASTM E1820

Fracture Toughness Results

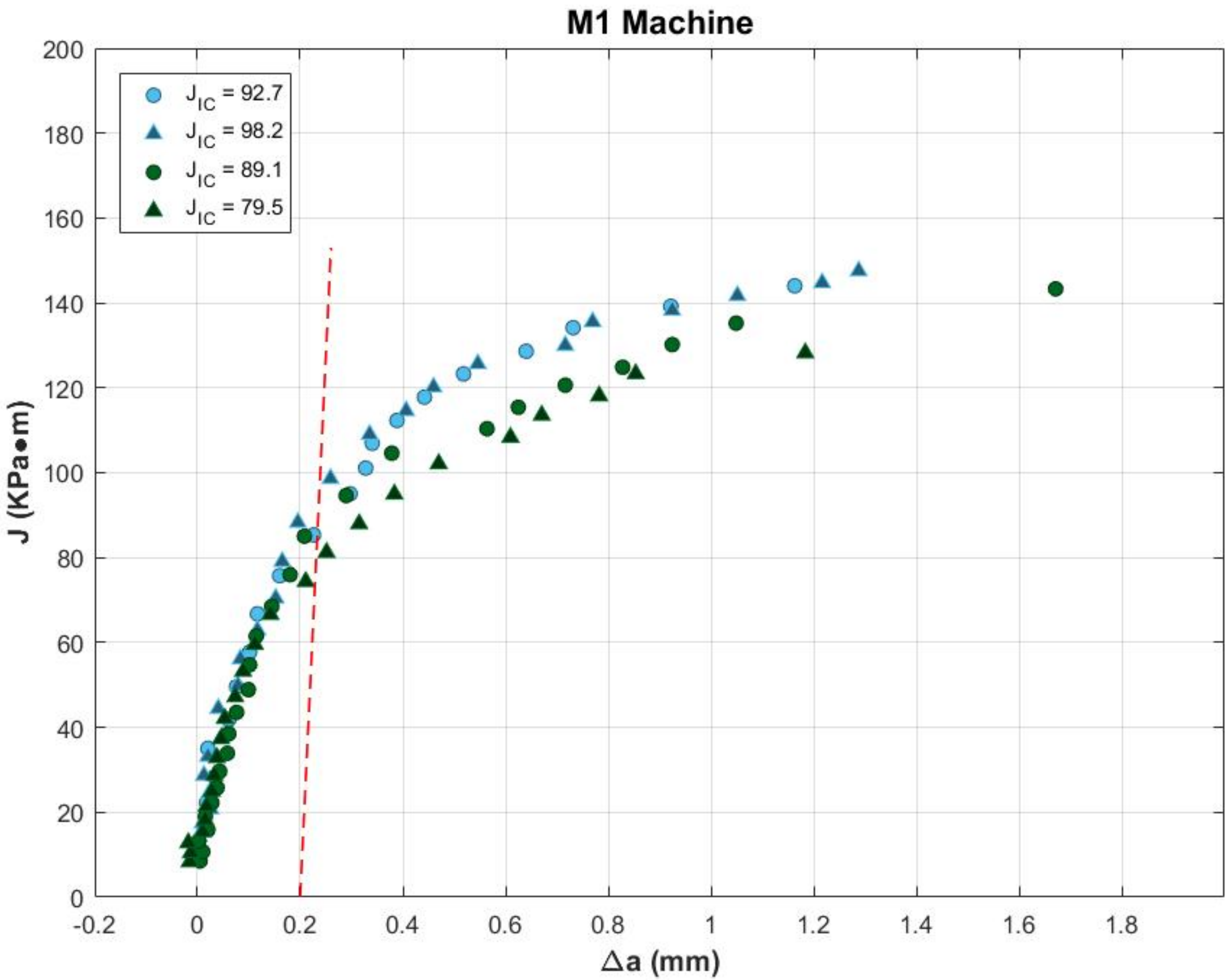

Fracture Toughness Results

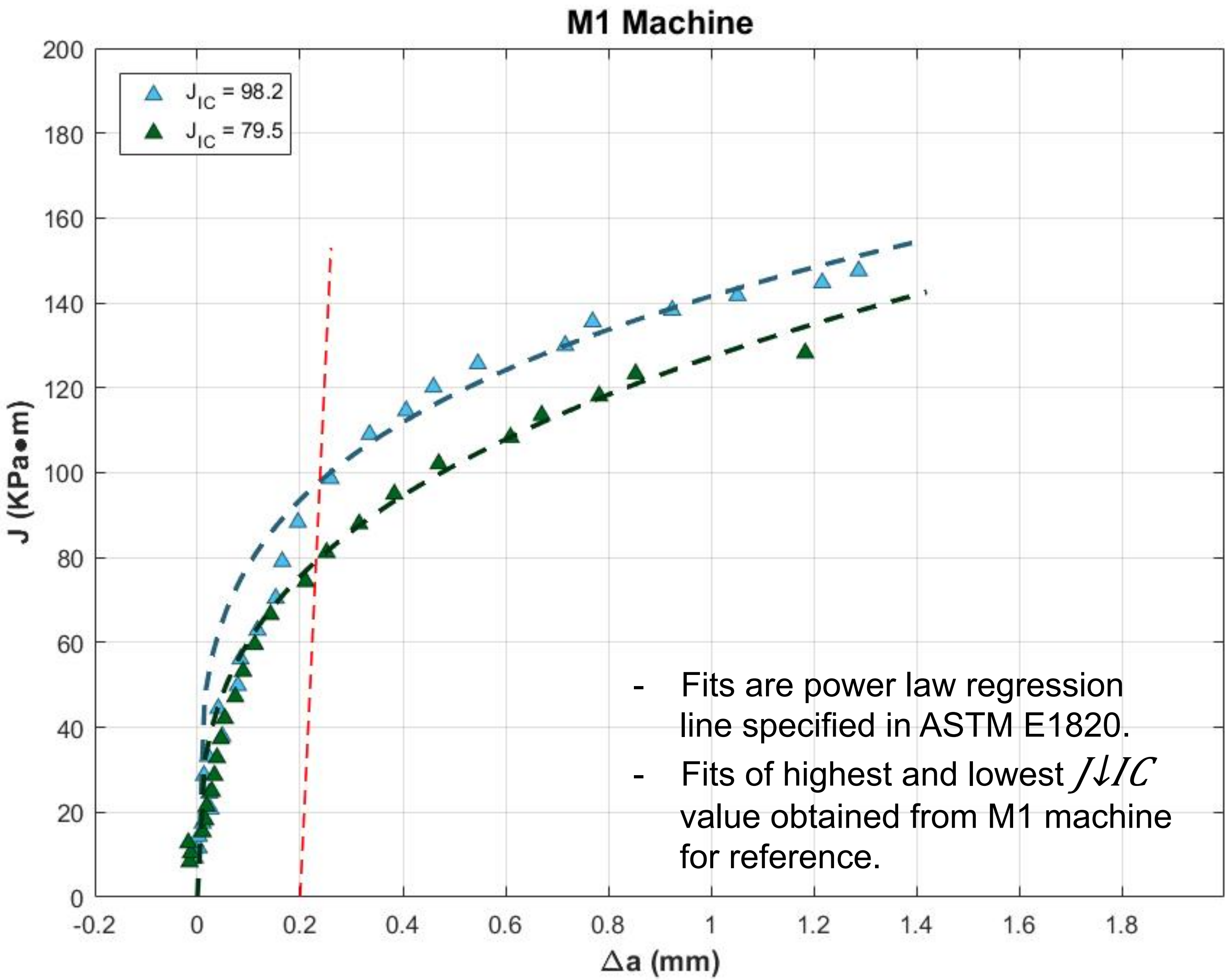

- Fits are power law regression line specified in ASTM E1820.
- Fits of highest and lowest J_{IC} value obtained from M1 machine for reference.

Fracture Toughness Results

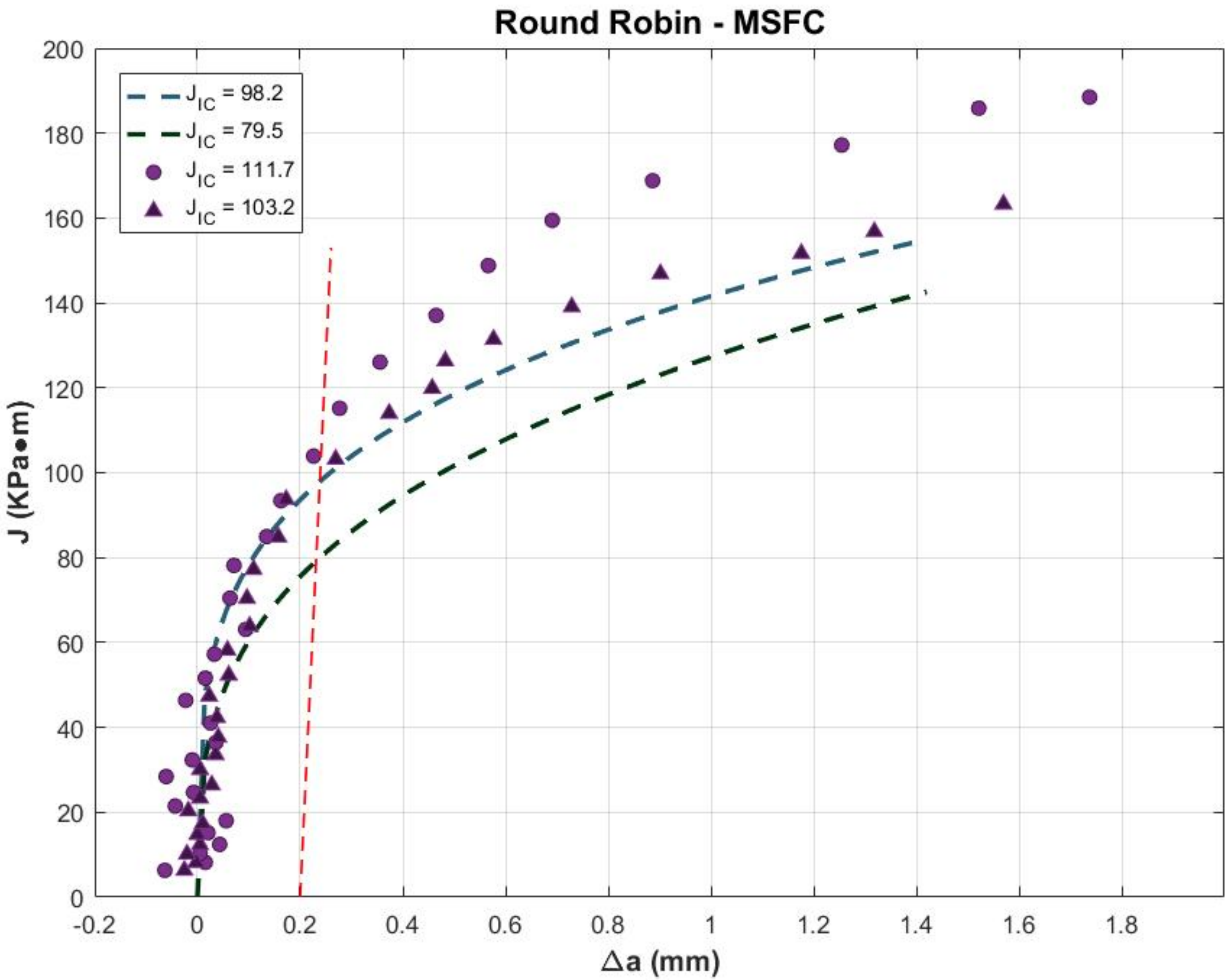

Fracture Toughness Results

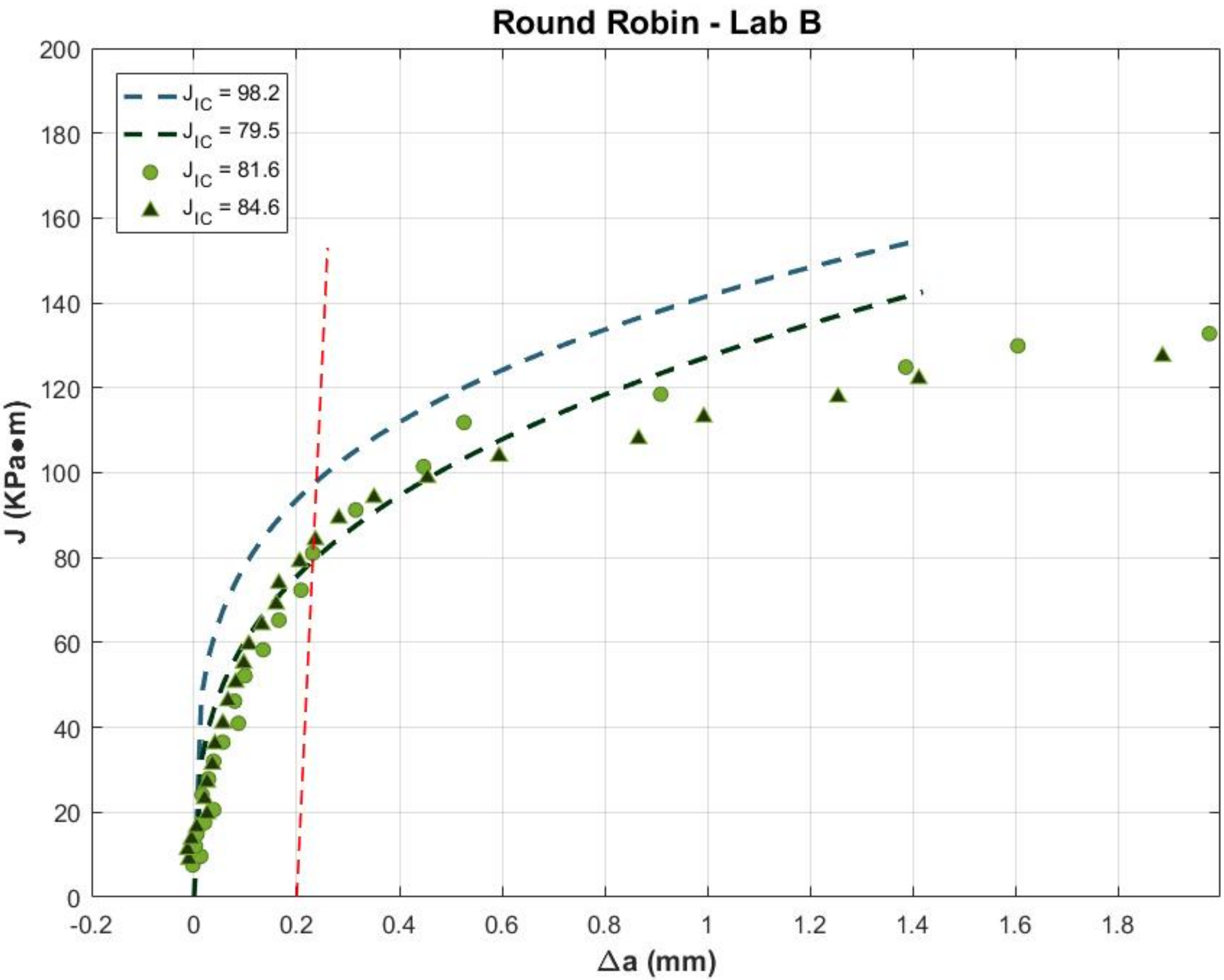

Fracture Toughness Results

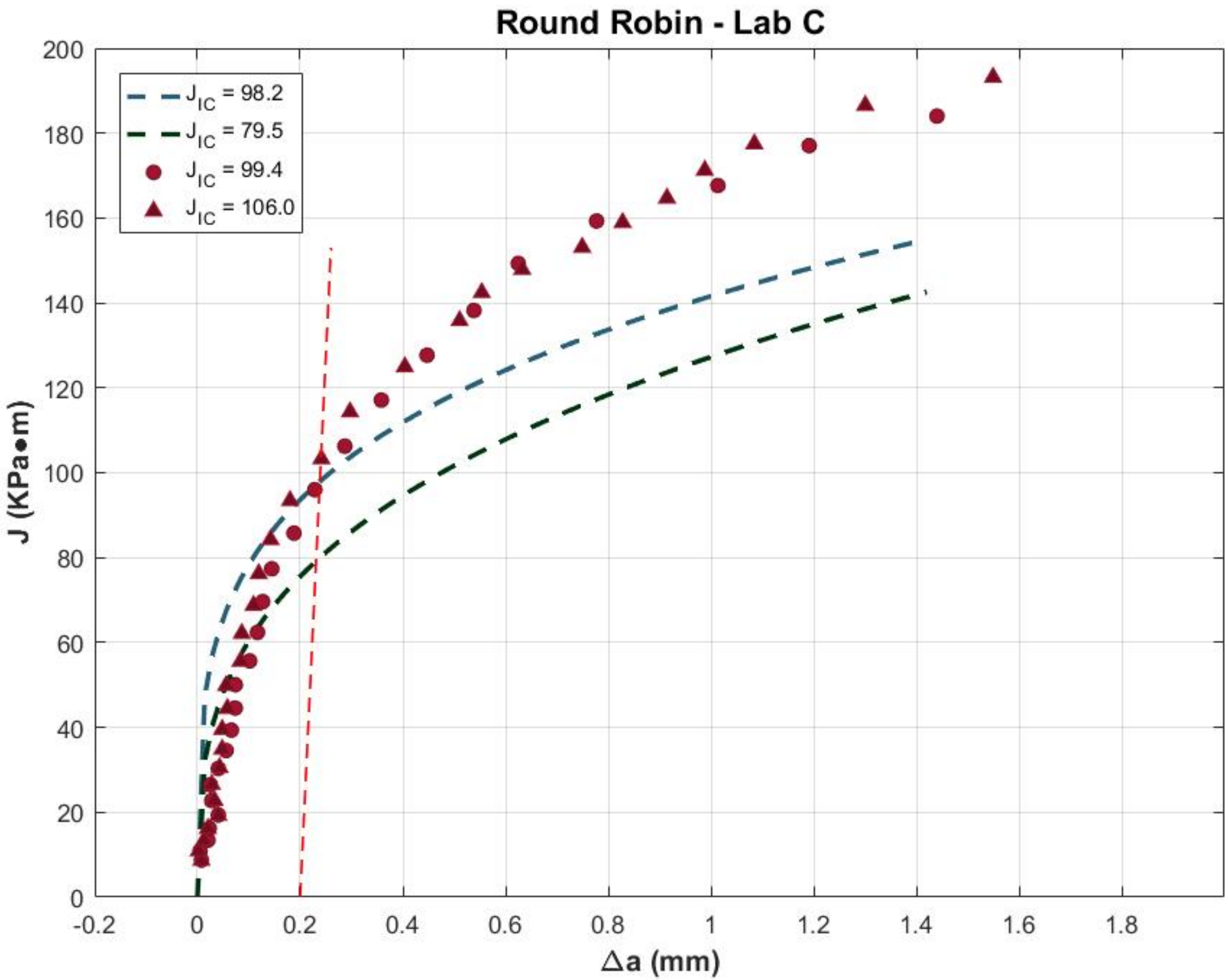

Fracture Toughness Results

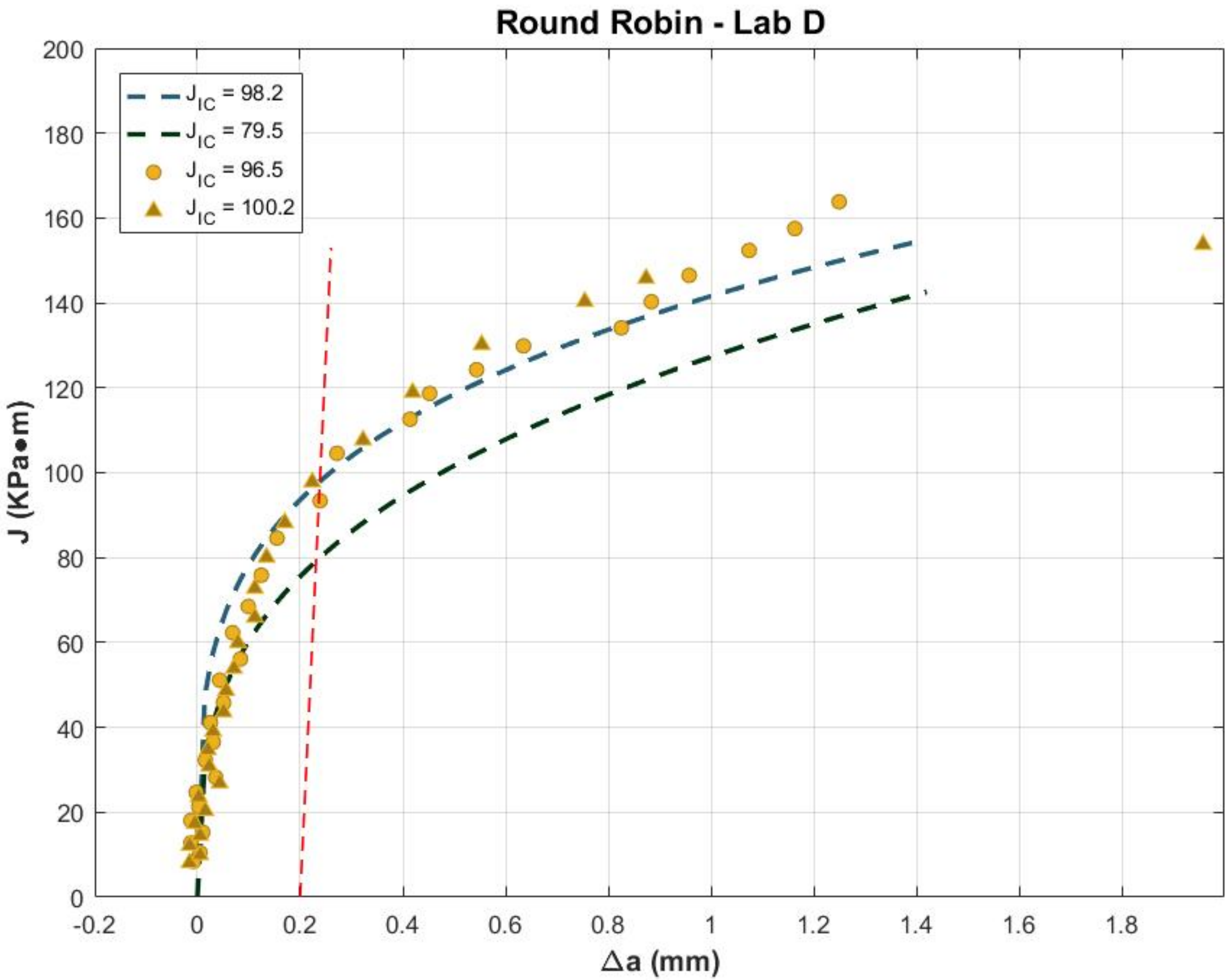

Fracture Toughness Results

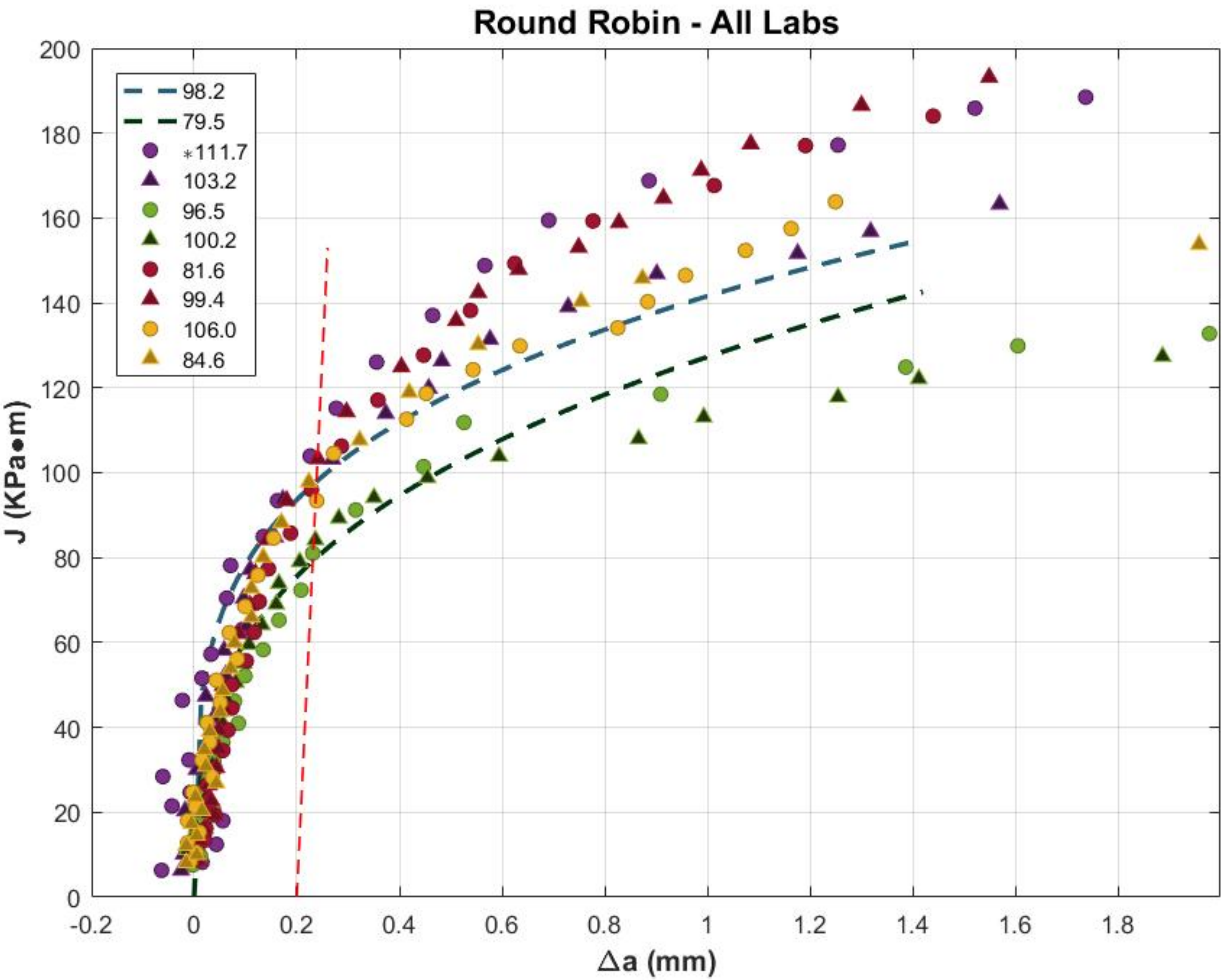

FINAL TECHNICAL PROGRAM

WORKSHOP ON MECHANICAL BEHAVIOR OF ADDITIVE MANUFACTURED COMPONENTS

Sponsored by ASTM Committee E08 on Fatigue and Fracture in conjunction with the National Institute of Standards and Technology (NIST).

May 4-5, 2016
Grand Hyatt San Antonio
San Antonio, TX

Workshop Organizers: Steve Daniewicz, Mississippi State University
Nima Shamsaei, Mississippi State University
Nik Hrabe, NIST
Nick Barbosa, NIST

WEDNESDAY, MAY 4, 2016
***separate registration is required for Wednesday and Thursday**

8:00 AM
Opening Remarks
Steve Daniewicz, Mississippi State University

8:15 AM
Additive Manufacturing in the Context of Structural Integrity
Michael Gorelik, FAA

8:45 AM
Reliability of Mechanical Behavior in Metallic Additively Manufactured Parts Used in Critical Applications
Doug Wells, NASA Marshall

9:15 AM
Ti-6Al-4V for Orthopaedic Implants in Fatigue
Mukesh Kumar, Zimmer-Biomet

9:45 AM BREAK

10:15 AM
Fracture Mechanics and Nondestructive Evaluation Modeling to Support Rapid Qualification of Additively Manufactured Parts
Craig McClung, Southwest Research Institute (SWRI)

FINAL TECHNICAL PROGRAM

10:45 AM
Extreme value analysis of defects on AM parts
Steffano Beretta, Politecnico di Milano

11:15 AM
Fatigue Life Manipulation of SLM® Parts
Wadim Reschetnik, Paderborn University

11:45 AM LUNCH

1:15 PM
Advanced Characterization of Additively Manufactured Materials, including Synchrotron–based 3D X-rays
Anthony Rollett, Carnegie Mellon University

1:45 PM
Effects of HIP Processing on Additively Manufactured, Titanium Materials Produced Using an Electron Beam – Directed Energy Deposition Process
Hank Phelps, Lockheed Martin Aeronautics

2:15 PM
Overview of Fatigue and Damage Tolerance Performance of Powder Bed Fusion Alloy N07718
William Tilson and William Campbell, NASA Marshall

2:45 PM BREAK

3:00 PM
Presentation of NEEDS and BARRIERS from pre-workshop survey
Nik Hrabe, NIST

3:30 PM
Expert Panel leads discussion of NEEDS and BARRIERS
Expert Panelists:
Bob Klein, Stryker
John Slotwinski, Johns Hopkins Applied Physics Laboratory (APL)
Gautam Gupta, 3D Systems
Craig McClung, Southwest Research Institute (SWRI)

4:30 PM
Entire group prioritizes NEEDS and BARRIERS

5:00 PM CLOSE 1st Day

FINAL TECHNICAL PROGRAM

THURSDAY, MAY 5, 2016
***separate registration is required for Wednesday and Thursday**

8:00 AM
Opening Remarks
Nik Hrabe, NIST

8:15 AM
Ongoing challenges in additive manufacturing of fatigue resistant materials
Nima Shamsaei, Mississippi State University presented by: Jutima Simsiriwong, Mississippi State University

8:45 AM
Breakout Sessions generate STRATEGIES for identified NEEDS and BARRIERS

10:00 AM BREAK

10:30 AM
Breakout Sessions prepare summaries of their discussions

11:00 AM
Breakout Sessions present summaries

11:45 AM
Closing Remarks
Steve Daniewicz, Mississippi State University

12:00 PM CLOSE Workshop

Ti-6Al-4V for Orthopedic Implants in Fatigue

Mukesh Kumar
Zimmer-Biomet

WORKSHOP ON MECHANICAL BEHAVIOR OF ADDITIVE MANUFACTURED COMPONENTS

Sponsored by ASTM Committee E08 on Fatigue and Fracture in conjunction with the National Institute of Standards and Technology (NIST).

May 4-5, 2016
Grand Hyatt San Antonio
San Antonio, TX

What does the Orthopedic Industry do

In the business of restoring mobility by replacing damaged bone / cartilage with metallic implants that

- Must survive years
- In a hostile (corrosive) environment
- (osseo) integrate with the surrounding bone to transmit 5-8 X body weight
- Under fatigue conditions

Titanium and Porous Structure

- Why do we need this porous structure
  - Bone – Implant Interface
    - Transmit load
- Animal
- Human

Animal Studies

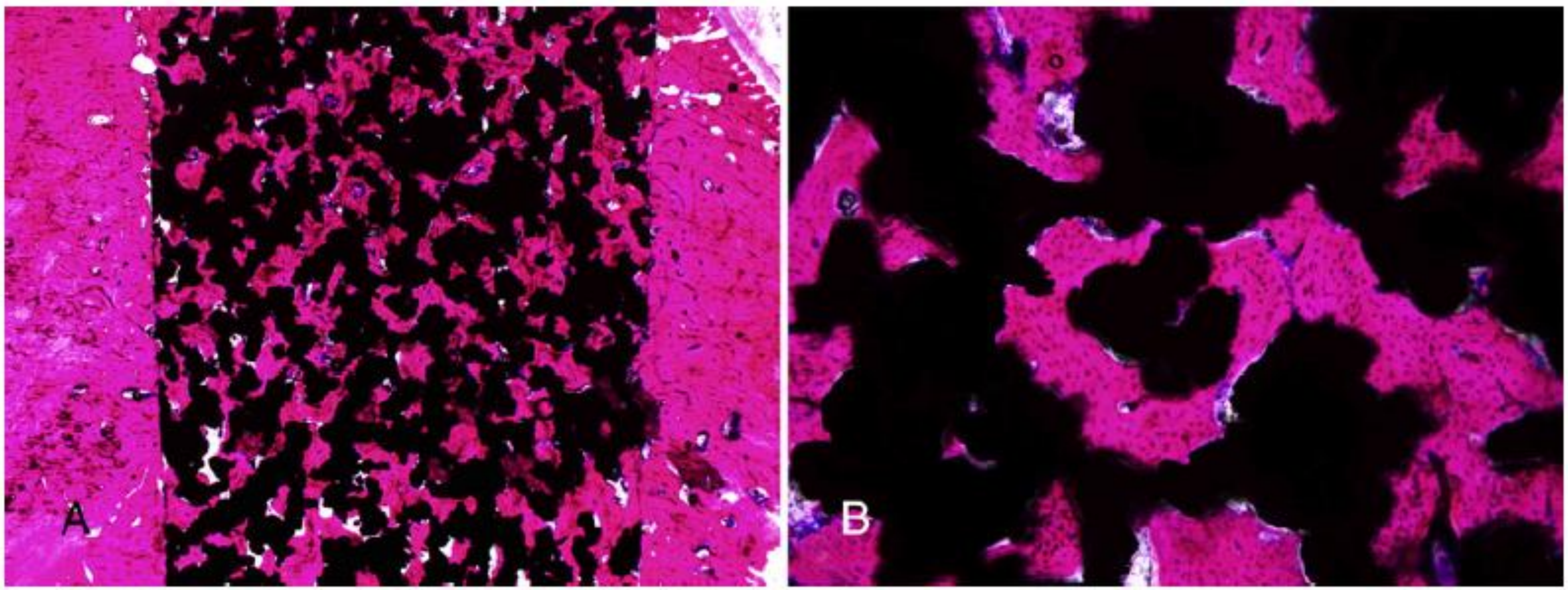

Human – Retrieval Analysis

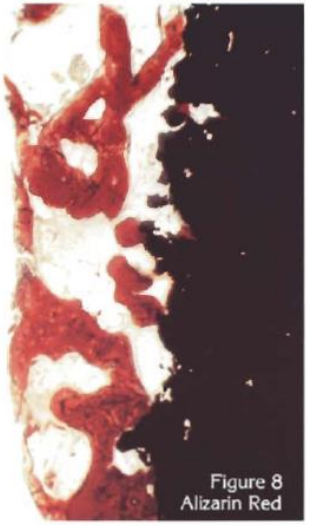
Figure 8
Alizarin Red

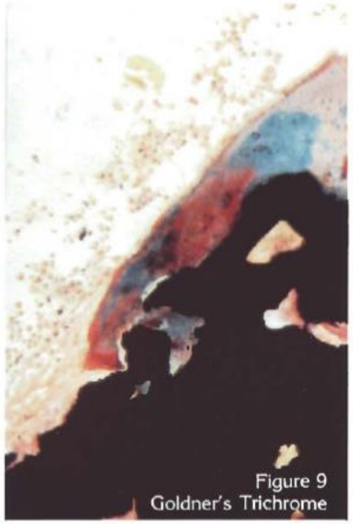
Figure 9
Goldner's Trichrome

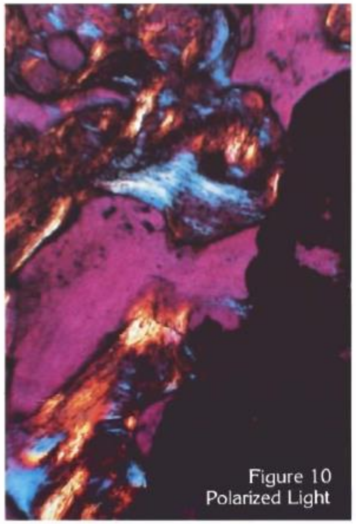
Figure 10
Polarized Light


Figure 11
Alizarin Red

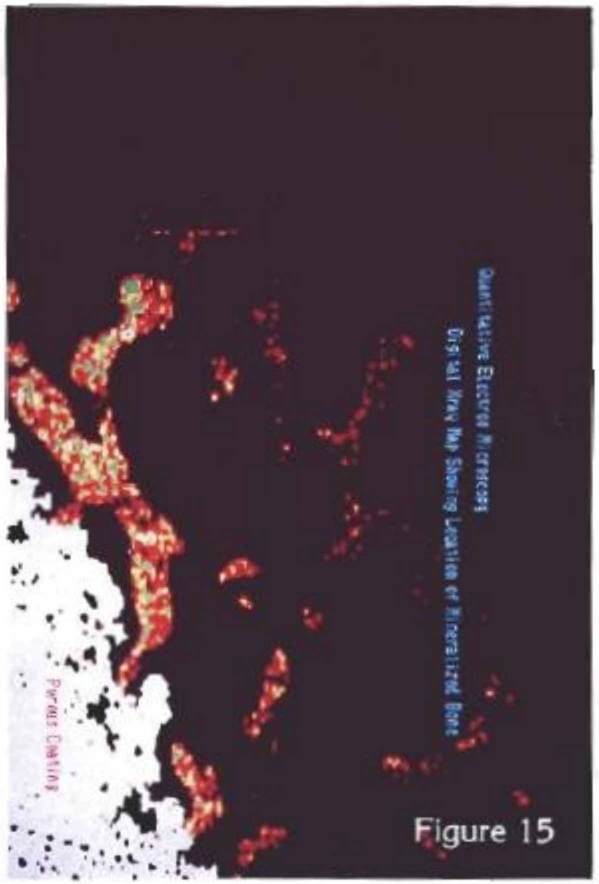

Figure 15

Porous Beaded Structure - Notch

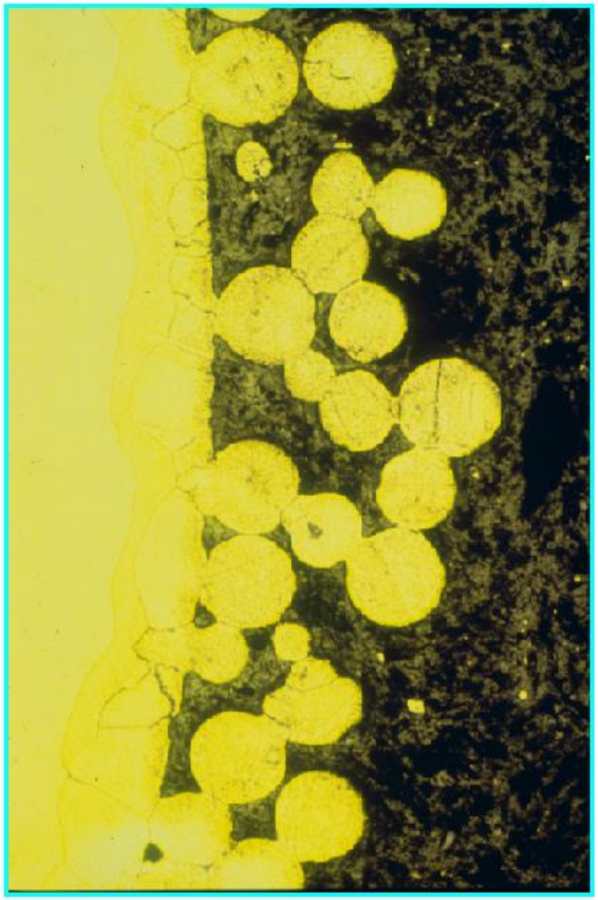

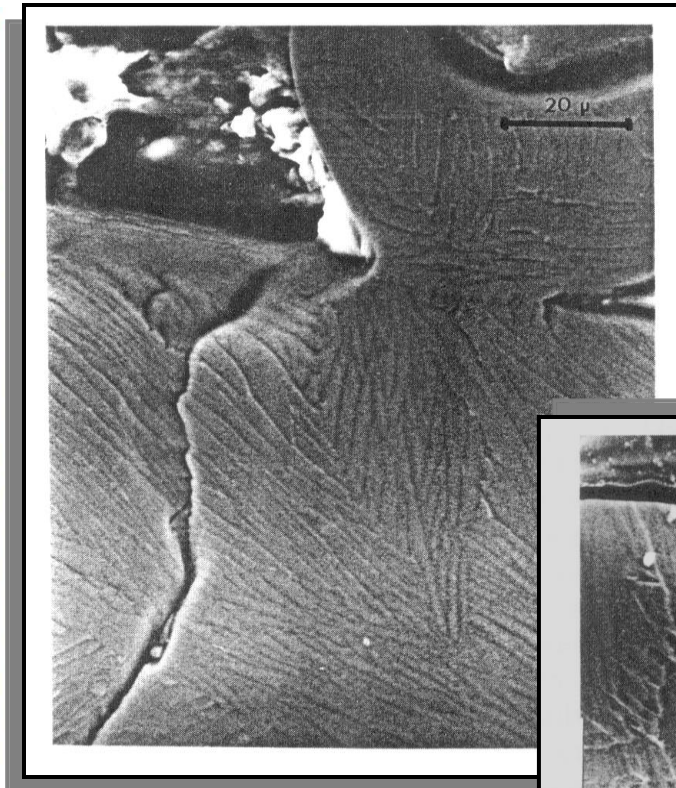

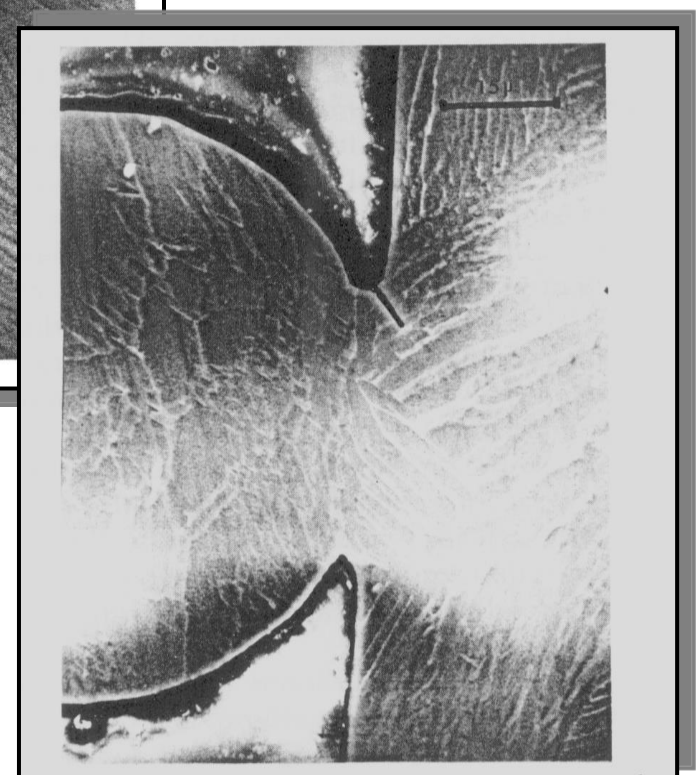

Orthopedic Industry and Additive Manufacturing

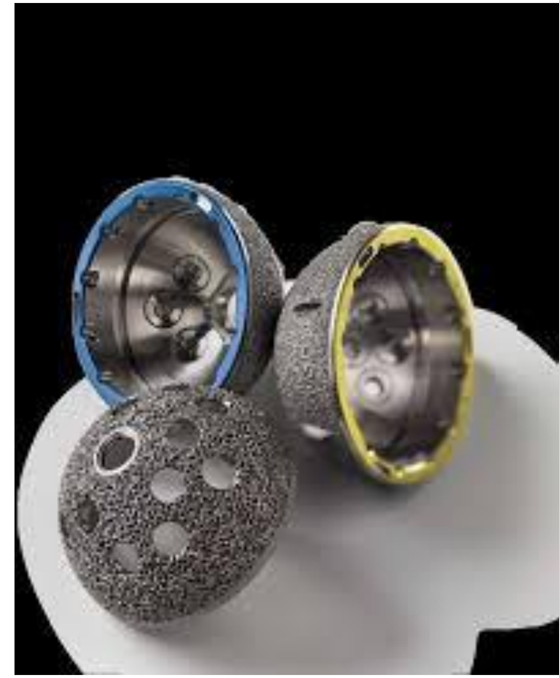

Additive Manufactured Implants now available

- Acetabular shells
- Spinal Implants

Low fatigue environment

Some Surgical Cases

Some clinical cases ….

- To get an idea of loads involved
  - Imagine your own anatomy

Why Additive Manufacturing makes perfect sense

Imagine the following work flow

Image (sometimes the contralateral side)

Create CAD

Make Implant / Bone Model / Fixtures and Guide

In many cases - Time is of the essence

18 year old patient

osteosarcoma of the proximal humerus

Expandable proximal humeral implant with a Compress stem

IMPLANT NOT FDA CLEARED

- Bilateral Triflanges

IMPLANT NOT FDA CLEARED

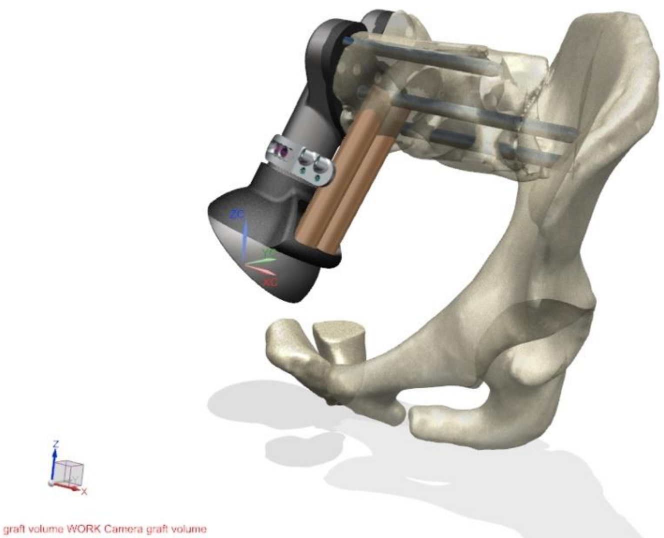

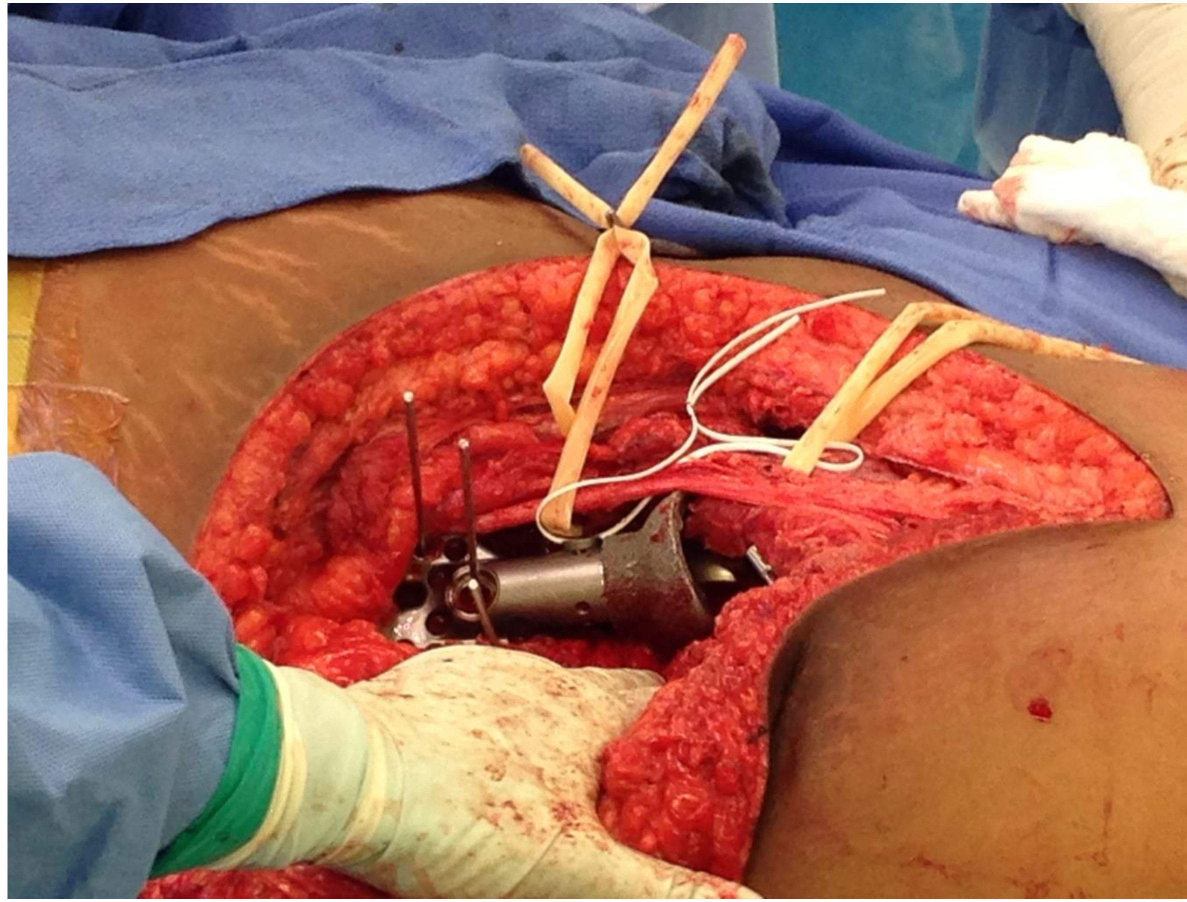

IMPLANT NOT FDA CLEARED

- Mid shaft Tibia

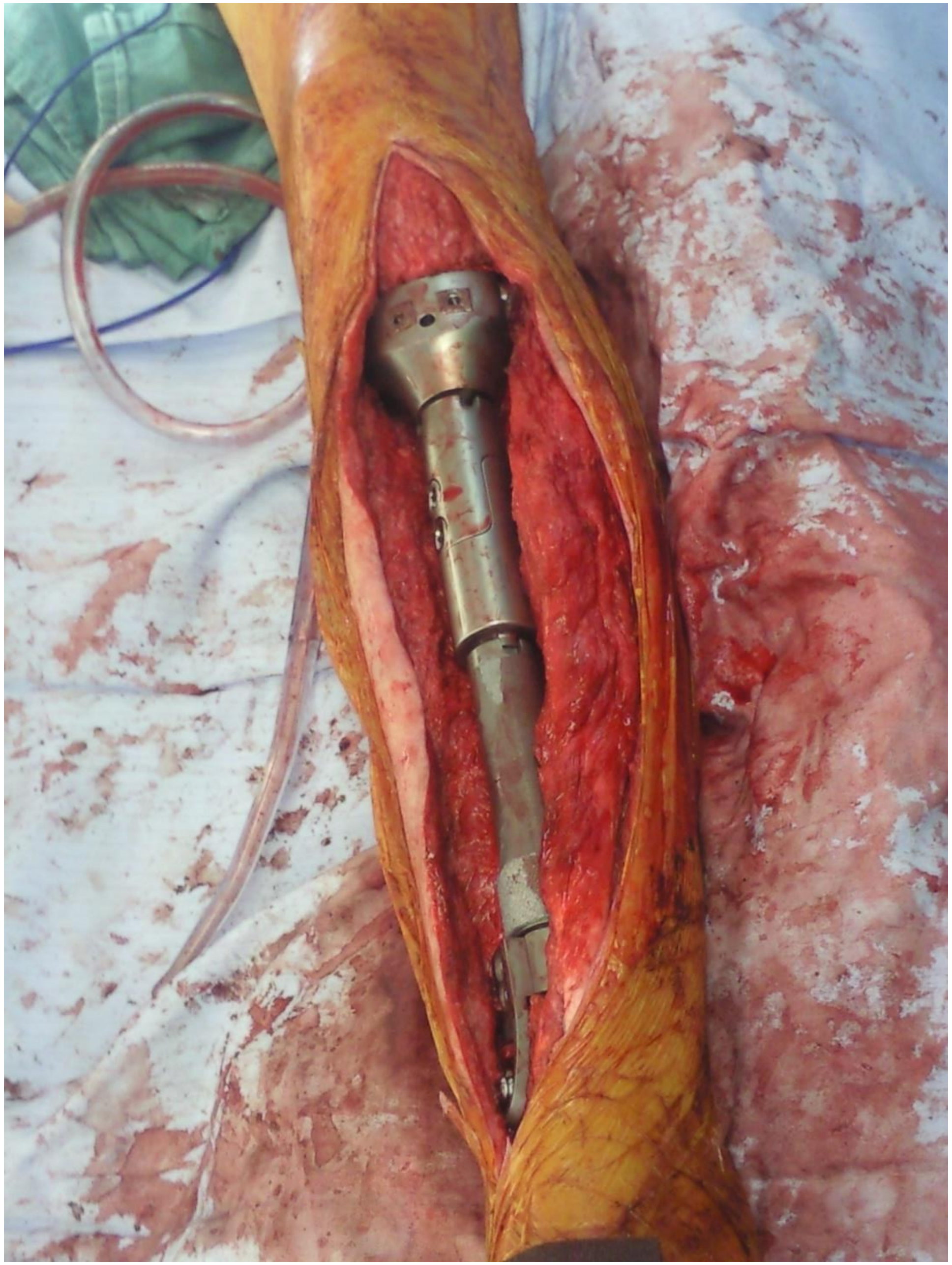

IMPLANT NOT FDA CLEARED

- Mid shaft femur

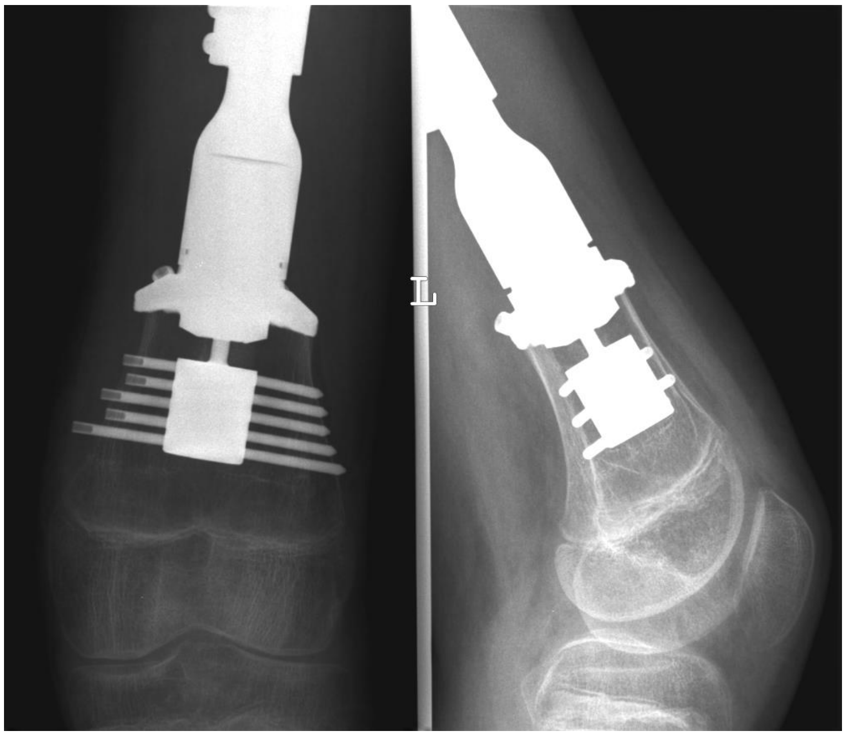

IMPLANT NOT FDA CLEARED

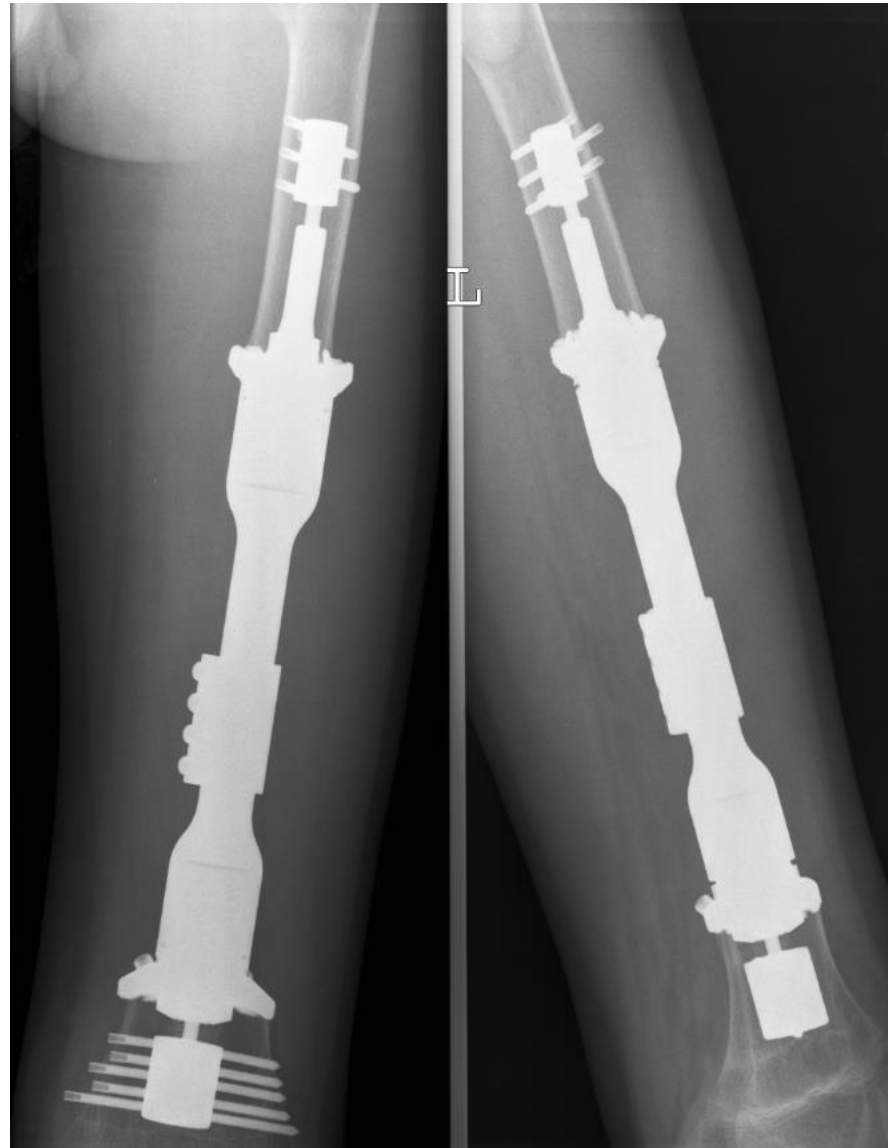

Work flow

What do we do today

- Scan of bone
- Evaluate contralateral side if available
- Design implant with surgeon (truly one of – so surgeon prescription)
- Surgeon approval
- Machine implant from bar stock
- Coat implant with porous structure
- Clean / passivate / package / sterilize

What we want to do

- Based on scan
  - 3D Print
  - Can print the porous structure
  - No need to program CNC machines
  - No issues of tolerance match ups
- Clean / passivate / package / sterilize

Can we define what we need to get Additive Manufactured Implant more main stream

Some Functional Requirements
The Patient

- All age groups
  - Young and Old

- Activity level
  - Sedentary and Active
    - And this can change with time
- Body Mass
  - And this definitely changes

Some Functional Requirements

Must be similar to ASTM F136

- Why?
  - We know ASTM F136 works
    - Maybe unnecessarily high
  - Surgeons have a comfort

What are we looking for …

- What heat treatment regimen can provide fatigue properties in excess of wrought material?
- How does the fatigue property change if there is semi-sintered loose powder on the "as built" surface?
  - Is there a way to simulate the decrease in fatigue from the presence of such semi-sintered surface particle clusters and thus help define acceptance criteria for such clusters?
- Design rules - recognizing that porous structures are essential features in orthopedic implants, but the presence of porous structures create stress risers and reduce fatigue properties, what design rules could be followed to help create a higher fatigue strength implant

Questions?

Fracture Mechanics and Nondestructive Evaluation Modeling to Support Rapid Qualification of Additively Manufactured Parts

ASTM Workshop on Mechanical Behavior of Additive Manufactured Components
May 4, 2016
San Antonio, Texas

Craig McClung, Michael Enright, John McFarland, Jonathan Moody
Southwest Research Institute

Irving Gray, Joe Gray
NDE Technologies, Inc.

Acknowledgments

- Funding for this SBIR effort provided by the US Air Force Research Laboratory
  - Andrew Nauss, AFRL Program Monitor for Phase I
  - Bill Musinski, AFRL Program Monitor for Phase II

Motivation

- Additive Manufacturing methods can produce defects
- NDE may be required to ensure structural integrity
- Key questions:
  - What size defects can be found in a complex part?
  - What size defects matter to structural integrity?
- Simulation modeling can be used to answer these questions without expensive physical testing
  - NDE simulation can determine what size defects can be found
  - Fracture mechanics simulation can determine what size defects matter to structural integrity
  - Coupled simulations can determine the impact of NDE reliability on fracture risk

Method:
Integrated NDE and Fracture Risk Models

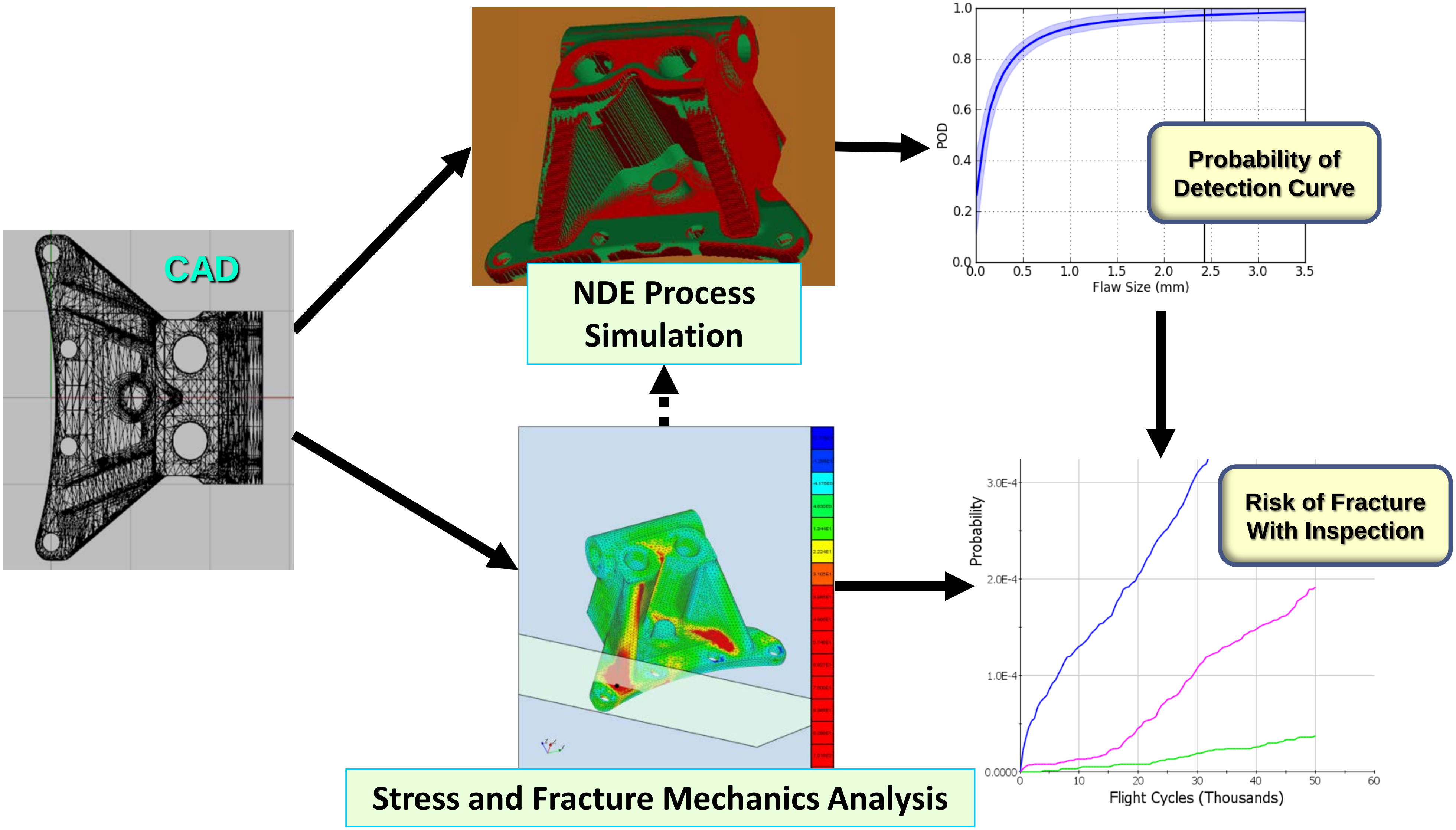

Overview

- Defect Morphology
  - Identify anomaly types associated with DMLS additive manufacturing processes
- POD Curve Simulation
  - Link NESSUS with XRSIM to generate location-specific POD curves
- Fracture Risk Simulation
  - Link NESSUS/XRSIM-generated POD curves with DARWIN to predict risk of fracture with inspection
- Application Example
  - Illustrate generation of location-specific POD curves and fracture risk assessment for actual component (engine mount)

Representative AM Defects

Low Energy- Lack Of Fusion

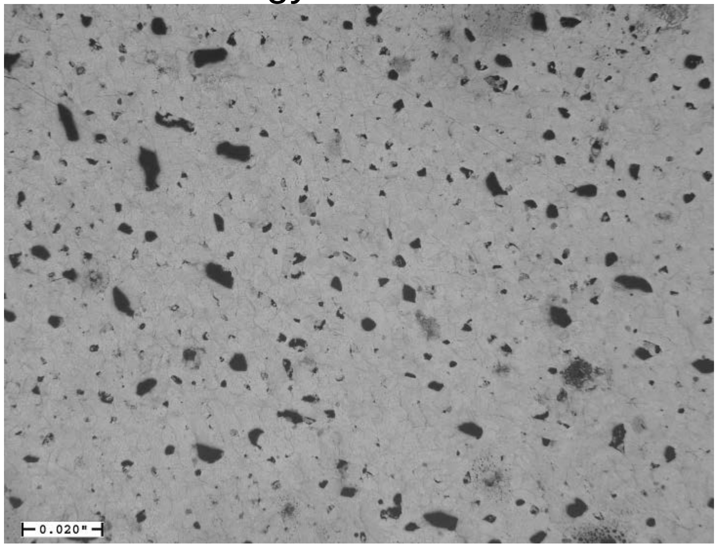

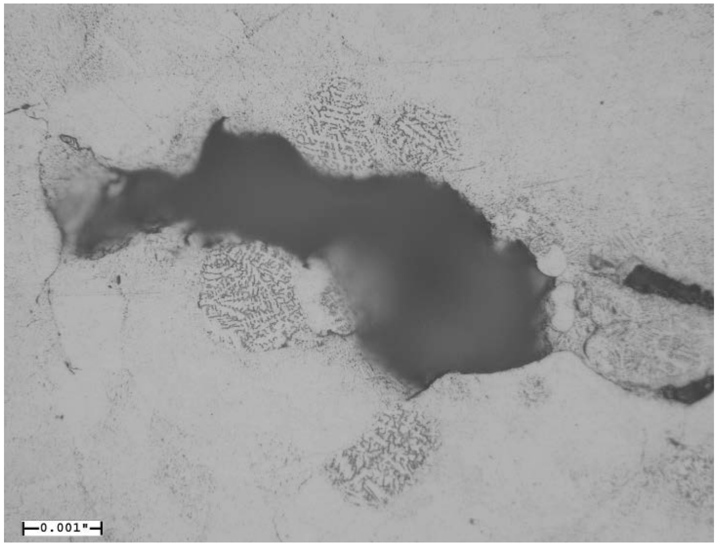

High Energy- Keyhole Porosity

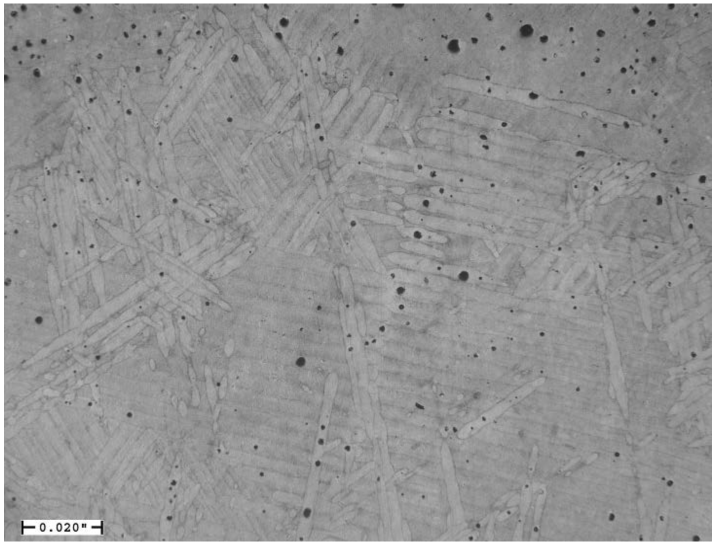

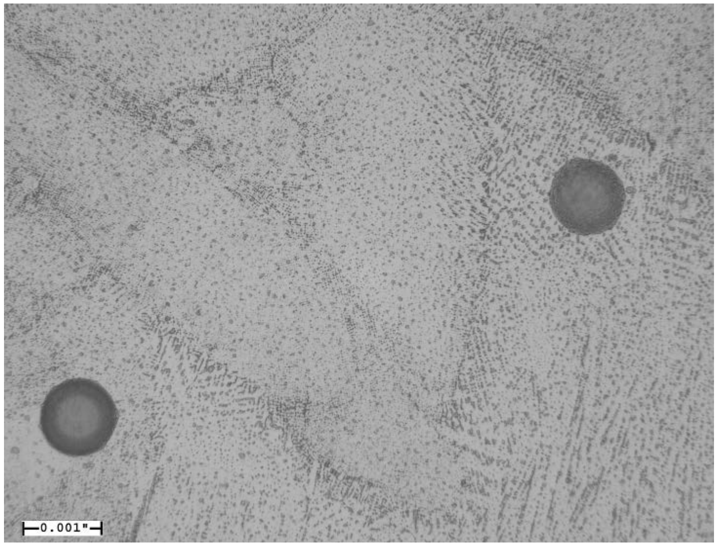

Simulating Non-Destructive Inspections Using XRSIM

- XRSIM simulates the application of X-Rays to a component to identify defects
- The intensity of the simulated X-Ray images is dependent on a number of factors
  - Equipment
    - Inherent filtration of x-ray tube, eddy current lift off and coil tilt, broad band center frequency
  - Setup
    - Placement of the central axis of the x-ray tube, orientation of the UT probe, scan variation in lift off and probe tilt
  - Signal Noise
  - Flaw morphology
    - Size, shape, position & orientation in the part

XRSIM Defect Detection Based on Contrast Values

- XRSIM provides virtual images that simulate the X-Ray NDE method
- Human detection of a defect is dependent on contrast values
  - Contrast is based on the image intensity at a defect versus the intensity of the surrounding image

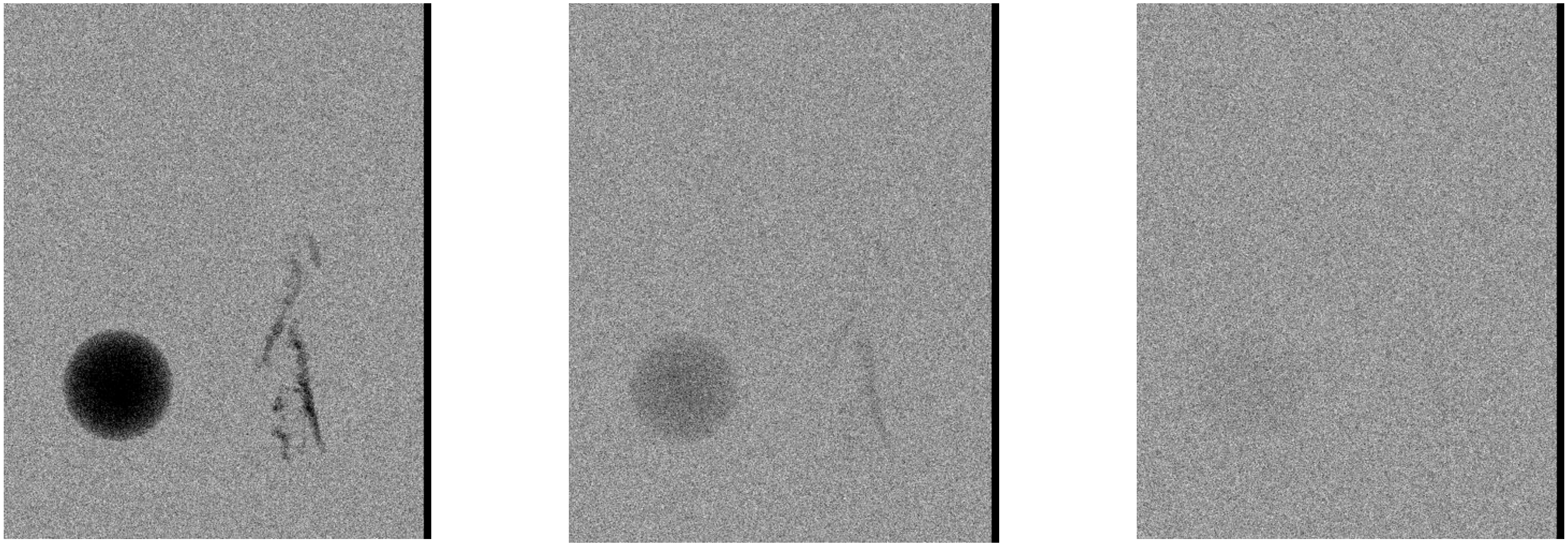

Simulating POD Curves Using Probabilistic Analysis

- The contrast value associated with a single defect size is modeled as a random variable
- The threshold contrast value at which a defect can be detected by a human is also modeled as a random variable

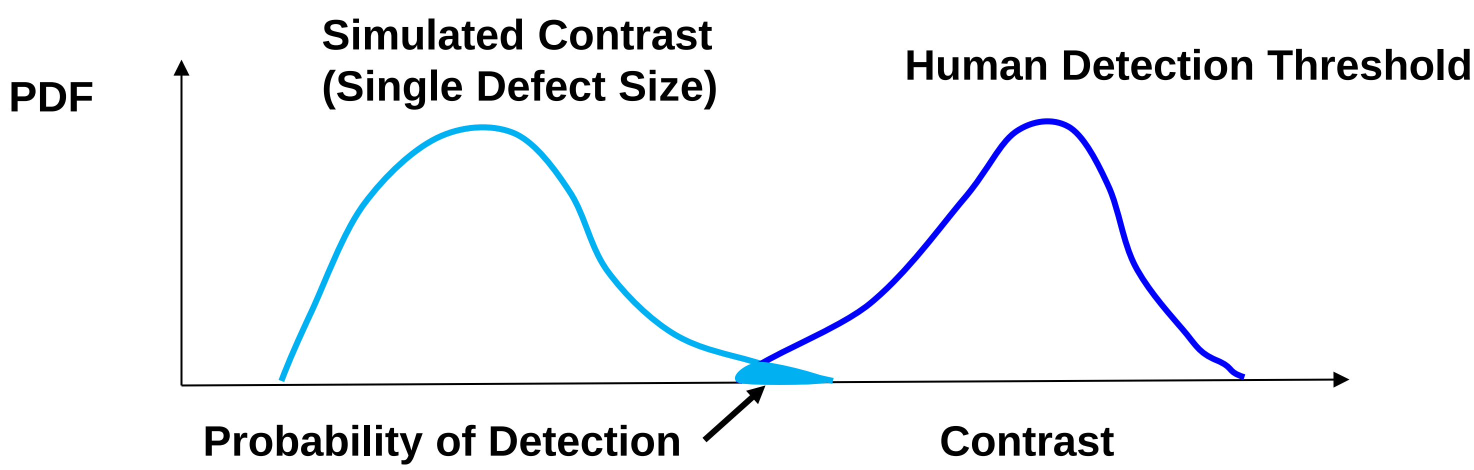

Simulating POD Curves Using Probabilistic Analysis (cont.)

- The POD values for each anomaly size can be used to construct the full POD curve

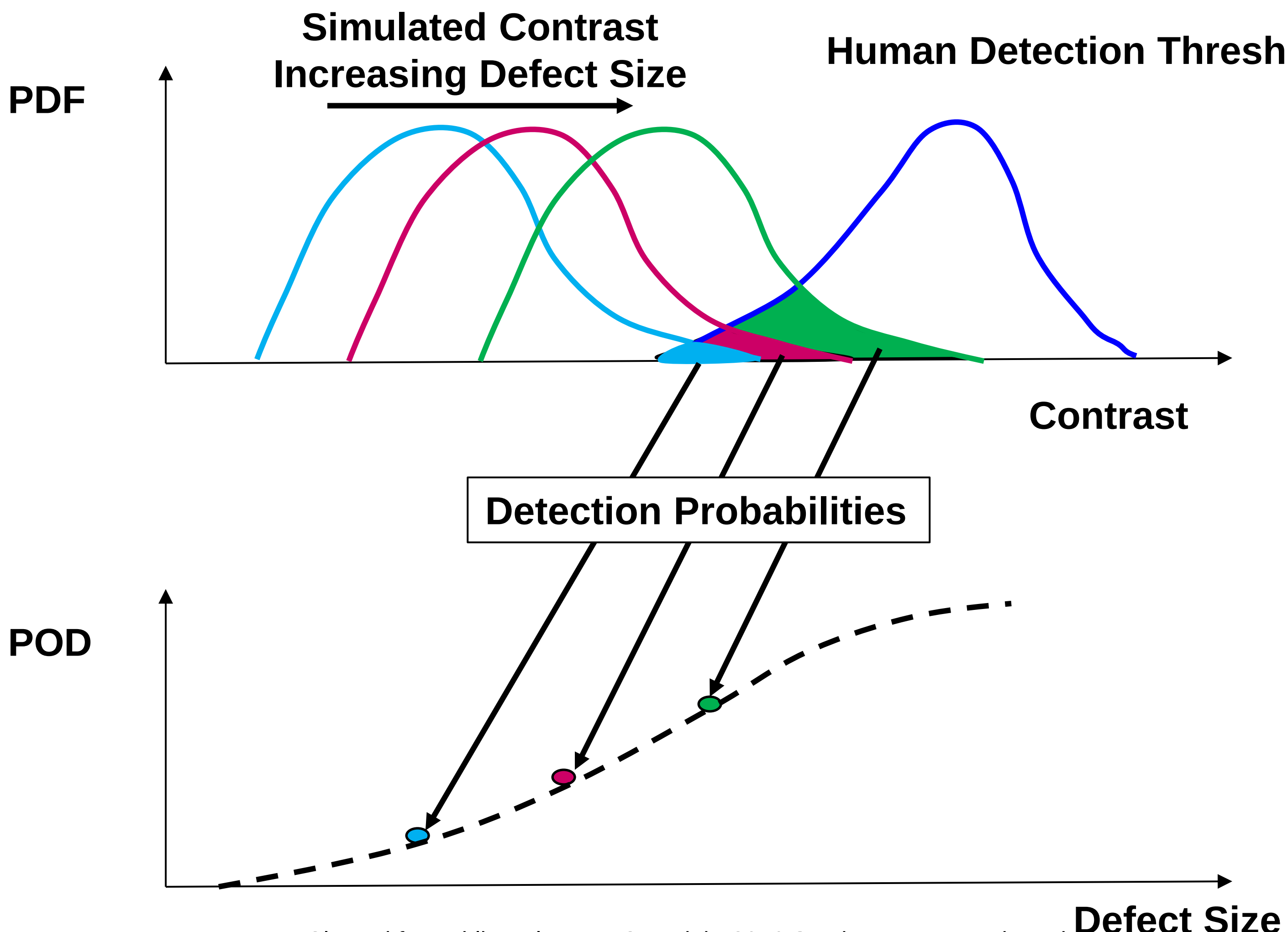

POD Curve Simulation Using NESSUS and XRSIM

- Create a response surface model
  - Relates contrast values with XRSIM input variables
- Propagate NDI random variables through response surface
  - Result: PDF of contrast values
- Create a probabilistic model (PDF) of human contrast detection threshold
  - Based on detect/no detect data
- Obtain POD curve
  - Achieved by comparing contrast PDF with contrast threshold PDF at each anomaly size

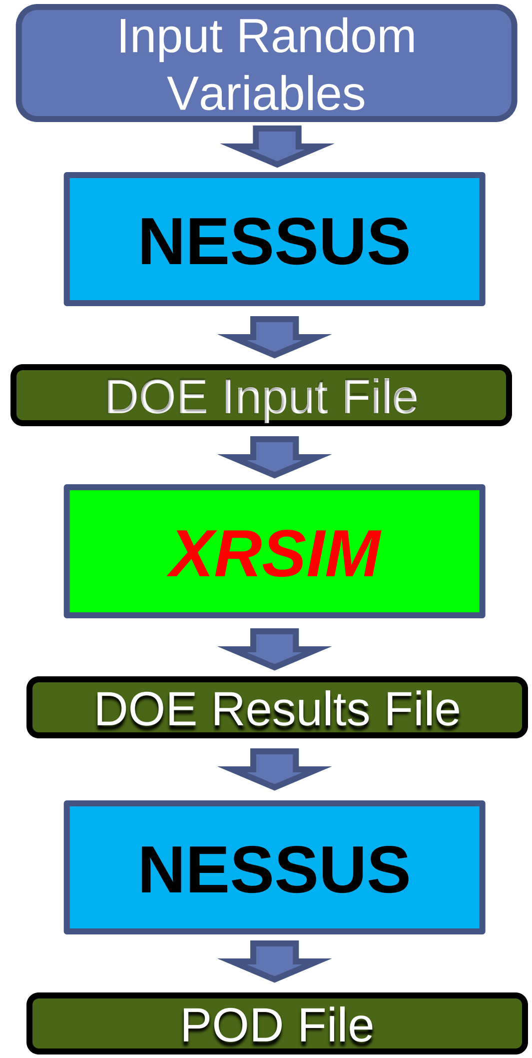

Process for Constructing Contrast Response Surface

- Identify ranges of XRSIM input variables
- Generate a table of XRSIM input data using design of experiments (DOE) approach in NESSUS
- Generate training data for each set in DOE table using XRSIM
- Construct a Gaussian Process response surface fit to the contrast training data using NESSUS

Variable	Units	Lower	Upper
Part orientation	deg	-2	2
Detector signal w/ grain diffraction	gs	1825	3175
Detector signal w/o grain diffraction	gs	2305	2695
Spherical porosity	µm	20	200

Input Variable Ranges

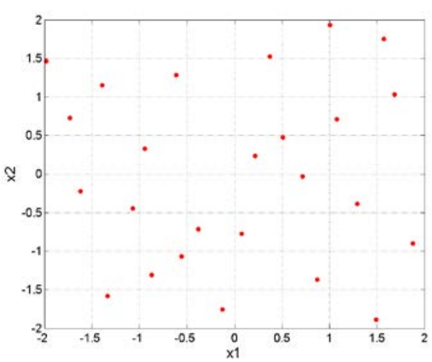

Design of Experiments

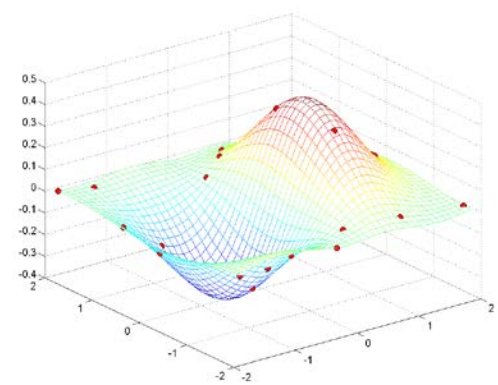

Response Surface

DARWIN GUI Overview

Design Assessment of Reliability With INspection

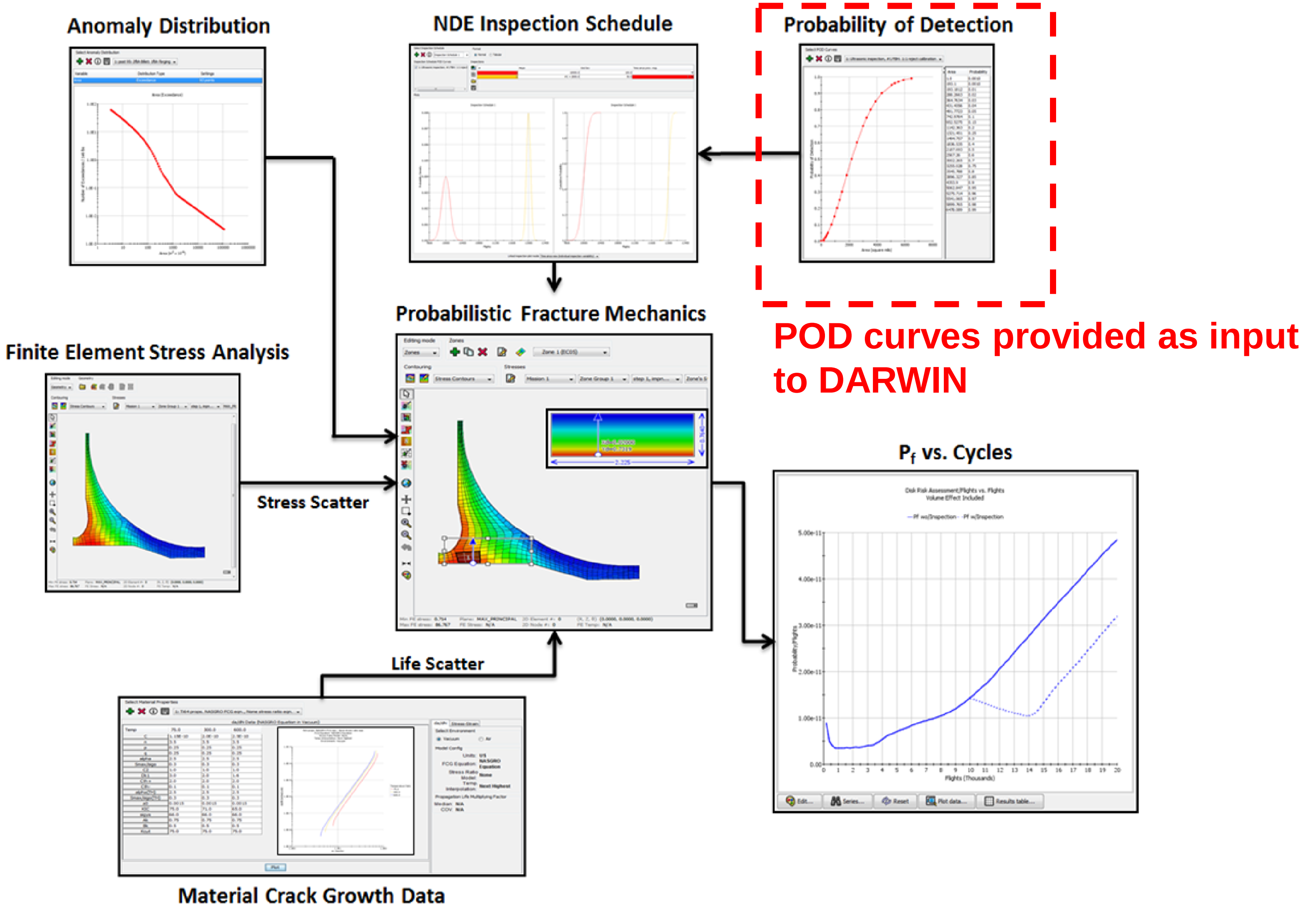

Linking XRSIM/NESSUS with DARWIN

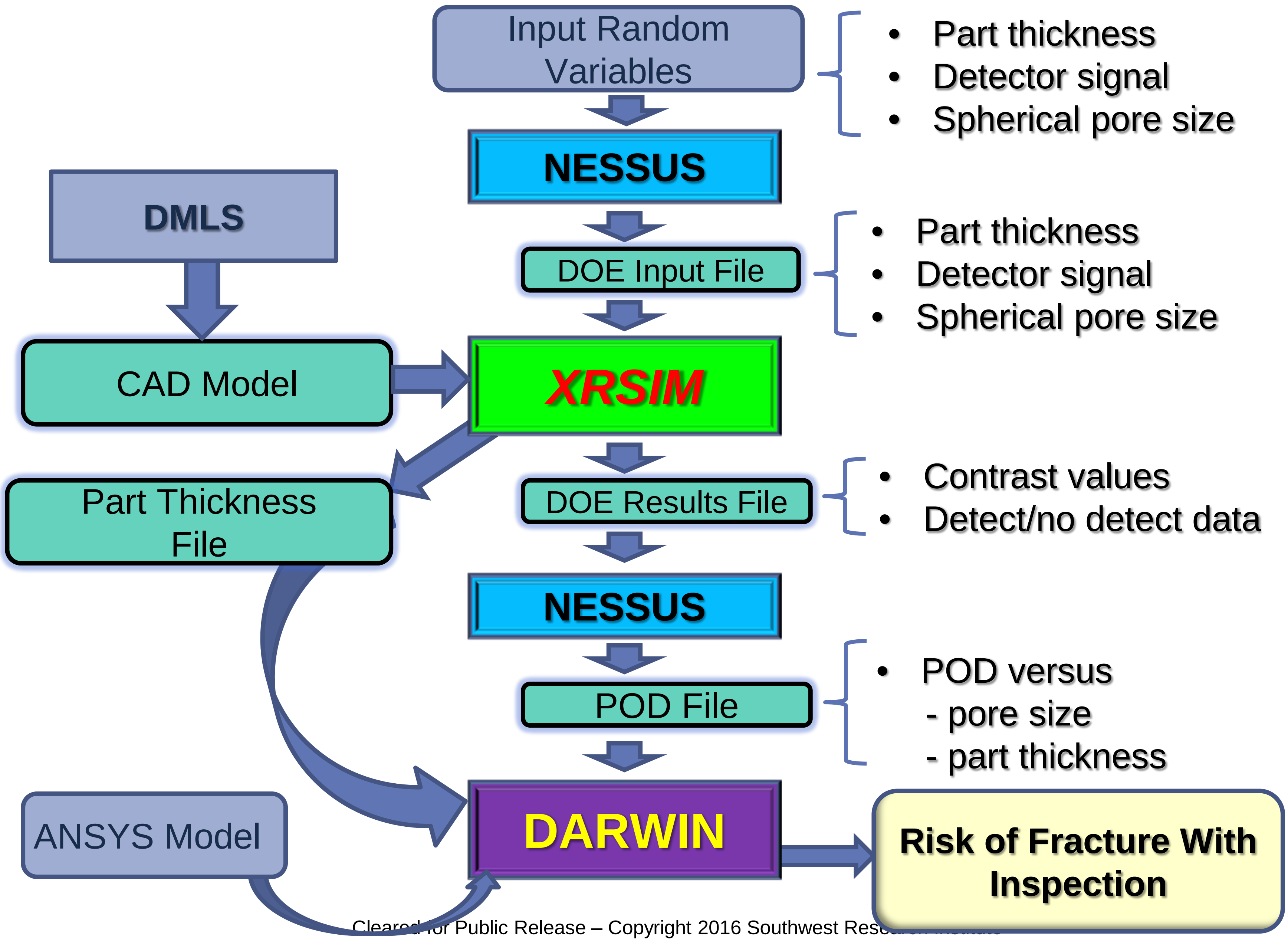

Application Example: Additive Manufacturing

- Actual engine mount developed under DARPA project (DMLS AM process, Ni 718 Alloy)

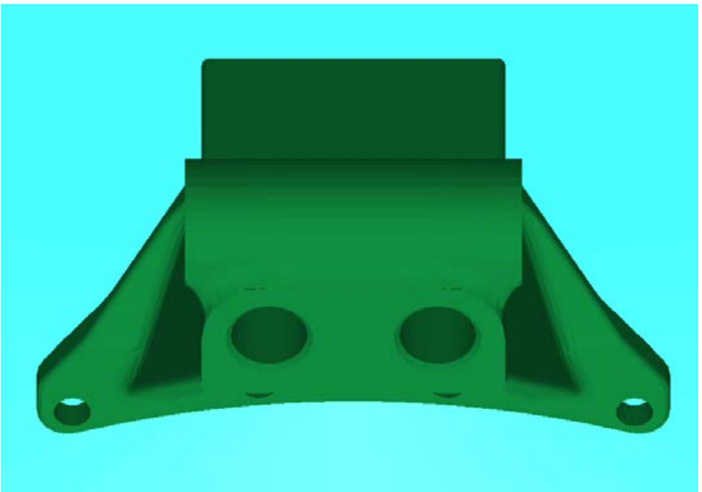

CAE Model

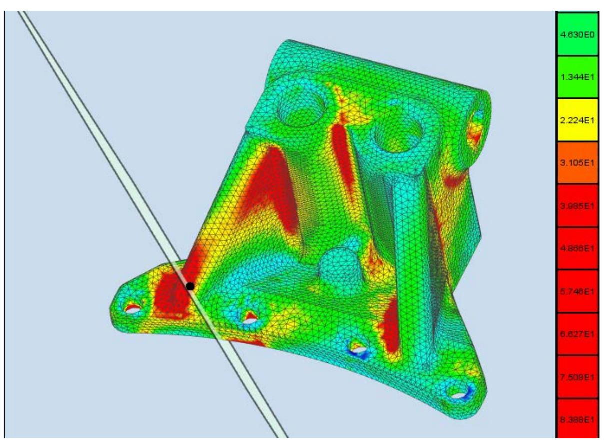

Location 1

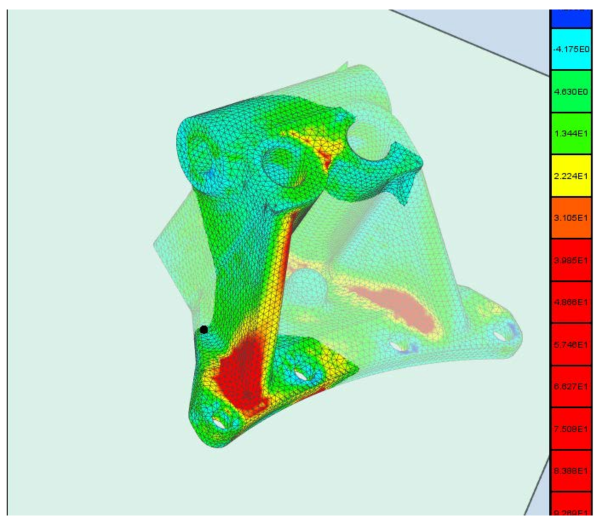

Location 2

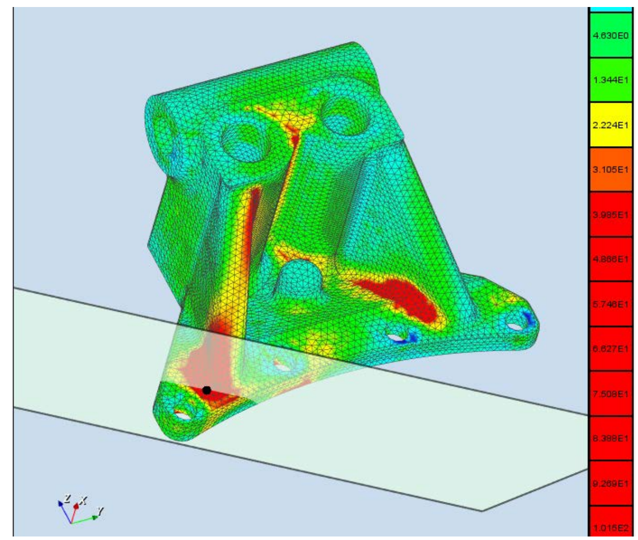

Location 3

XRSIM Input Variables

- Geometry complexity implies
  - Multiple orientations of the part
  - Several kilovoltage settings
- POD data assumes application of an inspection protocol where kilovoltage and orientations are fixed
- Key parameters controlling contrast
  - Part thickness
  - Pore size
  - Detector signal (grey scale)
  - Contrast noise

XRSIM Thickness Maps

Front View

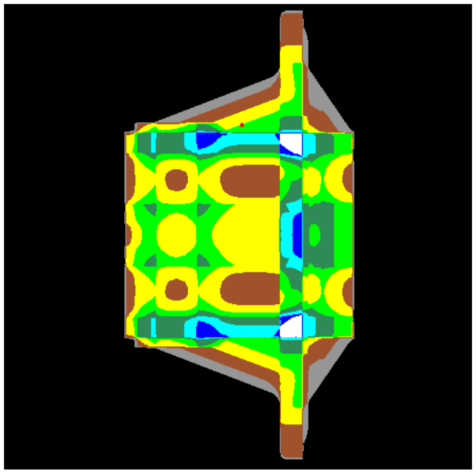

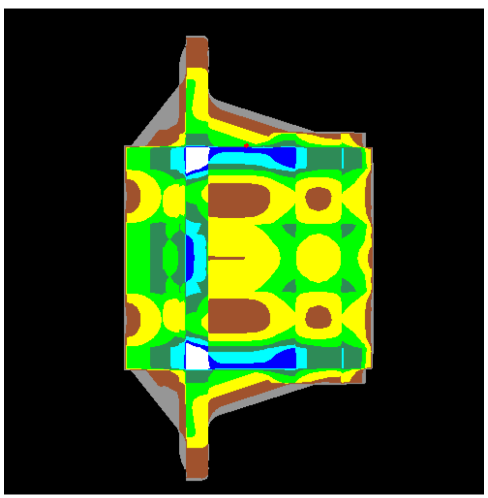

Back View

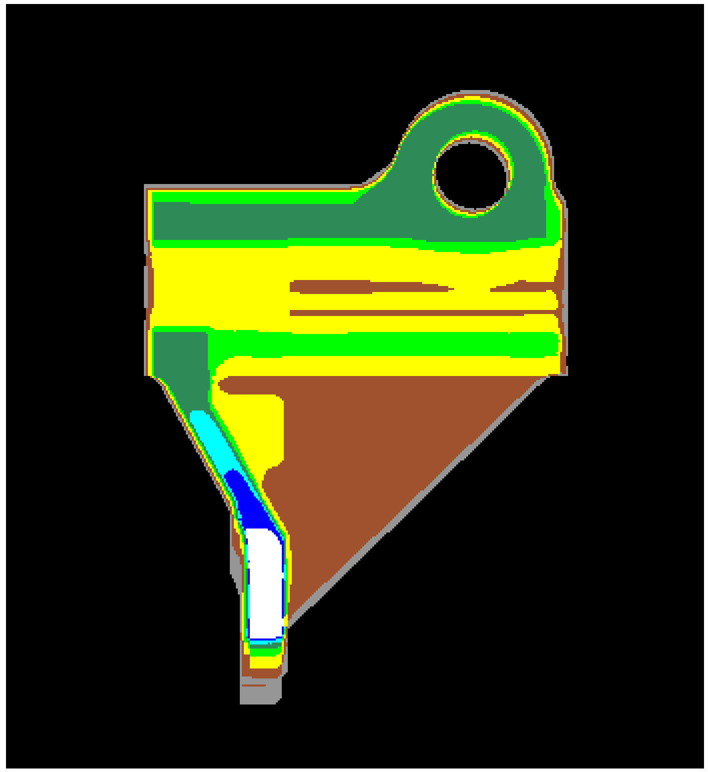

Top View

0.000 - 0.000 cm	0.634 - 1.269 cm
0.000 - 0.634 cm	1.903 - 2.537 cm
1.269 - 1.903 cm	3.171 - 3.806 cm
2.537 - 3.171 cm	4.440 - 5.074 cm
3.806 - 4.440 cm	

Thickness Legend

Right View

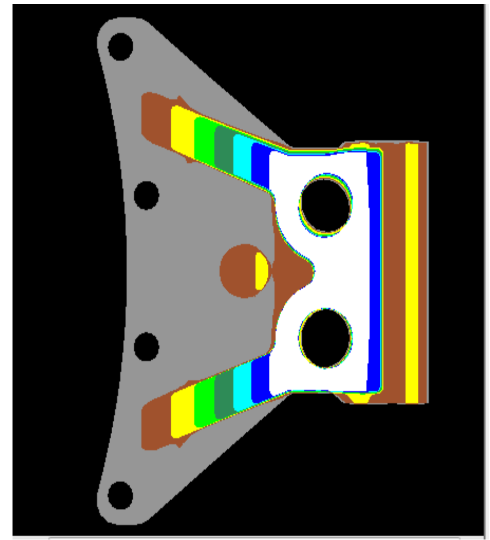

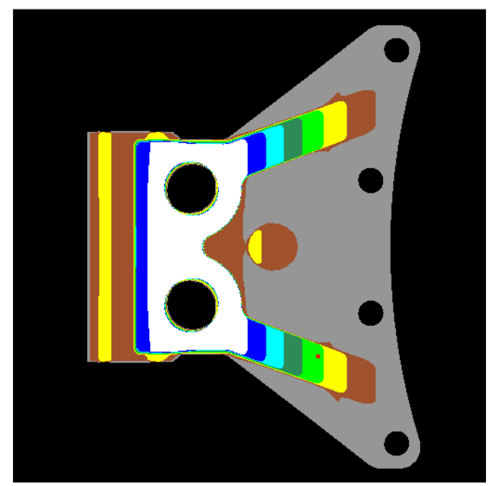

Left View

Detectability Maps from XRSIM at Several Orientations

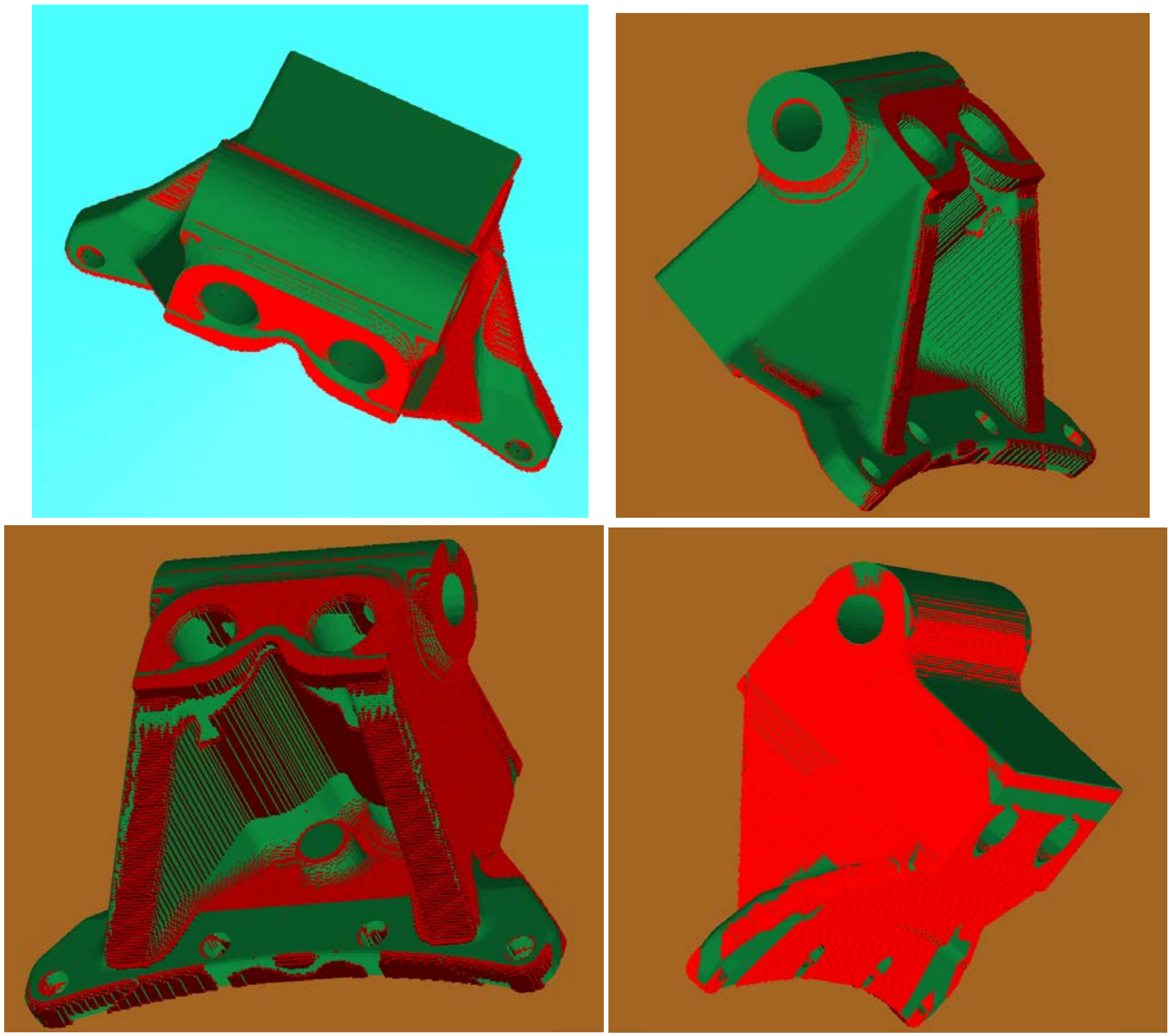

Probabilistic Model of Human Detectability Contrast Threshold

Detect/no detect results

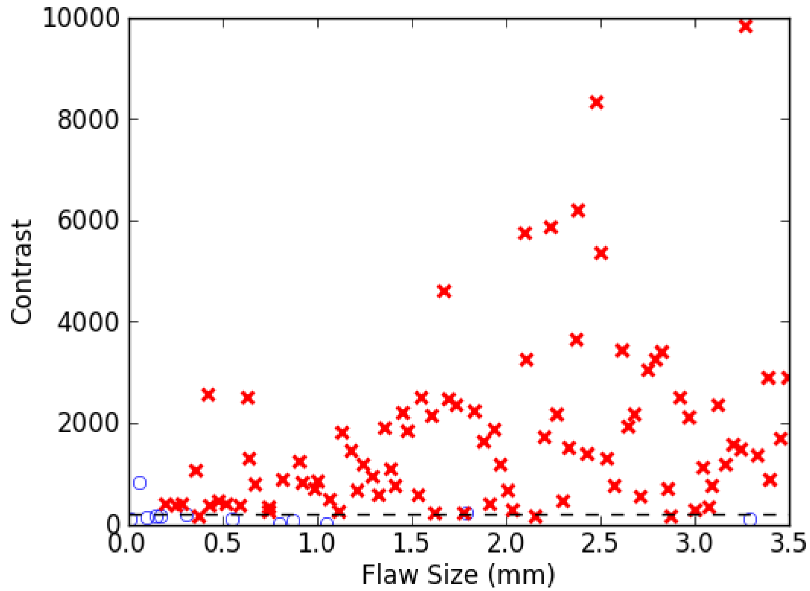

Zoomed in to show detail near threshold

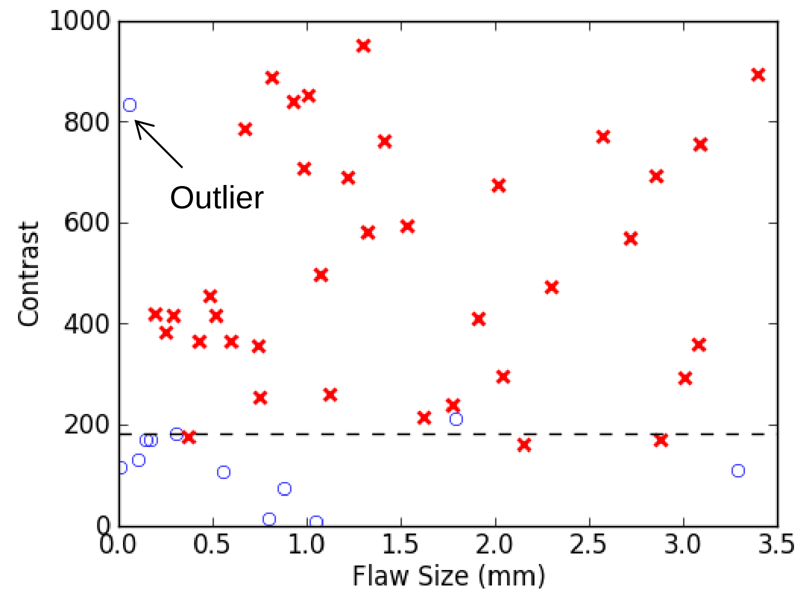

- Threshold value estimated based on 100 XRSIM results and corresponding detect/no detect data from NDE Technologies
- Detection does not follow a strict rule based on a single threshold value, so threshold modeled as a random variable
- Maximum likelihood used to estimate threshold mean and standard deviation, assuming normal distribution: Mean=183, Stdev=41

Probability of Detection Curves

- Deterministic input variables:
  - Part thickness
  - Pore size
- Random input variables:
  - Detector signal: Uniform (10,14000)
  - Contrast noise: Normal (0,79)
  - Contrast threshold: Normal (183,41)
- POD curves were computed using Monte Carlo simulation combined with conditional expectation
  - POD = Probability [Contrast > Contrast threshold]

Location 1 Results

Orientation 1 Thickness = 8.1 mm (0.319 in)

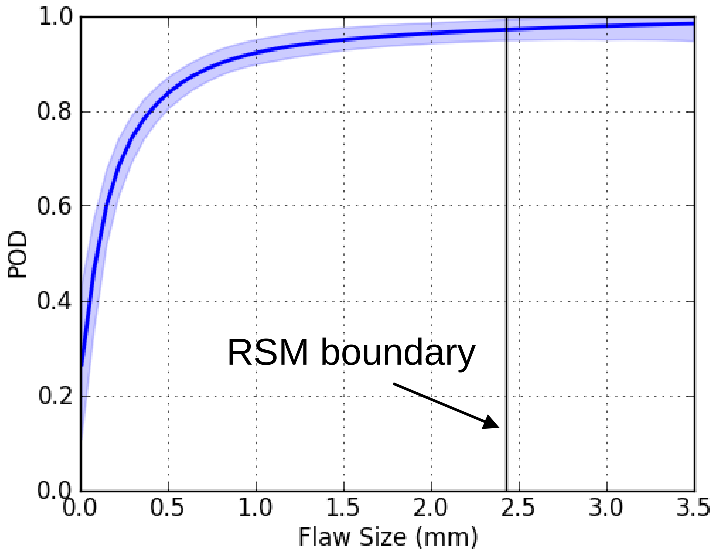

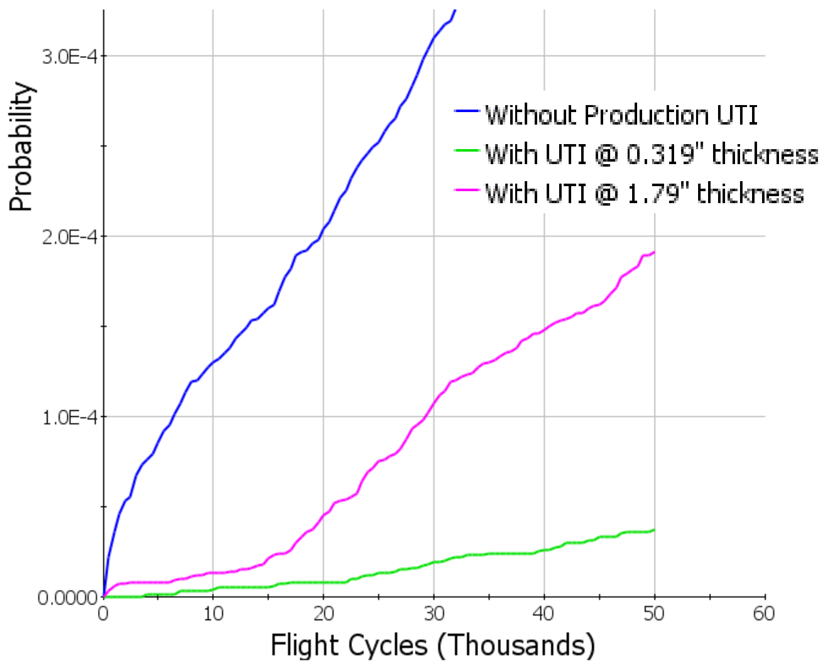

Orientation 2 Thickness = 45.45 mm (1.79 in)

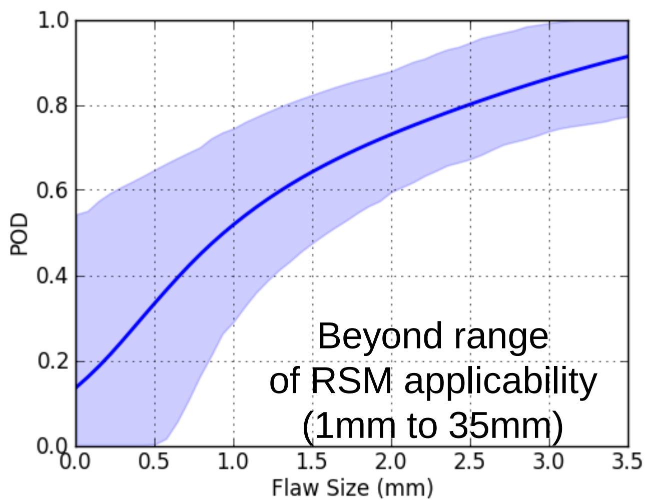

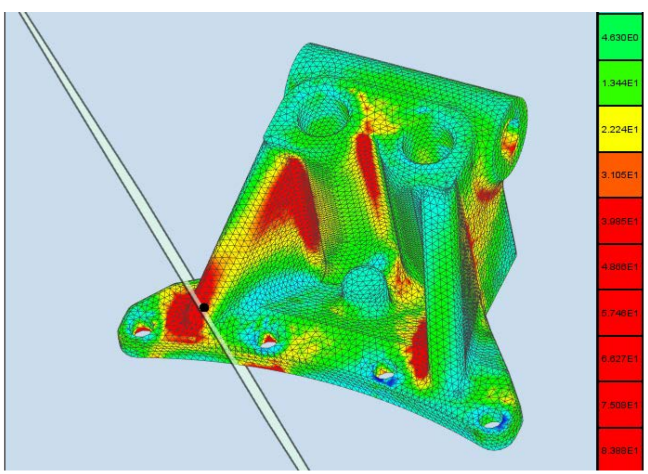

Influence of NDI on Manufacturing Anomaly Distribution

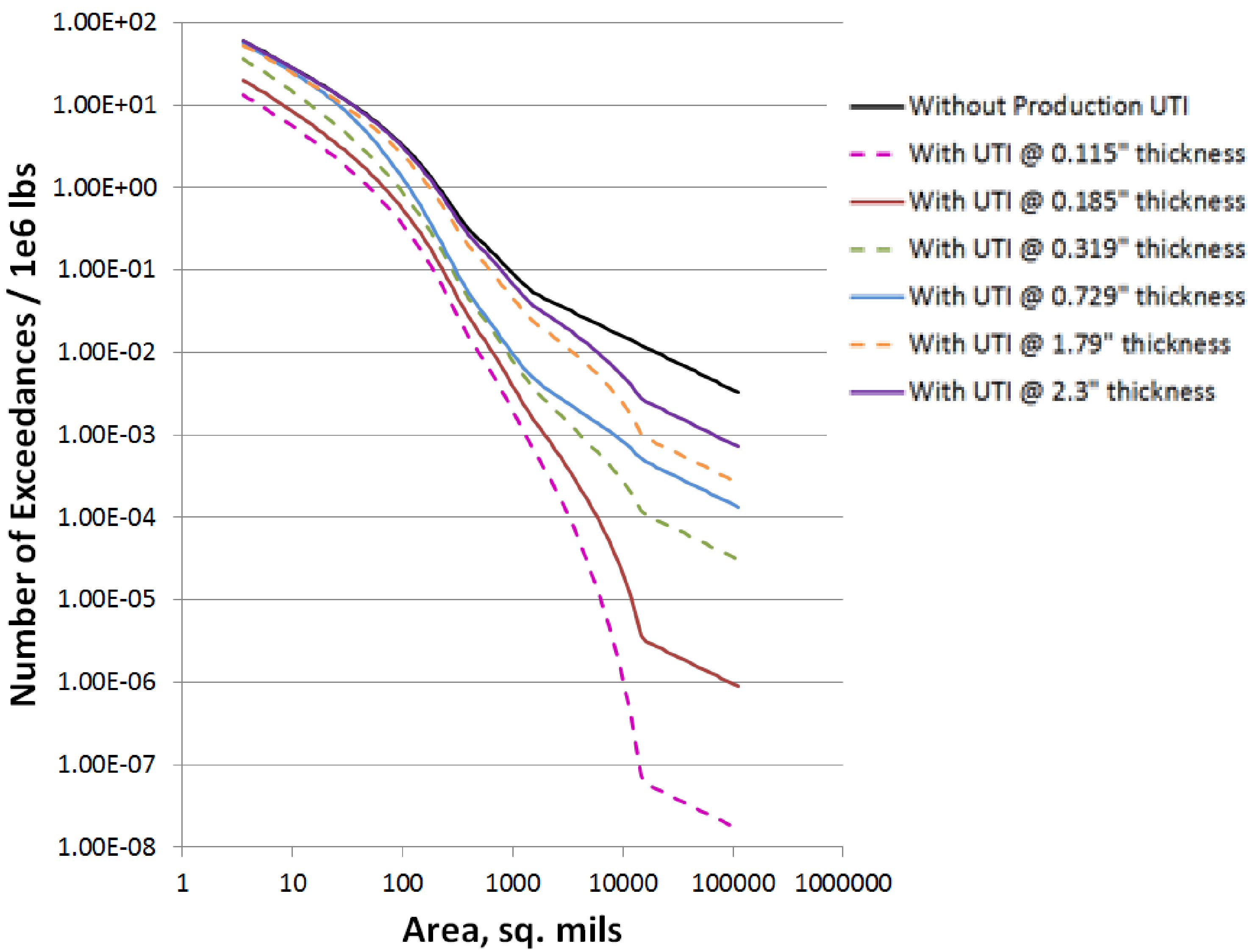

Summary

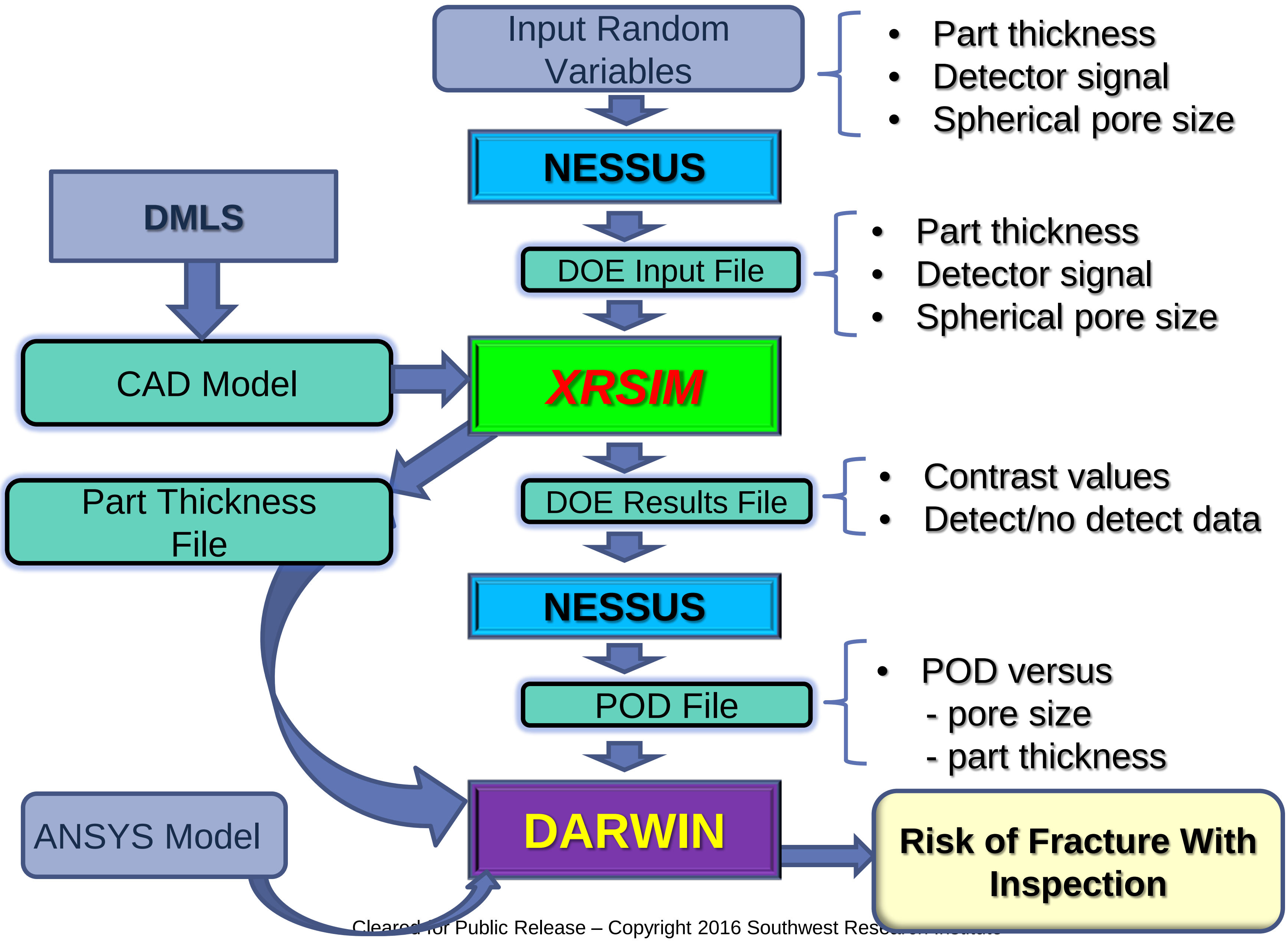

Input Random Variables
• Part thickness
• Detector signal
• Spherical pore size
NESSUS
DMLS
DOE Input File
• Part thickness
• Detector signal
• Spherical pore size
CAD Model
XRSIM
Part Thickness File
DOE Results File
• Contrast values
• Detect/no detect data
NESSUS
POD File
• POD versus
- pore size
- part thickness
ANSYS Model
DARWIN
Risk of Fracture With Inspection

Continuing Tasks

- Automate POD curve creation in XRSIM
- Automate transfer of location-specific POD curves from XRSIM to DARWIN
- Implement inverse calculation of critical initial crack size in DARWIN and transfer to XRSIM
- Verification and validation

Potential Future Extensions

- Use the integrated XRSIM-DARWIN modeling system to optimize NDE scan plans
- Combine with ICME models of the AM process (including models of microstructure and defect formation) to optimize the AM process itself

Role of Material Properties

- The fracture risk simulations also depend on known/assumed values of material properties (e.g., FCG)
- The uncertainties in these properties could be included as another random variable in the fracture risk simulations
- The material properties will be functions of the local microstructure, which will depend on the manufacturing process and the location/orientation within the part

Effects of HIP Processing on EB-DED Additively Manufactured Ti-64 Materials

LOCKHEED MARTIN

Hank Phelps
Jeff Langevin
Adam Sutton

Outline

- Background on EB-DED
  - Process
  - Flaw Types
  - Potential Applications
- Hot Isostatic Press Process
  - Why Considered
  - Benefits
- Impacts on Mechanical Properties
- Summary
- Conclusions

EB-DED Process

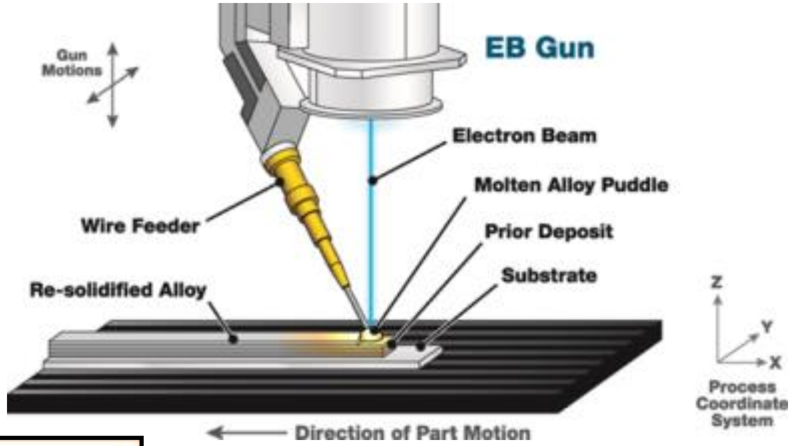

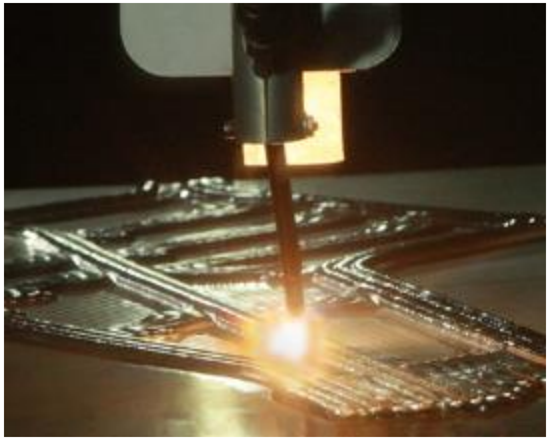

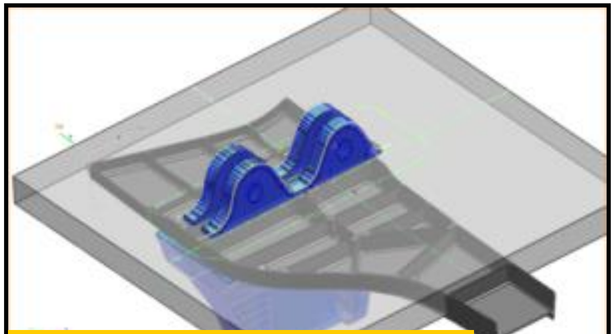

NC Path Planning and Deposition

Near-shape Article

Machine Part

Examples of Discontinuities

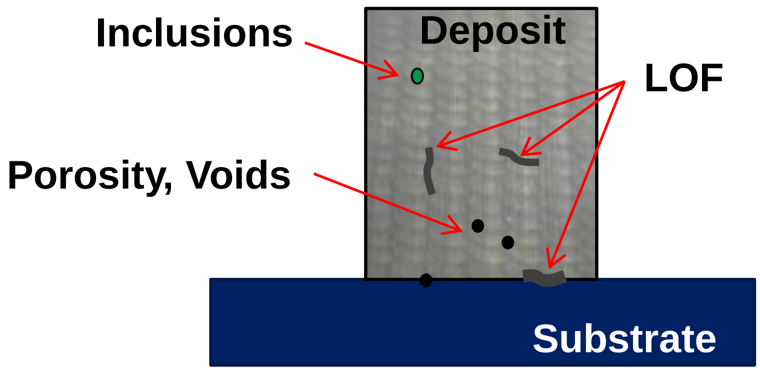

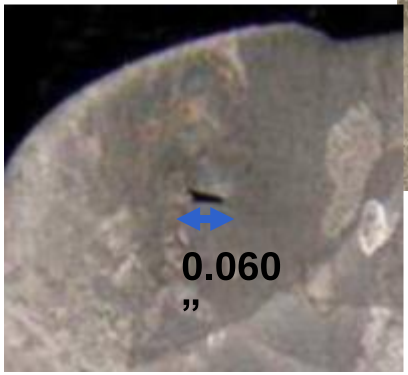

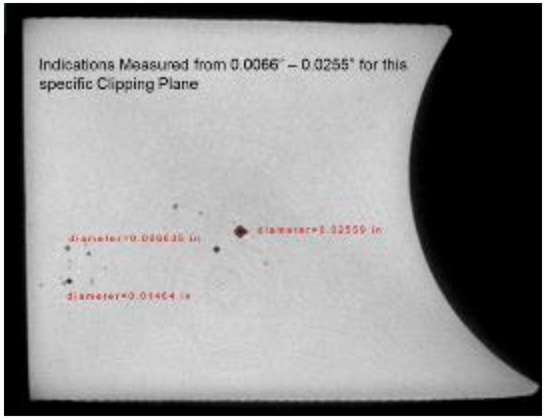

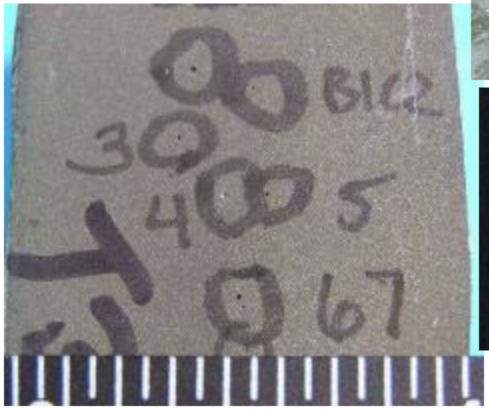

Potential Applications

Vertical Tail

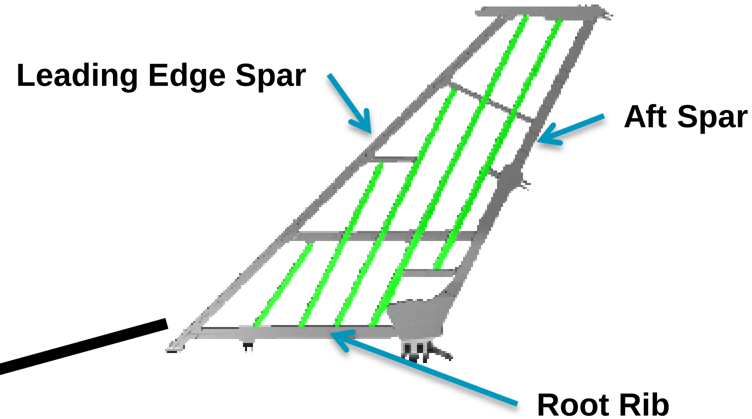

Canopy Bowframe

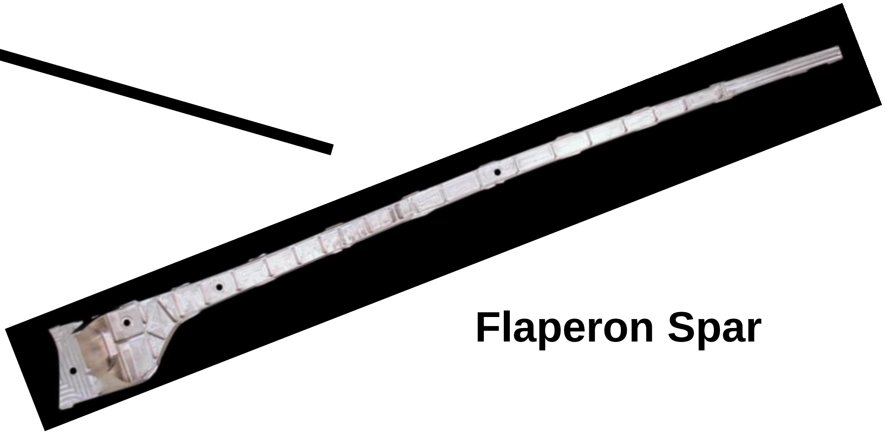

Flaperon Spar

Planned EB-DED Process Flow

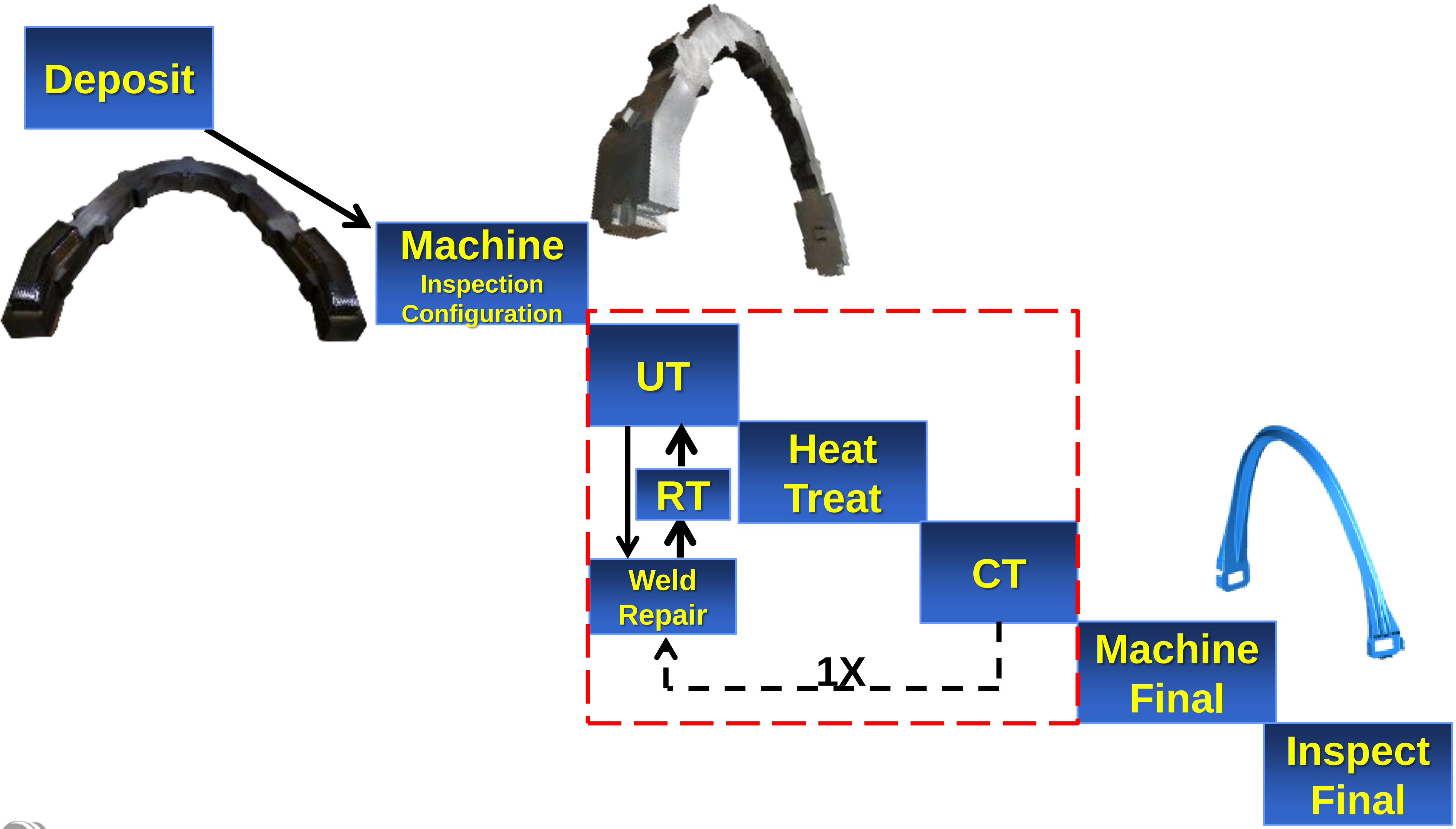

Alternative Process Flow

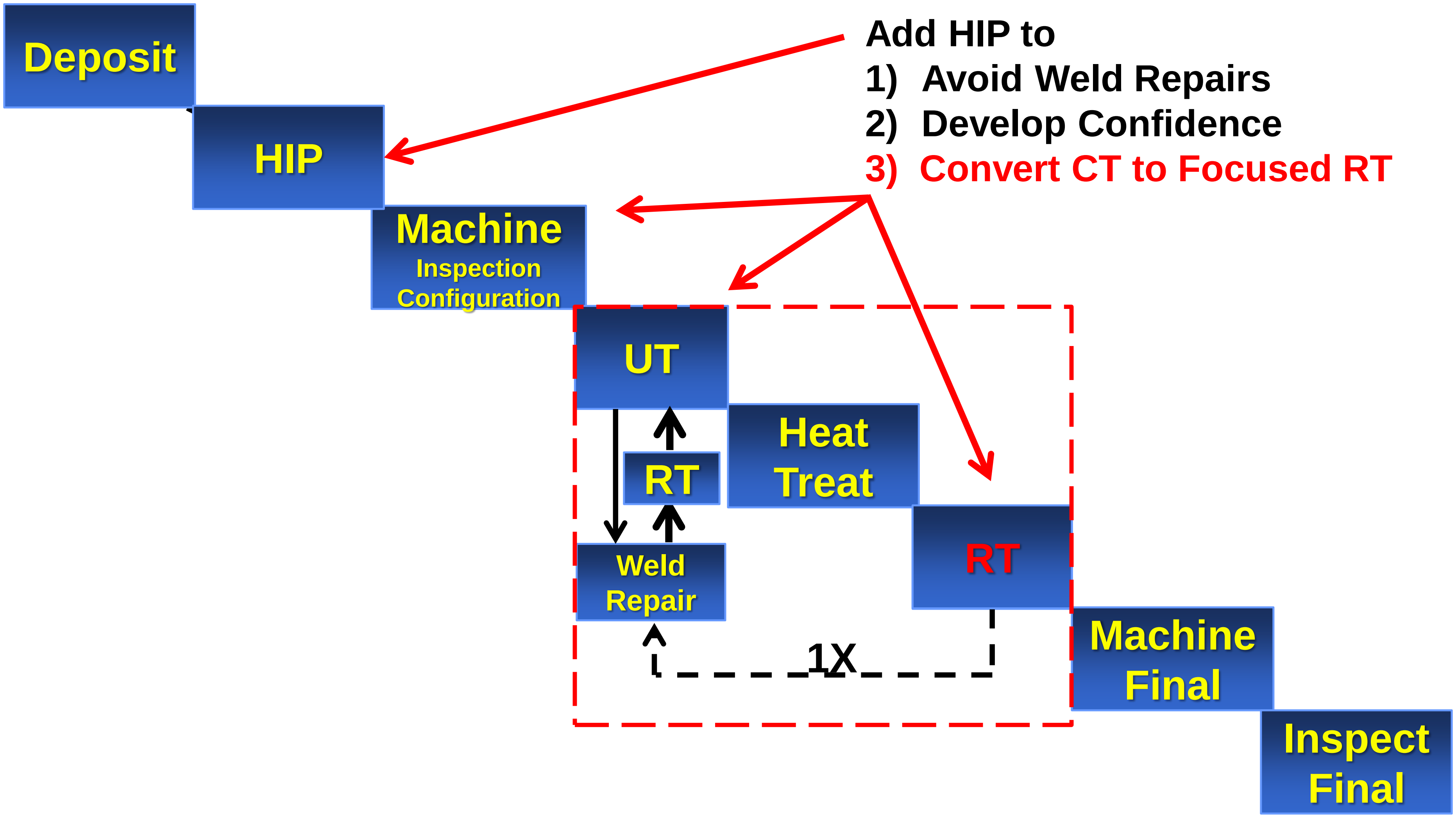

HIP Mitigation of Internal Flaws

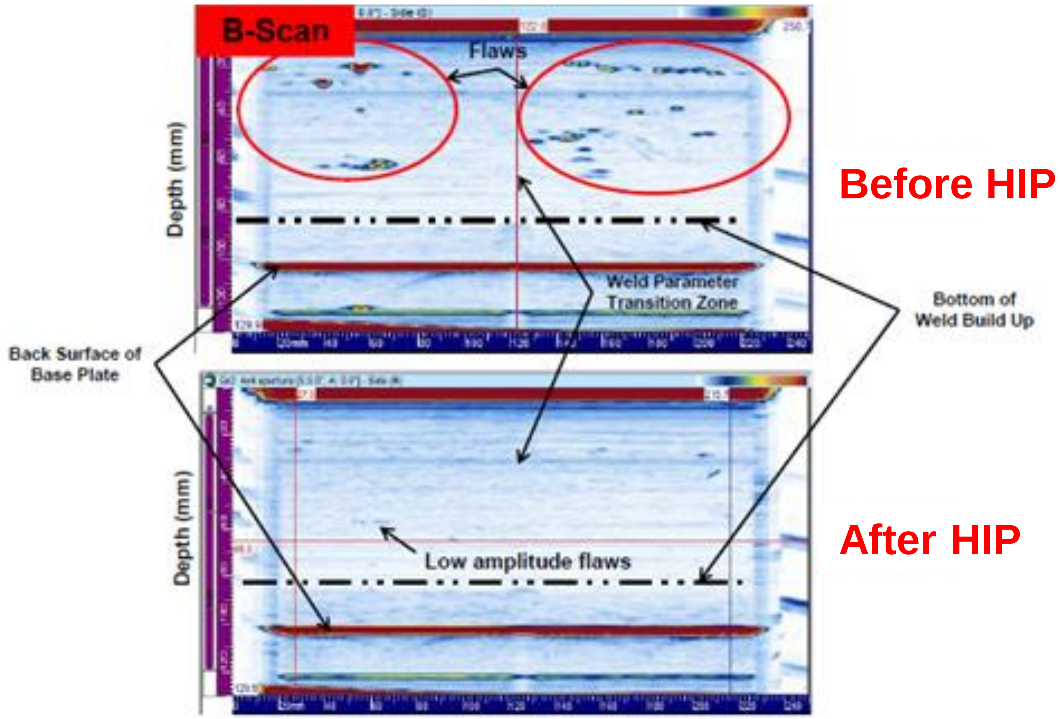

Refining Microstructure of Additive Manufacturing Materials to Improve Non-Destructive Inspections (NDI)(4034.001)

EB-DED Preforms

Condition	Process
Baseline	EB-DED + BA
HIP	EB-DED + HIP + BA

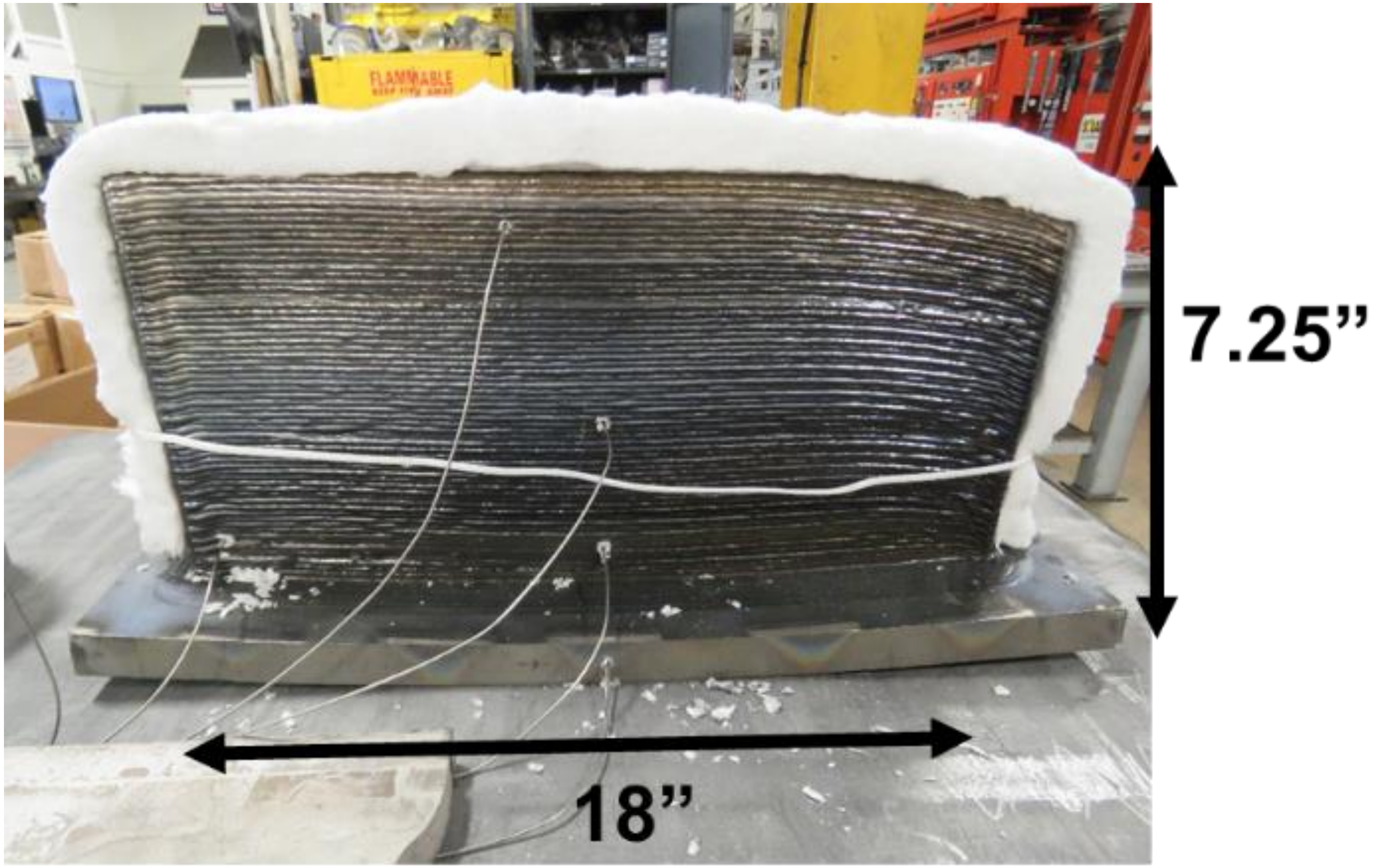

Tensile Results

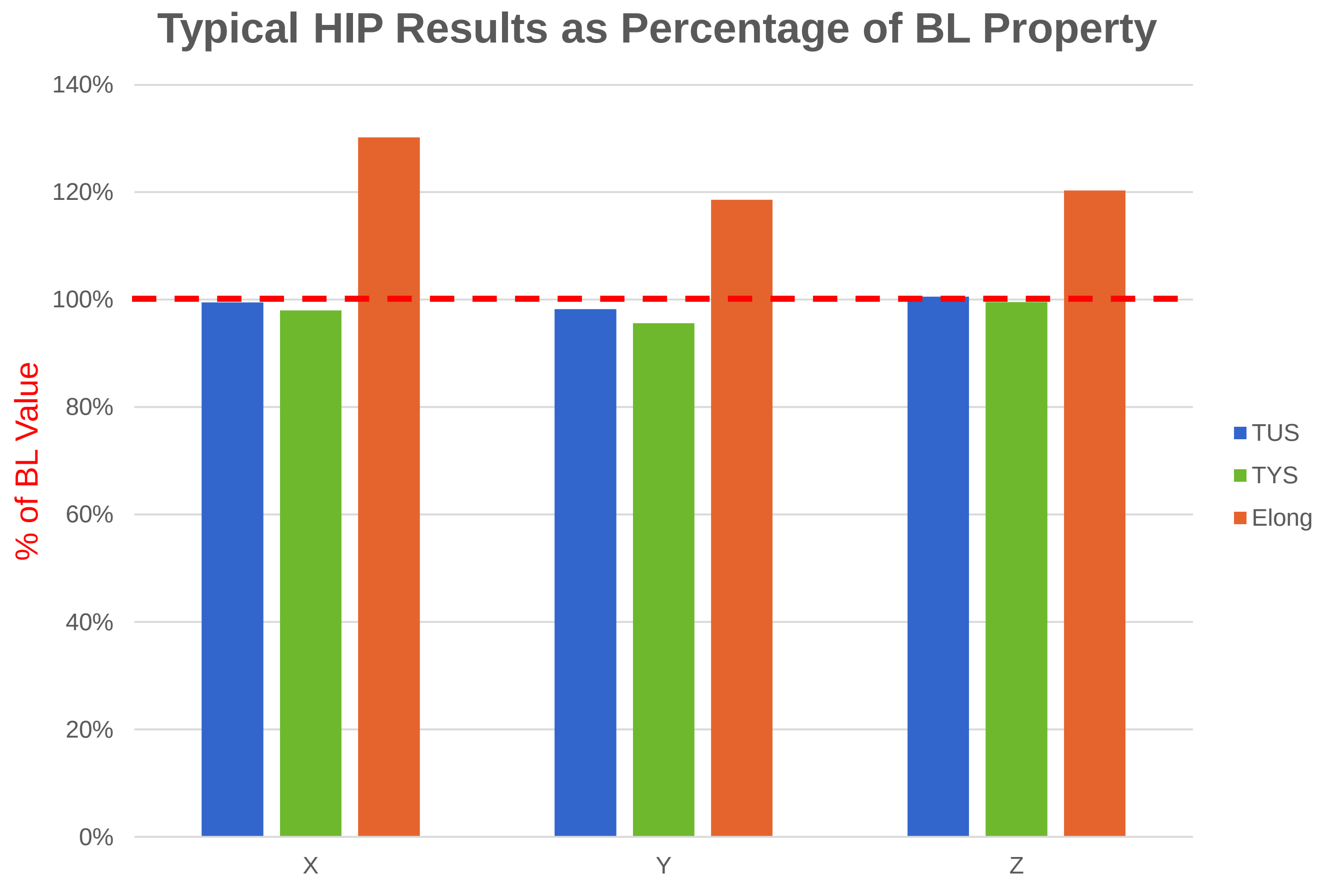

Fracture Toughness

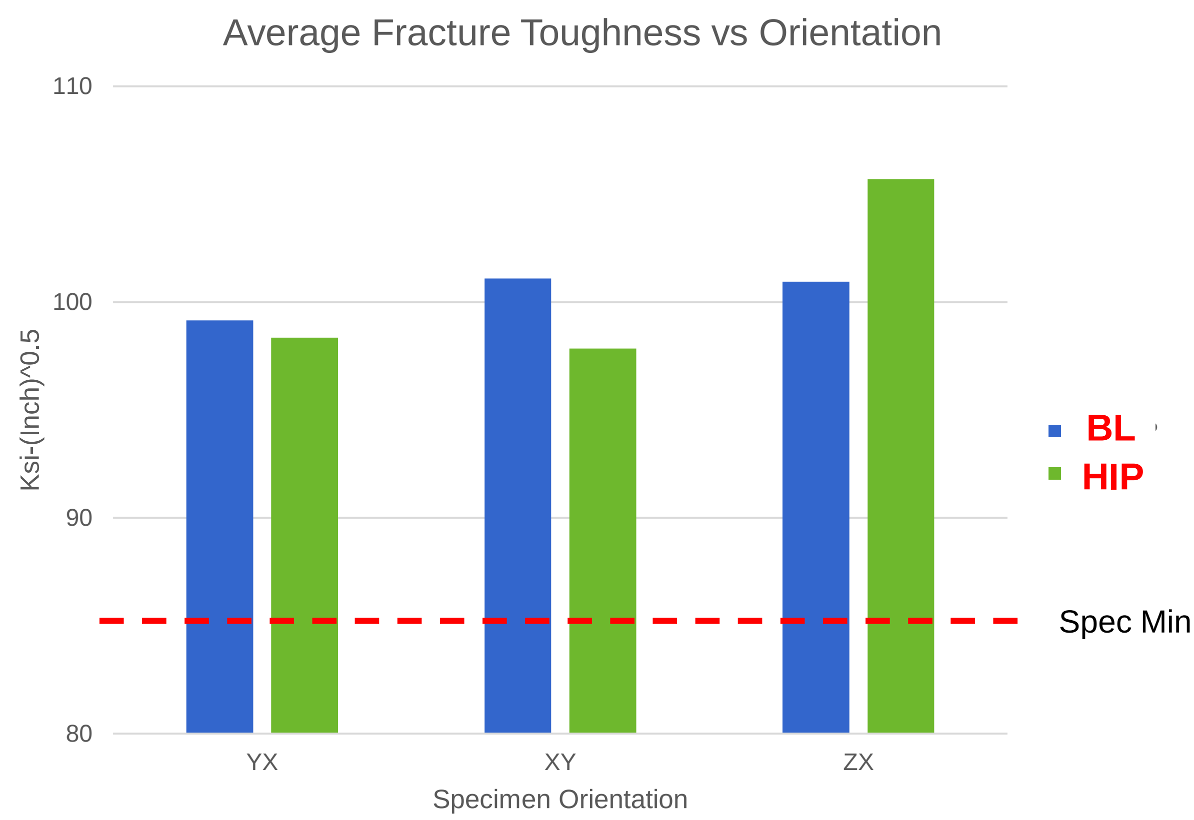

Strain Life Results (R=-1.0)

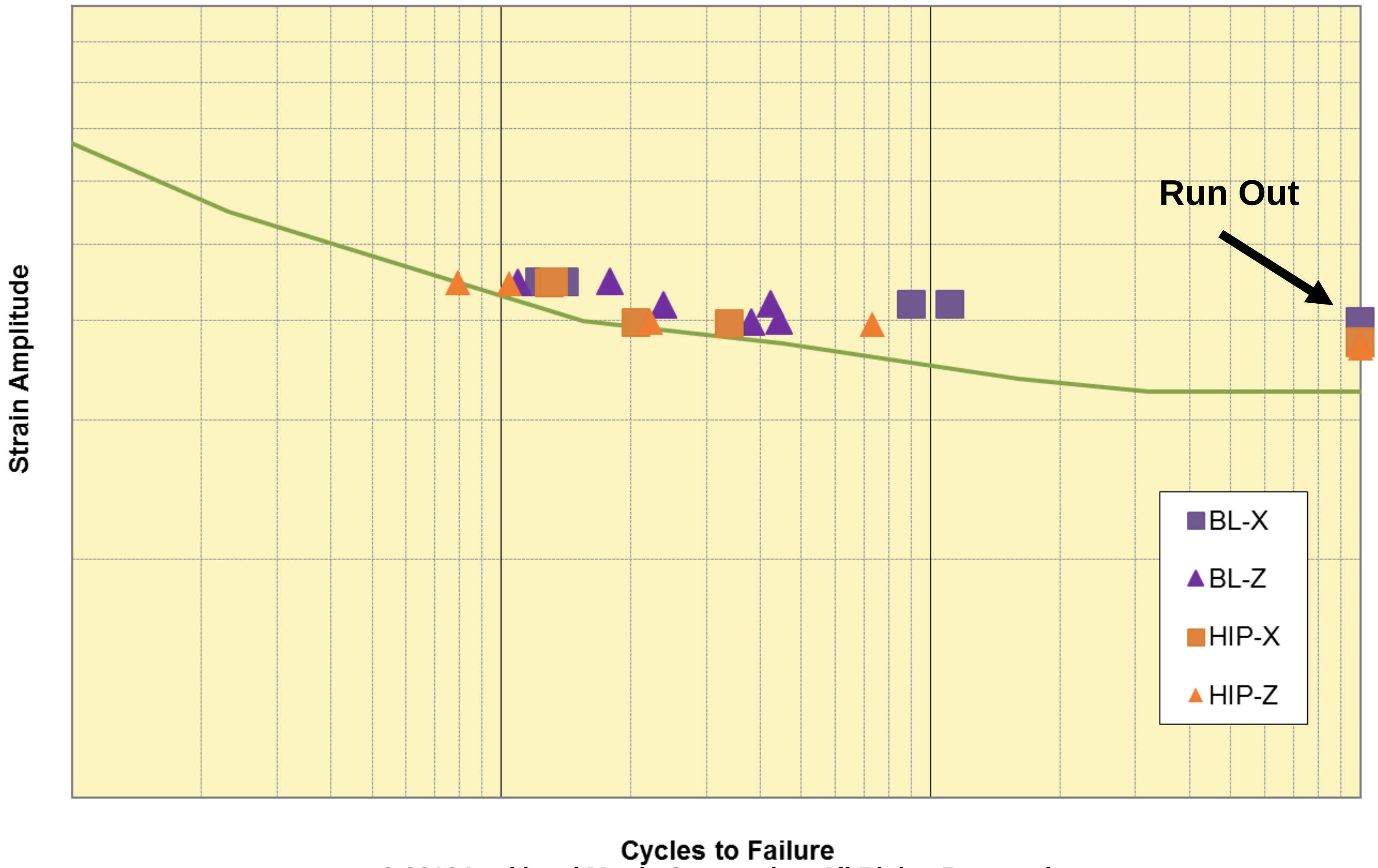

Fatigue Crack Growth Results

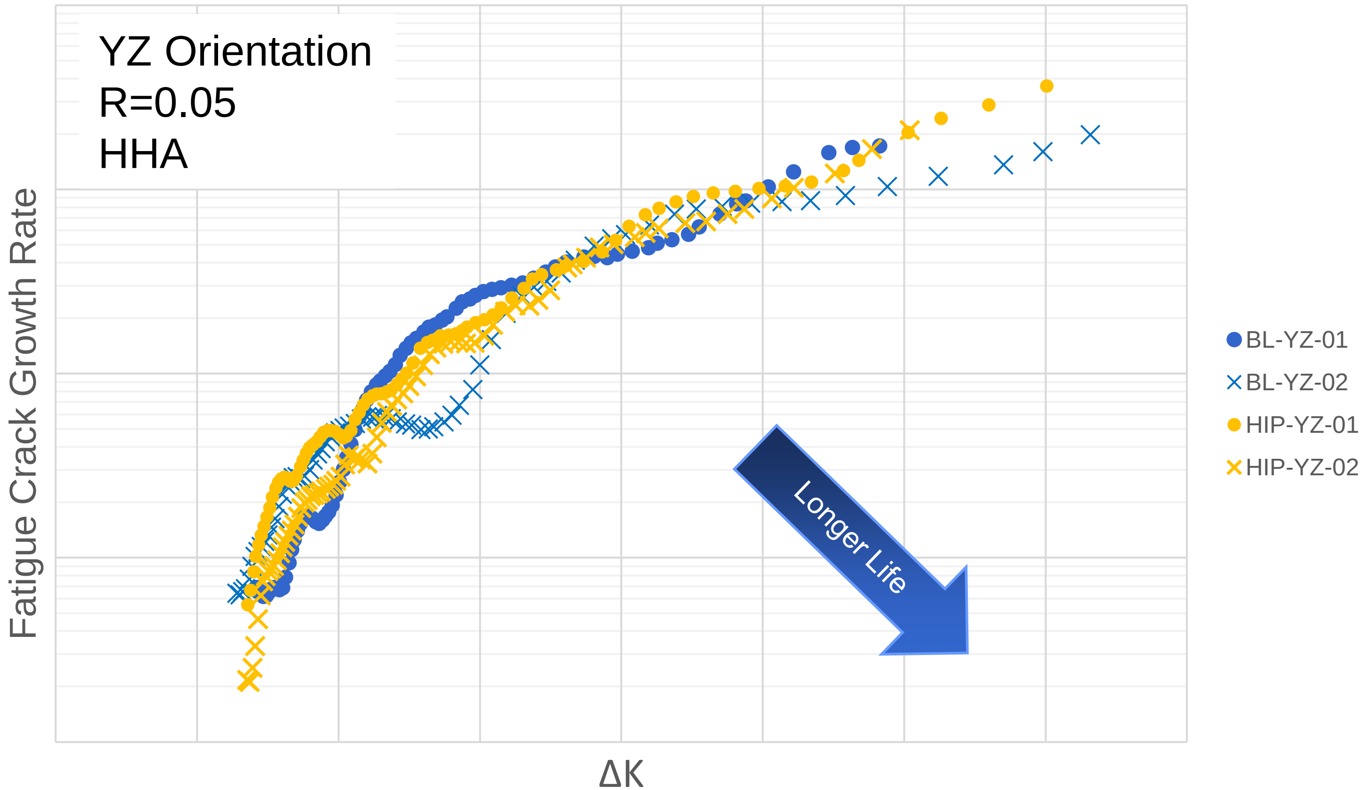

UT Inspection Results

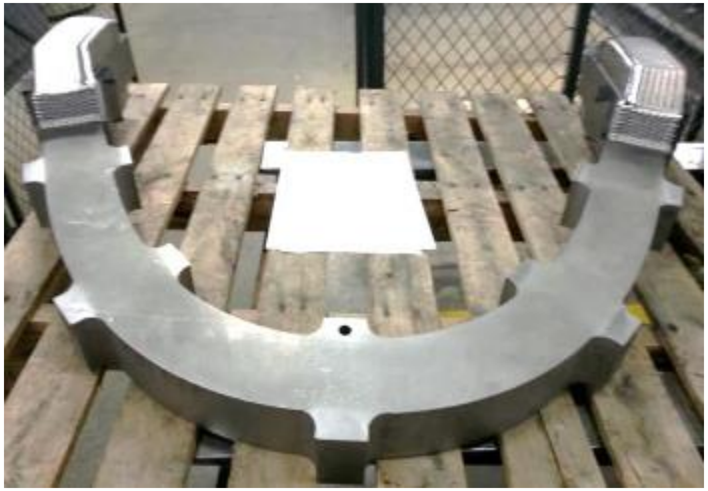

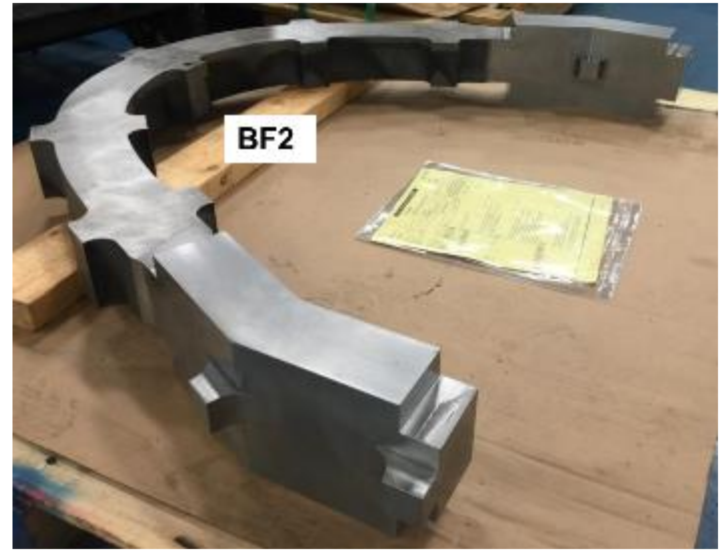

HIP

BL

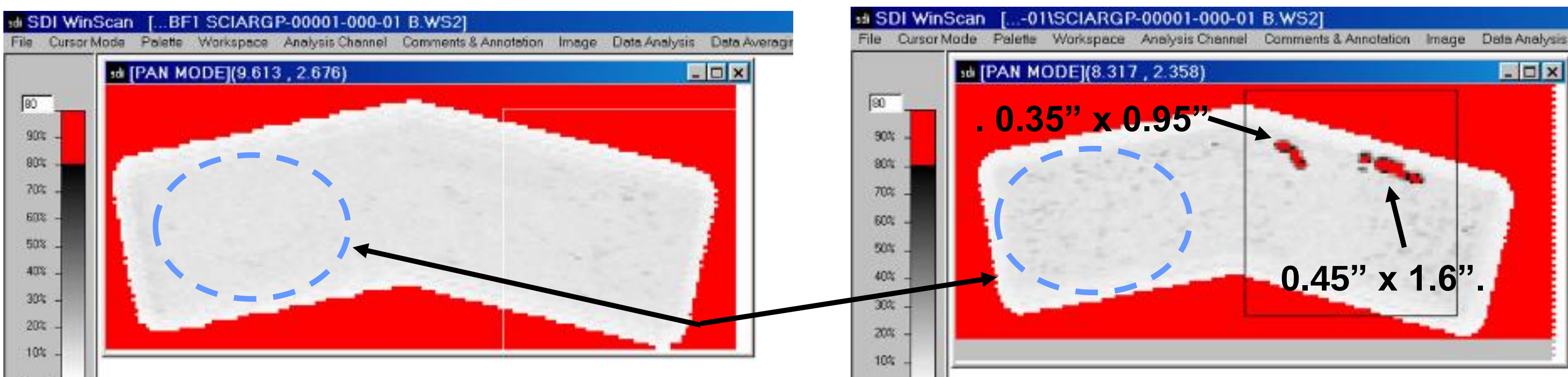

Transducer: 0.75” Diameter, 5 MHz, 6” Focus Immersion

Note – Lg LOF Result of Process Breakdown

Summary

Property	Effect of HIP	Note
Tensile UTS Yield Elongation	• X/Y < 2% Z Equivalent • X/Y < 5% Z < 1% • Increased 11 to 22%	Reduced Scatter
Fracture Toughness	• No Impact	
Strain Life	• Supports Existing Design Curve	
Fatigue Crack Growth	• Supports Existing Design Curve	
Ultrasonic Inspection	• Improved Inspectability • No Rejectable Indications	

Conclusions

- EB-DED Process Capable of Producing Large Aerospace Components
  - High Build Rates
  - Internal Material Quality Still an Issue
- Hot Isostatic Pressing
  - Capable of Closing & Healing Internal Flaws
  - Minimal In-Plane Strength Reduction Offset by Lower Scatter
  - Improves Out of Plan (Z Direction) Strength
  - No Other Significant Property Impacts
  - Recommended for Inclusion for Critical Components

Acknowledgements

- **Mike Mesick – LM NDI Level III**
- **Scott Stecker – Sciaky**
- **Andy Mugnaini – Sciaky**

ASTM E08 Fatigue and Fracture - Workshop on Mechanical Behavior of Additive Manufactured Components

Fatigue Life Manipulation of SLM® Parts

Wadim Reschetnik,
Richard Grylls, Benjamin Bauer,
Hans Albert Richard, Gunter Kullmer

Direct Manufacturing Research Center
Paderborn University – Germany
SLM Solutions NA, Inc.

Agenda

1. Additive Manufacturing – Selective Laser Melting - SLM®
   - SLM Solutions NA, Inc.
   - Selective Laser Melting System SLM® 280^{HL} and 500^{HL}
   - Qualified Materials

2. Project Fatigue Life Manipulation
   - Direct Manufacturing Research Center – DMRC
   - Motivation and Aims of the Project

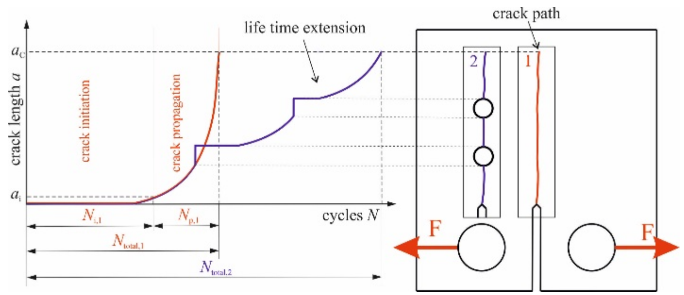

3. Experimental Investigation
   - Setup and Testing Methods
   - Fatigue properties of SLM® materials
   - Fatigue Life Manipulation by Notches

4. Conclusion

SLM Solutions NA, Inc.

Formerly: **HEK GmbH** • **MCP HEK Tooling GmbH** • **MTT Technologies GmbH**

SLM Solutions NA, Inc. | 28350 Cabot Drive, Suite #100, Novi, MI 48377 | 248.243.5400 | info@slm-solutions.us | www.slm-solutions.us

SLM Solutions Group AG – a deep rooted 3D printing heritage

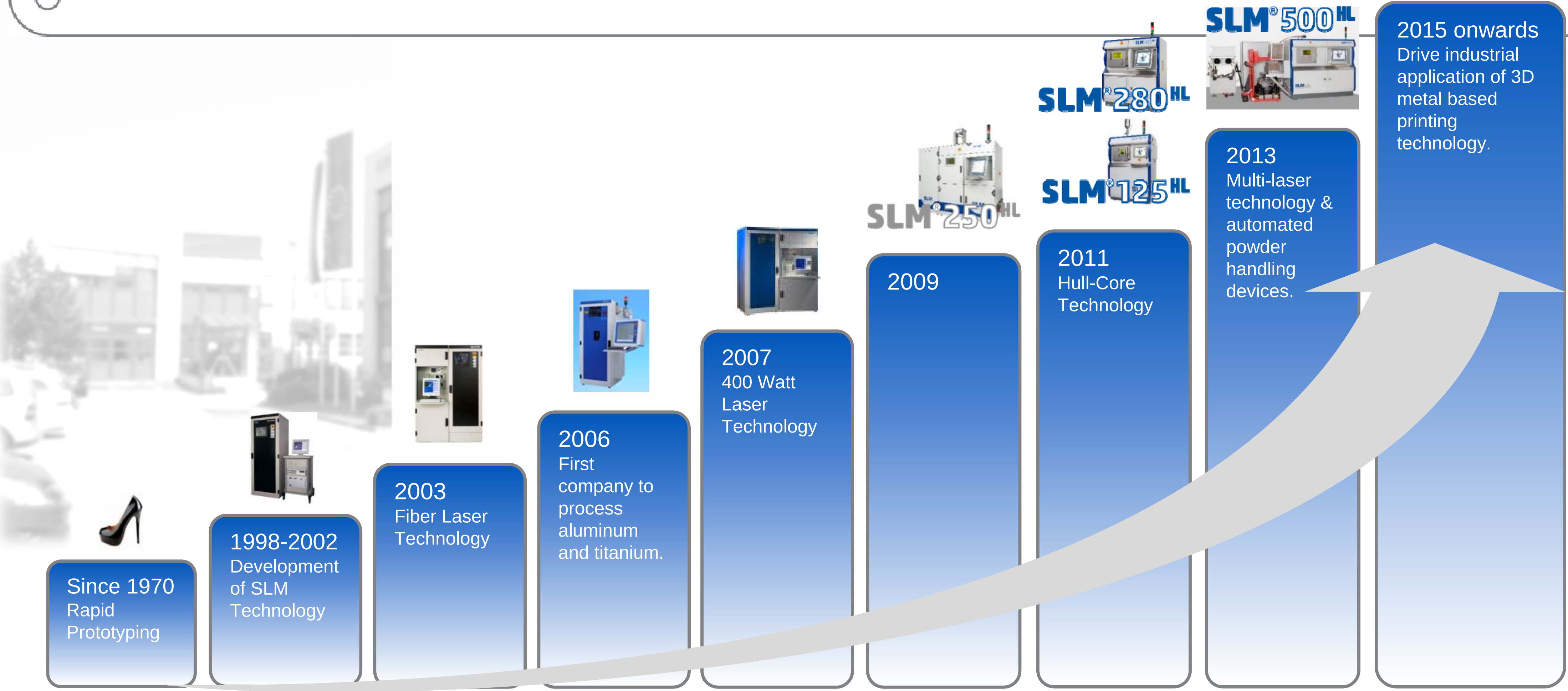

Note: History of SLM Solutions Group and its predecessors
Source: Company information

SLM®280HL

35% faster than the competition with twin-laser technology

- 280 x 280 x 350 mm build envelope
- Built-in 400 W laser
- Option to add 1 additional 400 W (twin) or 1000 W (duo) laser
- Ideal for medium to high volume part production
- Closed-loop powder handling
- Patented bi-directional powder recoater movement
- Upgraded process control
- Open software architecture and system parameters
- Optimized gas flow and recirculation

Build Speed	**20 – 45 ccm/h**
Layer Thickness	**20 – 75 / 100 µm**
Operational Beam Focus	**80 – 120 / 700 µm**
Dimensions in mm (B x H x T)	**1800 x 1900 (2400) x 1020**
Weight	**approx. 1000 kg**

SLM® 500HL

The flagship system for larger complex metal parts.

- 500 x 280 x 365 mm build envelope
- 2 standard 400 W lasers
- Option to equip 4x 400 W (Quad Laser Technology)
- Lasers may be used independently or parallel in the build process
- Closed-loop powder handling
- Patented bi-directional powder recoater movement
- Adapter for higher platform temperatures
- Open software controls
- Optimized gas flow and recirculation

Build Speed	**55 | 105 ccm/h Twin | Quad**
Layer Thickness	**20 – 75 µm**
Operational Beam Focus	**80 – 150 µm**
Dimensions in mm (B x H x T)	**5200 x 2700 x 2800 (incl. PRS & PSX)**
Weight	**approx. 3100 kg**

SLM® 500HL

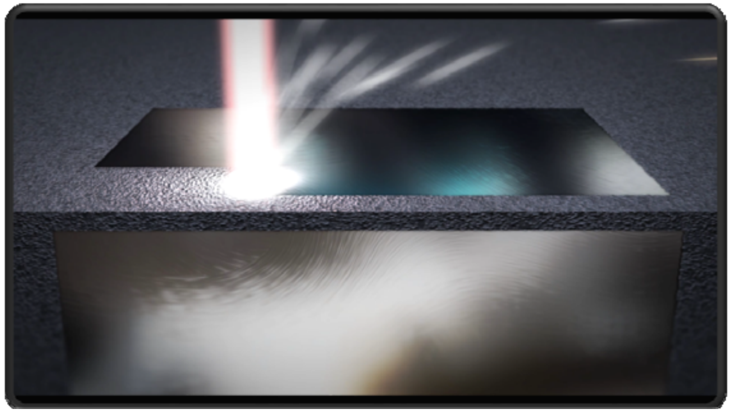

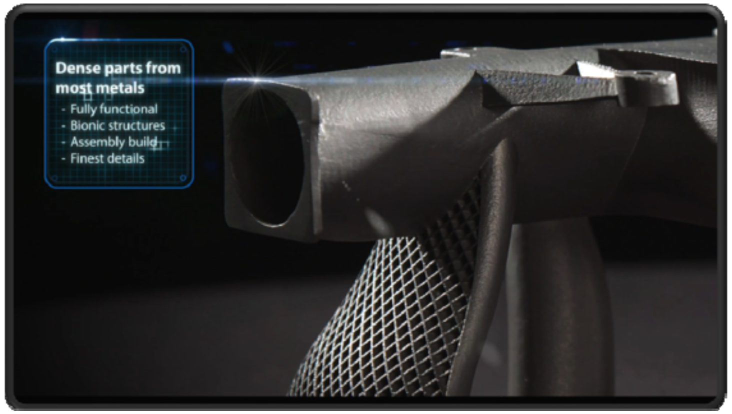

Dense parts from most metals
- Fully functional
- Bionic structures
- Assembly build
- Finest details

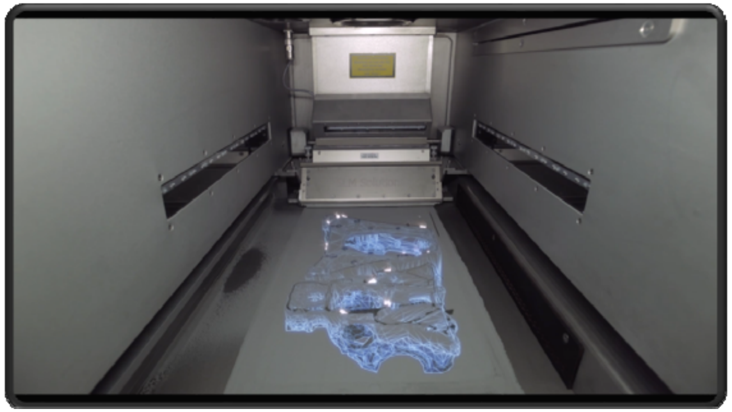

PRS 500
- Full powder removal
- Inert gas atmosphere
- Independent operation
- Full operator protection

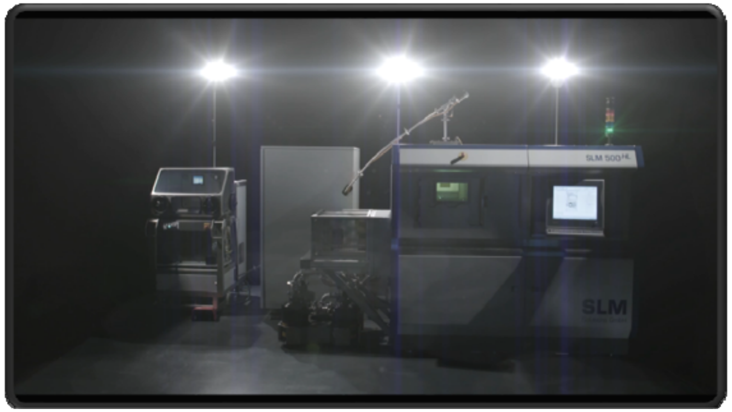

Qualified Materials

SLM Solutions

- **Continuous development of different materials. Certification due to customers needs and requirement.**
- Material data is available on a separate attachment. System parameters are available for the following materials:

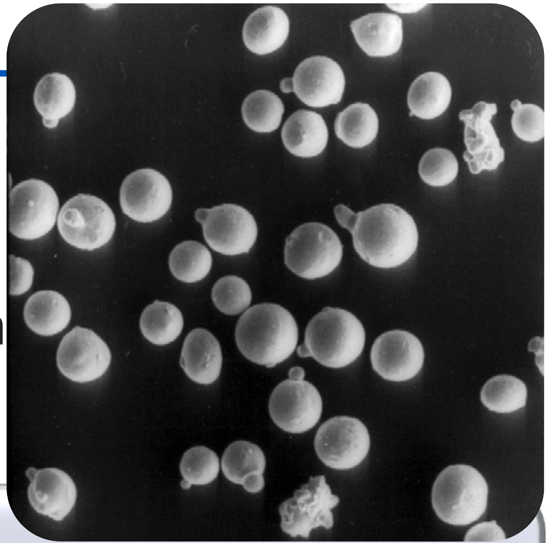

Stainless Steel:	316L (1.4404)	17-4 (1.4542)	
Tool Steel:	Maraging (1.2709)	H13 (1.2344)	
Titanium:	Ti Al6 V4	Ti Al6 Nb7	Ti (grade 1)
Aluminum:	AlSi10Mg	AlSi12	
Cobalt Chrome:	CoCr28Mo6 (ASTM F75)		
Inconel:	625	718	738

Direct Manufacturing Research Center – DMRC

- Institution of the faculty of mechanical engineering at the Paderborn University
- Flexible and very interdisciplinary structure
- Collaboration of 9 different chairs and a large number of industrial partners
- Funded by the State Government of North Rhine-Westphalia, industrial partners and public sources
- All project topics are guided by industry partners

Research → Materials → Machines → Service providers and end-users

★ = Founding member

Direct Manufacturing Research Center – DMRC

- Research fields in Laser Sintering, Fused Layer Modeling & Laser Melting

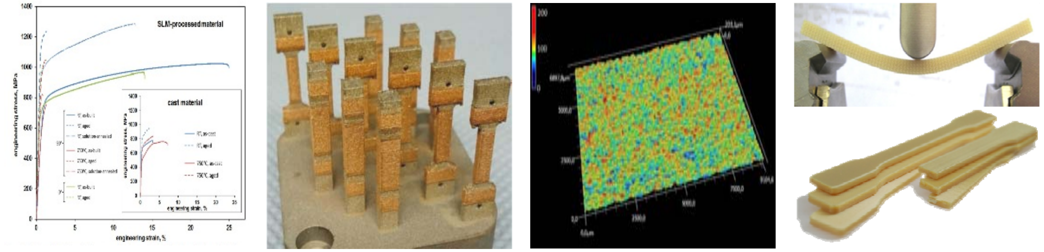

- **Material and process qualification:** LM.fatigue, LM, LS, FLM

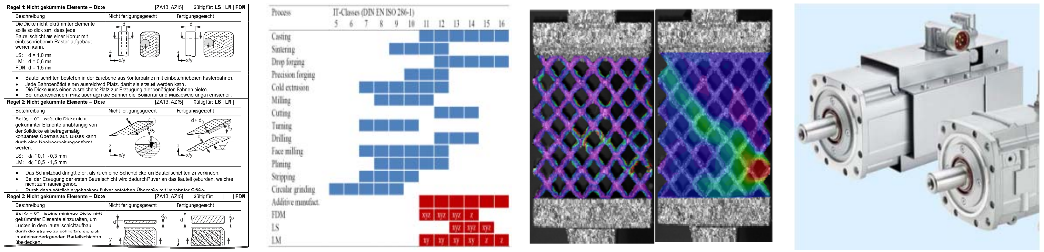

- **Design for AM:** Design Rules, Tolerances, Light weight design

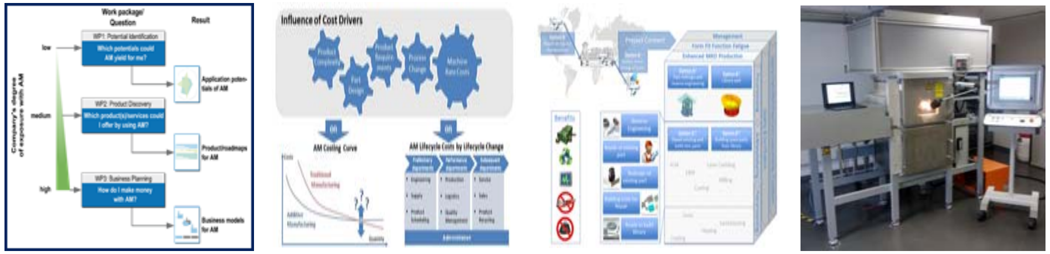

- Business development, Costs, Applications, Function Integration, Machine development

Motivation

- Technical components are subjected to various stresses
- Responsible for the limited service life

Main Goal

- **Extending the total life time of components**
- Using advantages of additive manufacturing
- Ingenious configuration of
  - Notch form
  - Notch position
  - Notch orientation

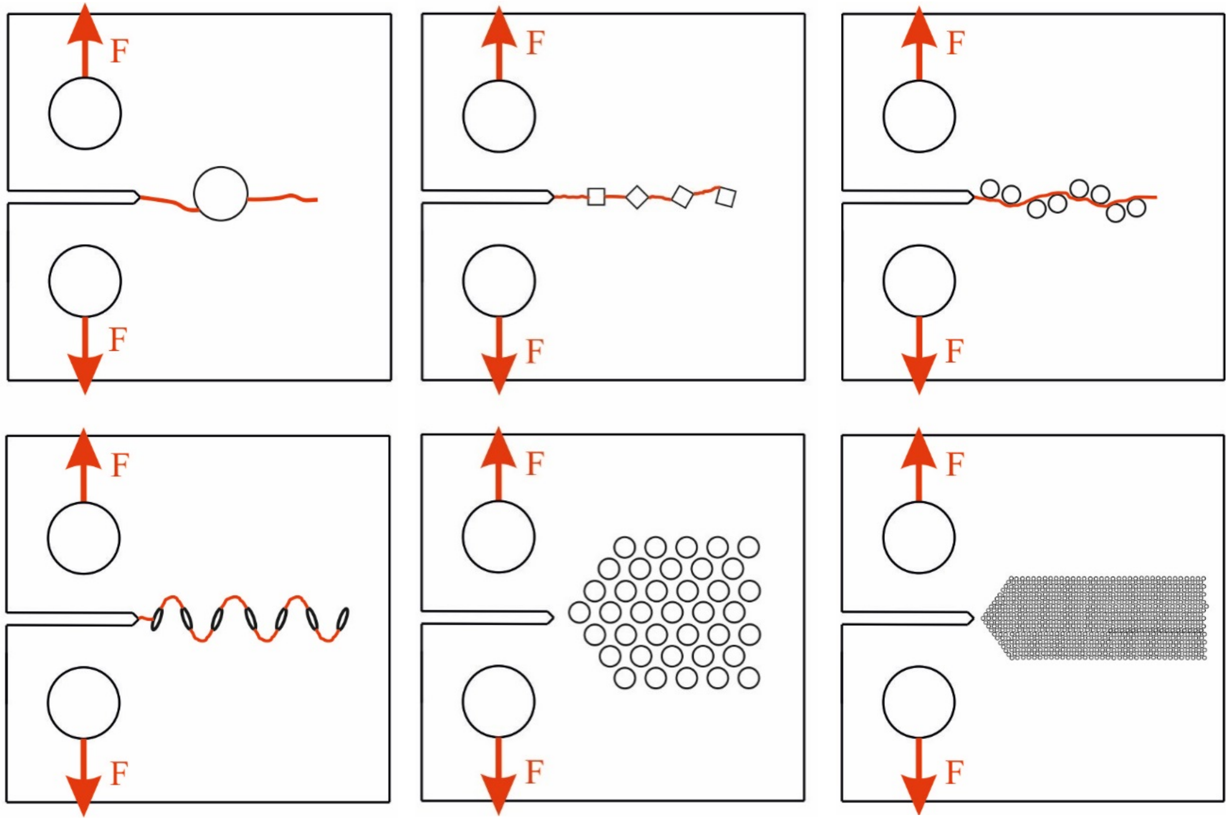

Schematic illustration of notch form, notch position and notch orientation for lifetime manipulation

Major measure for lifetime modification

- Lifetime under fatigue loading is divided into crack initiation and fatigue crack propagation
- “Jump” in a-N-diagram and shorten the lifetime
- Switching between fatigue crack propagation and crack initiation phase
- Initiating effect at each notch

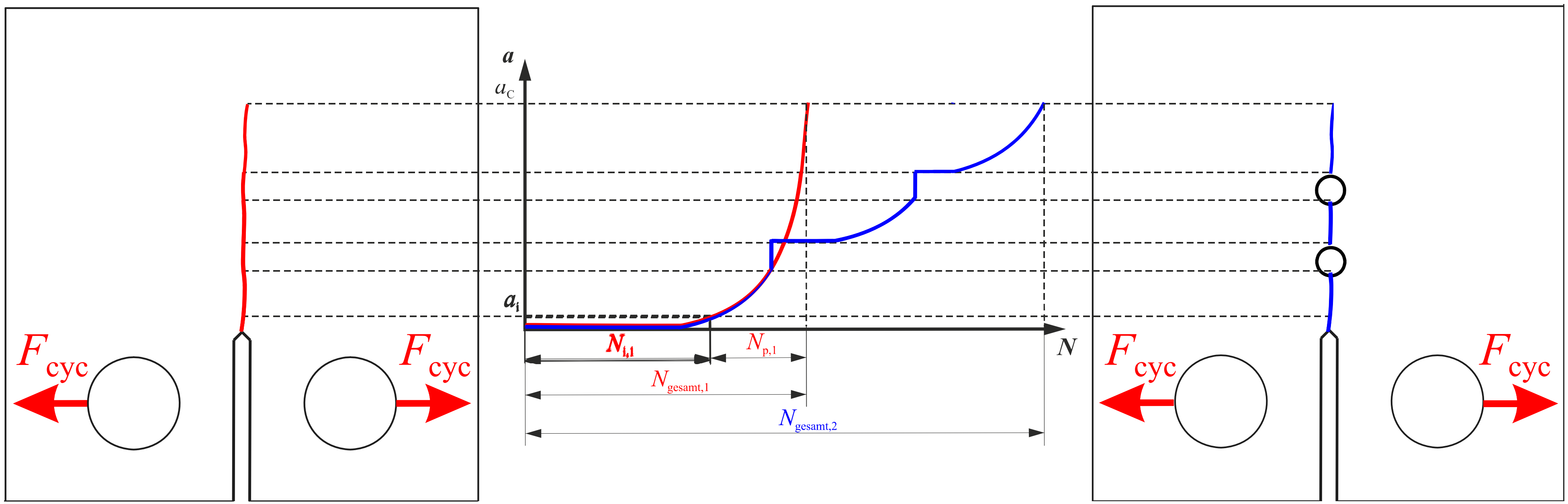

Schematic illustration of lifetime manipulation caused by notches

SLM SOLUTIONS

PADERBORN UNIVERSITY
The University for the Information Society

Experimental setup for fracture mechanics

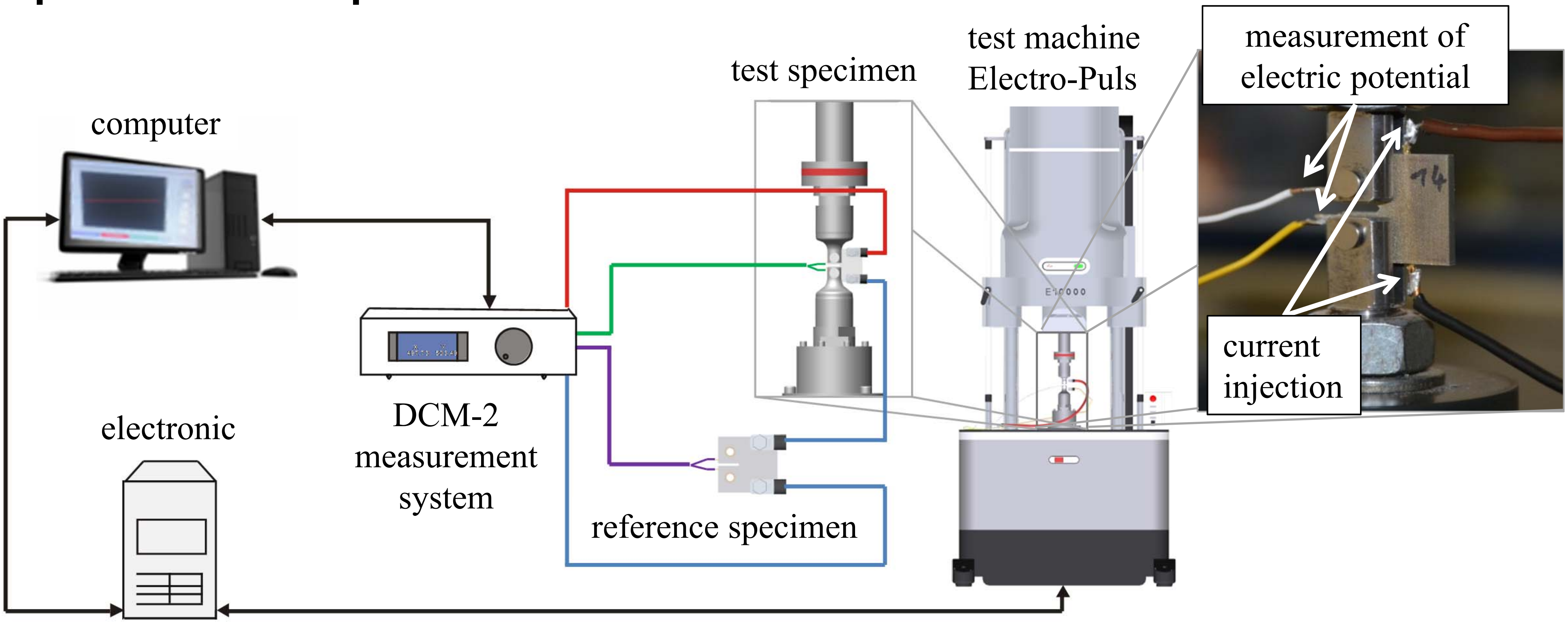

$$U = R_{\Omega} \cdot I_0 = \rho \cdot \frac{l}{A} \cdot I_0$$

U = voltage
R_{Ω} = resistance
I_0 = supply current

ρ = specific material resistance
l = length of specimen
A = cross sectional area

Testing Methods

mechanical load

cyclic stress intensity factor at the crack

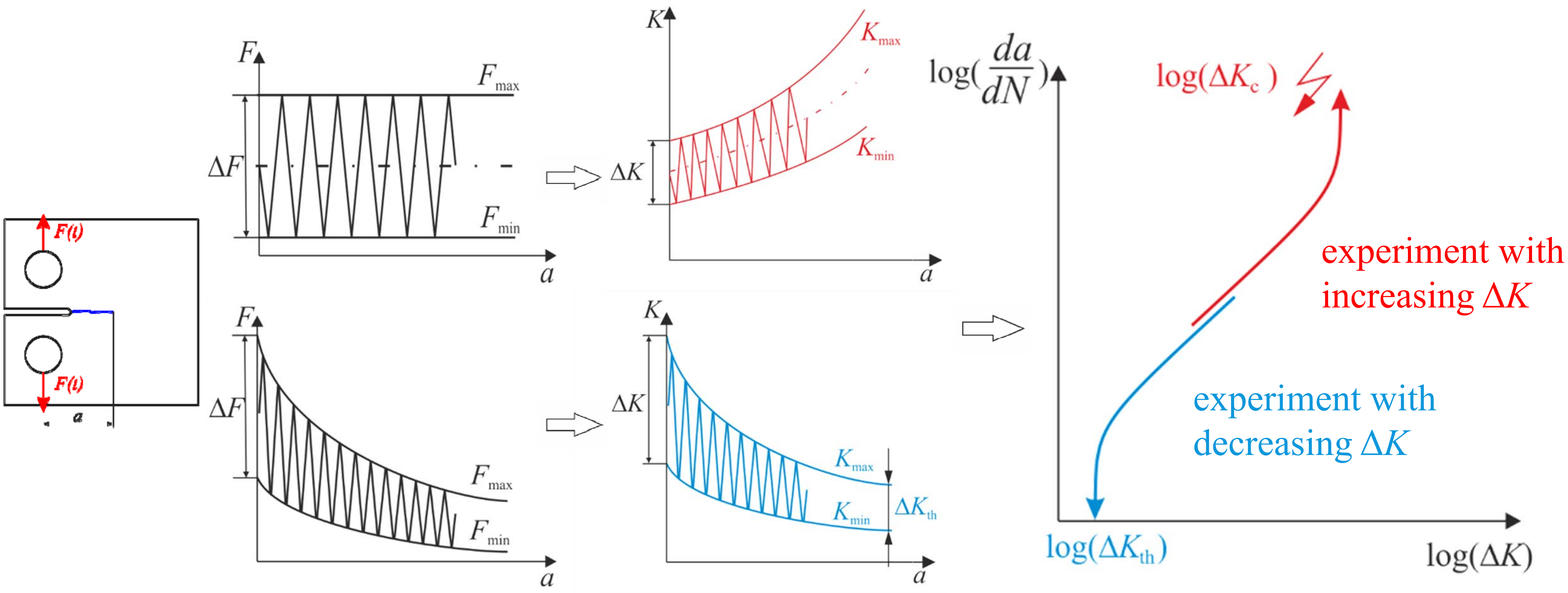

$\Delta K_I = \Delta\sigma \cdot \sqrt{\pi \cdot a} \cdot Y_I$ $\Delta\sigma =$ cyclic loading stress $a =$ crack length $Y_I =$ geometry factor

Fatigue properties of SLM® materials

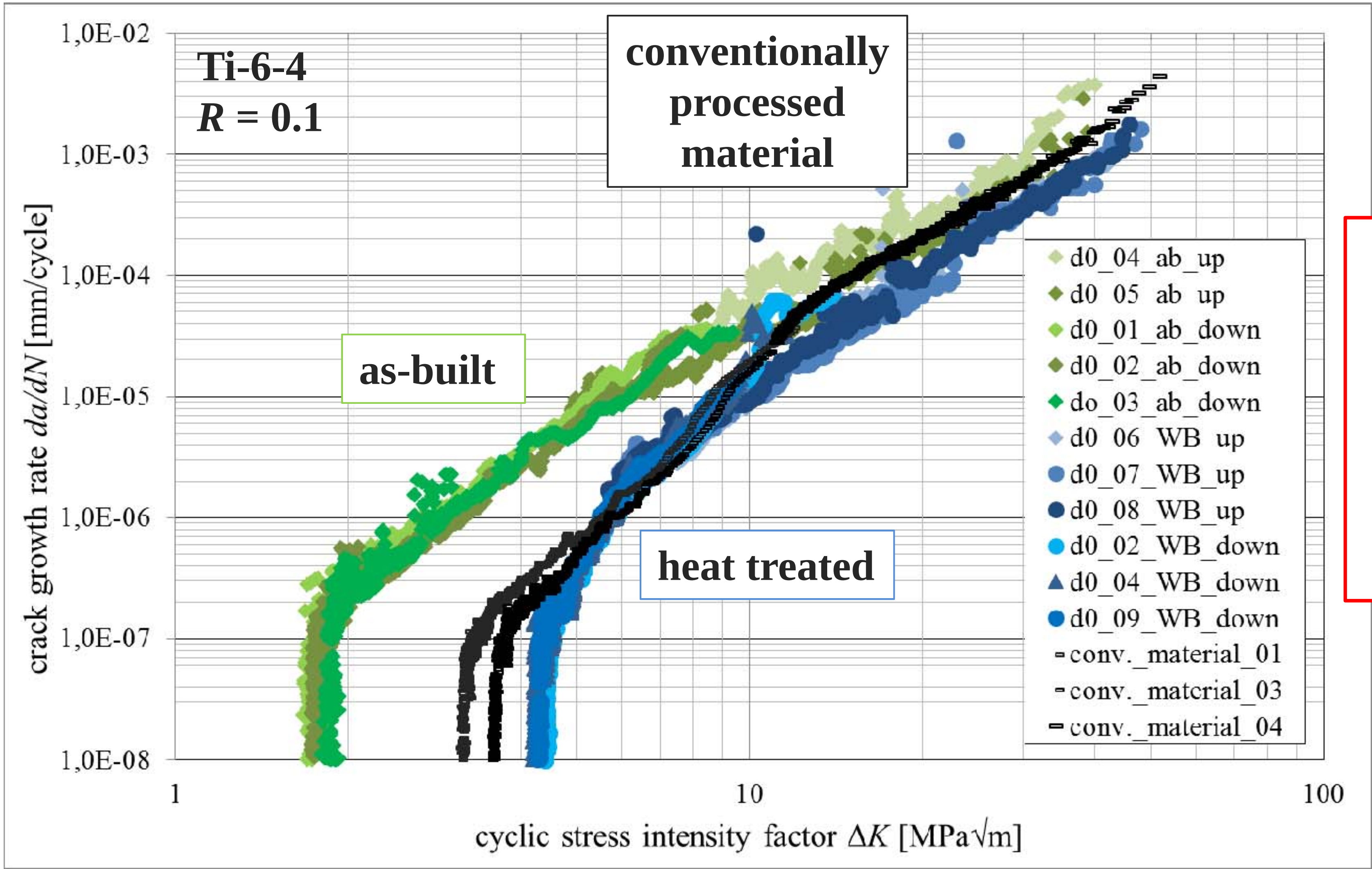

Heat treatment significantly improves the fatigue crack growth performance

Fatigue Life Manipulation by Notches – Lifetime Phases

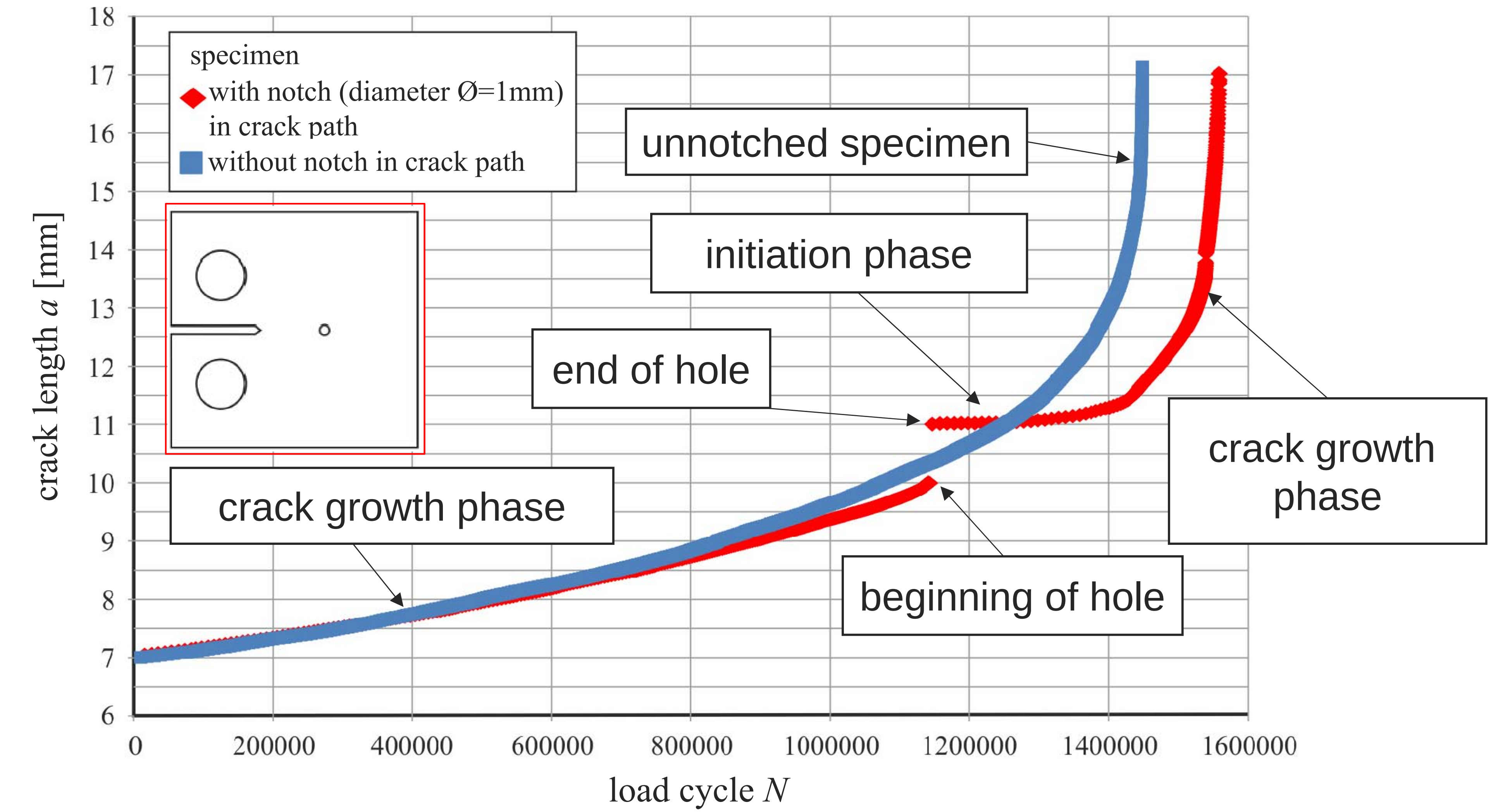

Fatigue Life Manipulation by Notches – Unnotched Specimen

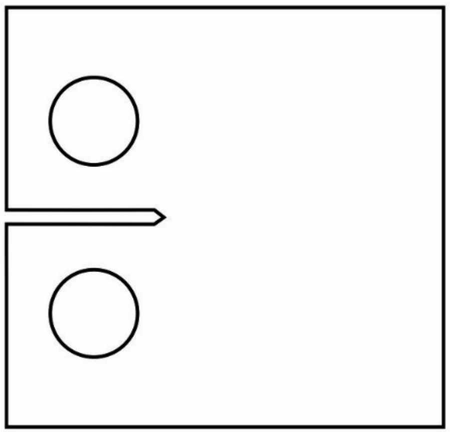

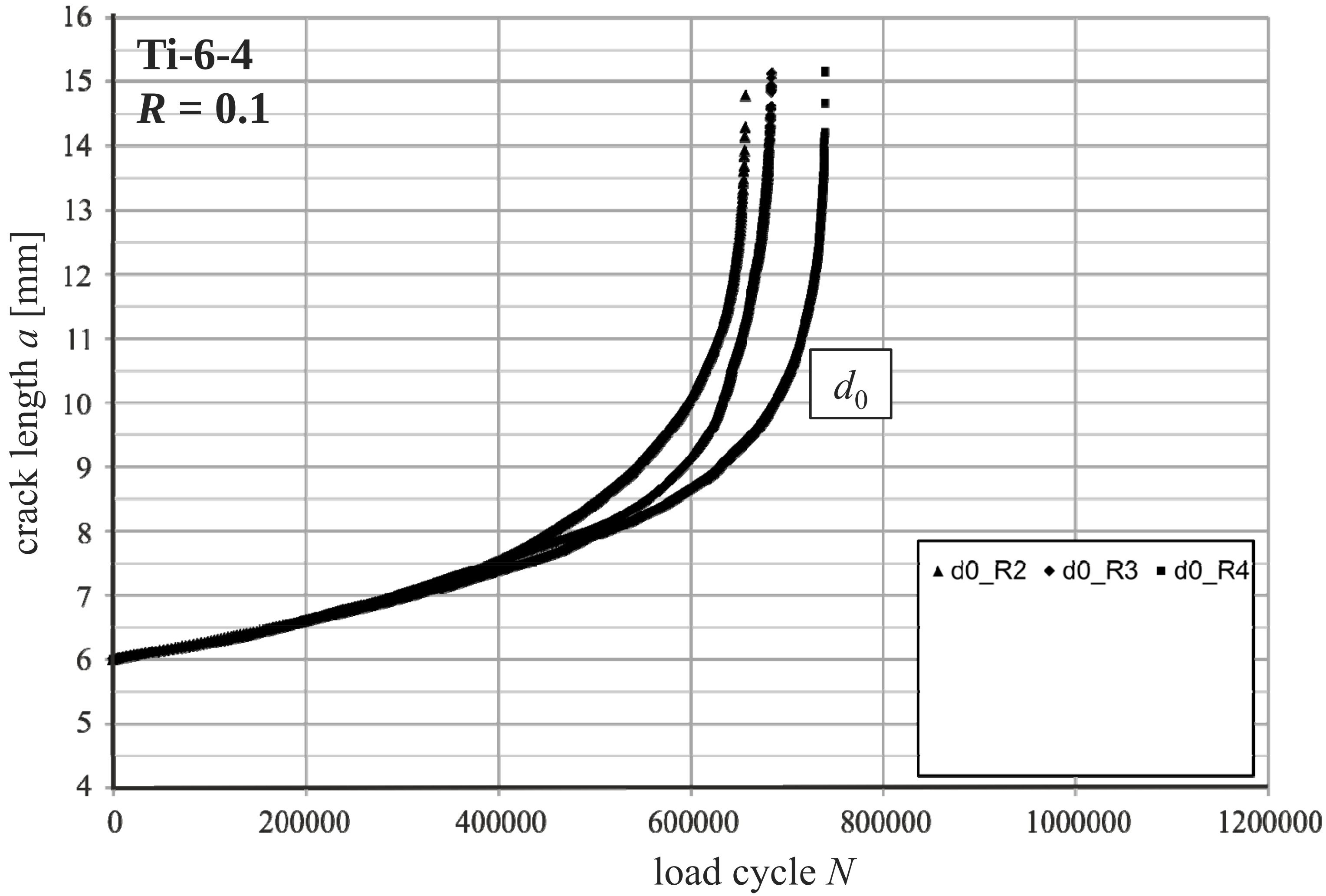

SLM SOLUTIONS

PADERBORN UNIVERSITY
The University for the Information Society

Fatigue Life Manipulation by Notches – One Hole with different Diameter

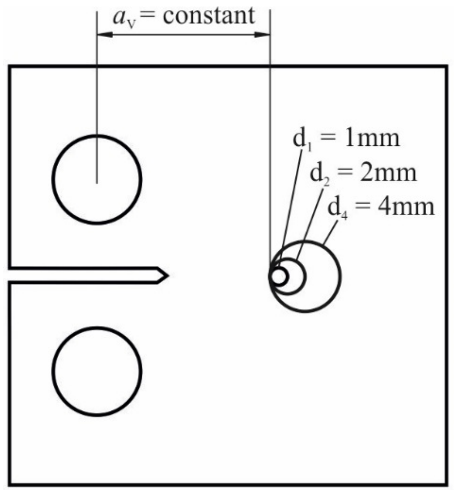

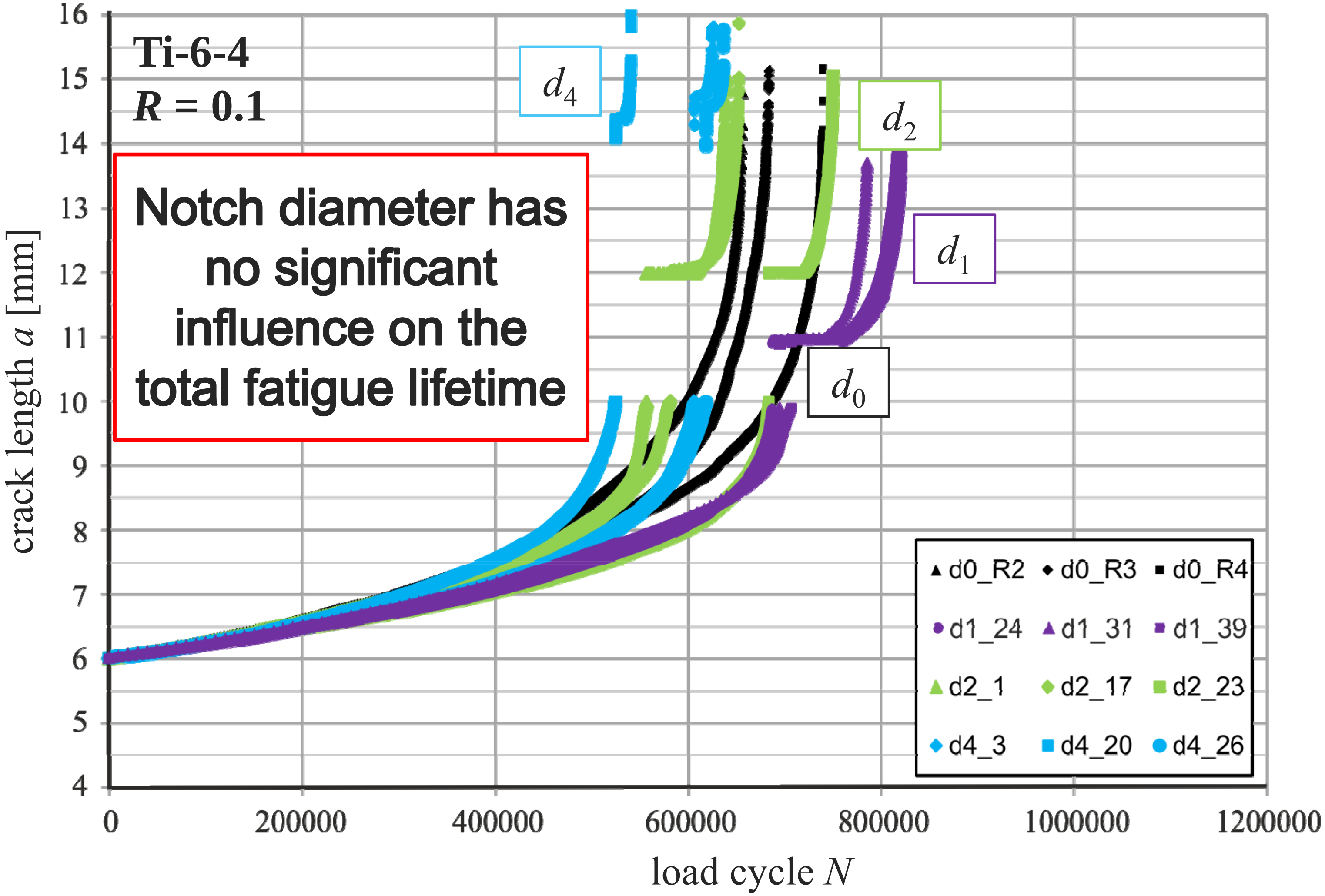

DMRC
DIRECT MANUFACTURING RESEARCH CENTER

SLM SOLUTIONS

PADERBORN UNIVERSITY
The University for the Information Society

Fatigue Life Manipulation by Notches – Row of Holes

- No re-initiation after growing at the first hole
- force increasing

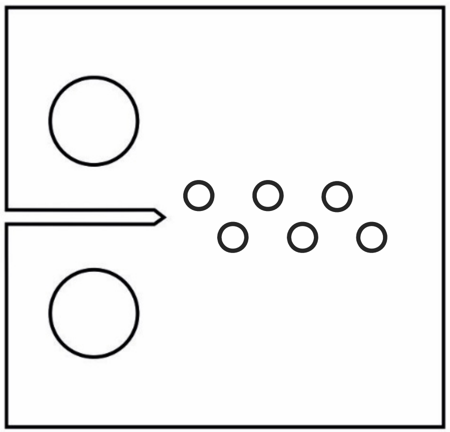

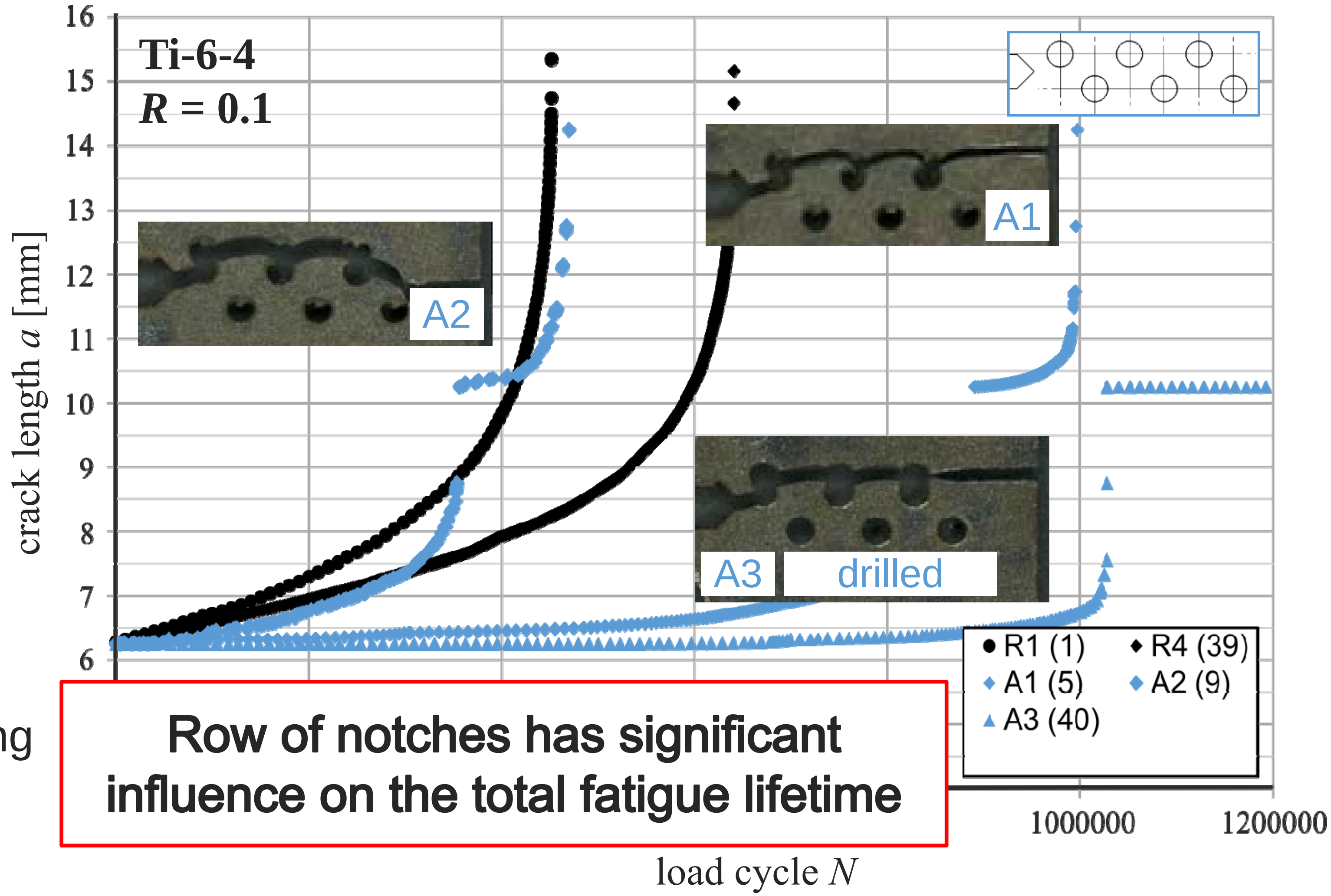

- deformed notches due to manufacturing process

Row of notches has significant influence on the total fatigue lifetime

Fatigue Life Manipulation by Notches – Elongated Notches

- No re-initiation after growing at the first elongated notch

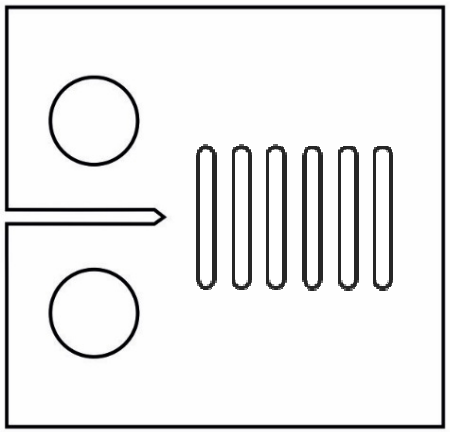

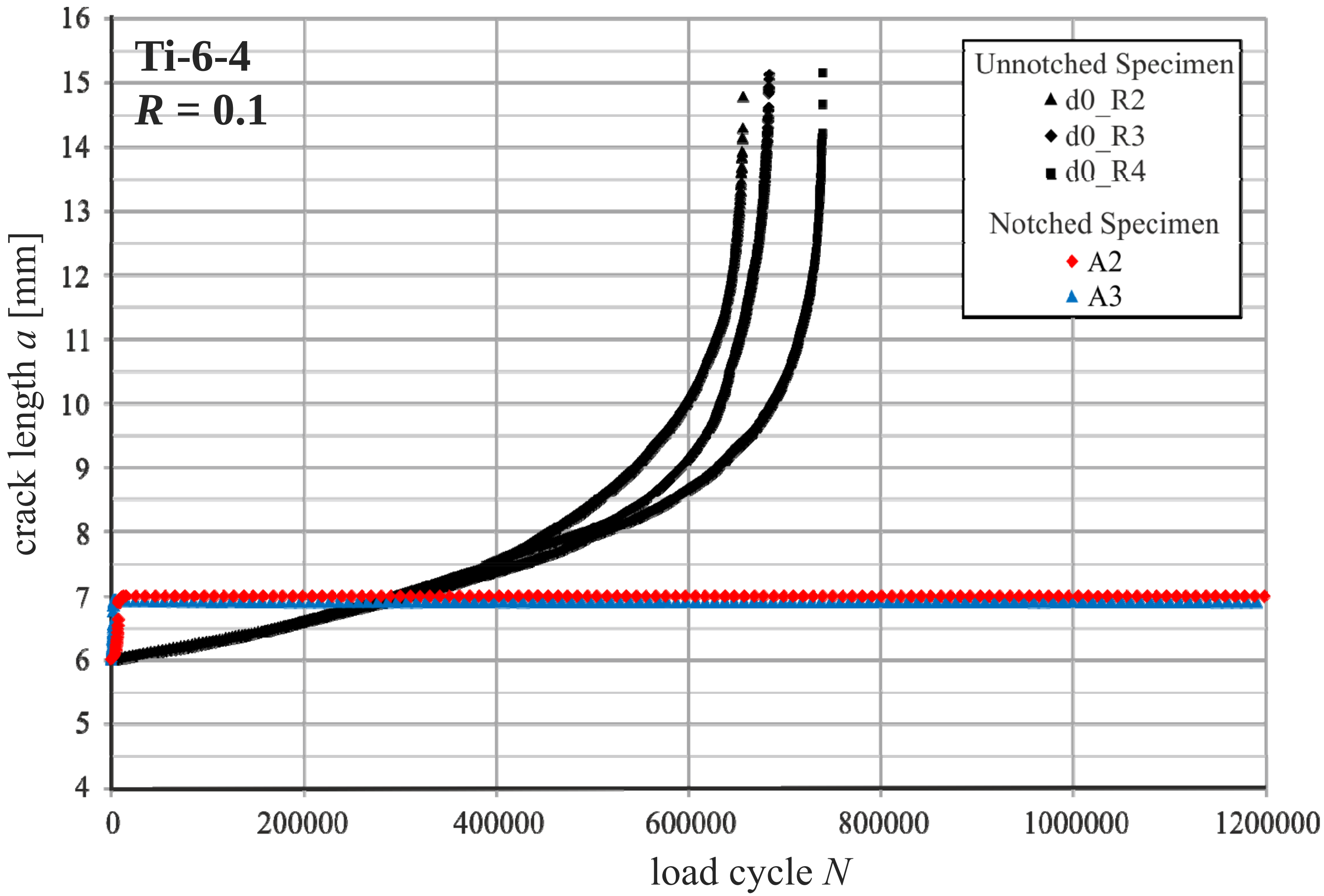

Fatigue Life Manipulation by Notches – Elongated Notches

- No re-initiation after growing at the first elongated notch
- Even after 10mil. cy.

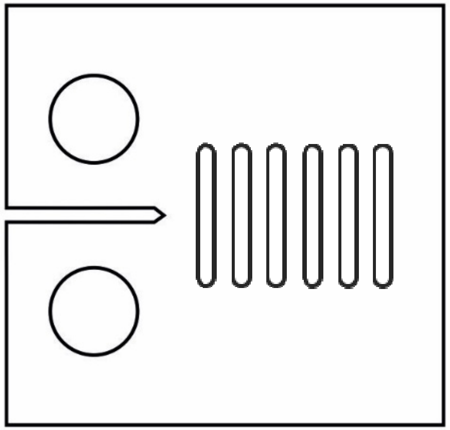

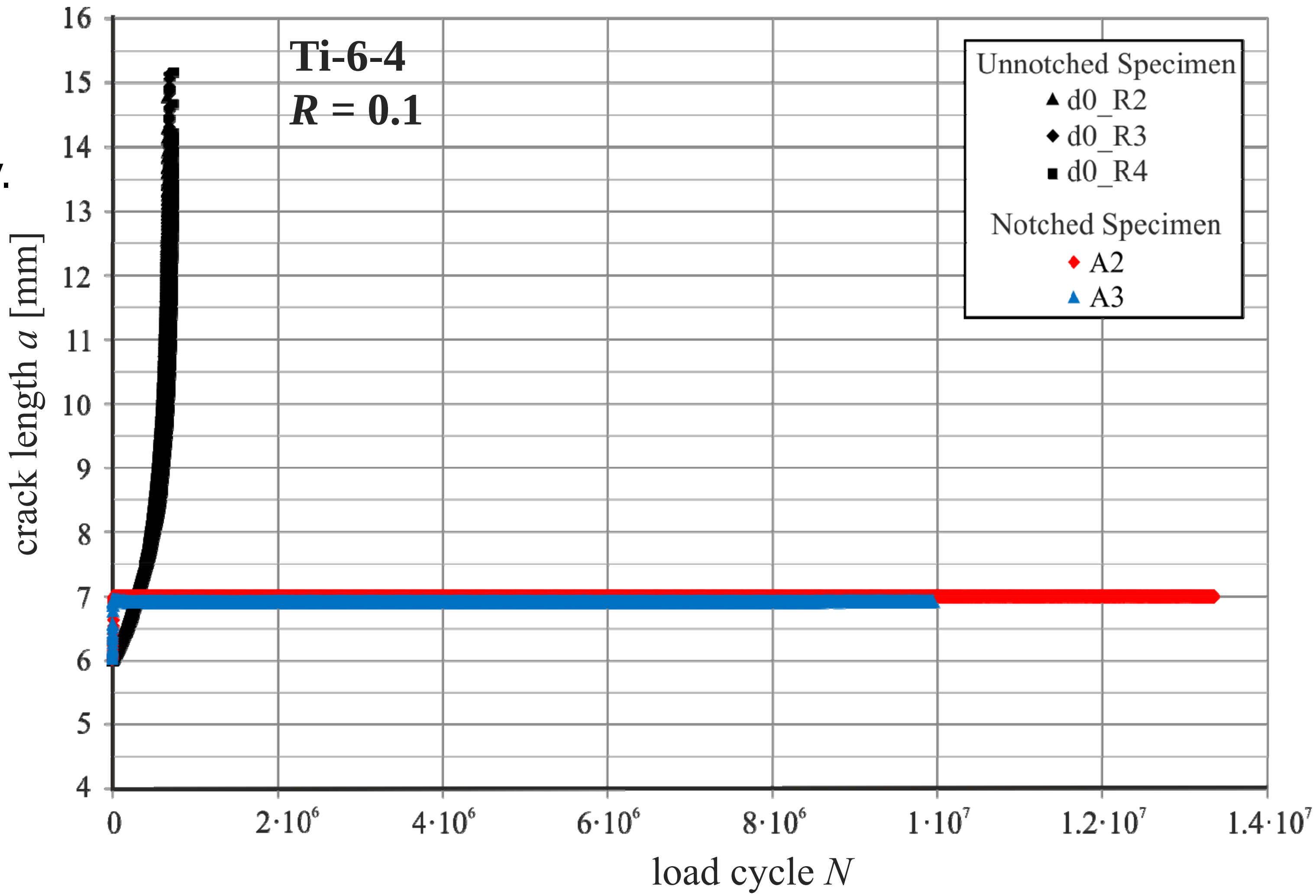

Fatigue Life Manipulation by Notches – Elongated Notches

- No re-initiation after growing at the first elongated notch
- Even after 10mil. cy.

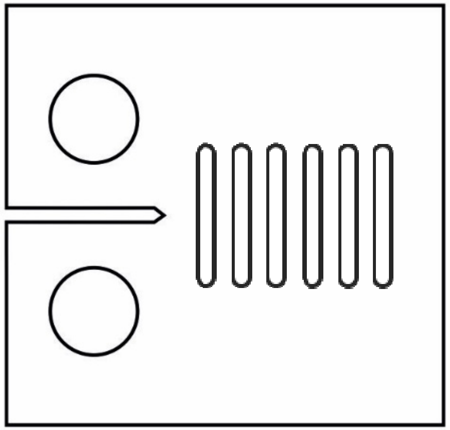

- force increasing

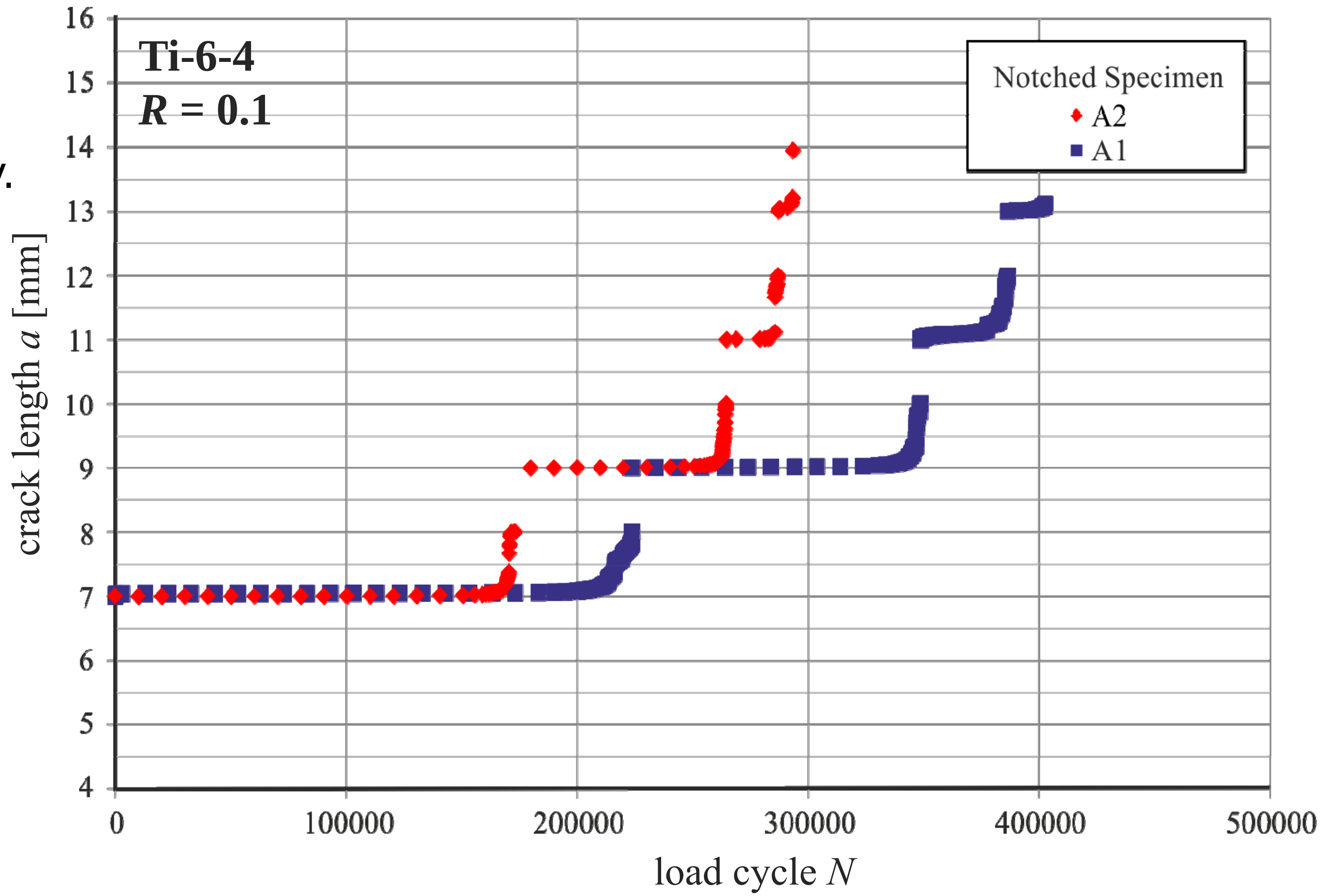

Fatigue Life Manipulation by Notches – Elongated Notches

- Comparison of different specimens with elongated notches – width 1 mm
- Notches lead to initiation effect
- This initiation effect increases with the number of notches
- But this effect is limited by the residual cross-section area of the specimen

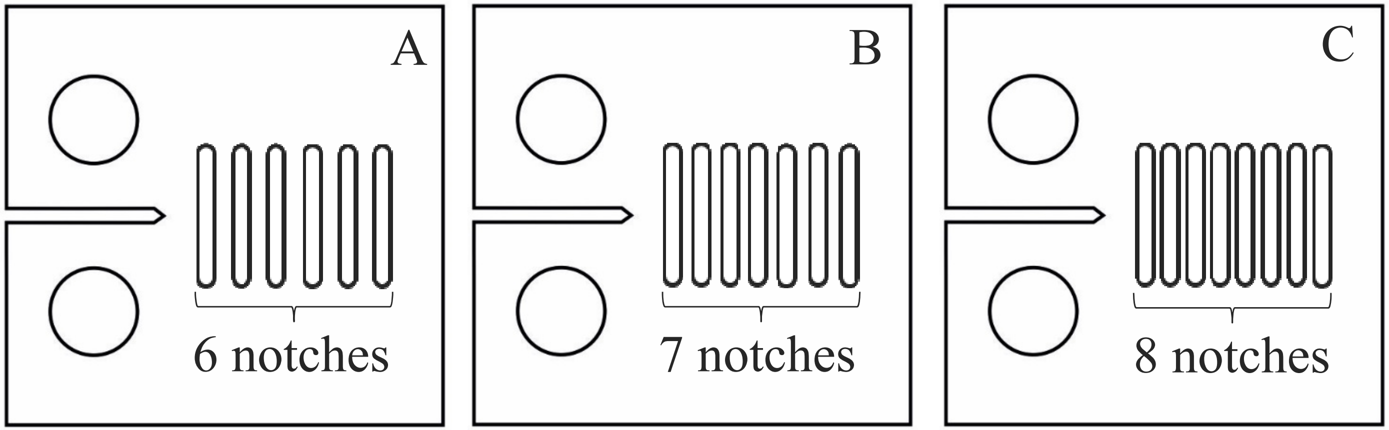

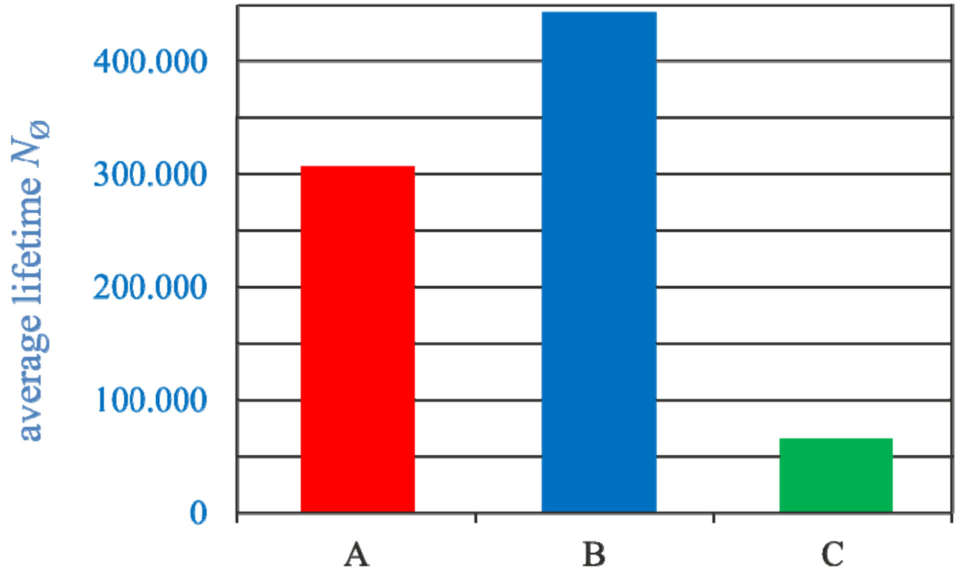

→ **The fatigue lifetime manipulation is possible and influenced by the number, size, form and position of the notches**

4. Conclusion

- Numerous experimental investigations were conducted on different SLM®-processed materials like titanium alloy and stainless steel
- Only a part of the results was presented
- Results show that the fatigue life (decrease or increase) can be manipulated by notches
- Significant crack growth retardation occurs if the crack initiation phase, caused by notches, plays a significant role in the total lifetime
- Taking the titanium alloy as an example, a significant lifetime extension can be achieved by using a row of notches
- Additive manufacturing offers the possibility to produce structures that have a longer fatigue lifetime

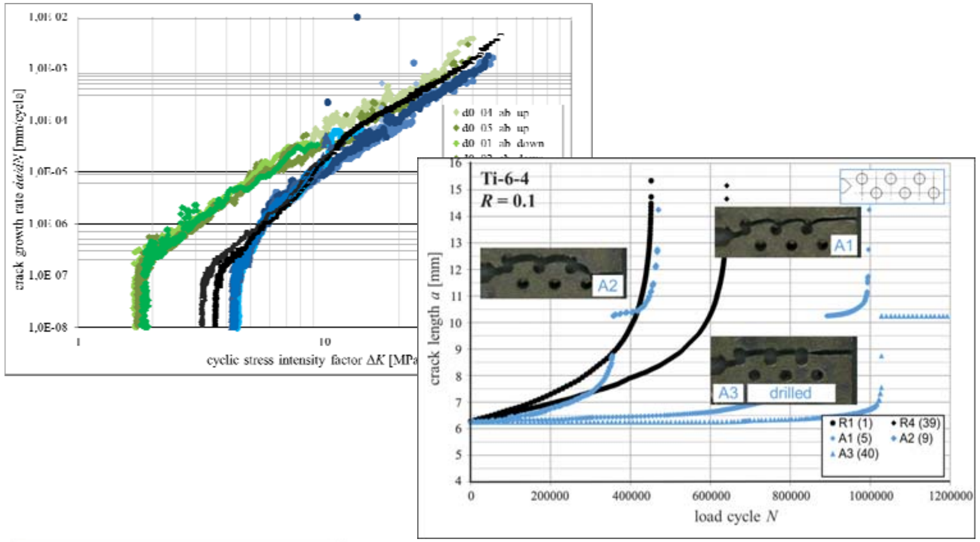

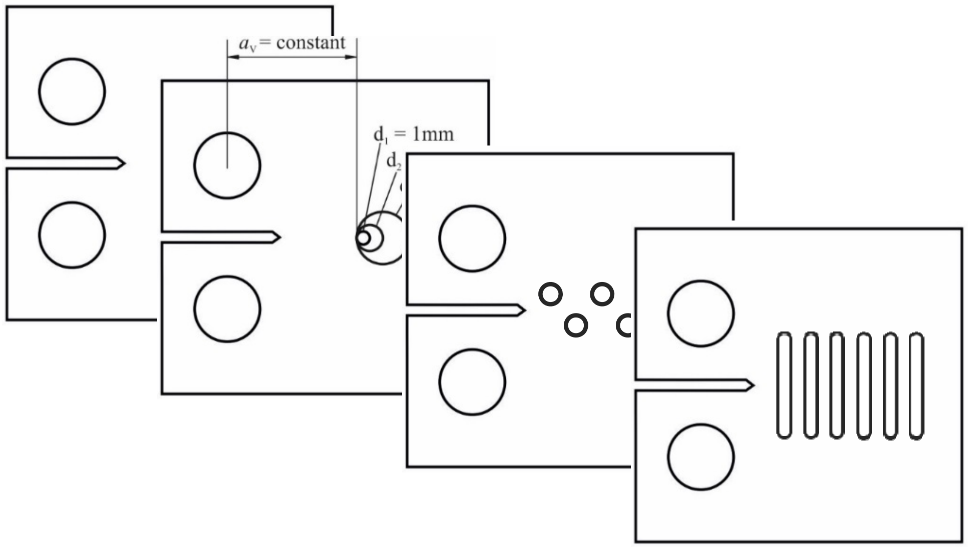

Fatigue Life Manipulation of SLM® Parts

THANK YOU FOR YOUR ATTENTION

M. Sc. Wadim Reschetnik

Institute of Applied Mechanics
Paderborn University
Pohlweg 47-49
33098 Paderborn

Phone : +49 52 51 / 60-5325
Fax : +49 52 51 / 60-5322
E-mail : reschetnik@fam.upb.de

W. Reschetnik, A. Riemer, H.A. Richard. Optimization of SLM structures with respect to crack growth and lifetime. Proceedings of ASPE Spring Topical Meeting, Dimensional Accuracy and Surface Finish in Additive Manufacturing, American Society for Precision Engineering, Berkeley, USA, 2014, S.190-195.

A. Riemer, W. Reschetnik, H.A. Richard. Fatigue Crack Growth in TiAl6V4 and 316L Manufactured by Selective Laser Melting – Influencing Factors and Measures for Lifetime Optimisation. ESA - Workshop on Additive Manufacturing for Space Application, 28.10.-29.10.2014, ESTEC, Noordwijk, Niederlande.

A. Riemer, S. Leuders, M. Thöne, H. A. Richard, T. Tröster and T. Niendorf. On the fatigue crack growth behavior in 316L stainless steel manufactured by selective laser melting. Engineering Fracture Mechanics, 120 (2014) 15-25.

S. Leuders, M. Thöne, A. Riemer, T. Niendorf, T. Tröster, H. A. Richard, H. J. Maier. On the mechanical behaviour of titanium alloy TiAl6V4 manufactured by selective laser melting: Fatigue resistance and crack growth performance, International Journal of Fatigue, 48 (2013) 300-307.

Advanced Characterization of Additively Manufactured Materials, including Synchrotron–based 3D X-rays

A.D. (Tony) Rollett, Ross Cunningham, Sneha Narra, Tugce Ozturk, Brian De Cost, Suraj Rao, Samikshya Subedi, Harshvadhan Jain, Ming Tang, Luke Scime, Paul Chao, Shuchen Cong, Jake Vries, Bryan Webler, Chris Pistorius, Jack Beuth, David Menasche, Liz Holm, Bob Suter.

With help from many others, especially John Siemon, Yanar Cagatay, Jaakko Suni (Alcoa Tech. Center) & Xianghui Xiao (APS)

Support:
America Makes
NSF
PA-RAMP
Adv. Photon Source
DOE
NIST
NASA
DOE-NNSA

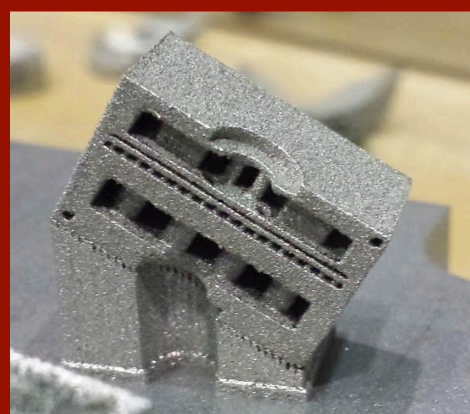

Prototype Heat Exchanger

GE Engine Brackets

Outline

- NextManufacturing Center at CMU; process model
- Quantitative prediction of microstructure: reduced order model to predict porosity
- Advanced characterization, e.g., 3D tomo (CT), HEDM
  - 3D High Energy x-ray Diffraction Microscopy (HEDM)
  - Pore size distributions, powder particle sizes, statistical presentation of data.
- Machine vision for microstructure
- Summary

Metals AM

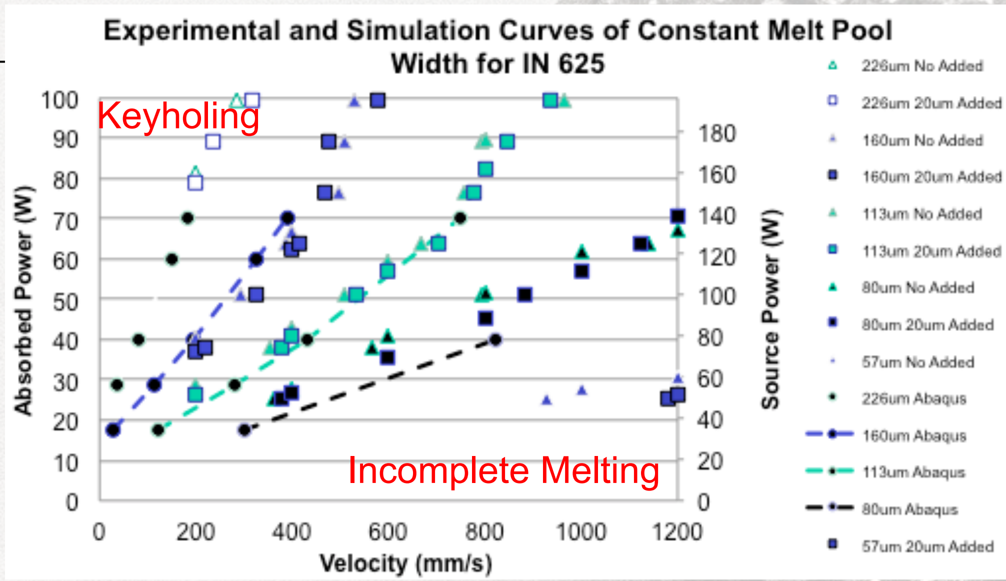

- CMU NextManufacturing Center
  - Broad AM group at Carnegie Mellon
  - Many inter-related projects with significant contributions
  - Strong emphasis on genomic approach
  - Brings together the AM ecosystem in the region
- Process Mapping Overview
  - Broad approach to process understanding
- Within 5 years AM users will be able to:
  - Vary microstructure spatially within parts
  - Monitor and control the process
  - Choose from a wide variety of powders
  - Eliminate or design for porosity
  - Design the process as they design a part (including cost estimates)

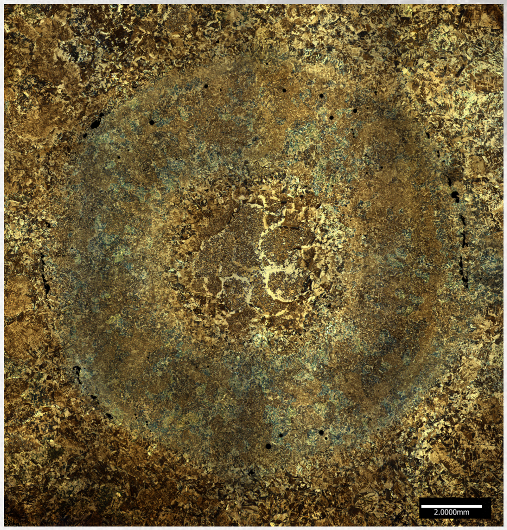

Work by Tang, Pistorius, Beuth

Porosity/Density Prediction

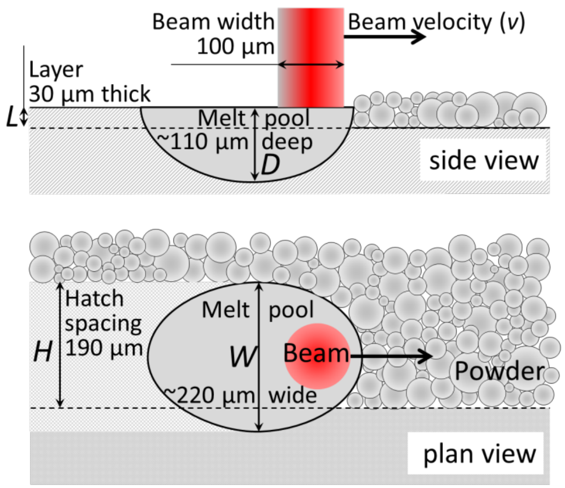

Melt pool geometry

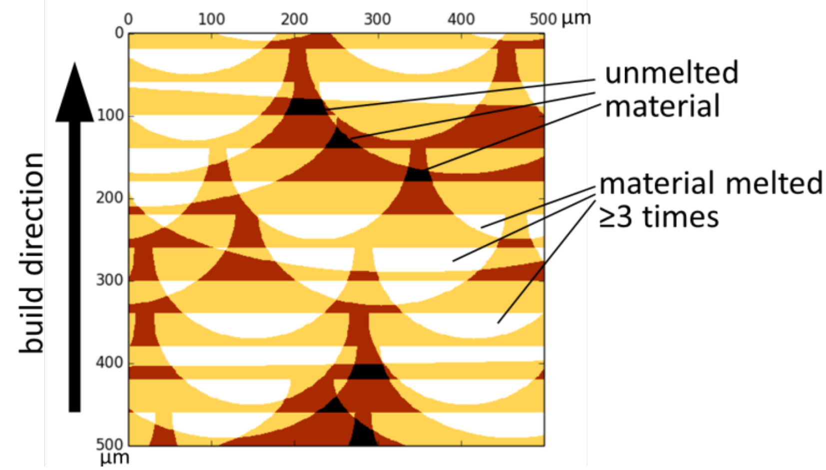

Melt pool overlap across layers

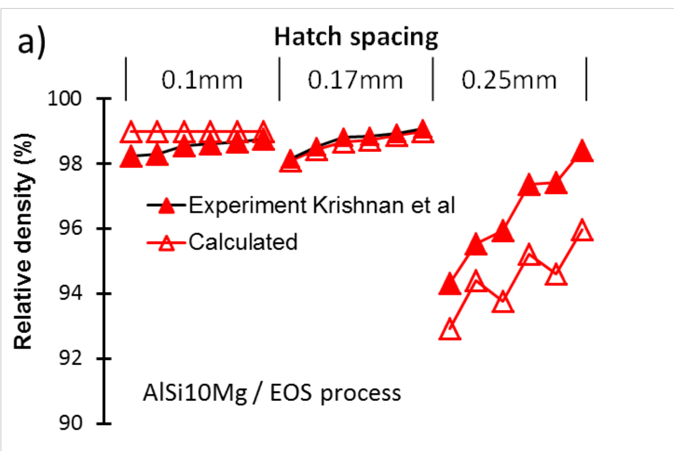

Comparison of model with literature data

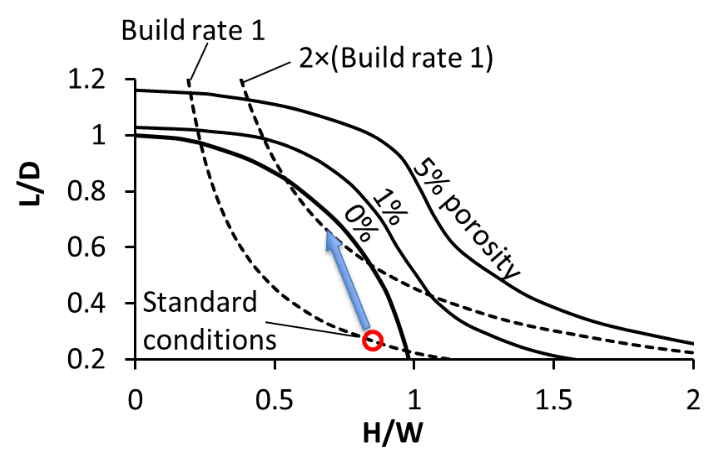

Comparison with standard operating point

Synchrotron Computed Tomography

- The Advanced Photon Source (APS) at Argonne National Laboratory provides high energy x-rays with **high brilliance (flux)**
- Synchrotron source is useful for computed tomography (CT):
  - Sample size (up to 2 mm diameter at 2BM)
  - Resolution (0.65 μm)
  - **Short scan times** (2-6 mins)
  - Terabytes of data; **long times** required to a) reconstruct each 3D image and b) analyze the results (e.g., segmentation)

Advanced Photon Source, Argonne National Lab, Chicago

Advanced Synchrotron Capabilities: CT+HEDM

- Recently NF- & FF-High Energy Diffraction Microscopy (HEDM) experiment at 1-ID on AM Ti-6-4
- 3D microstructure and orientation information with Near-Field mode
- 3D residual stress distribution via Far-Field mode
- Capability for in situ loading during CT, NF and FF; RAMS loading system developed by AFRL
- Schuren *et al.* (2015), 'New opportunities for quantitative tracking of polycrystal responses in three dimensions', COSSMS, **19** 235.

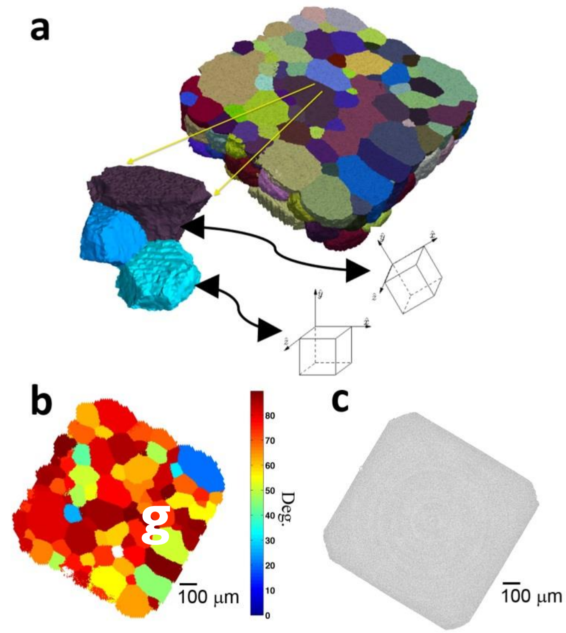

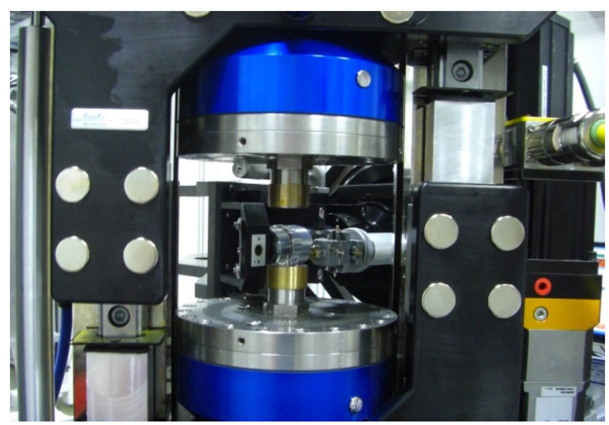

Porosity Measurement via CT

- "Evaluating the Effect of Processing Parameters on Porosity in Electron Beam Melted Ti-6Al-4V via Synchrotron X-ray Microtomography", R. Cunningham, S.P. Narra, J. Beuth, and A.D. Rollett, *JOM*, **68** 1 (2016)
- Aim was to characterize porosity size and shape distributions as a function of processing conditions
- Used computed tomography at the Advanced Photon Source at the Argonne Natl. Lab. In Chicago
- High energy x-rays permit rapid measurement (a few minutes per mm^3 sample volume) at high resolution (minimum pore size ~ 1 μm), which is suitable for pores ranging up to 100 μm.
- About 100 sample volumes can be measured per 24 hours of beamtime at 2BM (at APS), which uses "pink" radiation (parallel beam, limited range of energies, very high intensities). Each volume is of order 1 mm^3 with a resolution of approx. 1 μm. Substantial help from Xianghui Xiao (APS) is gratefully acknowledged.
- The void content of any material is particularly important with respect to fatigue resistance. Fatigue cracks typically start from voids in preference to other microstructural features (after manufacturing defects and corrosion pits).

CT on Beamline 2BM at APS

About XMI | Science and Research | Beamlines | Highlights | Software & Tools | Internal | Search APS...

Argonne Home > Advanced Photon Source > Xray Science Division › Xray Microscopy and Imaging › Beamlines › 2 BM ›

Contacts
FAQs
Beamlines
News
Publications

APS Email Portal
APS Intranet
APS Phonebook
APS Quick Links for Users
APS Safety and Training

Beamlines and Facilities: Beamline:2-BM

Introduction

The 2-BM beamline offers measurement capabilities for x-ray microtomography, x-ray topography and x-ray microdiffraction. X-ray microtomography and x-ray diffraction instruments are installed on separate optical tables for independent operation with fast switch over time. Optically-coupled high-resolution CCD system is used for microtomography and topography with up to 1 micron spatial resolution. X-ray microdiffraction setup consists of KB microfocussing mirrors (~3 micron minimum spot), four-circle Huber diffractometer, high-precision translation sample stage, two orthogonally-mounted video cameras for viewing sample, fluorescence detector (Si-drift diode) and diffraction detector (a scintillation detector or a CCD).

Three different levels of monochromaticity are available. Conventional monochromatic x-rays from a double-bounced Si (111) crystal monochromator (DCM, D E/E=1E-4), wide band-pass monochromatic x-rays from a double multilayer monochromator (DMM, D E/E=1~4E-2) and pink beam. The available x-ray range is from 5 keV to 30 keV. The lower limit is due to the x-ray windows and the upper limit is due to the critical angle of the x-ray mirror. Two different coatings (Cr and Pt) for the x-ray mirror allow either 20 keV or 30 keV energy cutoff.

Beamline Scientist:

Xianghui Xiao: xhxio@aps.anl.gov , (630) 252-9621

Francesco De Carlo: decarlo@aps.anl.gov , 630) 252-0148.

Beamline post-doc:

Yongshen Pan: pany@aps.anl.gov , (630) 252-5939

Techniques

- X-ray Tomography

Optical Components

Component	Distance from Source	Description	Installed
Filter assembly	23.2 m	8 filters on 2 carriers	05/1996
Hor. and vert. slits	23.5 m	25 µm reproducibility	05/1996
Vert. deflecting mirror	24.9 m	0.15 deg. plane w/ 2 coatings (Cr, Pt)	12/1997
Double multilayer mono.	27.4 m	Unfocussed	05/2000
Hor. and vert. slits	48.3 m	25 µm reproducibility	02/1997

Beamline Configurations

White Beam: (2-BM-A)	Beam at sample: 50 x 3 mm 2 (hor x vert), uncollimated
Pink Beam: (2-BM-B)	Beam at sample: 50 x 3 mm 2 (hor x vert), uncollimated
Monochromatic (multilayer): (2-BM-B)	Beam at sample: 25 x 4 mm 2 (hor x vert), E= 0.5-33 keV, dE/E= 10 -2

Detectors

Detector	Manufacturer	Description
Vortex	Radiant technologies	Energy dispersive solid state detector
Coolsnap HQ	Roper, Photometrics	Peltier cooled CCD camera
PCO Edge	PCO	sCMOS
PCO Dimax	PCO	CMOS
Bicron		Scintillator Point Detector
Ion Chambers		

2-BM-B X-ray Optics

KB-Mirrors, University of Chicago design

Parabolic refractive x-ray Be lenses

Ancillary Equipment

Micropositioning system

Time used: 3-5 minutes per volume

Data: approx. 0.2 Tbytes per volume

Software used for analysis:

tomopy

ImageJ

Avizo

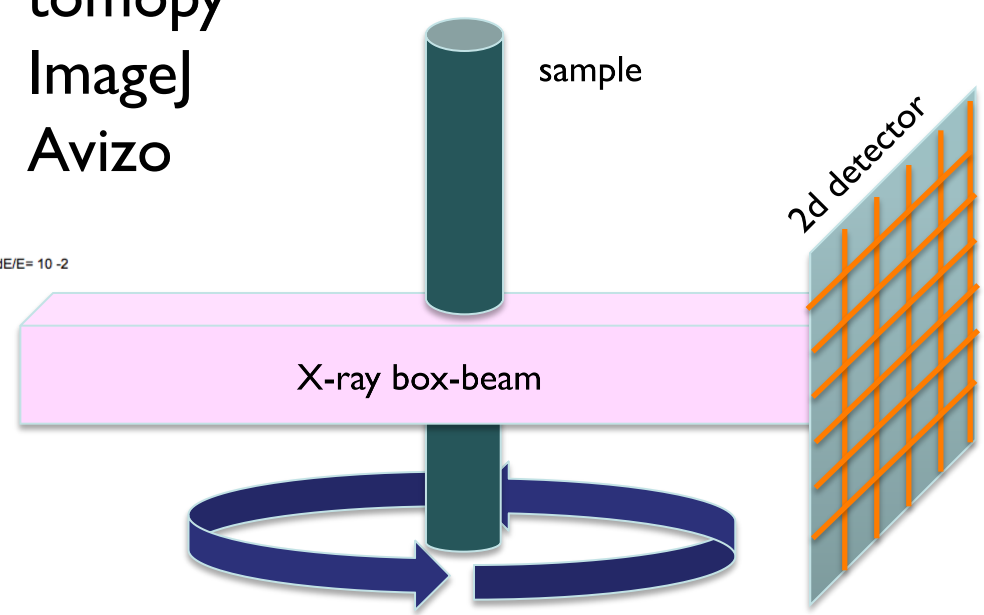

X-ray Computed Tomography (XCT)

- Conventional methods for porosity analysis inadequate
  - Archimedes
  - Metallographic analysis
- XCT: Constructs 3D model from a series of 2D radiographs
  - Contrast generated by difference in X-ray absorption as they travel through a material
- Provides information on size, morphology, and spatial distribution in 3D
- Most lab-scale XCT instruments have limited resolution (~25 µm)
- **Synchrotron source offers significantly better resolution (~1 µm), scan time**

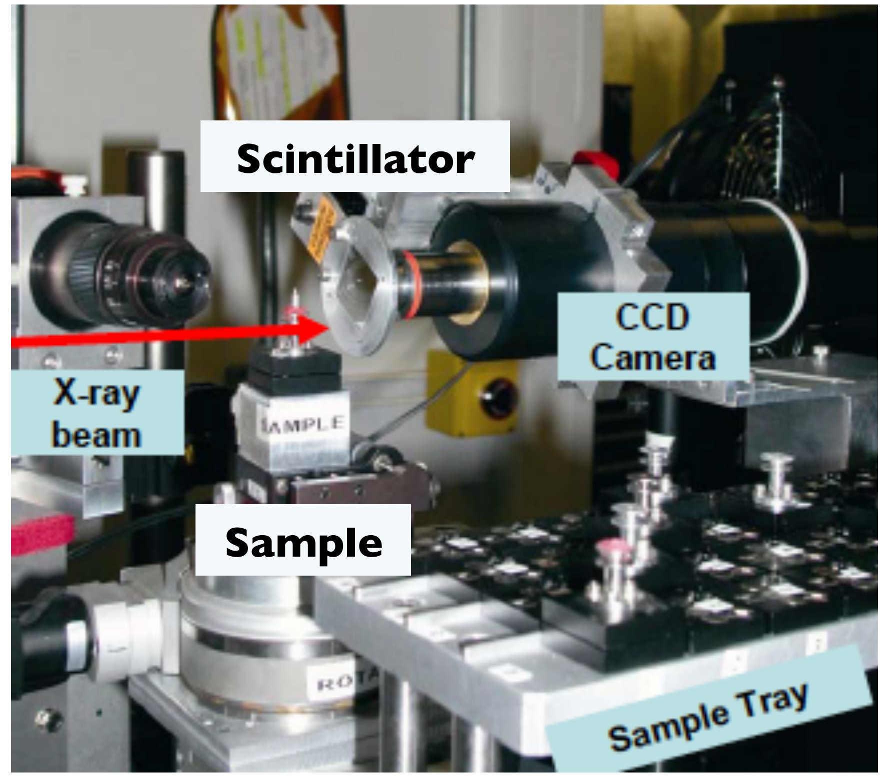

XCT setup at APS Beamline

https://www1.aps.anl.gov/files/download/Committees/InterCAT_Technical_Workgroup/2010/20100318decarlo.pdf

Microstructure in Ti-6Al-4V

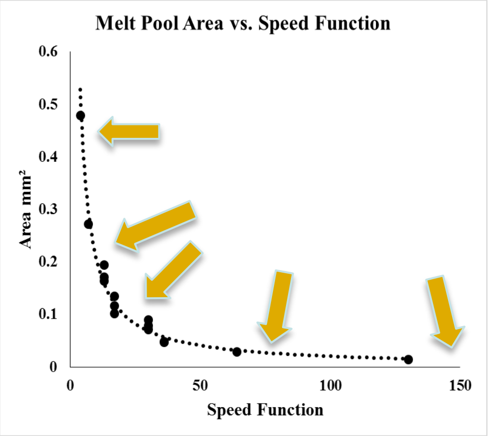

- Illustrate lamellar microstructures observed.
- **Five Ti-6Al-4V samples** (3 cm diameter, 1.5 cm height cylinders) were fabricated on Arcam EMB System at NC State
- **Beam velocity was varied to create melt pool areas corresponding to 1X, 2X, 4X, 1/2X, 1/4X of the "nominal" melt pool area**
- 1 x 1 x 15 mm imaging samples were cut from the bulk, and contour-bulk interface. CT-scans were taken from top ~ 8 mm of each sample
- CT on 2-BM beamline with 100 keV pink beam (parallel box beam), absorption mode; help from Xianghui Xiao (APS) acknowledged.
- Objective was to **characterize different types of porosity observed in AM metals**, and begin to **supplement process maps with intrinsic defect properties**

Ti-6Al-4V microstructure

- Standard microstructures are based on heat treatment in the two-phase range; this gives a mix of primary α and Widmanstätten $\alpha+\beta$.
- Despite the high cooling rate (~10^6 /s), the β structure is columnar and the transformation gives either martensite or acicular α.
- Variations in thermal history can give rise to significant transitions in microstructure. This example documents the variation in a Ti-6Al-4V build, which shows a martensitic microstructure near the top and a basketweave microstructure (or tempered martensite) towards the base.

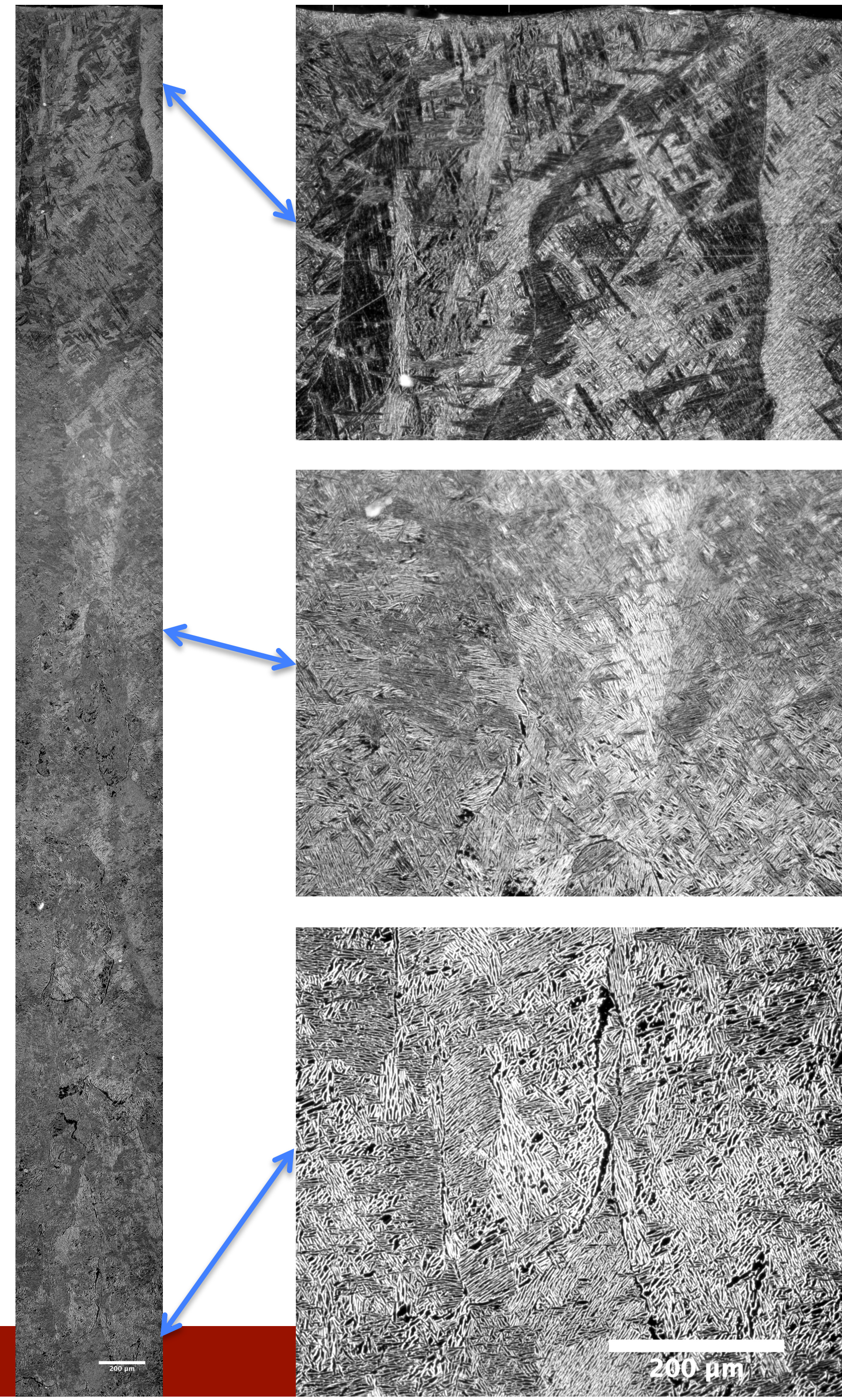

Ross Cunningham, Sneha Narra

Cunningham *et al*. (2016) *JOM*, **68** 1-7

Ti-6Al-4V

Increasing Melt Pool Area →

	1/2X	Nominal	2X	4X

0 mm-1.5 mm

6.5 mm-8.5 mm

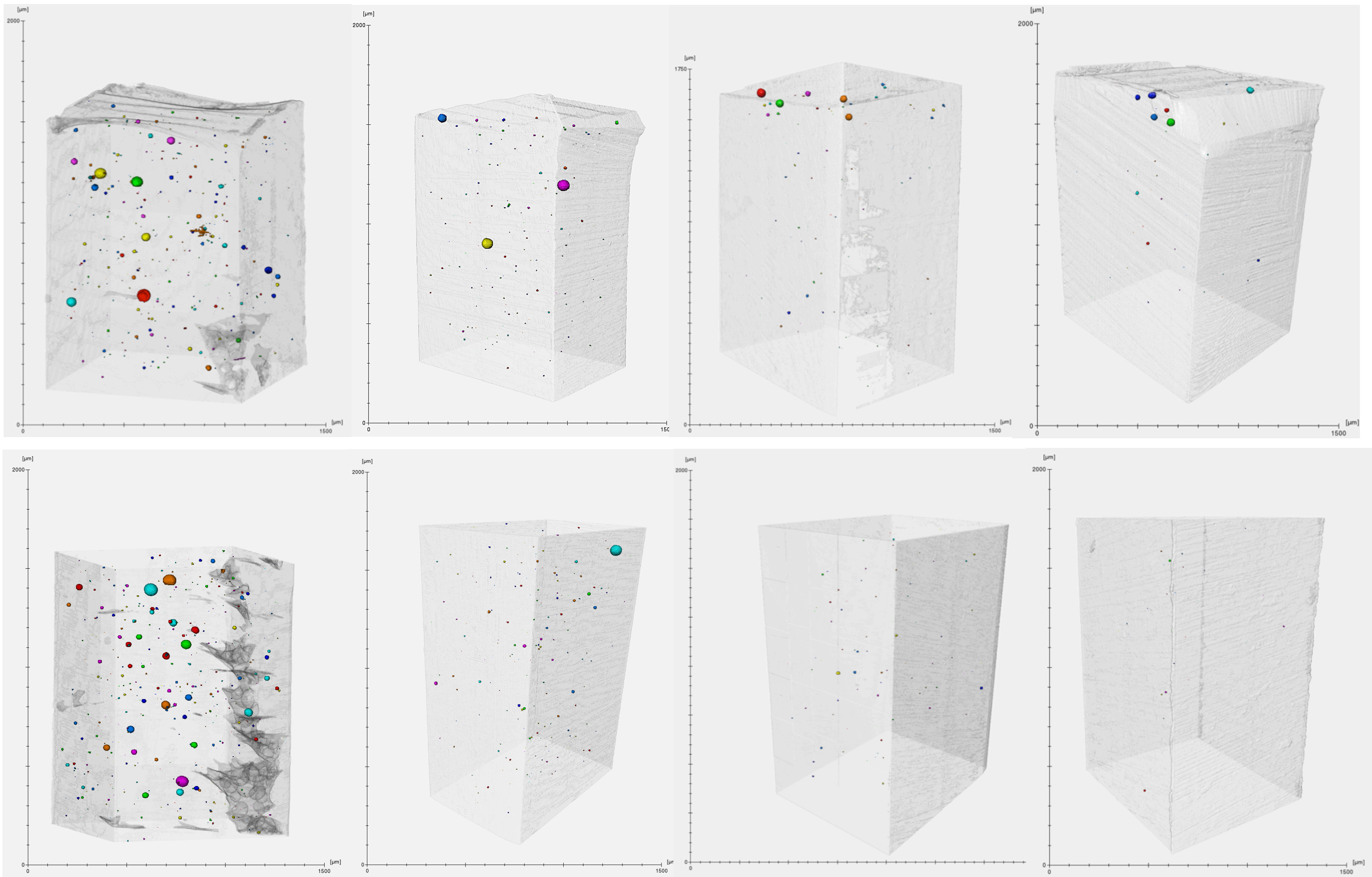

Cunningham *et al*. (2016) *JOM*, **68** 1-7

Ti-6Al-4V

Porosity Size Distribution in 6.5-7.9 mm from Top Surface

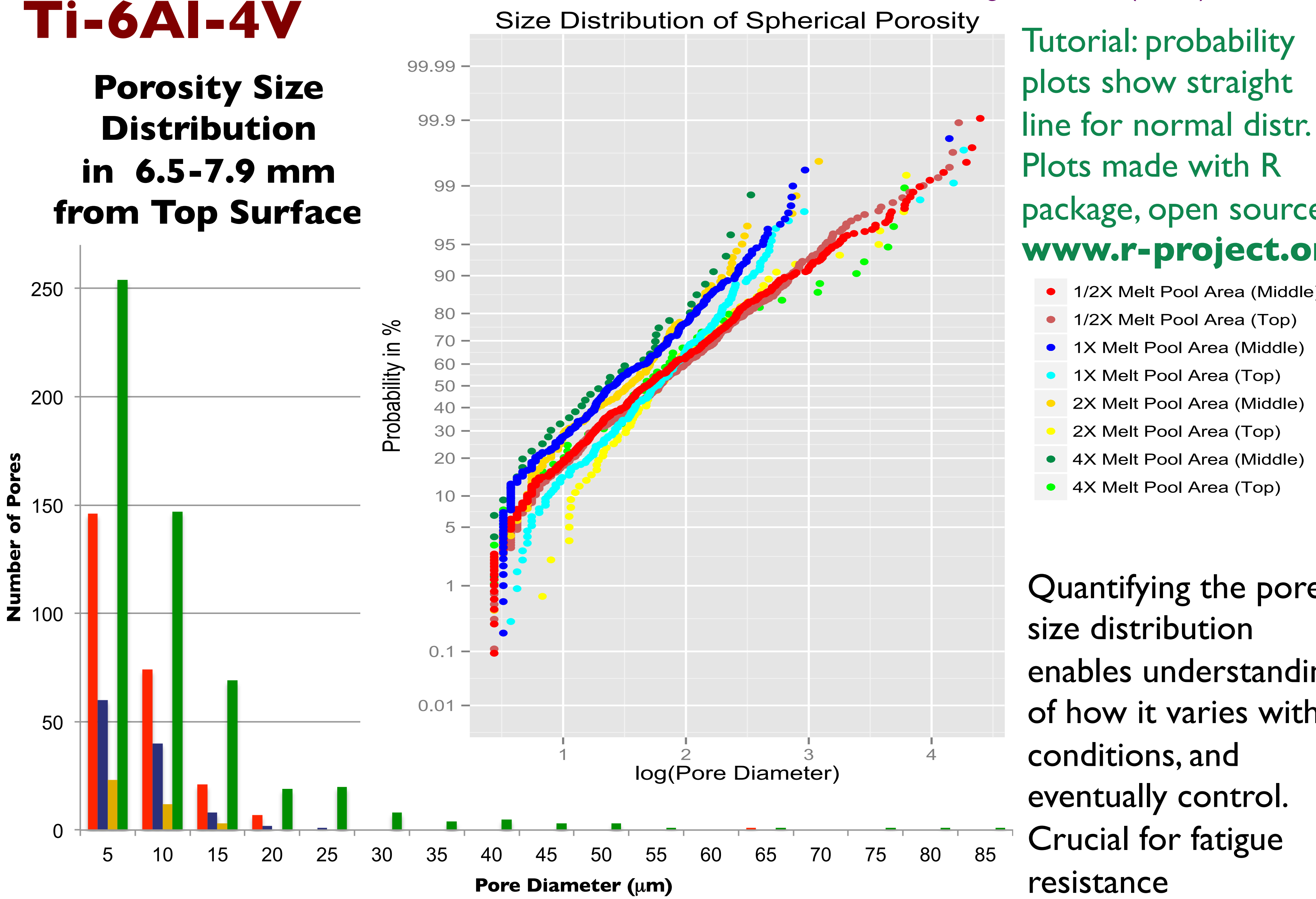

Tutorial: probability plots show straight line for normal distr. Plots made with R package, open source, **www.r-project.org**

Quantifying the pore size distribution enables understanding of how it varies with conditions, and eventually control. Crucial for fatigue resistance

Donegan *et al*. (2013) *Acta mater*. **61** 5595; application of peaks-over-threshold for quantifying tails

Ti-6-4 Sample 5B, contour-bulk interface: Intentionally porous

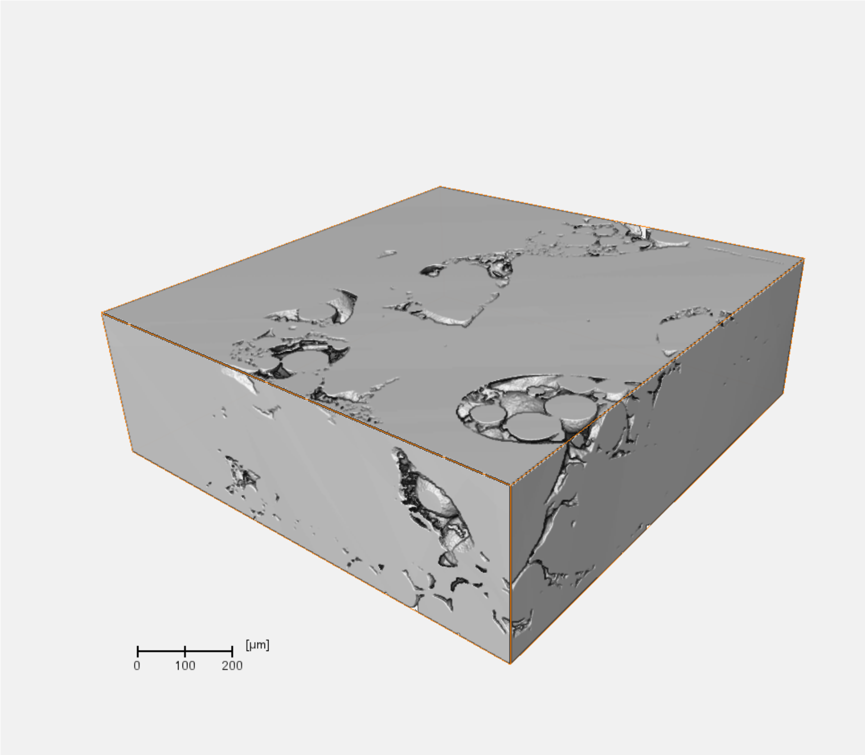

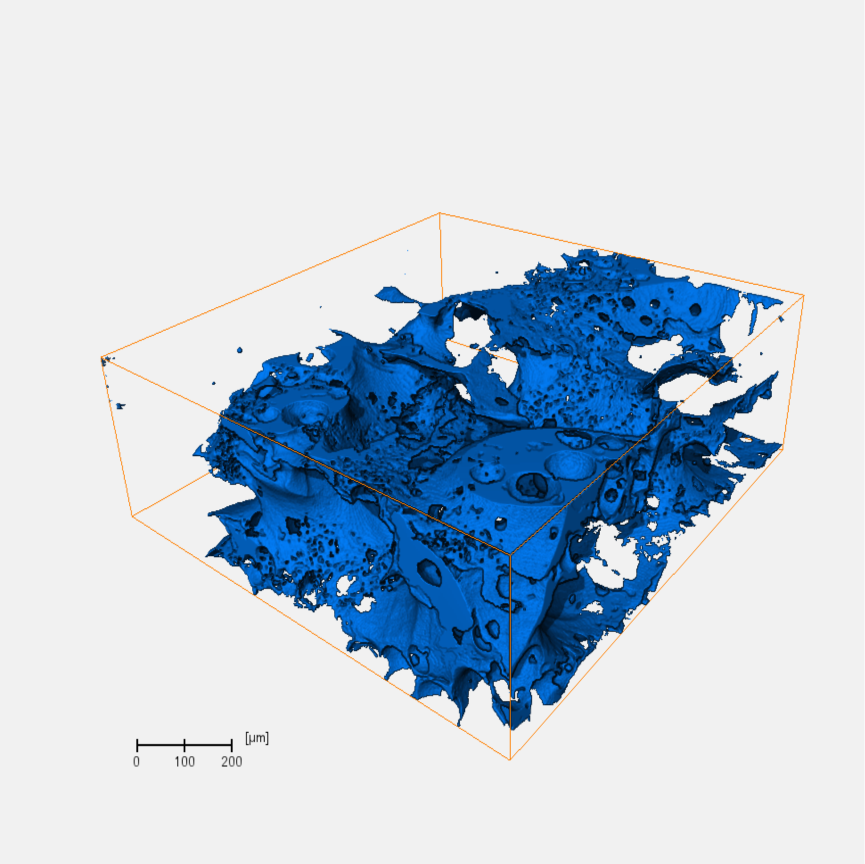

Powder Characteristics vs. Flow Behavior

- Gas-atomized powder generally display a log-normal size distribution[1]
- Log-normal distribution will appear linear on adjusted cumulative probability plot

- **Deviation from log-normal suggests sudden change in distribution (sieving)**
- **AlSi10Mg powder does not deviate from log normal**
- **EOS Ti-6Al-4V does not follow this trend**

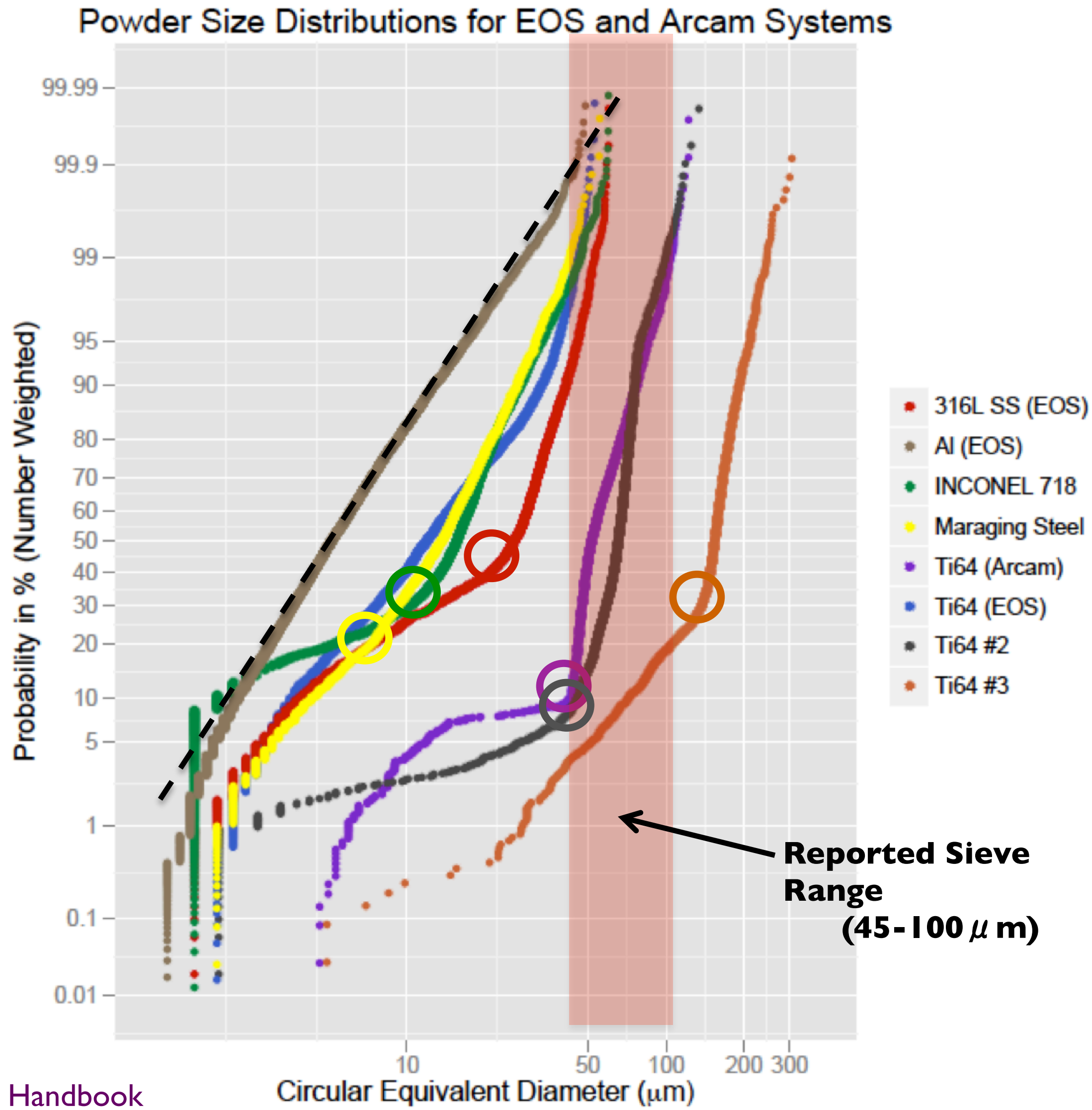

[1] O.D. Neikov, Chapter 5 - Atomization and Granulation, In Handbook of Non-Ferrous Metal Powders, edited by Neikov et al., Elsevier, Oxford, 2009, Pages 102-142

Powder Distribution vs. Flow

Distributions

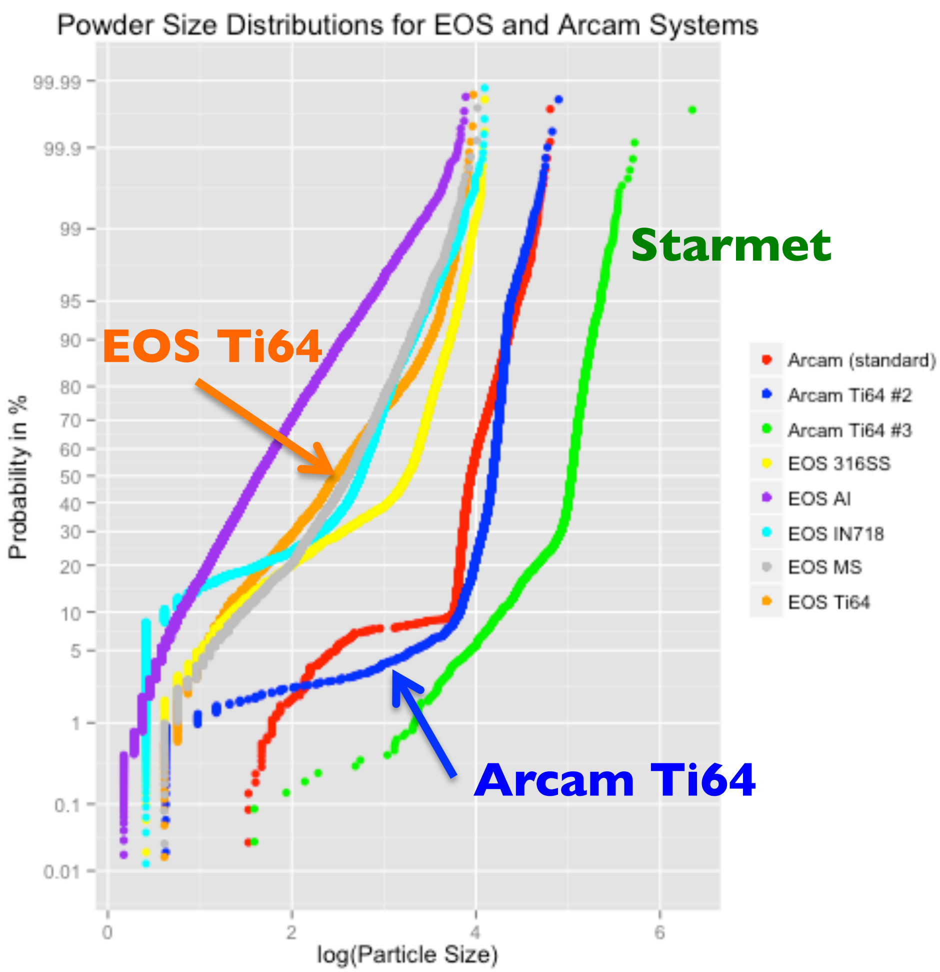

Flow

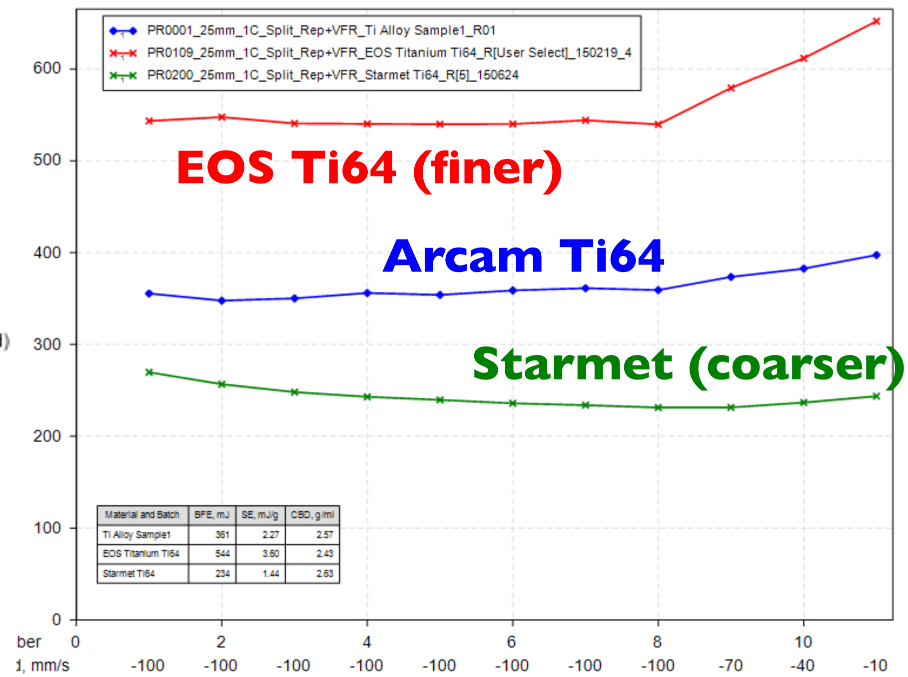

Material and Batch	BFE, mJ	SE, mJ/g	CBD, g/ml
Ti Alloy Sample1	361	2.27	2.57
EOS Titanium Ti64	544	3.60	2.43
Starmet Ti64	234	1.44	2.63

Flow measurements on a Freeman Rheometer
Propeller driven into a beaker full of powder
Confined flow effectively measured
Contrast with free flow with a Hall Cup

An automatic and objective system for finding relationships between microstructures

- Using machine vision and machine learning techniques, we automatically harvest, store, and compare microstructural image data.

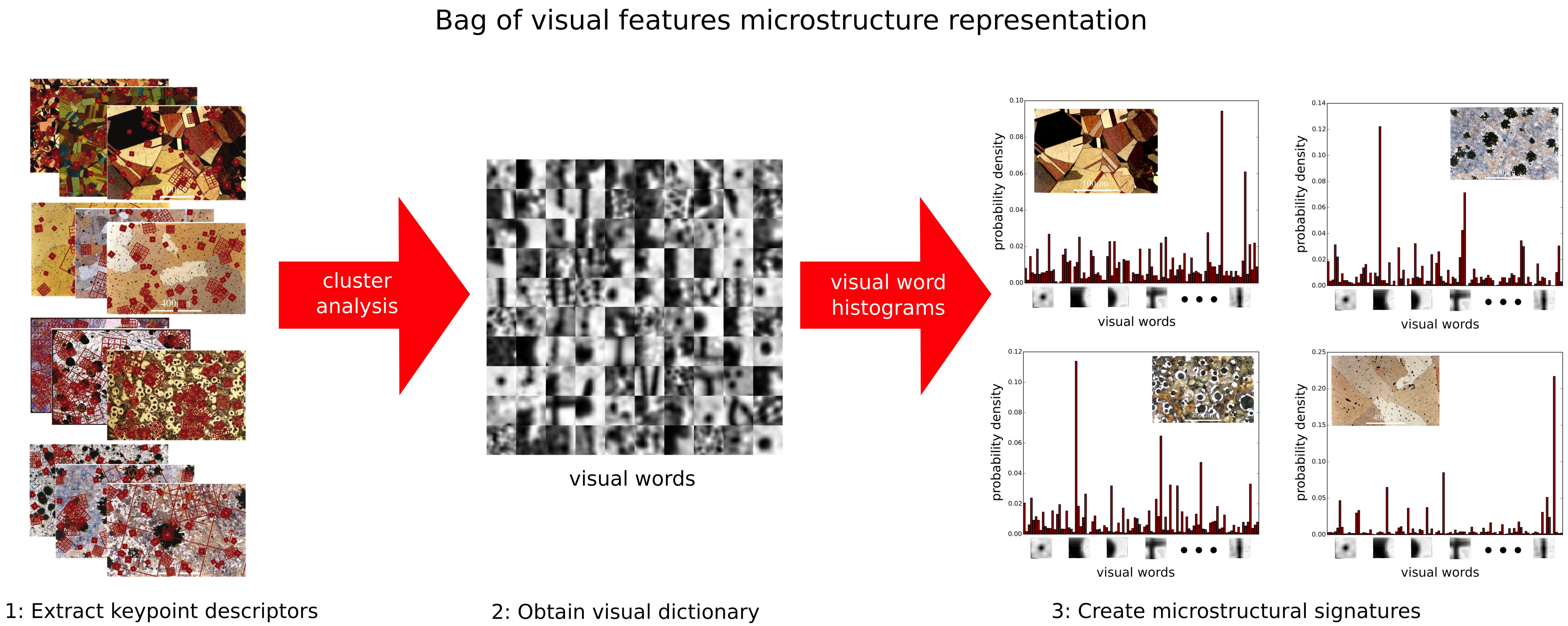

DeCost and Holm, *Computational Materials Science* **110** (2015) 126–133

Outcome: A microstructure classifier

- Given "training" micrographs divided into classes, we can classify new micrographs automatically and with high accuracy.

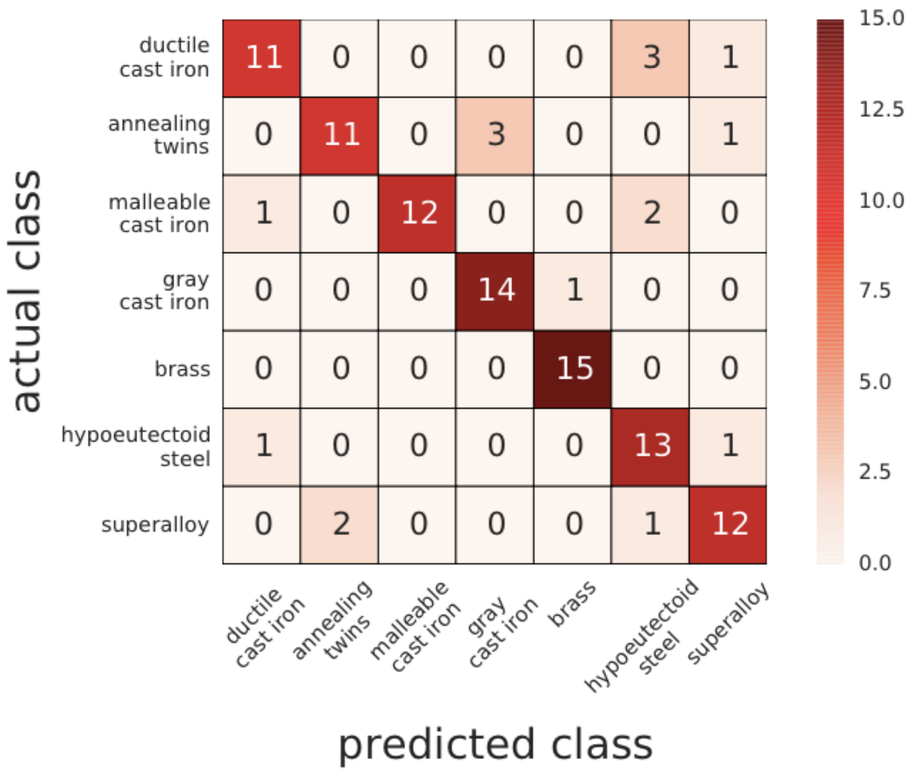

- 5-fold cross-validation on 15 microstructures per class (105 total)

∴ A score of '15' indicates perfect classification of validation images into the correct class:

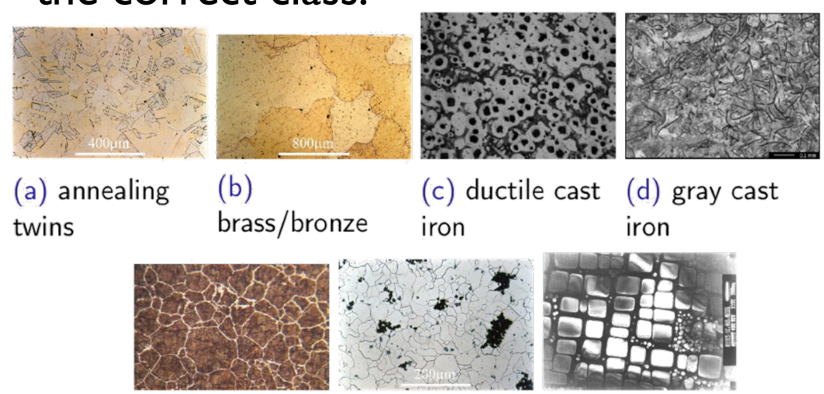

(a) annealing twins (b) brass/bronze (c) ductile cast iron (d) gray cast iron (e) hypoeutectoid steel (f) malleable cast iron (g) superalloy

- **Applications:** Process analysis, control and qualification; archiving; statistical analysis; finding correlations between structure and processing.

DeCost and Holm, *Computational Materials Science* **110** (2015) 126–133

Summary

- Understanding microstructure is important during every step in the additive manufacturing process. If you do not understand the details of the process, it is entirely possible to have a problem because of defects such as voids.
- Location of the voids relative to the surface is very important.
- This challenge can be addressing by combining
  - Measurement of powders and defects, especially pores: analysis with extreme value statistics, link to powder flow
  - Advanced characterization 3D microscopy with high energy synchrotron x-rays e.g. tomography of voids
  - Demonstrated ability to predict incomplete melting (and keyholing)
  - Development of micro-mechanical models for materials

National Aeronautics and Space Administration
Marshall Space Flight Center

Reliability of Mechanical Behavior in Metallic Additively Manufactured Parts for Critical Applications

Doug Wells
NASA MSFC
Huntsville AL

ASTM/NIST Workshop on Mechanical Behavior in Additive Manufactured parts

May 4, 2016

There is more to AM than manufacturing

AM machines create a unique material product form – typically purview of the foundry or mill

Subtractive Forging Process

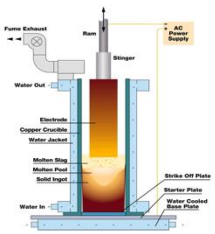

1. Ingot Making

2. Cutting

3. Heating

4. Forging

5. Heat Treating

6. Machining

7. Inspection

8. Delivery with CoC

Additive SLM Process

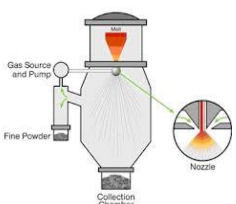

1. Powder Making

2. Printing

3. HIPing

4. Heat Treating

5. Machining

6. Inspection

7. Final Part

As the 'mill', the AM process must assure manufacturing compliance throughout the build process and material integrity throughout the volume of the final part.

AM Reliability Challenges

- AM responsibility serving as the material mill gives rise to additional reliability concerns
  - Low entry cost compared to typical material producers
  - New players in AM, unfamiliar with the scope of AM, lacking experience
  - Fabrication shops not previously responsible for metallurgical processes
  - Research labs converting to production

Concept Laser X-line Material Mill in a Box

- **AM machines operate with limited process feedback!**
  - **Reliability depends upon the quality and care taken in every step of AM operations => rigorous and meticulous controls**

Opportunities to Secure AM Reliability

Two primary opportunities to ensure AM reliability

1. In-Process Controls, (Control what you do)
   - Understanding fundamentals of the process
   - Knowing the process failure modes (pFMEA)
   - Identifying observable metrics and witness capabilities
   - Meticulous process scrutiny
   - *Future to provide detailed process feedback for post-process evaluation, eventually closed-loop controls.*
2. Post-Process Evaluation (Evaluate what you get, NDE)
   - Extensive subject, ASTM E07 and many partners involved
   - Not covered in this discussion

Part reliability rationale comes from sum of both in-process and post-process controls, weakness in one must be compensated in the other

The AM Process: Concept to Part

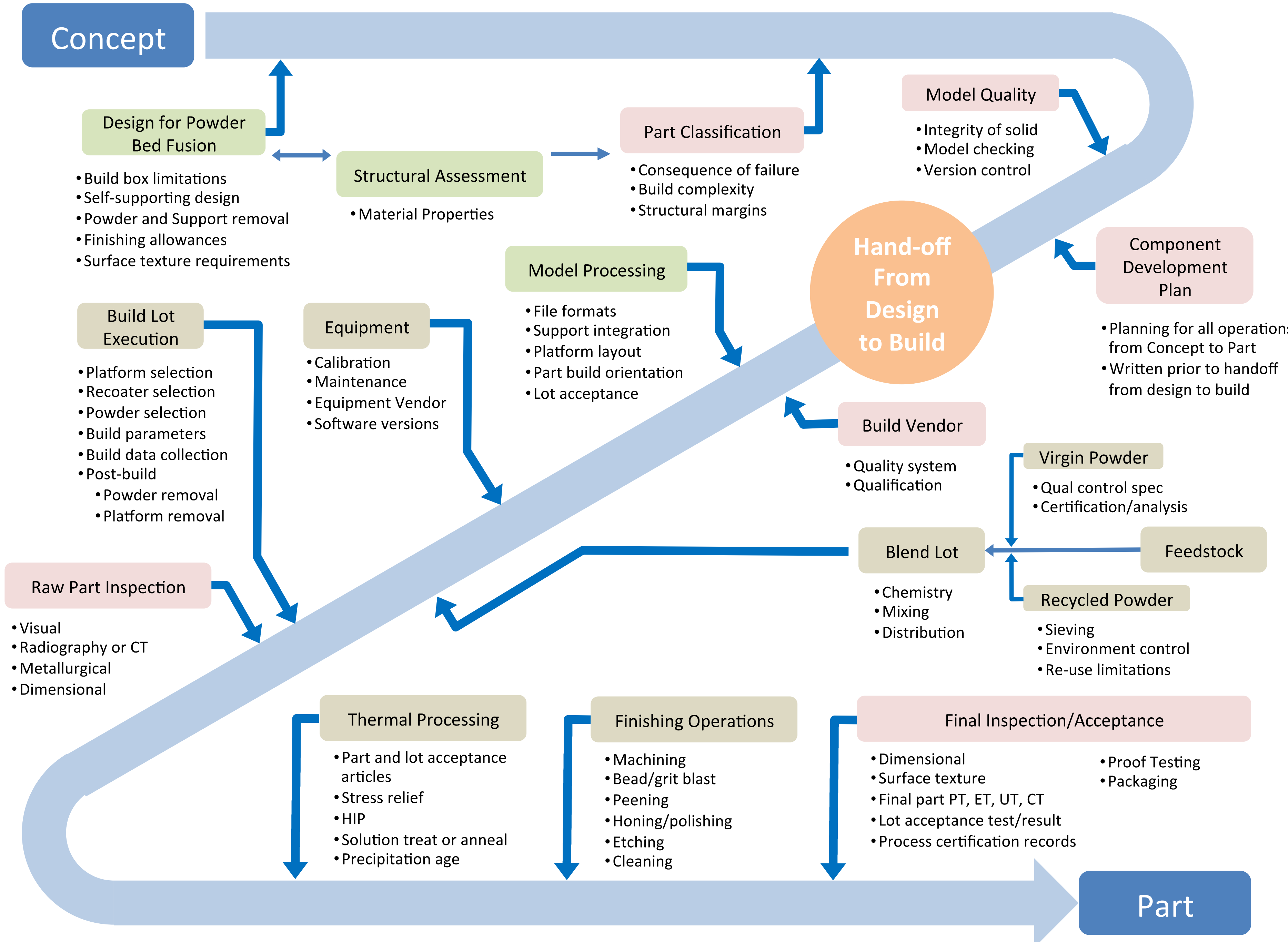

The AM Process: Concept to Part

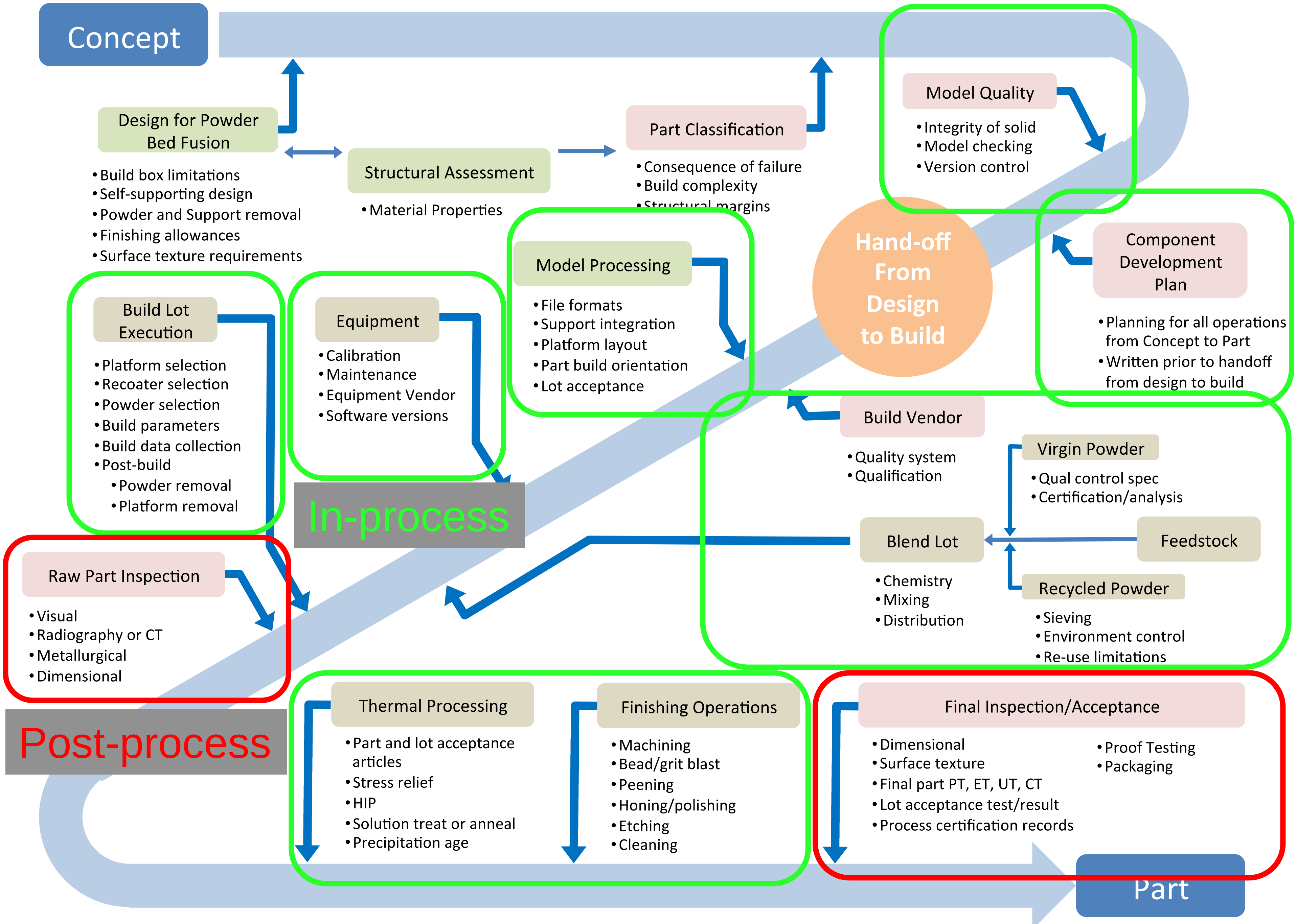

Standardization for AM Mechanical Reliability

- Systematic and controlled execution of AM processes is required to achieve requisite mechanical reliability
- Standardization of AM processes is actively pursued by private industry, government organizations, and standards development organizations worldwide.
  - ASTM F42, ISO collaboration
    - Only SDO with open, published AM standards
  - SAE AMS-AM
  - AWS
- NASA works with SDOs to bring open industry standards to AM
- Currently available open industry standards do not levy sufficient controls for spaceflight applications

Standardization for AM Mechanical Reliability

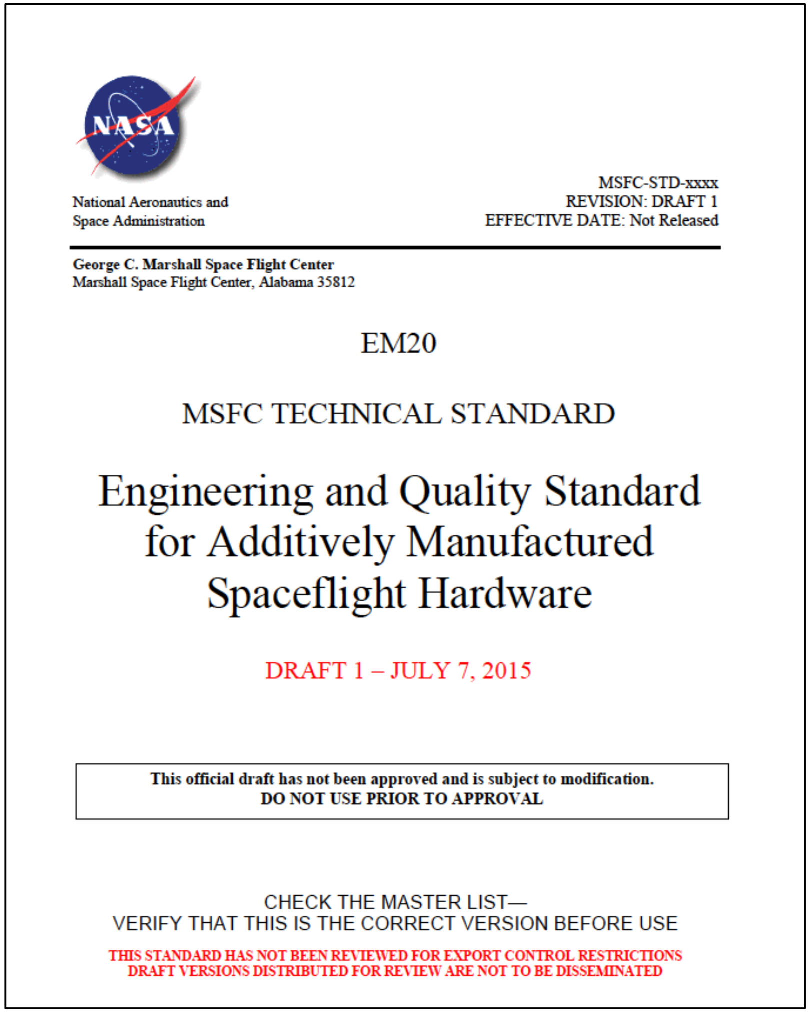

National Aeronautics and Space Administration

MSFC-STD-xxxx
REVISION: DRAFT 1
EFFECTIVE DATE: Not Released

George C. Marshall Space Flight Center
Marshall Space Flight Center, Alabama 35812

EM20

MSFC TECHNICAL STANDARD

Engineering and Quality Standard for Additively Manufactured Spaceflight Hardware

DRAFT 1 – JULY 7, 2015

This official draft has not been approved and is subject to modification.
DO NOT USE PRIOR TO APPROVAL

CHECK THE MASTER LIST—
VERIFY THAT THIS IS THE CORRECT VERSION BEFORE USE

THIS STANDARD HAS NOT BEEN REVIEWED FOR EXPORT CONTROL RESTRICTIONS
DRAFT VERSIONS DISTRIBUTED FOR REVIEW ARE NOT TO BE DISSEMINATED

- Draft NASA MSFC Standard
- Current methodology for AM reliability for critical applications
  - Space Launch System
  - Commercial Crew Program

Aerojet Rocketdyne RS-25

SpaceX SuperDraco

Aspects of Process Control

Draft NASA MSFC Standard implements four fundamental aspects of process control for AM:

Metallurgical Process Control

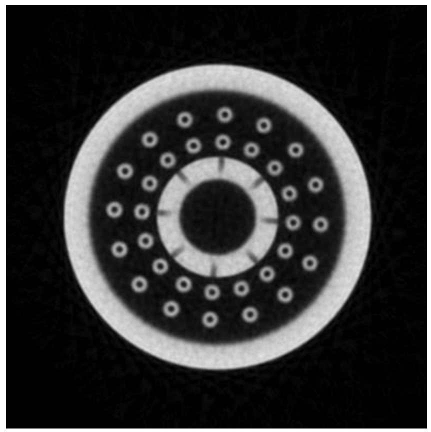

Part Process Control

Equipment Process Control

Build Vendor Process Control

- Each aspect of process control is essential to the production of critical AM parts with reliable mechanical behavior
- Discussion here focuses on process control fundamentals for production of mechanically reliable AM materials

Foundation: Qualified Metallurgical Process

- Draft NASA MSFC Standard identifies AM as a unique material product form and requires the metallurgical process to be qualified on ***every*** individual AM machine
- While aspects of this foundation are present in, for example, ASTM F3055 (IN718 AM spec), rigor, qualification, and traceability are currently lacking.

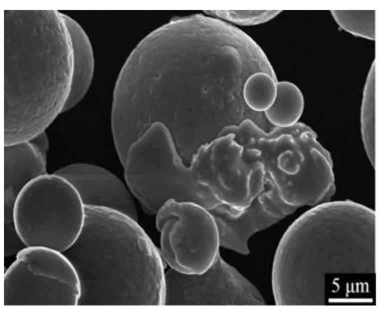

Powder

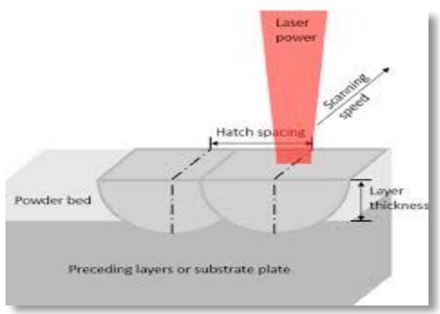

Process Variables

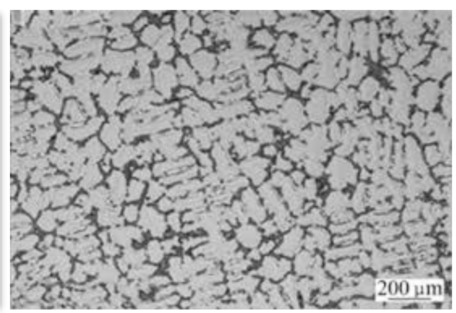

Microstructure

Properties

Foundation: Qualified Metallurgical Process

Qualified Metallurgical Process (QMP)

- Feedstock control or specification
- AM machine parameters, configuration, environment
- As-built densification, microstructure, and defect state
- Control of surface finish and detail rendering
- Thermal process for controlled microstructural evolution
- Mechanical behavior reference data
  - Strength, ductility, fatigue performance

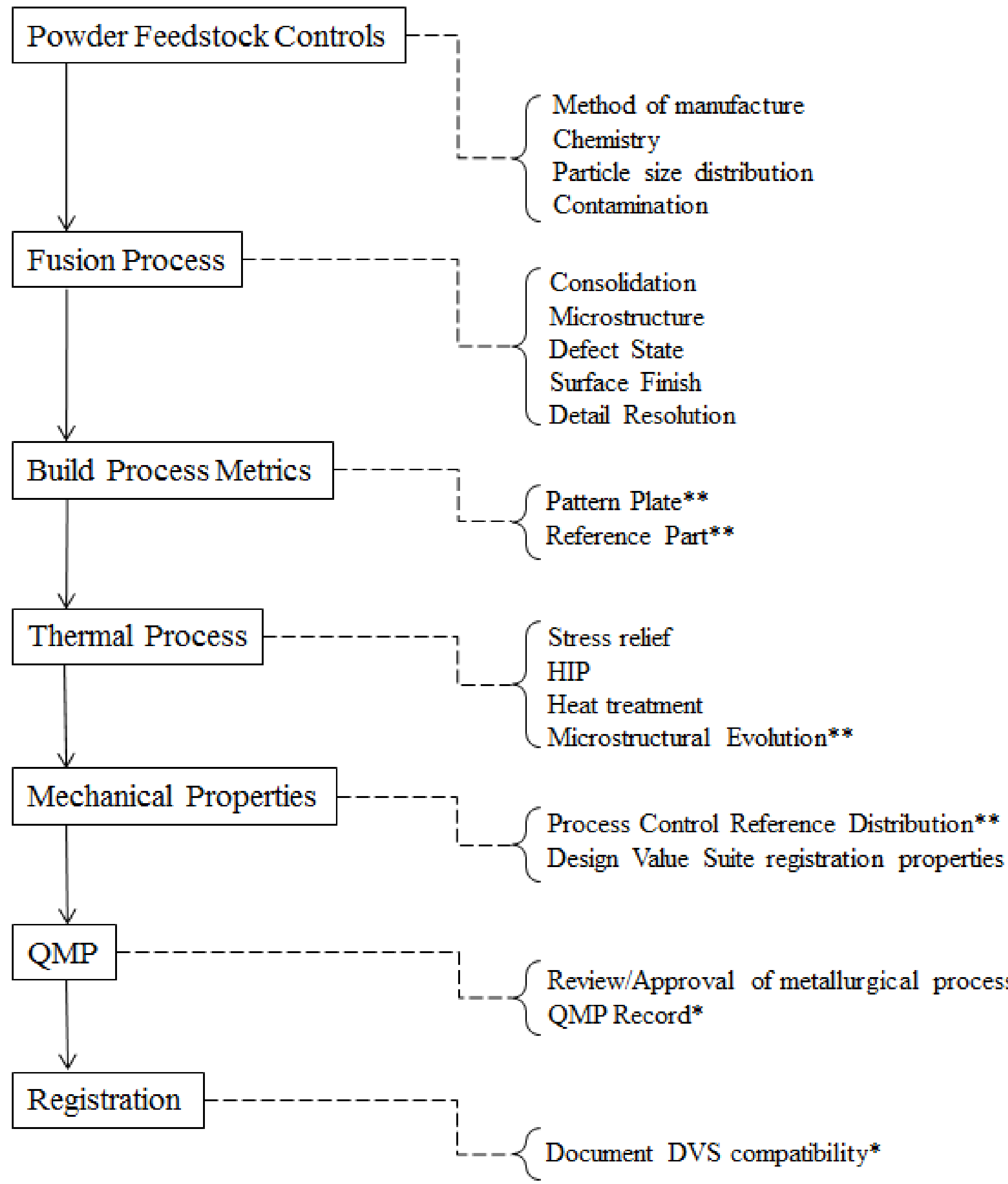

*Quality management system record
**Acceptance criteria metric

Foundation: Qualified Metallurgical Process

As Built

Stress Relieved

HIP & Final

Qualified Metallurgical Process (QMP)

- As-built densification, microstructure, and defect state
- Thermal process for controlled microstructural evolution

Foundation: Qualified Metallurgical Process

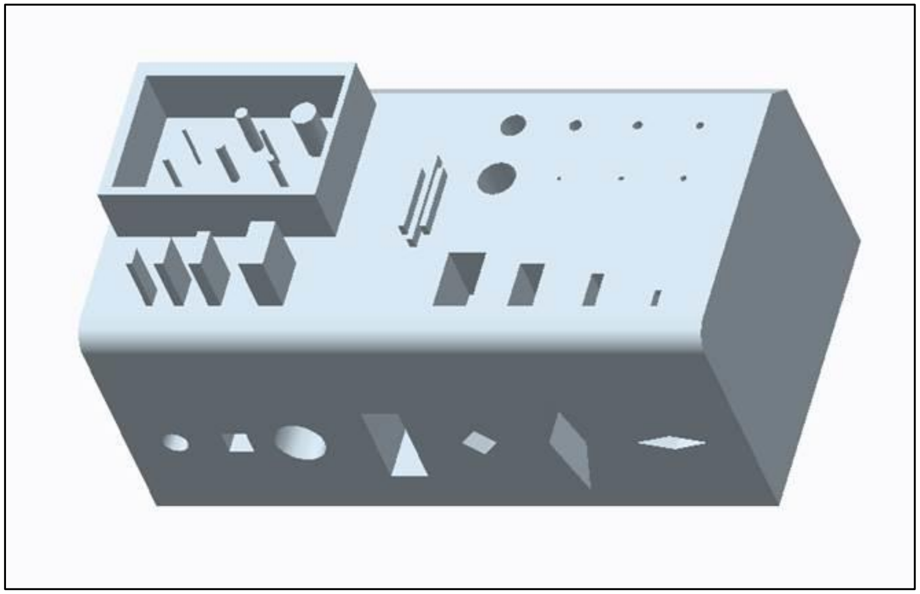

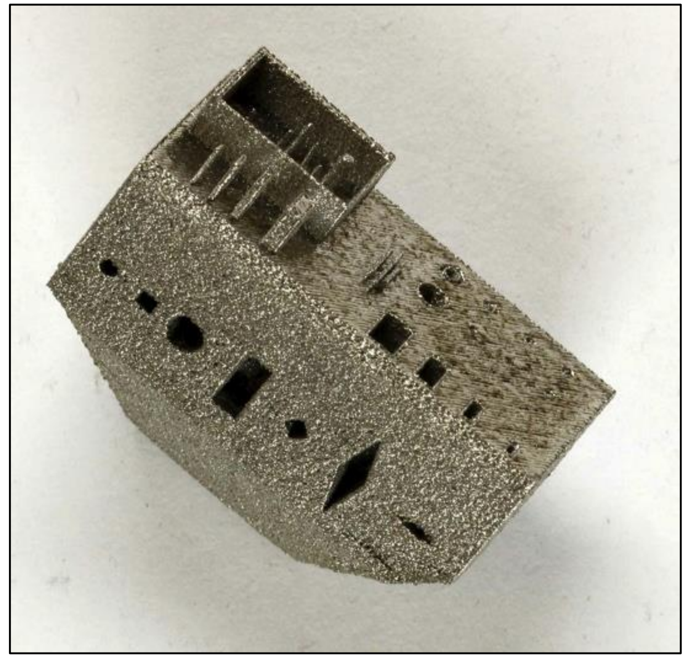

Reference parts:

Metrics for surface texture quality and detail rendering

Overhanging, vertical and horizontal surface texture, acuity of feature size and shape

Qualified Metallurgical Process (QMP)

- Reference Parts
- Control of surface finish and detail rendering
- Critical for consistent fatigue performance if as-built surfaces remain in part

Foundation: Qualified Metallurgical Process

- Mechanical behavior reference data
  - Strength, ductility, fatigue performance
  - Process Control Reference Distributions (PCRD)
- Establish and document estimates of mean value and variation associated with mechanical performance of the AM process per the QMP
  - Will evolve with lot variability, etc.
- Utilize knowledge of process performance to establish meaningful witness test acceptance criteria

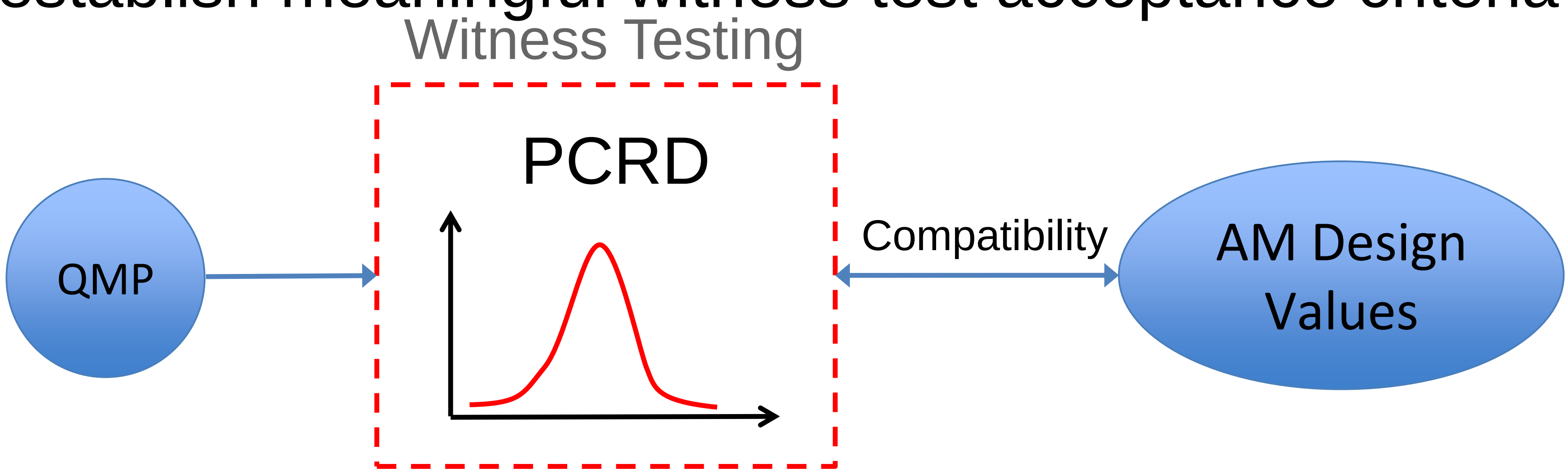

Foundation: Qualified Metallurgical Process

Types of AM build witness specimens

- Metallurgical
- Tensile (strengths and ductility)
- Fatigue
- Low-margin, governing properties

What is witnessed?

- Witness specimens provide direct evidence only for the systemic health of the AM process during the witnessed build
- Witness specimens are only an in-direct indicator of AM part quality through inference.

Foundation: Qualified Metallurgical Process

Types of AM build witness specimens

- Metallurgical

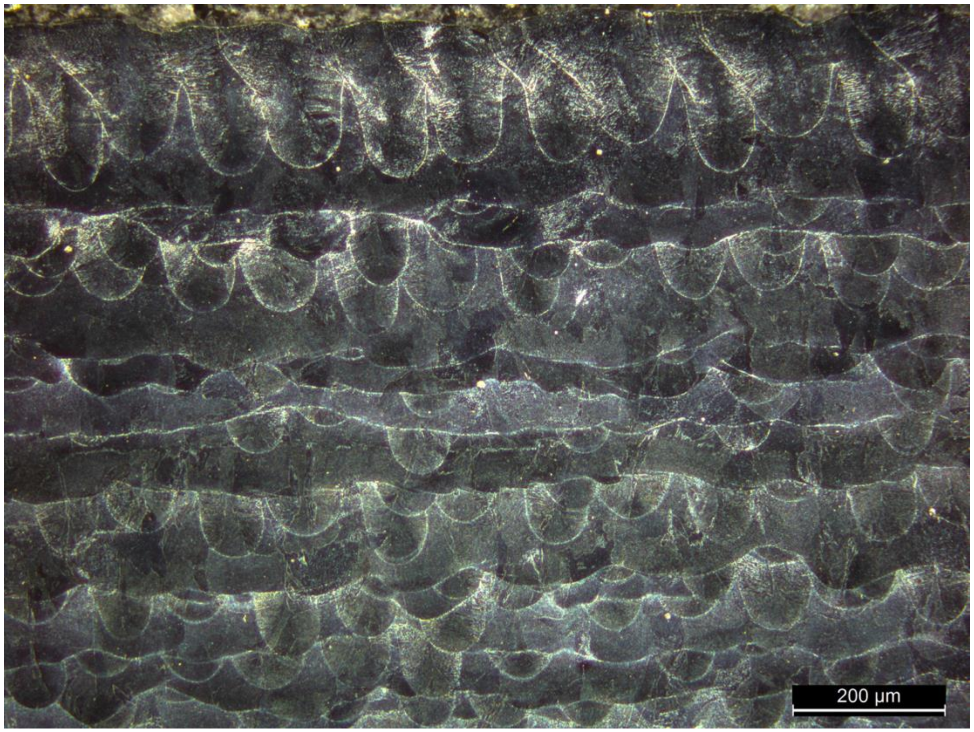

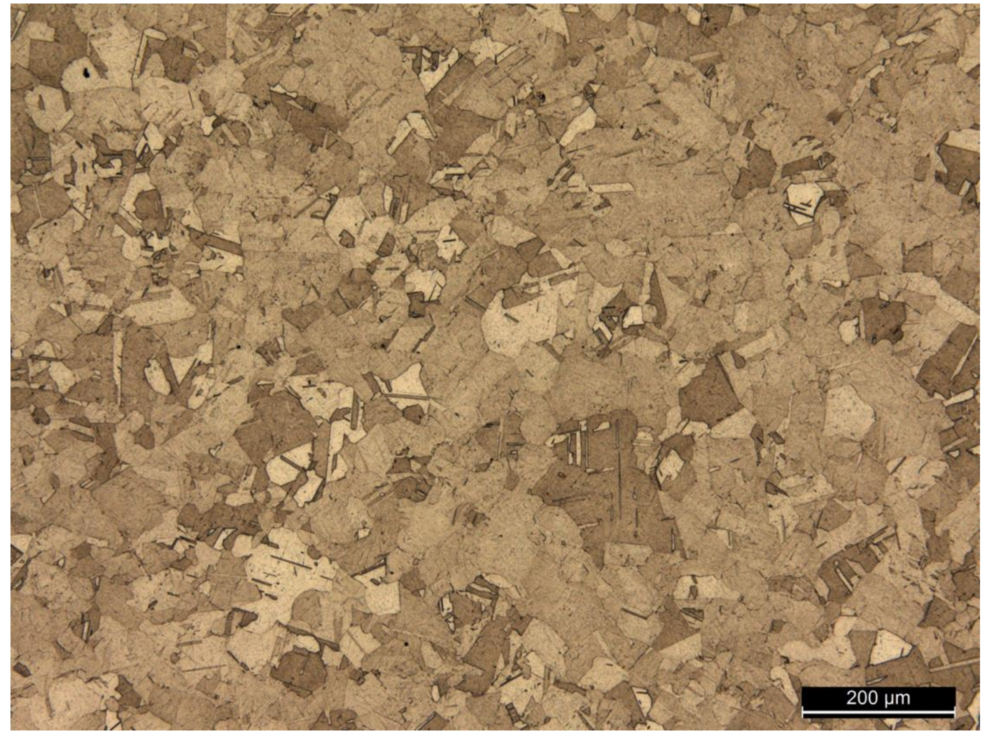

Example acceptance criteria - as-built state:
- Weld penetration depth and shape
- Grain nucleation patterns
- Porosity
- Lack of fusion / Cracks

Example acceptance criteria - final state:
- Grain size
- Expected phases or carbide sizes
- Grain boundary cleanliness
- Porosity
- Lack of fusion / Cracks

Foundation: Qualified Metallurgical Process

Types of AM build witness specimens

- Metallurgical

Example acceptance criteria - final state:

- Grain size
- Expected phases or carbide sizes
- Grain boundary cleanliness
- Porosity
- Lack of fusion / Cracks

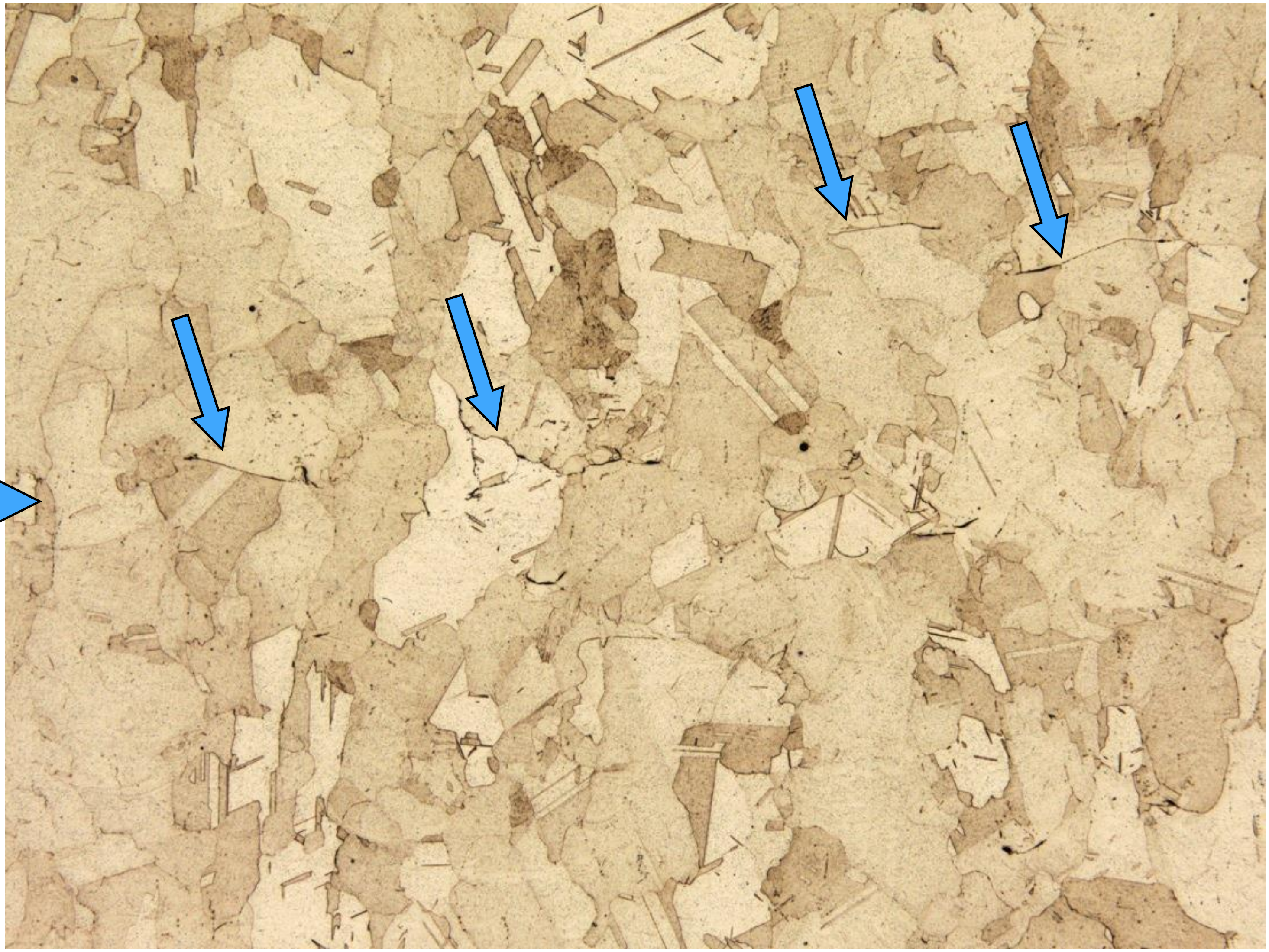

Foundation: Qualified Metallurgical Process

Types of AM build witness specimens

- Mechanical
  - Move away from spot testing for acceptance against 99/95 design values or specification minimums
  - Evaluate with sufficient tests to determine if the AM build is within family
  - Compromise with reasonable engineering assurance
  - Proposed
    - Six tensile
    - Two fatigue

Evaluate against the PCRD of the QMP

- **Ongoing evaluation of material quality substantiates the design allowable**
- **Only plausible way to maintain design values**

Example of AM build witness specimen evaluations

Nominal process is blue, off nominal in red

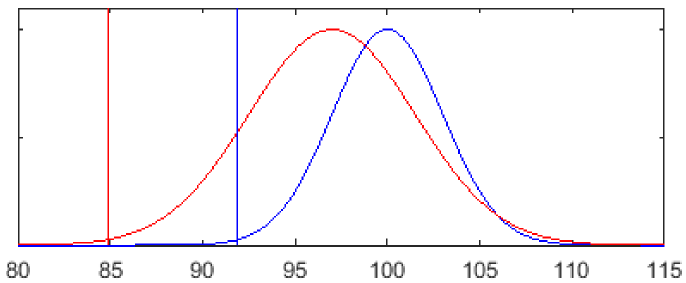

Two (2) witness tests per build

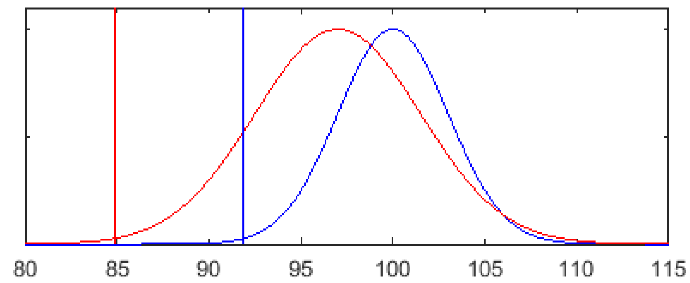

Six (6) witness tests per build

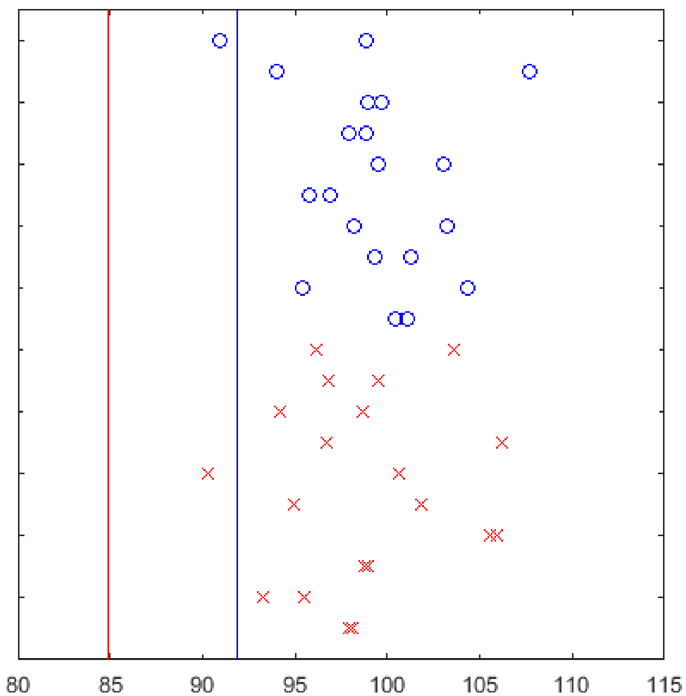

Process shift hard to discern

Random draw from nominal process 10 times

Random draw from off-nominal process, 10 times

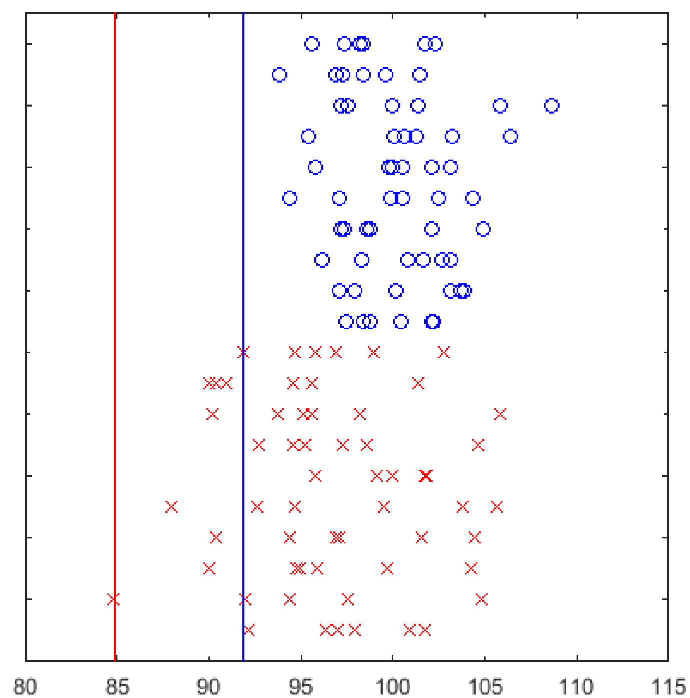

Process shift discernable with analysis of mean and variation

Witness for Statistical Process Control

Simulation is used to evaluate small sample statistical methods for witness specimen acceptance

Design acceptance criteria for the following:

- Keep process in family
- Minimize false negative acceptance results
- Protect the design values witnessed
- Protect the inferred design values

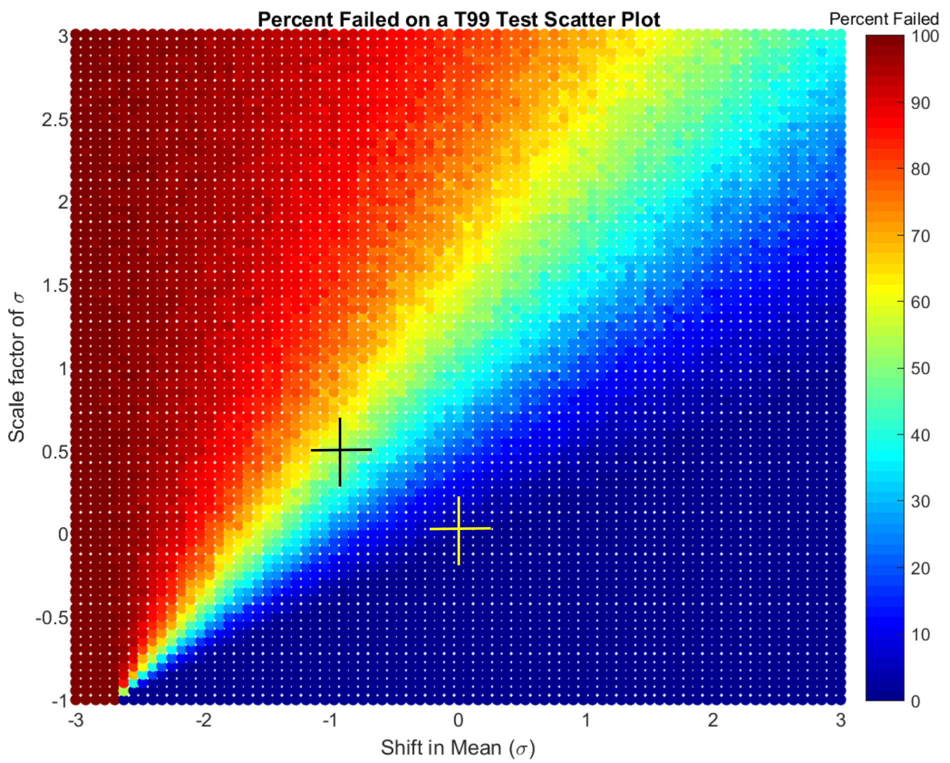

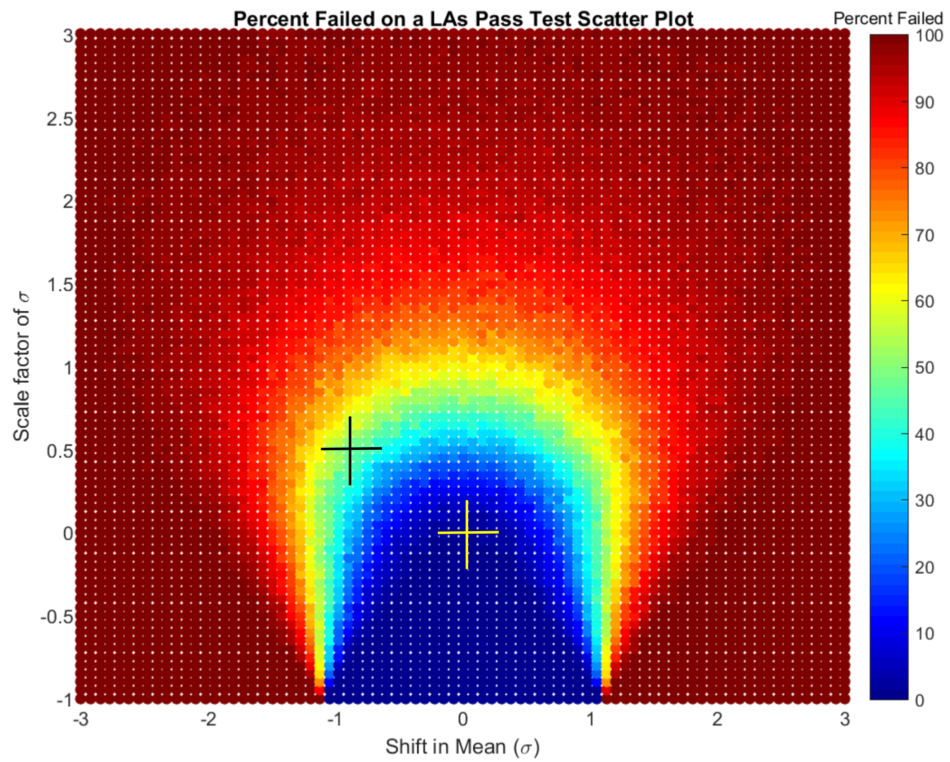

Role of Quality Management System

AM process controls cannot be meaningfully implemented without oversight and integration with strong Quality Management System

- Example, SAE AS9100

Mechanical reliability in AM cannot be established until:

- Process is defined and understood – Concept to Part
- Failure modes identified
- QMS engaged to monitor process and defeat failure modes

Standardization is key to developing a consistent approach

Summary of Points

To ensure mechanical reliability in AM:

- Requires thorough understanding and control of the process - Just as would be expected from a mill, foundry, or manufacturing house
- Requires sufficient process standardization to produce reliable parts in a routine fashion
- Requires quality management systems be in place
- Requires In-Process controls
  - Start with a solid foundation
    - Qualified metallurgical Process
  - Ensure mechanical reliability
    - Process witnessing, statistical evaluations
- Requires Post-Process controls
  - NDE
  - Proof testing
  - Etc.

Thank You

Additive Manufacturing at MSFC

Witness for Statistical Process Control